MASTER OF SCIENCE IN
AEROSPACE ENGINEERING
SPACE CURRICULUM

A versatile constellation of microsatellites with electric propulsion for Earth Observation: mission analysis and platform design

Andrea Papa

Anno Accademico 2013-2014

CENTROSPAZIO

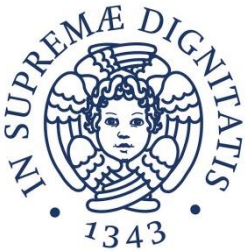

UNIVERSITY OF PISA

Master of Science in Aerospace Engineering
Space Curriculum

A versatile constellation of microsatellites with electric propulsion for Earth Observation: mission analysis and platform design

Supervisors:

Prof. Ing. S. Marcuccio

Ing. S. Gregucci

Candidate:

Andrea Papa

Anno Accademico 2013-2014

[…]when all are one and one is all, to be a rock and not to roll.
(Led Zeppelin, *Stairway to Heaven*, 1971)

"Quanto più piccolo è il treno più concentrato è il divertimento!"
(Sheldon Lee Cooper)

Alle due donne della mia vita

ABSTRACT

The increasing interest towards the exploitation of observations from the space to support daily human activities devoted to land and vegetation monitoring and management is the starting point for the study and creation of low-cost and high performance Earth Observation constellations.

This thesis is aimed at analyze and define a complete constellation of microsatellites with electric propulsion for optical Earth Observation (natural resources and environmental management, disaster monitoring, climatic assessments, agriculture and precision agriculture) considering as reference case the specific management of Tuscany croplands, and to design a suitable low-cost and high-performance standard platform. The work was carried out in collaboration between the University of Pisa and Alta SpA. In particular, the impact of a small electric propulsion device on-board the platform like the Alta SpA low power Hall thruster named HT100 has been studied exploiting the Alta SpA SATSLab (Spacecraft Attitude, Trajectory and Subsystems Laboratory) simulator. Several constellation architectures able to satisfy all users requirements (spatial and spectral optical images content, revisit frequency, ground coverage, operational flexibility) while maintaining a number of satellites low enough to ensure also the possibility of secondary payload single shared launches have been proposed. Recent technological improvements (in terms of power generation, electronic components miniaturization, electric propulsion readiness) allowed to design a very small platform able to be equipped with a large variety of optical instruments (large availability in terms of payload power, mass and envelope) while offering very interesting performance (power generation, data transmission, pointing accuracy, altitude maintenance, orbital transfers). Scientific requirements study, constellation architectures analysis and specifications and SATSLab drag compensation, orbital transfer, on-board power and energy management simulations results are shown, together with the platform design process adopted, final overall platform performance and specific considerations about future developments.

AKNOWLEDGMENTS

Desidero sinceramente ringraziare il Prof. Salvo Marcuccio e gli ingegneri Stefan Gregucci e Pierpaolo Pergola, per la costante disponibilità e collaborazione che mi è stata concessa durante questo periodo di tesi che, non lo nego, ha suscitato in me un interesse come forse non avrei mai immaginato. Ringraziamento naturalmente esteso ad Alta SpA ed a tutti i suoi dipendenti, con una parola in particolare per Cosimo e Tommaso, per le preziose consulenze, per i coleotteri bombardieri Angelo, Giovanni e Lucio, instancabili compagni di merende, per Andrea Bechi ed ancora per Stefan Gregucci, amici per me ormai irrinunciabili.

Un calorOSO grazie inoltre a tutti coloro che, *Don Chisciotte o Sancho Panza*, hanno da sempre accompagnato questo romantico rottame nelle sue disperate imprese. Perdonatemi se non vi annoio con uno dei miei soliti sproloqui in rima, se non evoco gatti, o serpenti, oppure barbadjanny, pini, scimmie, cotechi, peramoresoloperamoretuo, manzi, rastabanani, bruschette, vecchi bracaloni, tacchini, maratonde, Batacchi, suonatori Jones, kraken, giraffe, cutere, partners d'attacco, gamboni, Principi, maghi, dragoni, succhini&testoni, lanciarazzi, capitani, ASTREI, gabbianoni, pinze, gialloni, rugbysti, cantagalli, pararigori, marchigiani, abruzzesi, pisesi, butini, liguri, ciociari (già), tarantini, rossi, greci, romani, siculi, aerospaziali, Veri Pezzi Grossi, Sorelle o Pirati, ma tanto finirei per dimenticarmi qualcuno.

A ciascun cugino, zio e nonna, ed ad ogni amico di famiglia.

A Laura e Pasquale (e Pippo), perché forse non lo sanno, o forse non gliel'ho mai detto, ma mi hanno regalato i giorni più belli della mia vita.

A zio Michele, meraviglioso (e potenziale) interprete del calcio totale, costante guida ed ispirazione, faro anche nell'ora più buia.

A mamma e babbo, il mio cielo e la mia notte, la mia pentola d'oro alla fine dell'arcobaleno. Ah, e ovviamente anche a Jackone l'evaso.

A Matilde.

A mio fratello, perché è un Papa e perché se lo merita, e tornerà come è sempre stato, più forte di tutto e di tutti.

TABLE OF CONTENTS

ABSTRACT ..... **ix**

AKNOWLEDGMENTS ..... **xi**

TABLE OF CONTENTS ..... **xiii**

LIST OF FIGURES ..... **xxi**

LIST OF TABLES ..... **xxvi**

1 INTRODUCTION **1**

1.1 Thesis objectives and development of the work 3

2 REMOTE SENSING PRINCIPLES **5**

2.1 REMOTE SENSING OBSERVATION 6

2.1.1 Remote Sensing concept and fundamental characteristics ... 6

2.1.2 Energy source or illumination and the electromagnetic radiation 7

2.1.3 The Electromagnetic Spectrum 8

2.1.4 Radiation and atmosphere 10

2.1.5 Atmospheric windows 11

2.1.6 Interaction with the target 12

2.1.7 Target spectral response 12

2.1.8 Passive and active concepts of remote sensing observation 14

2.1.9 Remote sensing systems principal components 15

2.1.10 Remote sensing systems accuracy, precision and resolution 15

2.1.11 A fundamental distinction: images and photographs 16

2.1.12 Black & white images and color images 17

2.2 REMOTE SENSING SENSORS RESOLUTION TYPES 19

2.2.1 Temporal resolution 19

2.2.2 Spatial resolution 19
2.2.3 Spectral resolution 21
2.3 SUMMARY Chapter 2 22
3 REMOTE SENSING DATA APPLICATION FOR AGRICULTURAL MONITORING AND MANAGEMENT 23
3.1 USE OF OPTICAL SATELLITE REMOTE SENSING DATA 24
3.1.1 Relevant vegetation characteristics derivable from reflectance curves 25
3.1.2 Vegetation biochemical and biophysical parameters measurable from reflectance curves 27
3.1.3 Soil characteristics derivable from reflectance curves 29
3.2 VEGETATION AND SOIL INDICES 30
3.2.1 Most important VIS-NIR Ratios-Vegetation Indices 31
3.3 CROP POTENTIAL DESCRIPTIONS FROM OPTICAL REMOTE SENSING DATA 34
3.3.1 Crop acreage 34
3.3.2 Crop conditions 35
3.3.3 Crop changes and transformation 35
3.4 POTENTIAL CONTRIBUTIONS OF OPTICAL REMOTE SENSING DATA IN THE FRAME OF CROP MONITORING AND MANAGEMENT 36
3.4.1 Crop classification 36
3.4.2 Crop monitoring 36
3.4.3 Crop mapping 37
3.4.4 Crop yielding 41
3.5 SUMMARY 3.1 42
3.6 USERS' POINT OF VIEW AND REQUIREMENTS 43
3.6.1 Users' objectives 43

3.6.2 Priority information 43
3.7 TEMPORAL REQUIREMENTS 45
3.7.1 Temporal resolution 45
3.7.2 Turn-around time 45
3.7.3 Response time 46
3.7.4 Revisit time & Repeat Cycle 46
3.8 SPATIAL REQUIREMENTS 49
3.8.1 Spatial resolution 49
3.8.2 Location and measurement accuracy 52
3.9 SPECTRAL REQUIREMENTS 53
3.9.1 Suitable spectral domain 54
3.9.2 Number of bands and bandwidth: multispectral and hyperspectral analysis 58
3.10 PRECISION AGRICULTURE 64
3.11 SUMMARY 3.2 67
3.12 AN IMPROVED AND COMPLETE OPTICAL SYSTEM 68
3.13 SUMMARY 3.3 70
4 PAST, ACTUAL AND PLANNED EARTH OBSERVATION OPTICAL MISSIONS ANALYSIS 71
4.1 INTRODUCTION 72
4.2 MULTISPECTRAL OPTICAL EARTH OBSERVATION MISSIONS 73
4.2.1 Large satellites multispectral missions 73
4.2.2 Small satellites multispectral missions 78
4.2.3 Multispectral optical Earth Observation missions analysis conclusions 84
4.3 HYPERSPECTRAL OPTICAL EARTH OBSERVATION MISSIONS 86

4.3.1 Large satellites hyperspectral missions 86
4.3.2 Small satellites hyperspectral missions 87
4.3.3 Hyperspectral optical Earth Observation missions analysis conclusions 88
4.4 AN ATTRACTIVE OPPORTUNITY: THERMAL IR OBSERVATIONS 90
4.4.1 Thermal IR observation missions and instruments analysis 90
4.4.2 Thermal IR observation analysis conclusions 91
4.5 SUMMARY chapter 4 92
5 SAR OBSERVATION 93
5.1 NON-OPTICAL OBSERVATIONS: MICROWAVES SPECTRAL DOMAIN AND SYNTHETIC APERTURE RADAR (SAR) 94
5.1.1 SAR technology concept and principle of functioning 94
5.1.2 SAR signals target interaction mechanism 95
5.1.3 SAR Polarimetry (PolSAR) 98
5.1.4 Sar Polarimetry + SAR Interferometry (PolInSAR) 99
5.2 PAST, ACTUAL AND PLANNED EARTH OBSERVATION SAR MISSIONS AND STUDIES ANALYSIS 100
5.2.1 Large satellite Earth Observation SAR missions analysis 100
5.2.2 Actual and planned studies about microsatellites SAR applications 102
5.3 AGRICULTURE: OPTICAL IMAGES ARE SUFFICIENT . 103
5.4 SUMMARY Chapter 5 104
6 PRELIMINARY MISSION ARCHITECTURE DESIGN 105
6.1 CONSTELLATION DESIGN 106
6.1.1 A preliminary discrimination 108

6.1.2 Main technical requirements for an Earth Observation system 108
6.1.3 System drivers 109
6.1.4 Main parameters to define for an Earth Observation constellation design 109
6.2 ORBITAL CONSTRAINTS 110
6.2.1 Orbital altitude range 110
6.2.2 Orbital shape 111
6.2.3 Orbital inclination 112
6.3 SPECIALIZED ORBITS 114
6.3.1 Earthsynchronus Orbits: Repeating Ground Track Orbits (RGTO) 114
6.3.2 Sun-synchronus Orbits (SSO) 115
6.3.3 Sun-synchronus Repeating Ground Track Orbits (SSRGTO) 116
6.4 SUMMARY 6.1 117
6.5 GENERIC CONSTELLATION DESIGN 118
6.5.1 Repeat Cycle (RC) analysis to achieve the 1-day revisit time capability 118
6.5.2 Repeat coverage analysis to observe the whole Tuscany every day 125
6.6 SUMMARY 6.2 131
6.7 SPECIFIC-OPTICAL TASK MINI-CONSTELLATIONS 132
6.7.1 Specific-optical observation task mini-constellations 132
6.8 ACTUAL AND PLANNED SMALL MULTISPECTRAL, HYPERSPECTRAL AND THERMAL IR LAND AND VEGETATION OBSERVATION INSTRUMENTS 134
6.8.1 Multispectral optical Earth Observation sensors 134
6.8.2 Hyperspectral optical Earth Observation sensors 137

6.8.3 Single Thermal IR channel optical Earth Observation sensors 138

6.8.4 Specific mini-constellations satellites number analysis ... 139

6.9 COMPLETE OPTICAL CONSTELLATION PRELIMINARY ARCHITECTURE EXAMPLES 141

6.9.1 Proposed complete constellation architecture examples .. 141

6.9.2 Proposed complete constellation architecture examples discussion and selection of the most interesting examples 144

6.9.3 Description of most interesting selected architectures 145

6.10 SUMMARY 6.3 148

7 SATELLITE PRELIMINARY MASS BUDGET 151

7.1 SATELLITE PRELIMINARY MASS BUDGET 152

7.1.1 Satellite conceptual subdivision 152

7.1.2 Electric Propulsion subsystem: the Alta SpA HT100D ... 153

7.1.3 Telemetry, Tracking and Command subsystem (TT&C) 155

7.1.4 Primary structure 155

7.1.5 Thermal Control (TC), On-Board Computer (OBC) and Attitude & Determination Control (ADC) subsystems 156

7.1.6 Power Generation and Storage Subsystem 157

7.2 PRELIMINARY MASS BUDGET RESULTS 160

7.2.1 Mass budget results 160

7.2.2 GMAT simulations and preliminary mass budget results discussion and conclusions 163

7.3 SUMMARY Chapter 7 164

8 FIVE YEARS DRAG COMPENSATION AND ORBITAL TRANSFER SIMULATIONS 165

8.1 DRAG COMPENSATION GMAT SIMULATIONS 166

8.1.1 Five-years propellant expense GMAT simulations results 166

8.1.2 Available mass for an optical sensor derivation 167
8.1.3 Total mass selection for complete constellation architectures 169
8.2 Alta SpA SATSLab SIMULATIONS.....170
8.2.1 FIVE YEARS CONSTELLATION ARCHITECTURES Alta SpA SATSLAB SIMULATIONS 170
8.2.2 Alta SpA SATSLab simulations to model hypothetical orbital transfers.....174
8.2.3 Alta SpA SATSLab simulations results discussion.....175
8.3 SUMMARY Chapter 8 176
9 PLATFORM SIZING AND DESIGN 177
9.1 SATELLITE SUBSYSTEMS SIZING AND COMPONENT SELECTION 178
9.1.1 Platform dimensions 178
9.1.2 Power Generation subsystem and platform bus.....178
9.1.3 Primary Structure.....178
9.1.4 Thrusting Module 180
9.1.5 Telemetry, Tracking and Command subsystem (TT&C) .182
9.1.6 Attitude Determination and Control subsystem (ADC) ...186
9.1.7 On-Board Computer (OBC) and data storage subsystems192
9.1.8 Thermal Control subsystem (TC) 192
9.2 PLATFORM LOGIC DESIGN AND FUNCTIONS INDIVIDUATION 193
9.2.1 Mission scenario 193
9.2.2 Platform logic architecture 194
9.2.3 Platform begin of life (BOL) power budget and power storage subsystem sizing 194
9.2.4 Platform end of life (EOL) power budget and power storage subsystem sizing.....200

9.2.5 Alta SpA SATSLab simulations of complete mission BOL 201
9.2.6 Alta SpA SATSLab simulations of complete mission EOL 204
9.3 PLATFORM DESIGN 207
9.3.1 Platform conceptual definition 207
9.3.2 Platform external layout 207
9.3.3 Platform internal layout 214
9.3.4 Platform mass budget 219
9.4 ALTERNATIVE PLATFORM DESIGN 220
9.4.1 Alternative configuration 221
9.5 PLATFORM SIZING AND DESIGN CONCLUSIONS 229
9.6 SUMMARY Chapter 9 230
10 CONCLUSIONS 231
BIBLIOGRAPHY 233

LIST OF FIGURES

Figure 1.1 The NigeriSat-2 fully assembled flight model. 1
Figure 1.2: The DMC SLIM-6-22 12 kg instrument. 2
Figure 1.3: The Alta SpA HT100D. 3
Figure 2.1: Basic concept of a remote sensing observation system. 6
Figure 2.2: Schematic representation of an electromagnetic wave. 7
Figure 2.3: The Electromagnetic Spectrum 8
Figure 2.4: Atmospheric Windows and Sun-Earth characteristics. 11
Figure 2.5: Radiation absorption, reflection and transmission. 12
Figure 2.6: Water, soil and vegetation Reflectance Curves in the VIS and IR regions. 13
Figure 2.7: Passive and active observation concepts. 14
Figure 2.8: Digital Image of the original photograph. 17
Figure 2.9: Black & white image. 18
Figure 2.10: A color image compared to a black & white image. 18
Figure 2.11: The same scene acquired at three different spatial resolution levels. 20
Figure 3.1: Typical chlorophyll reflectance curve. 26
Figure 3.2: Healthy and unhealthy vegetation spectral behavior comparison. 30
Figure 3.3: NDVI thematic map of northeastern Kansas, 2011. 32
Figure 3.4: A true color map by RapidEye constellation. 38
Figure 3.5: A ground cover map by RapidEye constellation over Wurzburg, Germany. 39
Figure 3.6: A chlorophyll thematic map by RapidEye constellation. 40
Figure 3.7: A soil brightness thematic map. 40
Figure 3.8: Division in management zones according to NDVI measurements. 41
Figure 3.9: USA land cover and crop classification at national level. 50
Figure 3.10: In-field nitrogen content variability. 51
Figure 3.11: Ikonos multispectral image at about 4 m of spatial resolution. 52
Figure 3.12: RapidEye Red Edge band. 56

Figure 3.13: Hyperspectral imaging concept. 59
Figure 3.14: NDVI variability within adjacent small fields..... 65
Figure 4.1: Agriculture in Nevada by Landsat-7. 74
Figure 4.2: Landsat 8 satellite. 75
Figure 4.3: Deforestation in Rondonia, Brazil, by Landsat-8 (August 6, 2011). 76
Figure 4.4: RapidEye satellites at SSTL prior to launch site shipment. . 78
Figure 4.5: RapidEye image of Alaska, USA (September 11, 2012). 79
Figure 4.6: UK-DMC-2 and Deimos-1 at the launch facility in Baikonur. 81
Figure 4.7: First image of NigeriSat-X, Auckland, New Zealand (August 21, 20119). 83
Figure 4.8: CHRIS image of Uluru, Australia (April, 2004). 88
Figure 5.1: SAR concept representation. 95
Figure 5.2: Sentinel-1a (IW) image of the Gulf of Genua, Italy (August, 2014). 101
Figure 6.1: The satellite SC is directly placed over Tuscany at the starting time. 121
Figure 6.2: The satellite SC is again directly placed over Tuscany after 1 sidereal day. 121
Figure 6.3: The satellite SC is directly placed over Tuscany at the starting time. 122
Figure 6.4: The ground-track is shifted after 1 sidereal day and the satellite SC doesn't repass over the Tuscany. 122
Figure 6.5: Satellite is again directly placed over Tuscany after 2 sidereal days. 123
Figure 6.6: The satellite SC1 is directly placed over the region of interest at the starting time..... 123
Figure 6.7: After 1 sidereal day, the satellite SC2 is directly placed over the Tuscany. 124
Figure 6.8: After 2 sidereal days, the satellite SC1 is again placed directly over the Tuscany. 124
Figure 6.9: The Strip1 satellite images the most easterly Tuscany side during one pass. 127
Figure 6.10: The Strip2 satellite images the central portion of Tuscany during one pass. 127

Figure 6.11: The Strip3 satellite images the most westerly Tuscany side during one pass. 128
Figure 6.12: Acquisition of the entire Tuscany during a single pass from an inclination orbit. 129
Figure 6.13: 5-days acquisition of the Germany by RapidEye constellation. 129
Figure 6.14: Hodoyoshi-4 HRMS. 136
Figure 7.1: Alta SpA HT100D in operation. 153
Figure 7.2: Experimental HT100D total thrust efficiency. 154
Figure 7.3: Experimental HT100D Total Specific Impulse. 154
Figure 7.4: GMAT available mass to carry on-board a payload and propellant in the case of a thrust of 9 mN for altitudes comprised between 318 and 632 km. 160
Figure 7.5: GMAT available mass to carry on-board a payload and propellant in the case of a thrust of 9 mN for altitudes comprised between 661 and 1059 km. 160
Figure 7.6: GMAT available mass to carry on-board a payload and propellant in the case of a thrust of 12 mN for altitudes comprised between 318 and 632 km. 161
Figure 7.7: GMAT available mass to carry on-board a payload and propellant in the case of a thrust of 12 mN for altitudes comprised between 661 and 1059 km. 161
Figure 7.8: GMAT available mass to carry on-board a payload and propellant in the case of a thrust of 15 mN for altitudes comprised between 318 and 632 km. 162
Figure 7.9: GMAT available mass to carry on-board a payload and propellant in the case of a thrust of 15 mN for altitudes comprised between 661 and 1059 km. 162
Figure 8.1: Propellant expense to maintain altitude for 5 years up to about 404 km. 166
Figure 8.2: Propellant expense to maintain altitude for 5 years up to about 554 km. 167
Figure 8.3: Available mass to carry on- board an optical payload. 168
Figure 8.4: Available mass to carry on- board an optical payload. 168
Figure 8.5: Propellant mass consumption during the first 6 months of life at 358 km. 171

Figure 8.6: Propellant mass consumption during the first 6 months of life at 404 km. 171
Figure 8.7: Propellant mass consumption during the first 6 months of life at 554 km. 172
Figure 8.8: Propellant mass consumption during the last 6 months of life at 358 km. 172
Figure 8.9: Propellant mass consumption during the last 6 months of life at 404 km. 173
Figure 8.10: Propellant mass consumption during the last 6 months of life at 554 km. 173
Figure 9.1: EWC28 Syrlinks X-band transmitter and S-band receiver. 182
Figure 9.2: RUAG X-band helix antenna. 182
Figure 9.3: Ground station visibility from an altitude of 358 km. 183
Figure 9.4: Available channel capacity from an altitude of 358 km. 184
Figure 9.5: Ground station visibility from an altitude of 554 km. 184
Figure 9.6: Available channel capacity from an altitude of 554 km. 185
Figure 9.7: RW 90 of Astround Feinwerktechnik Adlershof GmbH reaction wheel. 188
Figure 9.8: ZARM MT5-2 magnetic torquer. 189
Figure 9.9: AMR ZARM digital magnetometer. 189
Figure 9.10: ST-16 Sinclair star trackers. 190
Figure 9.11: CSS-01,02 Space Micro coarse Sun sensor. 190
Figure 9.12: STIM300 Sensonor 3-axis MEMS gyroscope. 191
Figure 9.13: Platform logic architecture. 194
Figure 9.14: Different Sun-synchronus orbit configuration with respect the Sun vector. 195
Figure 9.15: Power Generation variation in relation to Sun-angle (first half of the year). 196
Figure 9.16: Power Generation variation in relation to Sun-angle (second half of the year). 196
Figure 9.17: Batteries DOD BOL vs time if observation and transmission are performed every orbit between +60° and -60° of latitude. 198
Figure 9.18: HT100D operation temperature. 199
Figure 9.19: Daily SMA BOL maintaining at 358 km of altitude. 199
Figure 9.20: Batteries DOD EOL vs time. 200
Figure 9.21: Daily SMA maintaining EOL at 358 km of altitude. 201

Figure 9.22: Power generation BOL during one completely operational day. 202
Figure 9.23: Power Consumption BOL during one operational day. HT100D ignitions are represented by the first and the last step. 202
Figure 9.24: Batteries Available Energy BOL during one completely operational day. 203
Figure 9.25: Batteries DOD and eclipse BOL during one completely operational day. Eclipse- thrusting is represented by the largest DOD decrease. 203
Figure 9.26: Power generation EOL during one completely operational day. 204
Figure 9.27: Power Consumption EOL during one completely operational day. HT100D ignitions are represented by the first and the last step.....205
Figure 9.28: Batteries Available Energy EOL during one completely operational day. 205
Figure 9.29: Batteries DOD and eclipse EOL during one completely operational day. Eclipse- thrusting is represented by the largest DOD decrease. 206
Figure 9.30: Isometric external view of the deployed platform. 208
Figure 9.31: Isometric external view of the deployed platform. 209
Figure 9.32: Isometric view of the deployed platform with in evidence the available volume of the *payload vane* (in blue). 209
Figure 9.33: Isometric external view of the deployed platform, solar panels side. 210
Figure 9.34: External view of the deployed platform, front of the *payload vane*. 211
Figure 9.35: External view of the deployed platform, in front of the *thrusting module*.....211
Figure 9.36: External view of the deployed platform, in front of the *thrusting module*.....212
Figure 9.37: External view of the deployed platform, from the top of the *payload vane*.....212
Figure 9.38: External view of the platform in the hypothetical launch configuration. 213
Figure 9.39: Isometric internal view of the platform.....214

Figure 9.40: Isometric internal view of the platform. 215
Figure 9.41: Internal view of the platform, front. 216
Figure 9.42: Internal view of the platform, back. 216
Figure 9.43: Internal view of the platform, top. 217
Figure 9.44: Internal view of the platform, in front of the *thrusting module*. 217
Figure 9.45: Interaction between the plume and the solar panel. 220
Figure 9.46: Platform external layout with only 3 deployable solar panels. 221
Figure 9.47: Batteries DOD BOL vs time. 222
Figure 9.48: Power generation BOL during one completely operational day. 223
Figure 9.49: Power Consumption BOL during one completely operational day. 223
Figure 9.50: Batteries Available Energy BOL during one completely operational day. 224
Figure 9.51: Batteries DOD and eclipse BOL during one completely operational day. Eclipse- thrusting is represented by the largest DOD decrease. 224
Figure 9.52: Batteries DOD BOL vs time. 225
Figure 9.53: Power generation EOL during one completely operational day. 226
Figure 9.54: Power Consumption EOL during one completely operational day. 226
Figure 9.55: Batteries Available Energy BOL during one completely operational day. 227
Figure 9.56: Batteries DOD and eclipse BOL during one completely operational day. Eclipse- thrusting is represented by the largest DOD decrease. 227

LIST OF TABLES

Table 2.1: Chapter 2 Summary. 22
Table 3.1: Chapter 3 Summary 1. 42
Table 3.2: Chapter 3 Summary 2. 67
Table 3.3: Chapter 3 Summary 3. 70

Table 4.1: Most representative large satellite multispectral missions principal characteristics. 78
Table 4.2: Most representative small satellite multispectral missions principal characteristics. 84
Table 4.3: Most representative large satellite hyperspectral missions principal characteristics. 86
Table 4.4: Chapter 4 Summary. 92
Table 5.1: Chapter 5 Summary 1. 104
Table 5.2: Chapter 5 Summary 2. 104
Table 6.1: Chapter 6 Summary 1. 117
Table 6.2: Values of altitude to achieve a nominal (RC) from 1 to 5 days. 120
Table 6.3: Chapter 6 Summary 2. 131
Table 6.4: Multispectral analyzed instruments and their satellite, altitude and mass. 134
Table 6.5: Multispectral analyzed instruments and their spatial and spectral performance. 135
Table 6.6: Hyperspectral analyzed instruments and their satellite, altitude and mass. 137
Table 6.7: Hyperspectral analyzed instruments and their spatial and spectral performance. 138
Table 6.8: TIR analyzed instruments and their satellite, altitude and mass. 138
Table 6.9: TIR analyzed instruments and their spatial and spectral performance. 139
Table 6.10: Architecture example n°1. 142
Table 6.11: Architecture example n°2. 142
Table 6.12: Architecture example n°3. 142
Table 6.13: Architecture example n°4. 142
Table 6.14: Architecture example n°5. 143
Table 6.15: Architecture example n°6. 143
Table 6.16: Architecture example n°7, relaxed temporal performance coming from the combination of previous examples and using a further lower altitude. 143
Table 6.17: Architecture example n°8. 143
Table 6.18: Architecture example n°9. 144

Table 6.19: Architecture example n°10. 144
Table 6.20: Proposed mission architecture I. 145
Table 6.21: Proposed mission architecture II. 146
Table 6.22: Proposed mission architecture III. 146
Table 6.23: Chapter 6 Summary 3. 149
Table 7.1: HT100D performance range. 153
Table 7.2: Electric Propulsion subsystem components mass. 154
Table 7.3: Thrust levels adopted to describe the HT100D operation with a nominal Total Specific Impulse of about 1200 s. 155
Table 7.4: TT&C subsystem mass for different cases. 155
Table 7.5: Primary structure percentage mass of satellite total mass for different cases (data derived by [3] are referred to the satellite dry mass). 155
Table 7.6: TC subsystem percentage mass of satellite total mass for different cases (data derived by [3] are referred to the satellite dry mass). 156
Table 7.7: OBC subsystem percentage mass of satellite total mass for different cases (data derived by [3] are referred to the satellite dry mass). 157
Table 7.8: ADC subsystem percentage mass of satellite total mass for different cases (data derived by [3] are referred to the satellite dry mass). 157
Table 7.9: Percentage mass of the satellite total mass assigned to TC, OBC and ADC subsystems. 157
Table 7.10: Triple junction GaInP/GaAs/Ge 3G30C Azur Space Cells characteristics. 158
Table 7.11: ABSL 18650 HC Li-Ion cell characteristics. 159
Table 7.12: Chapter 7 Summary. 164
Table 8.1: Mass of propellant needed to maintain 5 years a 50-kg microsatellite at three different altitudes. 170
Table 8.2: Transfers between Sun-synchronus orbits (with SMA increase) propellant mass expense results. 174
Table 8.3: Transfers between Sun-synchronus orbits (with SMA decrease) propellant mass expense results. 174
Table 8.4: Chapter 8 Summary 1. 176
Table 8.5: Chapter 8 Summary 2. 176
Table 8.6: Chapter 8 Summary 3. 176
Table 8.7: Chapter 8 Summary 4. 176
Table 9.1: Principal characteristics of proposed materials. 179
Table 9.2: VEGA and DNEPR frequency requirements. 179

Table 9.3: Simulations input parameters. 180
Table 9.4: Minimum tank capability computation. 180
Table 9.5: Physical properties of xenon. 181
Table 9.6: ATK spherical titanium pressurant tank specifications. 181
Table 9.7: Summary of Thrusting Module elements characteristics. 181
Table 9.8: Simulations input parameters. 183
Table 9.9: Simulations results.....183
Table 9.10: Characteristics of TT&C subsystem components. 186
Table 9.11: External torque acting on the satellite in the expected altitude range. 187
Table 9.12: Momentum storage required to RWs in the expected altitude range. 188
Table 9.13: characteristics of ADC actuators components. 191
Table 9.14: Characteristics of the ADC subsystem sensors. 191
Table 9.15: General mission scenario after the launch. 193
Table 9.16: Principal functions of nominal operational orbit sub-phases. 193
Table 9.17: BOL platform Power Budget for each mission nominal phase. 197
Table 9.18: EOL platform Power Budget for each mission nominal phase. 200
Table 9.19: Platform mass budget. 219
Table 9.20: BOL platform Power Budget for each mission nominal phase. 222
Table 9.21: EOL platform Power Budget for each mission nominal phase in the alternative configuration. 225
Table 9.22: Platform mass budget. 228
Table 9.23: Chapter 9 Summary. 230

1 INTRODUCTION

Small satellites with mass lower than 500 kg are becoming an attractive solution to perform very capable space missions. This is due especially to recent technological improvements, in particular from the point of view of electronic components miniaturization or high efficiency solar cells development. Interest in the small satellites sector arises from the warranty in terms of low-cost development, production and launch, this last ensured by the possibilities to define very convenient secondary-payload launch strategies [1]. Thanks to the limited costs promised, small satellites represent an unique opportunity to enter in the space business also for under development or even small countries, like South Africa or Nigeria, as testified by the NigeriaSat-2, shown in Figure 1.1 [2].

Figure 1.1 The NigeriSat-2 fully assembled flight model.

Small satellites use to operate at altitudes comprised between 600 km and 2000 km and could perform a large number of different scientific, remote sensing, specialized communications and technological demonstration space missions [3]. This results in the wide variety of worldwide government, commercial, industrial, civilian, military, and educational communities which are paying attention on this category [4].

Improvements in optical sensors design, data transmission and attitude determination and control devices technologies make nowadays small

satellites able to outclass larger spacecraft performance for example as a systematic, repetitive and continuous source of data in the frame of remote sensing Earth Observation [5]. Human activities related to natural resources management, like agriculture or disasters monitoring, offer an increasingly wide field of applications where small satellites observations could provide an unique and reliable support. Respect to larger satellites, constellations of many small satellites offer an irreplaceable solution to the need of very frequently observing specific problematic zones or monitoring dynamic processes [3].

The category of microsatellites, with mass comprised between 10 and 100 kg [1], appeared the most suitable to design an Earth Observation constellation, in relation to the mass of remote sensing instruments available on the market and to the on-board power generation levels achievable with state-of-art technologies. A standard and recurring platform bus aimed to accommodate different types of instruments in a certain range of mass and power, could result in a total freedom to create reliable, versatile and ad-hoc constellation missions with minimum efforts and expense. An example of actually in operation remote sensing instruments is provided by the SLIM-6-22, carried on-board by satellites of the Disaster Monitoring Constellation, and shown in Figure 1.2 [2].

Figure 1.2: The DMC SLIM-6-22 12 kg instrument.

The opportunity of equipping constellation microsatellites with an electric propulsion device like the Alta SpA low power Hall thruster named HT100 (shown in Figure 1.3) promises the possibility to create something of very innovative in terms of flexibility and performance. The use of electric propulsion is aimed to maintain the orbit at altitudes down to 300 km, and therefore to further increase observation performance of remote sensing instruments [6].

Figure 1.3: The Alta SpA HT100D.

1.1 Thesis objectives and development of the work

This thesis is aimed to define a versatile constellation of microsatellites with electric propulsion for Earth Observation and to design a simple and standard platform able to host a wide range of remote sensing instruments.

The objective is to develop a complete and manageable product aimed to respond to many different users involved in Earth Observation.

This product would be the result of a study about Earth Observation constellations completed by the design of a platform able to perform many different Earth Observation space missions while maintaining very limited costs and high performance. The mission analysis is also aimed at the identification of constellation architectures based on a number of satellites

small enough to be eventually launched by a single launch-vehicle. In parallel, the platform design is also aimed to demonstrate the possibility to conveniently carry on-board an electric propulsion device specifically designed for low power applications, like the Alta SpA HT100. The use of electric thrusters is finalized to the achievement (by means of orbital transfers) and maintenance of altitudes lower respect to those actually exploited by other satellites based on classical chemical propulsion systems [2], to improve spatial resolution performance.

The work is articulated into three steps:

- the first one, from Chapter 2 to 5, aimed to study the world of space Earth Observation, past, actual and planned programs, users requirements and purposes, technology limitations and perspectives. A significant attention is paid to land and vegetation observation, and in particular agricultural monitoring and management practices are set as reference application.
- The second one, from Chapter 6 to 8, aimed to define and simulate a wide range of suitable Earth Observation constellation scenarios, based on a low number of microsatellites with mass comprised between 40 and 80 kg and equipped with electric propulsion. The single observation of the Tuscany region is set as reference mission case. The Alta SpA SATSLab simulator is exploited to quantify the mass of propellant required to achieve and maintain altitudes identified during the constellation analysis.
- The last one, concentrated in Chapter 9, aimed to size and design a small standard satellite platform for Earth Observation, to simulate by means of Alta SpA SATSLab simulator the temporal behavior of platform power and energy sources (thruster ignitions, payload observation, data transmission, attitude determination and control) and to show overall platform performance.

2 REMOTE SENSING PRINCIPLES

This chapter introduces the remote sensing observation basic principles, basic mechanisms, fundamental components and characteristics, principal instruments and performance types that will be at the base of the successive discussion about the study and the design of a space mission devoted to support a system of remote sensing observation.

2.1 REMOTE SENSING OBSERVATION

2.1.1 Remote Sensing concept and fundamental characteristics

Remote sensing *is the science (and to some extent, art) of acquiring information about the Earth's surface without actually being in contact with it. This is done by sensing and recording reflected or emitted energy and processing, analyzing, and applying that information* [7].

Generally, this mechanism is based on the interaction between incident radiation and the objects that have to be acquired. This is the case for example of imaging systems, although remote sensing involves also the sensing of emitted energy and the use of non-imaging sensors.

The basic concept of remote sensing observation is illustrated in Figure 2.1:

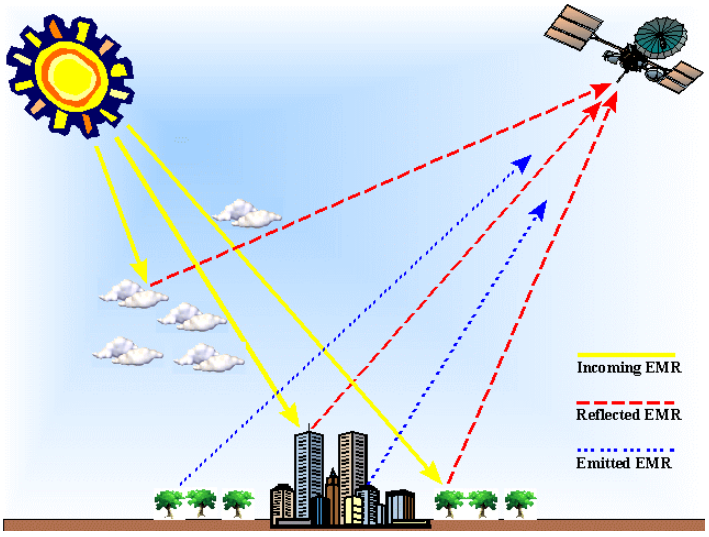

Figure 2.1: Basic concept of a remote sensing observation system.

In the frame of imaging systems, several factors have to be taken into account [7]:

- energy source or illumination.
- Radiation and the atmosphere.
- Interaction with the target.
- Recording of energy by the sensor.
- Data transmission, reception and processing.

- Images interpretation and analysis.
- Information application.

2.1.2 Energy source or illumination and the electromagnetic radiation

As previously listed, the first factor involved in the process of information acquisition by an imaging sensor is the presence of a source of energy that allows us to illuminate the target that we want to study (unless the sensed energy is emitted by the target). The energy produced by the source is available in the form of electromagnetic radiation.

Electromagnetic radiation *consists of an electrical field* $\vec{E}$ *which varies in magnitude in a direction perpendicular to the direction in which the radiation is traveling, and a magnetic field* $\vec{B}$ *oriented at right angles to the electrical field (Figure 2.2). Both these fields travel at the speed of light "c"* [7].

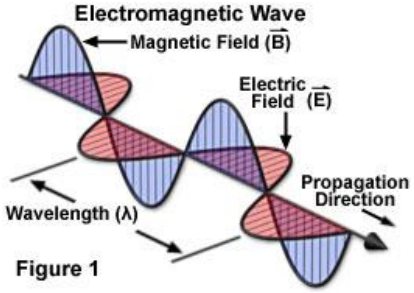

Figure 2.2: Schematic representation of an electromagnetic wave.

Hence, it is possible to describe all electromagnetic radiation thanks to the basics of the Wave Theory, which says that: *"[…]all electromagnetic radiation has fundamental properties and behaves in a predictable manner"* [7].

As shown by the Figure 2.2, there is another element that has to be considered when describing electromagnetic radiation: the wavelength λ. The wavelength is the distance between two successive peaks of the wave of the electromagnetic radiation; it is measured in units of length (from meters to nanometers) and is one of the two fundamental characteristics of electromagnetic radiation. The second fundamental characteristics is the electromagnetic radiation frequency ν, the number of cycles of a wave

passing a fixed point per unit of time. Frequency is typically measured in Hz. Electromagnetic radiation is completely described by these two quantities, which are linked by an inverse relation of proportionality. The relation between these two electromagnetic radiation characteristics is described by the equation [1.1]:

$$c = \lambda \nu \tag{1.1}$$

where $c \cong 3 \times 10^8\, m/s$.

Hence, the shorter the wavelength, the higher the frequency and *vice versa*. A description in terms of wavelength and of frequency of the electromagnetic radiation is a fundamental step to identify the suitable information to achievable from remote sensing data. The electromagnetic spectrum is typically subdivided in several different categories, characterized by different specific values of wavelength and frequency. This subdivision is of basic relevance when acquiring and interpreting remote sensing data [7].

2.1.3 The Electromagnetic Spectrum

The electromagnetic spectrum ranges from the shorter wavelengths (including gamma and x-rays) to the longer wavelengths (including microwaves and broadcast radio waves) [7]. There are several regions of the electromagnetic spectrum which are useful for remote sensing, as it is possible to see in Figure 2.3.

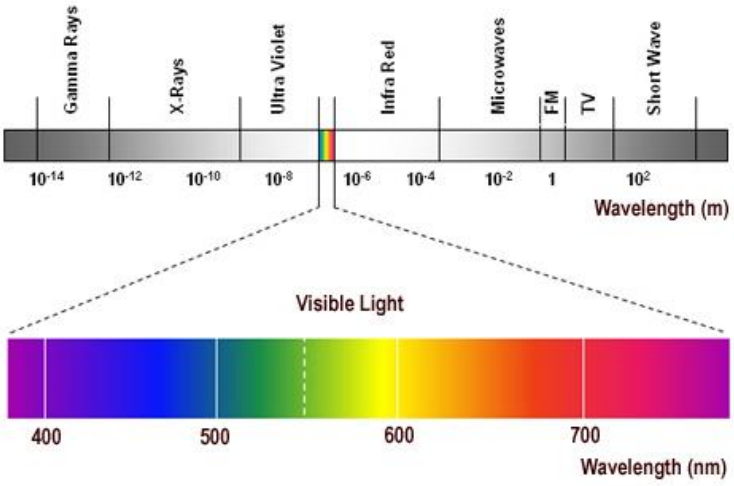

Figure 2.3: The Electromagnetic Spectrum

In the field of remote sensing, the ultraviolet (UV) region of the electromagnetic spectrum offers the shortest suitable wavelengths. This region is placed immediately beyond the visible (VIS) region, and for this reason is called ultraviolet. If illuminated by UV radiation, it is possible to appreciate the fluorescence or the visible light emission by some constituents of the surface of Earth, in particular minerals and rocks. [7] After the UV region, becomes the visible (VIS) one, which is the region of the spectrum that eyes can "*remotely*" detect. The VIS portion of electromagnetic spectrum goes from values of wavelength of about 400 nm (VIOLET channel) to values of about 700 nm (RED channel). This range of wavelengths is the unique region of the electromagnetic spectrum that we can associate with our concept of colors. As shown by the Figure 2.3, the VIS spectrum is divided in the following "channels" or "bands":

- **VIOLET** channel: from 400 nm to 446 nm.
- **BLUE** channel: from 446 to 500 nm.
- **GREEN** channel: from 500 nm to 578 nm.
- **YELLOW** channel: from 578 nm to 592 nm.
- **ORANGE** channel: from 592 nm to 620 nm.
- **RED** channel: from 620 nm to 700 nm. [7]

The following portion of interest of the electromagnetic spectrum is the so called Infrared (IR) region, which goes from values of wavelength of about 700 nm to 100 μm. Hence, it is more than one hundred times wider than the VIS region. The IR region could be further subdivided into two main categories, the reflected IR region and the emitted or more commonly thermal IR region. Thanks to its reflectance properties, it is possible to use the reflected IR region in the frame of remote sensing in a manner similar to the radiation in the visible region. Approximately, the reflected IR portion of the IR region of the electromagnetic spectrum goes from values of wavelength of about 700 nm to values of about 3.0 μm. Differently, the thermal IR region goes from values of about 3.0 μm to 100 μm. The behavior of the electromagnetic radiation in the thermal IR portion is different from the behavior of the visible and reflected IR electromagnetic radiation: in fact, this radiation is mainly composed by thermal energy in the form of heat emitted by the surface of the Earth. [7] Finally, the last region

which has more recently found application and interest in the frame of remote sensing is the region of the microwaves (MW), which goes from values of wavelength of about 1 mm to values of about 1 m. Differently from to the UV region of the electromagnetic spectrum, the MW region offers the longest wavelengths suitable for remote sensing purposes. This region shows a double behavior: the shortest wavelengths, from 1 mm, are characterized by properties similar to thermal IR wavelengths, while the longest are characterized by properties similar to those used for radio broadcasts [7].

2.1.4 Radiation and atmosphere

Before that electromagnetic radiation reaches the Earth's surface it has to travel through the thickness of the Earth's atmosphere. Particles and gases in the atmosphere can affect the incoming light and radiation. These effects are caused by the mechanisms of absorption and scattering.

Absorption *is a relevant phenomenon which takes place during the interaction between the travelling electromagnetic radiation and the interposed atmosphere. It results in the absorption from molecules present in the atmosphere of the energy at various different wavelengths. Ozone, carbon dioxide, and water vapor are the three main atmospheric constituents which are responsible of the absorption of the travelling electromagnetic radiation* [7].

Differently from absorption, the ***scattering*** *phenomenon consists in the redirection of the electromagnetic radiation from its original path caused by its interaction with particles or large gas molecules present in the atmosphere. The relevance of the scattering phenomenon is influenced by several factors like for example: the wavelength of the radiation, the abundance of particles or gases, and the distance the radiation travels through the atmosphere. There are three different types of relevant scattering mechanisms: the Rayleigh scattering, the Mie scattering and the nonselective scattering* [7].

2.1.5 Atmospheric windows

Electromagnetic radiation absorption from atmospheric constituents occurs in very specific portions of the electromagnetic spectrum; so, avoiding these specific portions allows to identify the regions of the electromagnetic spectrum that are really suitable for remote sensing observations [8].

Atmospheric windows *are those regions of the electromagnetic spectrum that are not strongly limited by atmospheric absorption and thanks to this results very useful for remote sensing purposes* [7].

To identify the wavelength regions that could be profitably used for remote sensing observations, it is necessary to compare the characteristics of the two most common energy source, the Sun and the Earth, with the atmospheric windows that are available [7], [8].

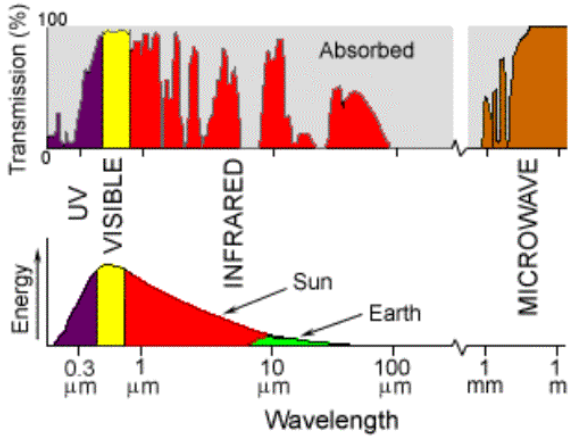

Figure 2.4: Atmospheric Windows and Sun-Earth characteristics.

As it is possible to appreciate from the Figure 2.4, in the VIS region of the electromagnetic spectrum is placed not only an atmospheric window, but also a peak of the energy irradiated by the Sun [7], [8]. Contemporarily, it is possible to register that heat energy emitted by the Earth corresponds to a window around 10 µm in the thermal IR region of the electromagnetic spectrum and that the large window at wavelengths longer than 1 mm corresponds to the MW regions [7], [8].

2.1.6 Interaction with the target

Passed the atmosphere, the electromagnetic radiation reaches the surface of the Earth and finally interact with the objects of interest. The interaction can be described by three different mechanisms: absorption, transmission and reflection. Once reached the surface, the total incident energy interacts with the target in one or more of these mechanisms. The mechanism of interaction adopted is influenced by electromagnetic radiation wavelength and by the properties (mainly material type and conditions) of the observed object [7].

Absorption *occurs when radiation (energy) is absorbed into the target while* ***transmission*** *occurs when radiation passes through a target.* ***Reflection*** *occurs when radiation "bounces" off the target and is redirected* [7].

Figure 2.5: Radiation absorption, reflection and transmission.

The three different interaction mechanisms are shown in the Figure 2.5. For remote sensing observations purposes, the most interesting interaction mechanism is that related to radiation reflected by targets. There exist two types of completely different reflection mechanisms: the specular reflection (in the case of smooth surfaces, almost all reflected energy is directed away in a single direction) and the diffuse reflection (in the case of rough surfaces, all reflected energy is almost uniformly directed in every directions). The predominance of one of reflection mechanisms depends on the wavelength of the incident electromagnetic radiation and on the surface roughness of the target [7].

2.1.7 Target spectral response

Hence, depending on the complex nature of the target of interest and on the wavelength of the incident electromagnetic radiation, it is possible to

appreciate deeply different responses to the mechanisms of absorption, transmission and reflection. Measuring the portion of the energy that is reflected, or emitted, by observed objects placed on the surface of the Earth over a wide variety of different specific wavelengths, it is possible to study the spectral response of the target and to build the so called "Reflectance Curves". Hence, comparing different response patterns of different scene characteristics, it becomes possible to distinguish between these characteristics. Differently, the distinction wouldn't be possible if the comparison would be performed only at a single wavelength. This is the case for example of water and vegetation spectral responses: in fact, they show significant differences in the IR region which allow to distinguish between them. These differences are highlighted by the Figure 2.6 [7].

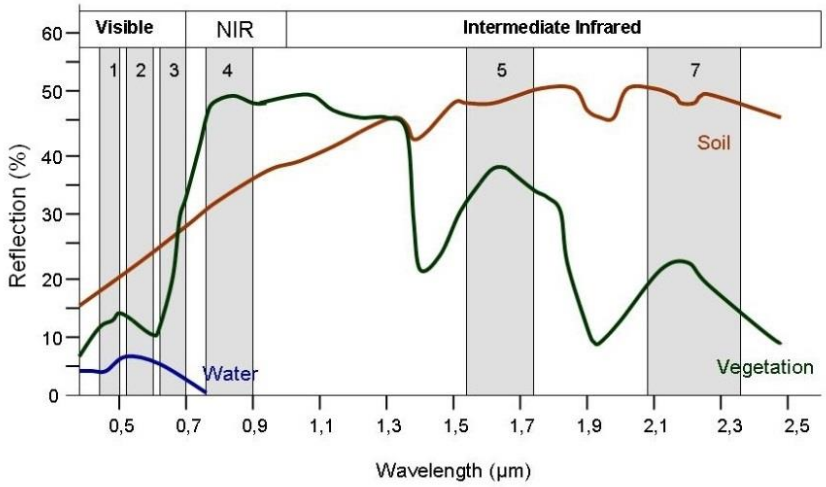

Figure 2.6: Water, soil and vegetation Reflectance Curves in the VIS and IR regions.

Finally, it is important to note that spectral responses could be slightly variable even for the same type of object observed and above all, and it is very important in the frame of vegetation study, they could vary with time.

So, knowing where to "look" spectrally and understanding the factors which influence the spectral response of the features of interest are critical to correctly interpreting the interaction of electromagnetic radiation with the surface [7].

2.1.8 Passive and active concepts of remote sensing observation

Remote sensors need a source of energy to illuminate targets of interest and to collect the energy that is either reflected (VIS and IR wavelengths) or absorbed and the re-emitted (thermal IR wavelengths). For example, the Sun is a natural available source of energy that is exploited by the so called passive sensors (Figure 2.7).

Passive sensors *are systems which measure energy that is naturally made available for example from the Sun, a natural source of energy* [7], [8].

Obviously, passive sensors can image targets only when the natural source of energy is available. For all reflected energy, like in the case of Sun energy, this can happens only during the time when the Sun is illuminating the Earth. So, at night, it is impossible to have available reflected energy from the Sun. They are clearly also limited by weather conditions. Differently, energy that is naturally emitted by surfaces, like in the case of thermal IR wavelengths, can be exploited during day and night, but it depends on the amount of energy emitted, and in particular if it sufficient to be recorded [7], [8]. Together with passive sensors, there exist also the so called active sensors, which provide their own source of illumination (Figure 2.7).

Active sensors *are instruments that emit the radiation which is directed toward the objects of interest. Hence, they detect and measure the radiation which is reflected by the object* [7].

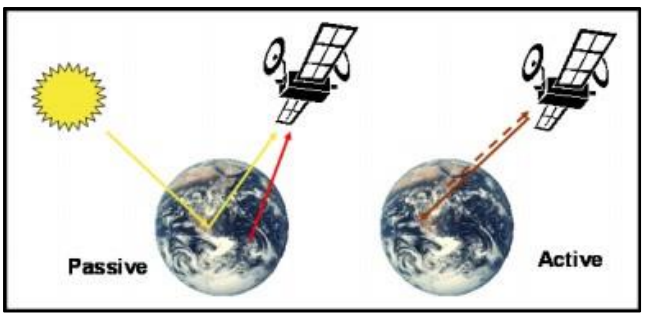

Figure 2.7: Passive and active observation concepts.

This specific characteristic of the concept of active observations allows active sensors to acquire images in every moment of the day and of the year, without limitations in terms of illumination and also of meteorological conditions. Hence, active sensors are particularly suitable to study those wavelengths that are not sufficiently ensured by the Sun, like the wavelengths of the MW region. However, in the frame of active sensors, it is necessary the generation of a significant amount of energy to profitably illuminate objects, and this could result hard to be obtained. Significant example of active sensors are the so called Synthetic Aperture Radar (SAR) [7], [8].

2.1.9 Remote sensing systems principal components

The radiation emitted, reflected, or scattered from an object propagates in the surrounding space bringing with it the information about the characteristics of the object. A set composed by a collector, followed by a detector, is used to capture the radiation and to measure the properties of the object [8]. The collector and the detector are the two main parts of a remote sensing instrument, and are those which initially work with the energy reflected or emitted by objects after the illumination provided by the source, natural or not.

*The **collector** is a collecting aperture that intercepts part of the radiated electromagnetic field. In the IR, visible, and UV regions, the collector is usually a lens or a reflecting surface that focuses the intercepted energy onto the detector. Differently, in the microwave region, an antenna is used to intercept the electromagnetic energy. Examples of antennas include dipoles, an array of dipoles, or dishes* [8].

The detection then occurs by transforming the electromagnetic energy into another form of energy such as heat or electric current [2].

2.1.10 Remote sensing systems accuracy, precision and resolution

In the frame of remote sensing instrument characteristics the most important are: the accuracy, the precision, the calibration and the resolution [8]. At this level of first analysis of remote sensing instrument, particular

attention will be given to different types of resolution: the temporal, the spatial and the spectral resolution.

Accuracy *is the capability of a measuring instrument to give results close to the true value of the measured quantity* [8].

Precision *is a gauge of how close the measured values are when multiple measurements are conducted. It is a measure of repeatability, i.e. the degree of agreement between individual measurements of a set of measurements, all of the same quantity. Therefore precision is a necessary, but not sufficient, condition for accuracy. It is affected by the measuring technique* [8].

In a general sense, the ***resolution*** *is the smallest increment of output that a measuring system can sense which is a characteristic of the measuring instrument* [8].

2.1.11 A fundamental distinction: images and photographs

Before describing the three different resolution types, it is very important to make a distinction between the concept of image and the concept of photograph.

An ***image*** *refers to any pictorial representation, regardless of what wavelengths or remote sensing device has been used to detect and record the electromagnetic energy* [7].

A ***photograph*** *refers specifically to images that have been detected as well as recorded on photographic film* [7].

Based on these definitions, we can say that all photographs are images, but not all images are photographs. Therefore, unless we are talking specifically about an image recorded photographically, the term image is used. A digital format could for example exploited to represent a photograph: the image is in fact subdivided into small area characterized by the identical shape and also area. These identical areas are called picture elements or pixels.

*In digital imaging, a **picture element or pixel** is the smallest controllable element of an image represented on a screen. Each pixel is a sample of an original image; more samples typically provide more accurate representations of the original. The intensity of each pixel is variable* [9].

Pixels represent the brightness of each area with a numeric value or digital number, as illustrated in Figure 2.8 [7].

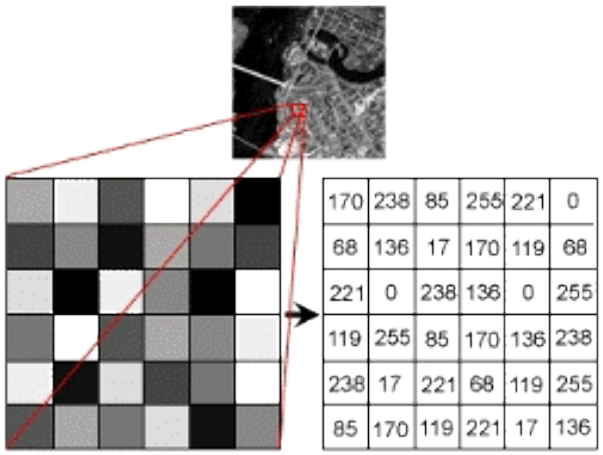

Figure 2.8: Digital Image of the original photograph.

2.1.12 Black & white images and color images

When an information is acquired over a certain range of wavelengths, more or less narrow, the information itself is stored in a channel, or in a band, which corresponds to the wavelength range. From a digital point of view, it is possible to combine and then display information within these channels exploiting the **BLUE**, the **GREEN** and the **RED** primary colors. Every channel contains a certain amount of information which are represented as one of the primary colors.

To form other colors, primary colors combine in a proportional measure which depends on the digital value shown by each pixels and hence on the relative brightness corresponding to these digital values.

If this process is used only to represent a single range of wavelengths, this range is effectively displayed exploiting contemporarily all three primary colors.

Considering that each pixels experience the same level of brightness level for each primary color, the result of the combination is an image

"black and white", characterized by different shades of gray, as depicted in Figure 2.9 [7].

Figure 2.9: Black & white image.

On the contrary, if more than one channel is represented as a different primary color, then the brightness levels differ from a different channel/primary color combination to another and the result of these combinations provides a color image. An comparison between a color image and a black and white image of the same scene is given by the Figure 2.10 [7].

Figure 2.10: A color image compared to a black & white image.

2.2 REMOTE SENSING SENSORS RESOLUTION TYPES

2.2.1 Temporal resolution

The concept of temporal resolution is very important in the frame of an Earth Observation remote sensing system and it is fundamental to define it.

*The **temporal resolution** refers to the interval of time needed to the instrument to image the same area at the same viewing angle* [7].

The real temporal resolution of a sensor is influenced by many factors, like the satellite orbital parameters, the instrument swath, the instrument pointing capabilities and finally also the latitude of the target of interest.

*As a satellite revolves around the Earth, the sensor "sees" a certain portion of the Earth's surface. The area imaged on the surface, is referred to as the **swath**. Imaging swaths for spacecraft sensors generally vary between tens and hundreds of km wide* [7].

2.2.2 Spatial resolution

For mostly of remote sensing instruments, the distance between the target of interest and the platform, so the satellite altitude, plays a fundament role in determining the detail of data acquired and the total area observed by the instrument. Sensors mounted on-board platforms which fly so much far away from the objects of interest, like spacecraft sensors, typically view wider areas, but cannot discern very fine details [8].

The detail discernible in an image is dependent on the spatial resolution of the sensor and refers to the size of the smallest possible feature that can be detected on -ground [7].

Spatial resolution of remote sensing instruments depend mostly on the so called instrument Instantaneous Field of View (IFOV).

*The **IFOV** is the angular cone of visibility of the sensor and determines the area on the Earth's surface which is "seen" from a given altitude at one particular moment in time* [7].

The extension of the area imaged by the sensor is determined by multiplying the IFOV by the distance from the instrument to the target of interest. This area on the ground is called the resolution cell and determines the sensor's maximum spatial resolution [7]. There exist a one-to-one correspondence of the ground-resolution element's size to the pixel size at the image plane [8]. Parallel to the concept of pixels and on-ground resolutions, has to be defined the On-ground Sample Distance (GSD):

In remote sensing, the ground sample distance (GSD) of the ground from air or space is the distance between pixel centers measured on the ground [10].

Instruments able to detect and image only extended characteristics of the scene are defined coarse or low resolution instruments. On the contrary, instruments able to detect and image very fine details, very small characteristics of the scene, are called high or very high resolution instruments. Three examples are given in Figure 2.11 to have a comparison.

Figure 2.11: The same scene acquired at three different spatial resolution levels.

For a satellite at an altitude h from the ground, the ground-resolution X' at nadir is expressed by equation (2.1):

$$X' = 2.44\, h\, \frac{\lambda}{D} \tag{2.1}$$

where:

- λ is the sensor wavelength.

- *D* is the collecting aperture. [7]

2.2.3 Spectral resolution

In sub-Paragraph 2.1.7, there are references related to target spectral response and reflectance curves. Target spectral response and targets reflectance curves are used to describe the reflectance and/or emittance behavior of an imaged scene over multiple wavelengths of study. Different and specific details present in a scene can be generally discriminated if their spectral responses are compared over different and specific wavelength ranges. To discriminate wide classes, like for example to discriminate water from vegetation, are typically sufficient broad wavelength ranges, such as the VIS and the IR channels. Differently, to discriminate similar and more fine differences in a scene, is generally required to compare spectral responses in spectral ranges much finer. Hence, to discriminate even more fine and small details, it is necessary an instrument characterized by an high spectral resolution.

*The **spectral resolution** describes the ability of a sensor to define fine wavelength intervals. The finer the spectral resolution, the narrower the wavelength range for a particular channel or band* [7].

Some remote sensing instruments record energy over several distinct wavelength ranges and at various spectral resolutions. These instruments are the so called multispectral instruments. There exist another class of spectrally-improved multispectral instruments, the so called hyperspectral instruments. Hyperspectral sensors record energy in hundreds up to thousands of very narrow spectral bands distributed in the visible, near and mid-infrared portions of the electromagnetic spectrum. This results in a very high spectral resolution which make possible to discriminate between different observed targets that have similar but not identical spectral responses in the narrow bands [10]. Multispectral and hyperspectral instruments specific characteristics, possibilities and potential applications will be described in greater details in the following chapters.

2.3 SUMMARY Chapter 2

Remote sensing observation concept and system main characteristics (Table 2.1).

OBSERVATION MECHANISM	
Main elements	• energy source or illumination. • Radiation and the atmosphere. • Interaction with the target. • Recording of energy by the sensor. • Transmission, reception and processing. • Interpretation and analysis. • Application.

Electromagnetic Spectrum regions studied by remote sensing systems	• UV.
	• VIS.
	• IR:
	  o reflected IR.
	  o Thermal IR.
	• MW.

System types	• Passive. • Active.
Resolution types	• Spatial. • Temporal. • Spectral.

Table 2.1: Chapter 2 Summary.

3 REMOTE SENSING DATA APPLICATION FOR AGRICULTURAL MONITORING AND MANAGEMENT

This chapter presents an overview of potential application of satellite remote sensing images in the frame of Earth Observation, with particular attention to land and vegetation. As reference case, remote sensing possible applications to agriculture and precision agriculture is described. Therefore, a brief description of biochemical and biophysical parameters usually measured in this frame is given. An accurate analysis about different users scientific requirements is performed to understand the main specifications required to the observation system.

3.1 USE OF OPTICAL SATELLITE REMOTE SENSING DATA

In the frame of land and vegetation observation and of the study of their processes, remote sensing images could play a very determinant and innovative role. In particular, the eventual application of remote sensing images to all practices involved in agriculture monitoring and management will be initially exploited as starting point to fully describe the world of Earth Observation.

From satellite remote sensing data is possible to obtain many spatial, spectral and temporal measurements: these measurements could be determinant to improve agricultural practices and so to enhance, at a first analysis, the production and to reduce costs and risks. Remote sensing images derived from spacecraft observations could provide a significant support for the decision making process which is at the base of every agricultural management activity. Remote sensing observations could find intense application, and they result useful both to observe large field areas at national level, to observe mid-sized crops at regional level and finally also to observe single small farms at local level. The result is a very interesting starting point for the creation of politics for a sustainable agricultural development [11].

Satellite remote sensing images offer a very wide source of reliable, non-destructive, systematic and repetitive sets of data which could cover some gaps in the knowledge of crops and land in general. From these data, it is possible to obtain indisputable information which could reveal some details that couldn't be highlight with other observation tools.

Starting from these information, farmers and other interested users could construct suitable spatial reference frames and temporal statistical models which can be used to plan targeted and timely appropriate agricultural interventions and the possibility to monitor the results of these interventions during the growing season.

Hence farmers are provided by the capability of correcting in almost real-time the treatments [12].

In conclusion, satellite remote sensing images offer a great possibility to improve the management of available resources, by both quantifying, qualifying and locating them very accurately. The result is a statistical inventory of data which is capable at any time to say "*what was grown and*

when" [11], and to predict with a certain level of confidence the results of adopted agricultural interventions.

As initial step of the analysis of potential applications of satellite remote sensing observations to the field of agriculture and managed agriculture, the attention will be principally paid on optical remote sensing systems. Data achievable from optical images ensure an higher level of confidence and a deeper historical heritage in this particular field respect for example to microwaves images.

Anyway, in Chapter 5, also non-optical observation systems will be analyzed as an alternative or complementary tool, in order to have a better understanding of their potential contribution and also a comparison [13].

The large amount of available information about optical remote sensing observations and their frequent application in the past as a support tool for agricultural monitoring and management practices, has allowed to perform a very deep analysis, which has been then completed and also qualified by the analysis of other candidate sources of information.

3.1.1 Relevant vegetation characteristics derivable from reflectance curves

Optical satellite remote sensing data are principally used to produce reflectance curves to describe the spectral response of a certain studied target over a certain number of wavelength ranges. Reflectance curves are influenced by target properties and this is particularly true for land and vegetation.

Reflectance curves could provide several information about land and vegetation, especially some biochemical and biophysical significant parameters and some soil characteristics [13], [14].

In the frame of vegetation observation, typical reflectance curves are able to give information related to:

- vegetation type.
- Vegetation density.
- Vegetation phenological state.
- Vegetation phytosanitary state.
- Moisture content.

The typical reflectance curves trends are regulated by many factors, like for example:

- plants water content.
- Structure of plants and leaves [14].

The structure of plants and leaves could be very accurately appreciated especially by analyzing the spectral bands in the near-infrared region, where it is possible to observe very high values of reflectance. Other relevant factors which influence vegetation reflectance curves are the content and the typology of foliar pigments. In particular, the reflected energy in the visible region is strictly related to the presence of three very important foliar pigments: the chlorophyll, the xanthophyll and the carotene. From the accurate analysis of these pigments is possible to derive many information related to vegetation and vegetation response to the environment [15]. Chlorophyll is the most determinant pigment in the vegetation behavior: there exist several interesting regions of the electromagnetic spectrum which could provide many very suitable information. As illustrated by Figure 3.1, these regions of study of the chlorophyll characteristics are placed between 540 nm (where generally it is possible to observe a minimum of chlorophyll absorption) and 680 nm (where, instead, it is possible to observe a maximum of chlorophyll absorption) [16].

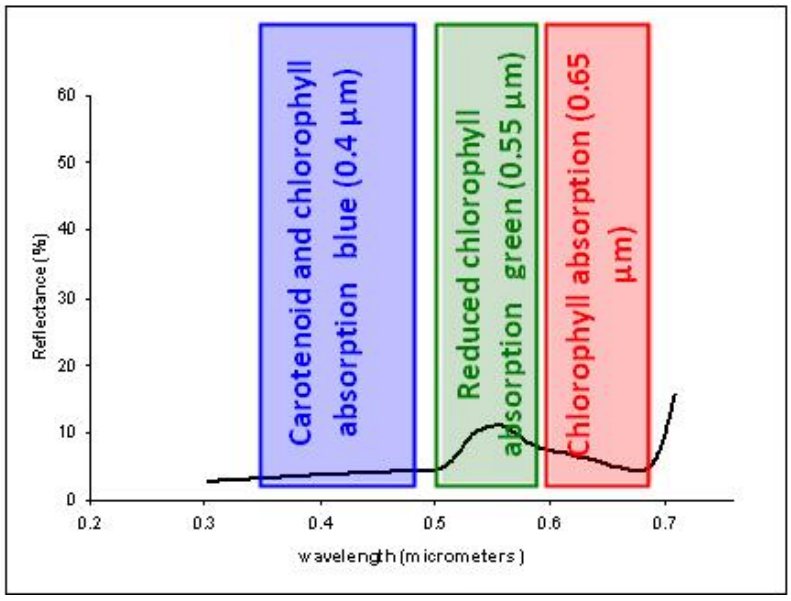

Figure 3.1: Typical chlorophyll reflectance curve.

This spectral range is placed in the visible region of the electromagnetic spectrum. In particular, the strong reflectance values in the GREEN channel, centered around the wavelength of 540 nm where it is possible to observe the minimum of chlorophyll absorption, are those that confer the typical green color in the visible band to leaves [16].

3.1.2 Vegetation biochemical and biophysical parameters measurable from reflectance curves

There exist many parameters which describe the chemistry and the physics of land, vegetation and cultivated areas in particular. Many of these parameters could be derived from the analysis of the reflectance curves produced using satellite remote sensing data. These parameters could be used as indicators for the definition of decision making processes, or as input data for the creation of crop dynamical models, to allow validation practices and to eliminate uncertainties during interventions [14].

The main biochemical and biophysical parameters which could be derived from remote sensing reflectance curves are:

- *Biochemical concentration* [17].
- *Wet and dry biomass and (wet and dry) green biomass*.
  The biomass is an important indicator which gives information about the condition of the crop and about its potential yield. It could be also used to achieve better performance in terms of vegetation classification. It assumes different specific values for different specific vegetation species. It is quantitatively derivable from the analysis of remote sensing data [17].
- *Leaf Area Index (LAI)*.
  LAI is a key descriptor of the vegetation canopy state. It is influenced by many factors, including nutrient imbalances, disease and soil conditions. LAI is largely used as main indicator of the heath state of crops and of the intensity of agricultural practices on environment (e.g. the amount of fertilizer applied). Its study and description could be easily performed exploiting information made available by satellite remote sensing images. Thematic maps devoted to describe its spatial distribution are usually created with a spatial resolution of about 10 m [18]. An heterogeneous distribution of LAI means that there are some difference in the health state of crop and

in crop vigor. This indicates that particular zones of the vegetation are more stressed respect to others. With LAI is generally possible to relate detected stresses to problems in the vegetation response to soil properties or to nutrients availability for given weather conditions [16], [17], [19]. It is also strictly linked to those organic processes which influence the crop growth. It is largely exploited as input data to derive crop growth models, to derive potential yield predictions suitable for the inception of any type of management practice. Generally, this indicator reaches its maximum value one or two months before the harvest time: thanks to this, LAI represents a reliable point of reference for crop yield predictions. By means of LAI, it is possible to predict for example some relevant factors like foliage cover, photosynthesis and evapo-transpiration (ETo) which are strictly linked to crop yielding. The ETo is particularly interesting: in fact, it is strictly related to the hydric content of plants and, if accurately estimated, this factor is very important for the definition of strategies of irrigation. It is also used to predict potential drought times. There are some spectral bands in which is possible to evaluate the LAI; mainly these bands are placed between 690 nm and 880 nm.

- *Green Fraction.*
  The Green Fraction is mainly relatable to: fAPAR (very important for crop yielding estimates); fCOVER (used to evaluate the production and the water content); photosynthesis; evapo-transpiration and phenology [17].
- *Leaf Cover (LC)* [17].
- *Leaf Water Content (LWC).*
  The Leaf Water Content is mainly related to optimization of irrigation practices. It is useful for example to detect plant pathologies, to quantify the amount of water required for irrigation or, like ETo, to predict drought seasons [17].
- *Leaf Chlorophyll Content (LCC).*
  The LCC gives an idea about the content of nitrogen of vegetation and about the amount of fertilizer assimilated by the plants. Hence it is strictly related to fertilization practices.

There are three bands in which is possible to study the LCC [16]:
  - 540 – 560 nm.
  - 662 – 682 nm.
  - 692 – 712 nm.
- *Nitrogen content* [11].
- *Mineral content* [11].
- *Vegetation height*.
  Vegetation height is a parameter of secondary importance, mostly related to particular types of non-optical remote sensing observations (SAR, for example).
  By means of the knowledge of the vegetation height, it is possible to obtain indirect information related to biomass and phenological state [17], [20].
- *Vegetation indices*, that are algebraic combinations of measurements of reflectance in two or more spectral channels, mainly in the RED channel and in the near-infrared channel. They are typically used to estimate LAI and other relevant biochemical and biophysical parameters [21].

3.1.3 Soil characteristics derivable from reflectance curves

Accurate analysis of soil is important to manage land and so it is fundamental for all human activities devoted to agriculture. Starting from reflectance curves, it is possible to derive the soil type (with a spatial resolution up to 100 m, [18]), the soil salinity and the soil moisture content, which is a key parameter for irrigation practices. Soil moisture content has to be measured on a quasi-daily base [11].

Satellite remote sensing images could finally play a relevant role in the measurement and description of the soil erosion and degradation mechanisms and their temporal development. The erosion of soil could be easily monitored by remote sensing satellite images thanks to appreciable differences in color, tone and structure of eroding soil layers respect to those non-eroding. Indeed, it is possible to create erosion temporal models, directly relatable to vegetation cover [11].

3.2 VEGETATION AND SOIL INDICES

Vegetation indices are "remotely sensed" algebraic combinations of measurements of reflectance in two or more spectral channels. The most used are the RED channel and the NIR channel.

These indices are based on the very different behavior exhibited by vegetation in these two bands: the RED one, characterized by a very strong absorption of the incident light, and the near-infrared one, characterized instead by a very strong reflection and transmission of the incident light. Moreover, stressed vegetation exhibits an higher reflectivity in the RED channel and a lower reflectivity in the near-infrared channel respect to healthy vegetation, as shown in Figure 3.2.

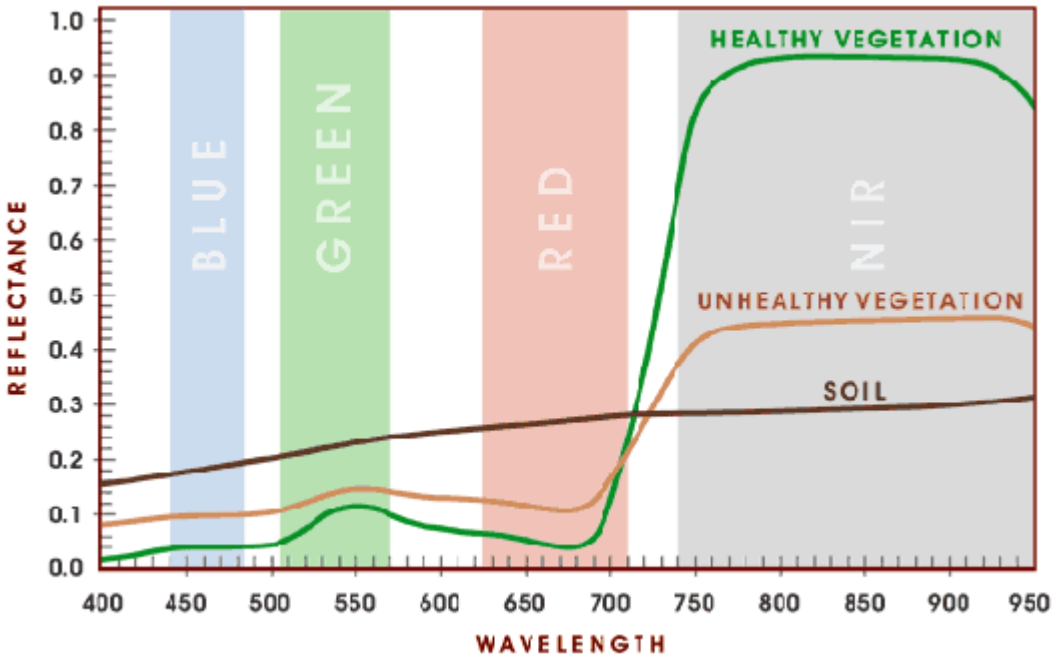

Figure 3.2: Healthy and unhealthy vegetation spectral behavior comparison.

Hence, vegetation indices are the classical way widely used to characterize the type, the amount and the conditions of vegetation and soil present within a scene in an accurate, quantitative and repetitive manner. They have provided many benefits in crop monitoring and management. Once computed, vegetation indices could be empirically associated to those parameters which describe the health state of vegetation, which model the

phenological development of crops and to some other parameters which are used to evaluate crop potential yield and production. Examples of these biochemical and biophysical parameters associable to vegetation indices computation are: LAI, Leaf Chlorophyll Content, vegetation density and canopy, biomass, soil use, Net Primary Production (NPP) and fAPAR (fraction of Absorbed Photosynthetically Active Radiation). Vegetation indices are determinant to estimate the plant nitrogen content by means of measurements of the chlorophyll content. Hence, they result in an optimum way to define strategies for a suitable application of the fertilizer. Vegetation indices are simple and rapid to be used and allow to eliminate some factors of disturbance, like for example particular effects related to soil, to topography and to viewing-angle. By the fact that vegetation indices are based on the combination of more than one spectral bands, they allow also to reduce the influence of the atmospheric conditions [19], [21].

3.2.1 Most important VIS-NIR Ratios-Vegetation Indices

SR: *Simple Ratio*

The vegetation index called Simple Ratio (SR) enables the discrimination between vegetated soil and non-vegetated soil. It also offers some general and marginal information about vegetation health. The SR could be for example calculated using NIR and RED reflectance values, as shown in equation 2.1:

$$SR = \frac{(NIR\ refl.)}{(RED\ refl.)} \tag{2.1}$$

The values of SR result higher than 1 in case of vegetated lands, and become higher and higher for more dense and more sane vegetated lands [22].

NDVI: *Normalized Difference Vegetation Index*

The Normalized Difference Vegetation Index is related to vegetation density, vegetation physiological state, biomass and potential yield. It allows to make temporal comparisons between different periods of the year.

The NDVI could be for example calculated using the NIR and RED reflectance values, according to equation 2.2:

$$NDVI = \frac{(NIR\ refl.) - (RED\ refl.)}{(NIR\ refl.) + (RED\ refl.)} = \frac{SR - 1}{SR + 1} \tag{2.2}$$

NDVI values goes from a lower limit of 0 to an upper limit of 1. Occasionally, NDVI could become negative due to several sensor characteristics or to units of input variables. Values of NDVI approaching 1 refer to more dense presence of vegetation and to a better health of the vegetation itself [22]. It is possible to create NDVI thematic maps which, at a good spatial resolution levels (about 30 m, [18]), enable users to identify some particular zones of the field where the vegetation is particularly stressed and not sufficiently vigorous. These information give the possibility to plan a preventive intervention in order to eliminate the eventuality of destructive pathologies. NDVI thematic maps contain information spatially distributed which enable the user to pay attention just on particular specific zones of the crop, and so to define very targeted treatments. An example is provided by Figure 3.3 (image produced thanks to Landsat Thematic Mapper), where high NDVI values represent healthy and vigorous vegetation while low NDVI values represent non-vegetated lands [23].

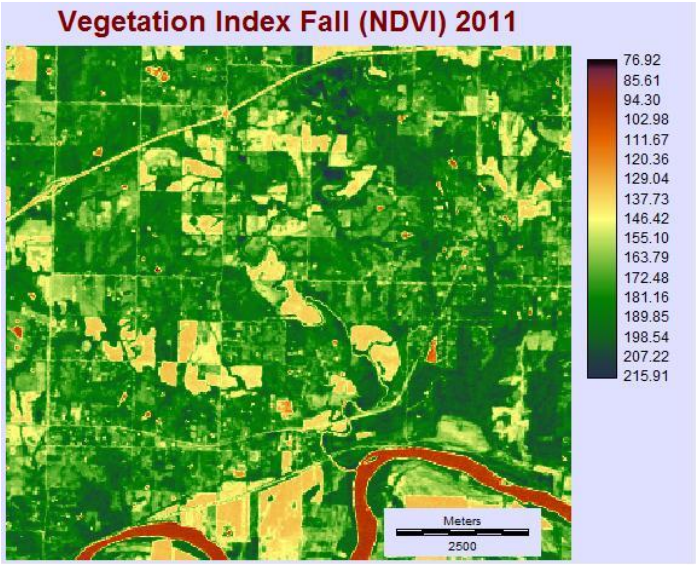

Figure 3.3: NDVI thematic map of northeastern Kansas, 2011.

It is very important to couple NDVI remote sensing data with archive data to identify variations in the general behavior respect to past trends of the specific crop.

NDVI-G: *Normalized Difference Vegetation Index – Green*

NDVI-G could be calculated according to equation 2.3:

$$NDVI - G = \frac{(NIR\ refl.) - (GREEN\ refl.)}{(NIR\ refl.) + (GREEN\ refl.)} \quad (2.3)$$

The Normalized Difference Vegetation Index – Green is a vegetation index developed for the remote estimation of chlorophyll content, especially in highest plant leaves. The NDVI-G allows to detect plants stresses which are strictly linked to variations in the content of foliar pigments, principally to the chlorophyll. This is possible thanks to the addiction of the GREEN channel [22].

SAVI: *Soil Adjusted Vegetation Index*

SAVI could be calculated according to equation 2.4:

$$SAVI = \frac{(1 + 0.5) \times (NIR\ refl. - RED\ refl.)}{(NIR\ refl. + RED\ refl. + 0.5)} \quad (2.4)$$

It is probably the most important vegetation index related to soil properties. It is used to minimize the effects of soil brightness in those vegetation indices which are based on the RED and NIR channels. It is derived from the definition of NDVI. In fact, a constant soil adjustment factor L is incorporated into the denominator of the NDVI equation. L varies according to the reflectance characteristics of the soil and is also influenced by the density of the vegetation cover analyzed [22].

3.3 CROP POTENTIAL DESCRIPTIONS FROM OPTICAL REMOTE SENSING DATA

From the combined analysis of biochemical and biophysical parameters, it is possible to create a background of information which is the starting point for the application of satellite remote sensing observations to agricultural monitoring and management practices. From the contemporary knowledge of these parameters and from the complementary support of vegetation indices, complete descriptions of large and small crops and reliable predictions of their temporal development trends are possible. This knowledge allows to plan appropriate, targeted and timely strategies of intervention and to control their real effects.

In conclusion, the precise and complete description of crops properties given by satellite remote sensing products provide many fundamental information. Satellite remote sensing images provide: precise location of crops and the discrimination of them from non-cultivated areas; precise measurements of crops actual dimensions (crop acreage); exhaustive and deep analysis of their actual conditions; finally, the creation of reliable temporal and spatial models which describe the future trends of crops.

3.3.1 Crop acreage

The crop acreage is a very important practice. It results to be the starting point for successive crop classifications and crop mappings. Satellite remote sensing images guarantees both to estimate the extension of very large crops and also to have an auxiliary tool for the estimation of small areas. This permits for example to discriminate adjoining crops managed by different farmers. Generally, first reliable estimates of crop acreage are performed by optical imagery at the end of April. From this moment, a projected statistical estimate of annual percentage variation of crop dimensions is derived and sent to devoted agencies every months until the end of October [24].

A precise crop acreage (and a precise projection of their growth trend with time) is finally also a very determinant tool to confirm farmers' declarations. The control of farmers' declarations is becoming a very actual feature, especially at regional and local level: adopting images produced by satellite remote sensing instruments would result in the creation of an undisputable and absolutely reliable tool, devoted to identify individual crop

classes relative to a specific farm on a field-by-field base, and so very useful to resolve administrative disputes [24].

3.3.2 Crop conditions

Remote sensing images allow to identify those zones within crops which are for example affected by conditions too dry or too wet, and consequently to define appropriate, timely and targeted irrigation strategies. Furthermore it is possible, if required, to identify crops affected by nitrogen deficit, by insects, weeds or fungal infestations or weather related damages [17]. By means of a preliminary identification of these dangerous factors, satellite remote sensing images offer the possibility to the farmer (at any field-scale) to intervene in the right place, in the right manner and in the right moment with preventive actions. The aid that satellite remote sensing observations could provide in the frame of prevention is very wide and it is probably the most determinant innovation introduced by these systems, together with the improvement in the field of control of the farmers' declarations [24].

3.3.3 Crop changes and transformation

Vegetation is characterized by a very dynamical behavior which is very hard to be appreciated. Consequently, it is important to monitor continuously vegetation transformations during the year and to create a very accurate analysis of these dynamical processes. A systematic and continuous description of crop transformations and transition periods is very useful both for food security, which is for example basic for emerging countries, and also for politics on sustainability. To study the dynamical vegetation behavior, it is necessary to directly make comparisons between spatial and spectral responses in different periods of time, and also for example compare the lasts data acquired with data collected by other systems (not necessarily satellite systems) in the past [17].

3.4 POTENTIAL CONTRIBUTIONS OF OPTICAL REMOTE SENSING DATA IN THE FRAME OF CROP MONITORING AND MANAGEMENT

3.4.1 Crop classification

The capability of identifying, discriminating and classifying crops, is one of the basic performance required to satellite remote sensing images. Crops classification is an information of primary importance both at national, regional and local level [17]. Is in the frame of crop classification capabilities that the actual community for the Earth Observation for agriculture is focusing its attention, in particular in understanding how to improve the actual abilities in the spectral analysis of vegetation behavior [11].

3.4.2 Crop monitoring

Crop monitoring by means of satellite remote sensing data could be performed over a very wide range of crop features and under many points of view. At a first analysis, satellite remote sensing images could monitor every most relevant crop and soil characteristic, and the systematic and repetitive nature of this kind of observations results in a very interesting and complete service.

The capability of monitoring croplands is mainly based on the possibility of describing in a continuous, systematic, reliable and undisputable manner those biochemical and biophysical parameters previously listed. Typical parameters such as vegetation density, vegetation type, vegetation phenology (in particular, the biomass and the green biomass content) and also the chlorophyll content, form a set of variables which give a very detailed and accurate description of the possible targets of interest, a very complete overview of their principal and most interesting conditions [17].

In particular, monitoring the phenological state is very important; a good knowledge of this phenomenon could result in reliable and accurate predictions about crop potential yield and also about possible interventions.

Phenology refers to the study of periodic plant and animal life cycle events and how these are influenced by seasonal and inter-annual variations in climate, as well as habitat factors.

Each plant species has a specific phenological state which influence its specific spectral response. For appropriate agricultural management practices is necessary that farmers and other commercial users interested know very accurately the specific phenological stage in every moment of the year and also the almost exact moment at which another certain phenological stage will be reached. The identification of the different phenological stages allow a better study of vegetation canopy and a good quantification of the biomass. From a general point of view, there exist three fundamental phenological stages, which goes from sowing to harvest: the vegetative stage, the stage of reproduction and the stage of maturation [25].

The phenology of a crop has to be described at least on a weekly base especially in the summer period, although phenology information are important at every moment of the year [25]. From this point of view, thanks to quantitative relations which could be systematically derived, satellite remote sensing data offer a great occasion to monitor and describe this phenomenon.

An accurate monitoring of the dynamics of phenological stages and the consequent prediction and identification of the successive phenological stages, is fundamental for the definition and for the planning of optimum strategies of fertilization and irrigation. Hence, a good control of phenology dynamics could result in appropriate optimization of available resources, a significant increase of production efficiency and consequently in very large savings of agriculture costs [25].

In agricultural practices monitoring, it is finally necessary to comprehend the control of crop rotation cycles, that is very useful for purposes of crop diversification and of crop intensification programs, and mostly in the so called practice of "crop residue covering". With crop residue we refer to those residual materials leaved on cultivated zones after sowing times. In fact, good management of those residual materials it's important to improve the soil quality [17].

3.4.3 Crop mapping

Satellite remote sensing data are at the base for the creation of many types of maps (like those of figures 2.3 and 2.4) which show lands, crops and all their fundamental characteristics: their extension, their geographical distribution, their placement and the specific cultivations within any crop.

Maps are also very useful to discriminate between vegetated and non-vegetated lands [17].

Information contained in satellite remote sensing derived maps could be added to traditional methods of census and ground surveying and so result in a significant increase of actual capabilities and amount of data thanks. Not only, maps obtained from remote sensing data could be very successfully used to identify and monitor also wastelands, which could be a characteristics for example very interesting for large emerging countries, such as India [26].

Within these categories of products are very important:

- true color maps.
- ground cover maps, which are color coded maps showing particularly the quantity of land covered by green leaf.

An example of true color map is given in Figure 3.4. The true color map reported is produced thanks to RapidEye constellation observation [27].

Figure 3.4: A true color map by RapidEye constellation.

A color coded ground cover map is given in Figure 3.5. The ground color map is produced thanks to RapidEye constellation observations over Wurzburg, Germany. A map of this type is used to classify lands: agriculture and forest lands are indicated by green, water by blue, urban lands by violet and bare soil by red.

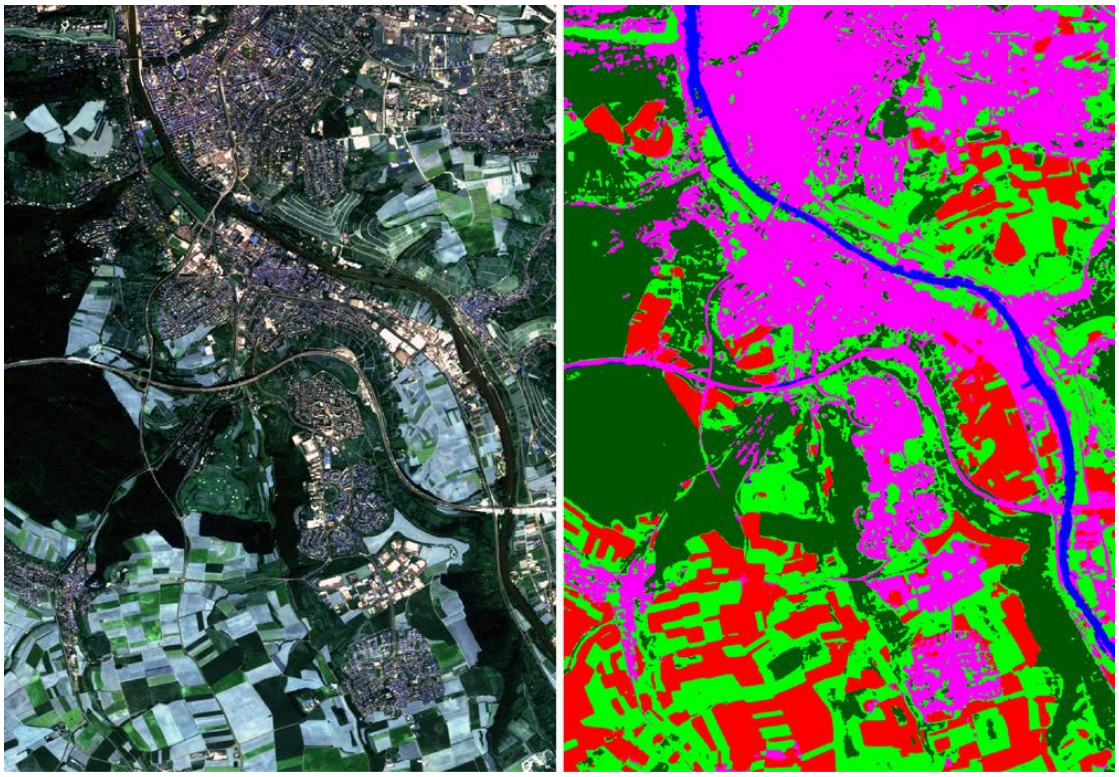

Figure 3.5: A ground cover map by RapidEye constellation over Wurzburg, Germany.

With satellite remote sensing spectral and spatial data is possible to create more accurate and specific maps, the so called "thematic maps". Thematic maps are used to give an idea of spatial distribution of the most important and significant biochemical and biophysical parameters (like LAI, chlorophyll content, or hydric resources distribution) or of some other indicators (like NDVI) which are empirically related with previous parameters [27].

Figure 3.6 shows a thematic map produced thanks to RapidEye observation and devoted to describe spatial distribution of chlorophyll content.

High content of chlorophyll in are indicated by green, while a poor chlorophyll content is highlighted by yellow and red.

Figure 3.6: A chlorophyll thematic map by RapidEye constellation.

Other useful thematic maps which could be obtained by satellite remote sensing data regard soils, like for example the "soil brightness" maps shown by Figure 3.7, again derived thanks to RapidEye observation.

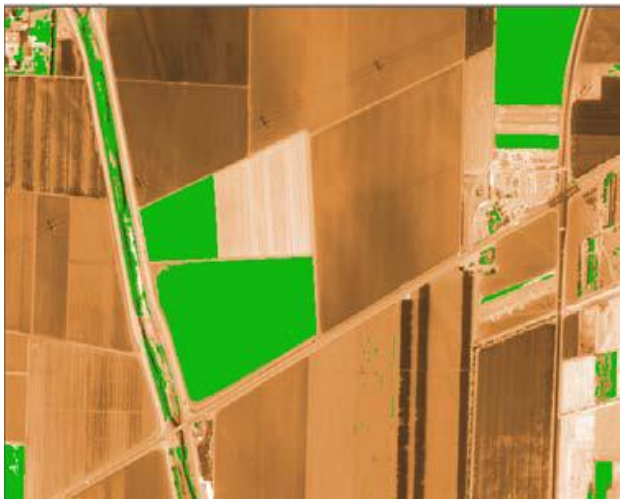

Figure 3.7: A soil brightness thematic map.

In particular, this type of map, show several characteristics related specifically to the soil, like its use, its color, its structure and about the organic matter which is present. A map of this type could be for example used like input for the creation of management zones [27].

3.4.4 Crop yielding

With remote sensing satellite is possible to make very accurate and reliable estimates of crop yielding, also valid for long periods of time, in order to estimate seasonal production. There exist many ways to estimate crop yielding from satellite remote sensing data. Of particular interest is the one based on statistical large-scale analysis. These statistical analysis are conducted on large areas and then are appropriately scaled to single small units; after this operation, scaled statistical analysis are also projected forward in time. Statistical analysis could be eventually coupled for example with weather forecasts, in order to have a very global idea of the situation. Typical time length of these yielding projections are of the order of 6 months [17]. To provide very reliable predictions on crop yield, satellite remote sensing images have to be characterized by a very high accuracy and precision. An high accuracy is very important for example in the practice of the identification of management zones [28].

Management zones *are sub-regions of a field that express a relatively homogeneous combination of yield-limiting factors and for which a single rate of a specific crop input is appropriate* [28].

This division of the crop in specific management zones that require a particular different set of treatments one from each other could result in an unique occasion to monitor particularly problematic areas and to incentive their production by planning a suitable cycle of timely and targeted interventions [28]. An example of management zones division based on NDVI measurements is provided by Figure 3.8, where non-productive zones are identified by the red and problematic zones by yellow.

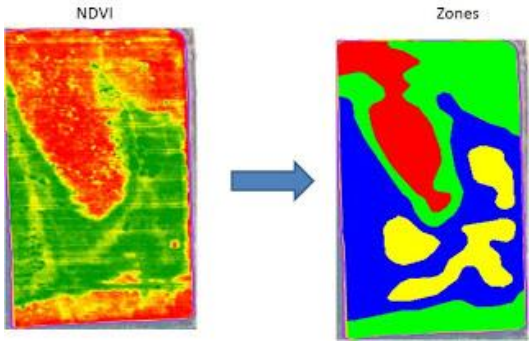

Figure 3.8: Division in management zones according to NDVI measurements.

3.5 SUMMARY 3.1

Potential services achievable with optical remote sensing observations in the frame of agricultural monitoring and management practices (Table 3.1).

POTENTIAL SERVICES	
From reflectance curves, identification of the most relevant vegetation features	• Vegetation type. • Vegetation density. • Vegetation phenological state. • Vegetation phytosanitary state. • Moisture content.
Vegetation biochemical and biophysical parameters	• LAI. • Biochemical concentration. • Biomass. • Leaf Chlorophyll Content. • Vegetation Indices.
Crop description	• Acreage. • Conditions. • Changes and transformation.
Crop monitoring and management	• Monitoring. • Classification. • Mapping. • Yielding.

Table 3.1: Chapter 3 Summary 1.

3.6 USERS' POINT OF VIEW AND REQUIREMENTS

3.6.1 Users' objectives

Users in many domains require information or information related services that are targeted, concise, reliable, low cost, timely, and which are provided in forms and formats specific to a user's own activities [29].

There are many general objectives which users' are interested to realize, and satellite remote sensing information represent a very attractive way. First of all, users want to increase the production efficiency, by means of more appropriate and timely interventions, by the reduction of wastes and by the ability to detect crop stress and anomalies with a certain advantage to properly plan these interventions. Hence, improve the prevention capabilities is an essential guideline to design a land and vegetation observation space system. Satellite remote sensing images offer the occasion to increase the potentialities of a single farmer interested in a single small unit and also of national agencies devoted to administrate larger fields: hence, remote sensing images could permit the reduction of costs of typical agricultural practices at different production levels and a general improvement in the management of available resources.

Important objectives which are at the base of the application of satellite remote sensing observations are the reduction of production risks and the reduction of potential environmental impact of agricultural practices; this last one is for example strictly related to the increase capability of an appropriate use of fertilizer or pesticide or fungicide [29], [30].

3.6.2 Priority information

Fundamental information which satellite remote sensing images have to provide are mainly related to crop identification and to the definition of reliable and statistical models describing their temporal development processes. Furthermore, especially in the case of single-farm units, becomes more and more attractive to achieve information suitable for external interventions of management planning. These external interventions (like fertilization or irrigation) allow farmers or general users of other domains to improve the conditions of cultivations, reducing for example crop stresses or maintaining a good level of health [30].

Hence, farmers and other involved users are particularly interested to obtain information suitable for the application of fertilizer, which is a large part of agriculture management costs and which could result dangerous for the environment if it is not appropriately used. With satellite remote sensing images is possible to assess the specific location where fertilizer has to be applied and also the exact amount of fertilizer required and the exact moment for the application. This allows the farmer to be ready to any eventualities and to intervene in the right manner every time, and this results fundamental in the purpose of prevention.

Clearly, farmers are also interested to obtain information suitable for appropriate applications of pesticides and herbicides, agents that are necessary to eliminate parasites and weeds. Like fertilization, a good management of these resources could result both in the reduction of costs and also in the reduction of environmental impact [30].

Furthermore, measurements related to the moisture content of the soil, to the water content of the plants and to the crop temperature are also very interesting. The availability of these measurements allow to define very accurate and appropriate strategies for irrigation practices management. The evaluation of crop hydric stress, which is possible to perform with satellite remote sensing images, permits farmers to have an adequate idea about the water required by soil and vegetation, about the exact location where water has to be applied and the appropriate moment for the application, like in the case of fertilizer [31].

Main vegetation characteristics, biochemical and biophysical parameters, or other vegetation indicators are used to understand the crop actual state in all its complexity; evaluating the state of the crop allows to identify crop deficiencies, crop deficiencies types and their relevance, and hence to plane adequate intervention to prevent losses at the harvest moment.

3.7 TEMPORAL REQUIREMENTS

3.7.1 Temporal resolution

Temporal resolution refers to the frequency that a satellite, or constellation of satellites, can collect imagery over a given area of interest [13]. Temporal requirements are the most important performance required to a satellite remote sensing system by farmers and general users in agricultural applications. They are obviously strictly related to the specific application of study, to the particular region of study, to the dimensions of the region of study and in this sense is possible to find a very wide range of possibilities [30]. Very good temporal resolution performance are the principal advantage in land and vegetation observation from spacecraft platforms respect for example to aerial observations.

The use of a satellite systems offer an unique occasion of repetitive coverage and systematic revisit of zones of interest. Thanks to it, becomes possible a continuous monitoring which is fundamental to build a very reliable modeling of dynamical vegetation processes and of vegetation continuous changes and transformations. The timeliness is fundamental in agricultural management, and this continuous capability of observation makes satellites' images very attractive for farmers and other users interested in agriculture [32]. Very good temporal requirements are for example fundamental for purposes of prevention by means of a potential service of "early warning".

This service provides the identification of problematic zones where a timely intervention is required, allowing to prevent complications and to safeguard crops. It is very important the timely identification of nitrogen deficit zones, of mineral deficit zones, hydric stress spots, potential diseases, presence of weeds and pests in order to plan appropriate and preventive interventions [30], [11].

3.7.2 Turn-around time

The most important temporal performance required by agricultural users is the so called turn-around time.

*The **turn-around time** is the time which elapses from the acquisition of a certain target to the delivery of the product* [30].

Typically, turn-around times required by farmers are of the order of 48-72 hours for most of the applications related to medium and large-scale agricultural practices. Turn-around time requirements could reach the value of about 24 hours in the case of more specific and stringent applications, like for example precision agriculture [30], [33].

3.7.3 Response time

Strictly related to turn-around time requirements, there is the response time capability of the satellite system. Typically, the satellite system should ensure the possibility of acquiring a certain demanded target within 24 hours from a specific unplanned request, for example if a preliminary general overview of the crop has been performed and a potential problem has been identified. A good combination of turn-around time and response time capabilities allow the system to guarantee the timely delivery of required images, making possible to prevent problems or complications with appropriate strategies [30].

3.7.4 Revisit time & Repeat Cycle

The achievement of turn-around time and response time requirements becomes possible if a very good and targeted satellite system "Repeat Cycle" and related "Revisit Time" frequency are ensured.

*The system **revisit time** is the time elapsed between observations of the same point on Earth by a satellite; it depends on the satellite's orbit, target location (target latitude), and on the swath of the sensor* [3].

*The **repeat cycle** is the interval of time which elapses before that the satellite repeats its ground track* [3].

A rapid revisit time frequency allows the system to repass on all targets of interest in a desired and designed range of days. Again, the possibility of a systematic and repetitive revisit of a certain target is an unique occasion offered by satellite observations and it is unreachable with aerial observations, which are limited by flight planes [32].

Generally, a frequent revisit time capability is necessary in agricultural practices because it is the only way to study very accurately and in a

continuous manner the dynamical processes related to vegetation variability, which is very difficult to be predicted [7]. Depending on the nature of the specific case of study, satellite revisit time capabilities could range from 1 year for land cover discrimination, to 2 months for a simple monitoring (especially if vegetation species within very large regions have to be identified), to 7-5 days to evaluate LAI and the soil moisture content, to 3 days to measure the land surface temperature, up to 1 day if for example to measure NDVI, to accurately monitor hydric stress or to control active fires [16], [18], [35].

Mostly, the revisit time has to allow the farmer to define a weekly planning strategy for agricultural activities. In this weekly planning farmers and other users interested in agriculture could require many different types of information [30].

Obviously, if the zone of interest has a reduced extension or if the satellite system has to be particularly concentrated on a specific region, like in the eventual case of Tuscany, it would be possible to specifically set the system to improve farmers planning capabilities, resulting in a very good support for management activities.

An important external factor affecting the system revisit time capability is the influence of cloud covering. The system should be able to acquire, and then release, the required information in the expected range of days even if the acquisition occasions are reduced by weather conditions. To guarantee this capability, in the case of an optical instrument which cannot acquire images through clouds, the satellite system has to be designed to ensure an appropriate revisit time performance [30]. Due to this fact, it appears very interesting to have revisit times as closest as possible to 1-3 days. If the system is able to acquire every target within the region of interest almost every day, then it could be exploited by many different users with different specific needs, and its services can be tailored to every desired situation [30].

Meteorological conditions are not a limiting factors for active instruments, such as imaging radar and in particular Synthetic Aperture Radar (SAR), described in Chapter 5 [34].

In conclusion, information produced by satellite remote sensing observations has to provide temporal descriptions of the development of the properties of monitored soils and crops. This temporal characterization is

intended to provide a planning capability such that the farmer could manage his cultivation during every week of the year, and, exceptionally, to intervene within a day. Moreover, thanks to the large amount of data produced by a satellite system, it is possible to build statistical temporal models exploitable by farmers to manage croplands not only on a short-term base, but also to forecast crop development during the whole year. Hence, a system of observation devoted to agricultural monitoring and management practices has to provide also the farmer with a service available on a yearly subscription basis. By combining weekly and eventually daily products and then projecting these data to have statistical predictions regarding seasonal changes during the year, the satellite system becomes a very complete source of information and results in something of irreplaceable [11].

3.8 SPATIAL REQUIREMENTS

Images obtained with very good spatial discrimination performance allow farmers and other users to monitor and manage the variability of crop conditions in very small agricultural sections, to discriminate fine details of the observed scene and to direct targeted and timely interventions in particular specific zones. The higher the spatial performance, the higher will be the homogeneity of crop and soil characteristics within the scene.

Many different levels of spatial discrimination performance could be suitable for several agricultural monitoring and management practices, and they clearly depend on the particular application of interest. In a general sense, spatial requirements depend mainly on the dimension of the unit to be managed and so on the areas that have to be monitored and managed.

Remote sensing images could be used to analyze large-scale factors, such as crop type or soil general characteristics, up to study the variability within a single small field, at the so called "farm level", where higher spatial resolution performance are needed.

Spatial requirements are strictly related to the specific type of cultivation, to the management objectives and to the equipment available for the farmer and so to the effective capabilities of intervention [30].

Finally, at a first analysis, there not exist very precise and fixed requirements on spatial resolution performance for the satellite system because there isn't a single or a standard type of user. Spatial resolution performance vary according to the specific target and to the specific application.

Becomes very important to make a preliminary discrimination between different eventual cases to obtain a more general overview of the situation. This overview will allow to understand in a deeper way what kind of spatial resolution performance a satellite system for Earth Observation particularly devoted to agricultural monitoring and management practice has to guarantee.

3.8.1 Spatial resolution

Theoretically, there aren't limits to spatial resolution in agricultural applications.

For example, one could imagine to reach very high spatial resolution levels and to study up to the plant level. A capability of this type is not

anyway really required when observing and monitoring crops. Generally, the most stringent spatial performance cover the range which goes from tens of meters (indicatively, from 10 to 30 m for agriculture monitoring, as measurement of LAI and NDVI, or to 50 - 100 m for land cover and vegetation species discrimination, crop classification and soil type identification) up to the order of 1 m for very precise agricultural applications (between 2 m and 5 m for example for precision agriculture practices) [18], [30], [36].

As shown by Figure 3.9for the USA, to obtain just a general overview of large-scale crops, for example for monitoring at the national level, are sufficient spatial resolution performance up to about hundreds of meters (realistically up to 500 – 1000 m), simply to obtain superficial information about crop type and their extension [17], [18].

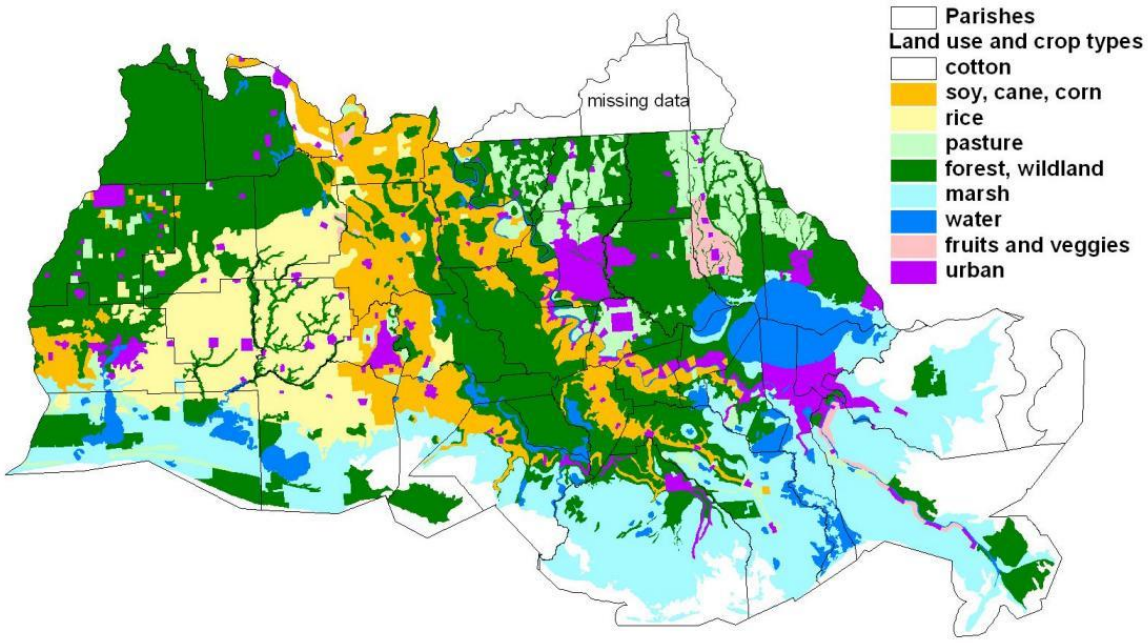

Figure 3.9: USA land cover and crop classification at national level.

Looking at some particular specific case, like for example identification of hydric stress of the crop, fundamental for strategies of irrigation, is generally sufficient a spatial resolution of about 20 m.

A further improved spatial resolution, comprised for example between 5 meters and 10 m, provides consistent savings in irrigation costs, allowing the farmer to focus interventions only in very specific zones of the crop [31].

Also to establish strategies of variable rate of application of fertilizer is required a spatial resolution comprised in a range which goes from 5 m to 10 m. Figure 3.10 shows the in-field variability of nitrogen content.

Dark regions need an higher rate of fertilizer application to increase production.

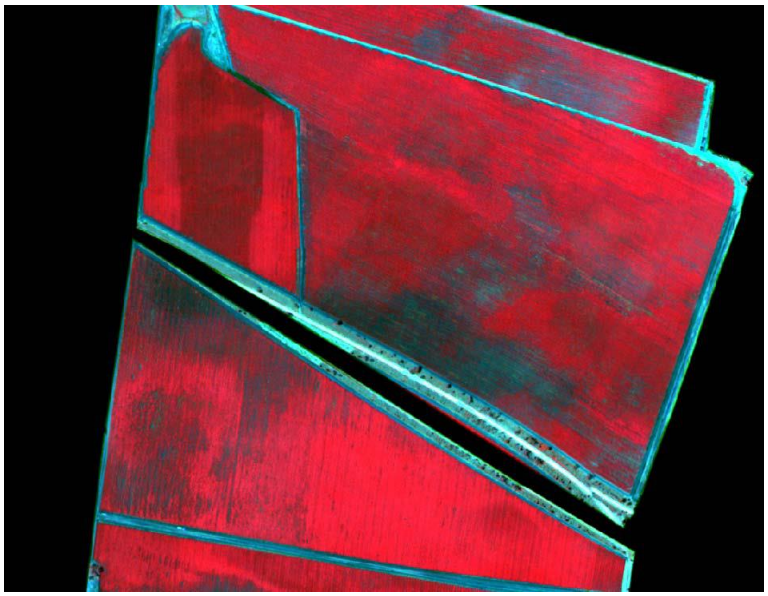

Figure 3.10: In-field nitrogen content variability.

Besides, a resolution level of this type could be useful also for simple monitoring at local level, for example at the single farm level, in the frame of precision agriculture [36].

Very important are also the study and the evaluation of spatial models in the biomass distribution and in the crop potential yield. These spatial models could then be used to create temporal models useful to make predictions on crop phenology dynamical cycle.

Precise study of biomass distribution and crop potential yield requires levels of spatial resolution around 3 m and represents a product of very high level in the frame of agriculture, a fundamental step to create a complete archive of information [17].

An example of an image at a spatial resolution lower than 5 m is provided by Ikonos observation and is illustrated in Figure 3.11:

Figure 3.11: Ikonos multispectral image at about 4 m of spatial resolution.

Looking at agricultural practices which require very high spatial resolution levels like those relative to herbicide application, which is a very delicate practice, and to precision viticulture practices. In these two applications could be necessary spatial resolution levels around 1 m [37], [38].

3.8.2 Location and measurement accuracy

Actually, due to the fact that location-based systems have become an integral part of life, high accuracy is an aspect needed to ensure that imagery and derived information can be used for actionable intelligence [29].

Referring to purposes of land and vegetation observation, in particular the location accuracy of the target in the scene is a determinant performance required to the remote sensing system.

Generally, both for simple agricultural monitoring and also for agricultural management practices are required a measurement accuracy of about 70-75% and a location accuracy within 1 pixel. Obviously, this is particularly true and hence required for application devoted to manage small units, for example of 10-20 m of size [30].

3.9 SPECTRAL REQUIREMENTS

*The **spectral resolution** is a measure of the capability of a spectrograph, or, more generally, of a frequency spectrum, to resolve details in the electromagnetic spectrum* [3].

The spectral resolution of an instrument could be described in terms of the division of the spectral space in: range of wavelengths, number of sampled wavelengths, contiguous nature of sampled wavelengths, spectral width of each wavelength sample. Large spectral resolution data imply both a large number of spectral bands both a contiguous cover of the spectrum [7].

The spectral resolution is becoming of primary importance in the remote sensing instruments performance in relation to agricultural monitoring and management practices and it is now probably one of the observation performance that we are mostly trying to improve [39].

The highest possible spectral resolution is researched to achieve the best capability of analyzing the smallest shades and differences in the reflectance curves of the vegetation. From the identification of these small shades and differences in spectral responses will be possible to achieve many and many interesting results, from a better capability of discrimination of the species, to a targeted capability of detecting specific agricultural problems and then of evaluating them. With an high spectral resolution is possible to discern and describe very well a certain target, like land and vegetation, and to acquire information that on the contrary would be lost with analysis at a worse spectral resolution [40]. A very high spectral resolution is fundamental to discriminate species that have similar spectral responses, and also to discriminate croplands from those residual materials remained after the sowing times. The capability of deeply analyze the spectral response of the vegetation or of the soil is very important to evaluate accurately some details in the stress state of the objectives (for example, nutrients or water stress), allowing preventive interventions which ensure the survival of the crop or the "reliability" of the soil for successive practices [17].

Like spatial resolution requirements, also spectral resolution requirements are strictly related to the purposes and to the extension of the

study, to management objectives, to the equipment available for the farmers (and so, to their possibilities of intervention) and to the size of the specific area of interest [30].

3.9.1 Suitable spectral domain

Visible (VIS) *(from 400 nm to 700 nm)*

The visible domain is of primary importance in the analysis of the spectral behavior of vegetation and soil and so it is at the base of the study of certain characteristics which allow an optimum application of remote sensing observations to agricultural activities.

Specifically to agricultural applications, the visible region of the electromagnetic spectrum is essential for the photointerpretation of crops' images by means of the produced maps, which are important for example to define test areas, and for the creation of vegetation indices like NDVI [17].

RED channel *(from 620 nm to 700 nm)*

The most important visible channel in the spectral analysis of land and vegetation characteristics is the RED channel. The RED channel is characterized by a strong absorption of the solar radiation (low reflectance level) by the vegetation. In the RED channel is placed a region of absorption of the chlorophyll and thanks to its analysis it is possible to discriminate between vegetated land and bare soil and also between different types of vegetation. At a first analysis, a RED channel is fundamental to provide vegetation indices, to measure LAI, and hence to describe the health state of the vegetation and crops and to monitor them during the seasons. In this band is registered a reduced atmospheric diffusion respect to the rest of the visible region, and thanks to this the RED channel is also used to perform geometrical controls also for images produced in the other bands [22].

GREEN channel *(from 500 nm to 578 nm)*

Another important channels is the GREEN channel, where the vegetation registers a very high absorption. The GREEN channel is suitable to study the chlorophyll, to measure the NDVI-G vegetation index and to produce true color maps. It is used to provide measurements of the Photochemical Reflectance Index [41].

BLUE channel *(from 446 nm to 500 nm)*

The third visible channel in order of importance is the BLUE channel, which covers the region of the electromagnetic spectrum from 446 nm to 500 nm. This channel is mostly used for dust corrections in the other bands. Generally, is added to RED and GREEN channel to permit the creations of true color maps [41].

XAN channel *(from 520 nm to 540 nm)*

An additional interesting channel could be the so called xanthophyll (XAN) channel, which is sensitive to another important foliar pigment of vegetation, the xanthophyll. This channel, which covers the region of the electromagnetic spectrum from 520 nm to 540 nm (so, is a very narrow band, placed between the BLUE and the GREEN channels) could be used to create with the GREEN channel an interesting vegetation index, the Photochemical Reflectance Index (PRI) [41].

Panchromatic (PAN) channel

The panchromatic acquisitions are very interesting in the frame of agricultural monitoring and management practices. It allows to reach higher resolution levels respect to the classical RGB channels. PAN information could be used to perform statistical analysis (especially at small-field level, very interesting for emerging nations) of crop and to produce pan-sharpened images [41].

Infrared (IR) *(from 760 nm to 1 mm)*

The Infrared portion of the electromagnetic spectrum is of primary importance together with the visible region. Infrared light is very sensitive to crop vigor as well as crop stress and damage. So, observations in this region of the electromagnetic spectrum allow a proper detection of the variations in the vigor of the vegetation, in the water content of plants, in the estimation of the amount of the biomass of the vegetation and many other features [17].

Near-Infrared (NIR) channel *(from 760 nm to 2500 nm)*

In particular it is very important the near-infrared channel. In this channel the reflectance curves show very strong reflectance values of the incident

light. Comparing the high reflectance values in the near-infrared channel together with the low reflectance values in the RED channel, it is possible to create many of the most important vegetation indices. Not only: the spectral behavior of the vegetation in this region of the electromagnetic spectrum is strictly related to soil structure and texture, to the foliar structure of plants, to their health state, to their specific nature and to their phenological state. Hence, this channel results to be a very powerful tool of survey for the discrimination between different species, for the analysis of the different crop stages of evolution and for the detection of eventual pathologies within an homogeneous vegetal community of cropland [17].

RED-EDGE band *(from to 690 nm to 730 nm)*

Between the RED channel and the NIR channel is placed the so called RED-EDGE band. This band is very useful to quantify the content of chlorophyll and to deeply analyze the foliar structure. It is useful to discriminate between different species of vegetation and also to monitor the vegetation canopy. It is primarily exploited to achieve an optimum analysis of the health and nutrition state of the vegetation. This band is strictly related to the nitrogen level. The nitrogen is at the base of many fertilizers (used, for example, with corn, wheat and rice) and the nitrogen amount could be quantified by measuring the content of its principal indicator, the chlorophyll. Looking at the Figure 3.12, it's possible to say that the chlorophyll concentration grows if the flex of the curve is very near to the NIR region of the electromagnetic spectrum.

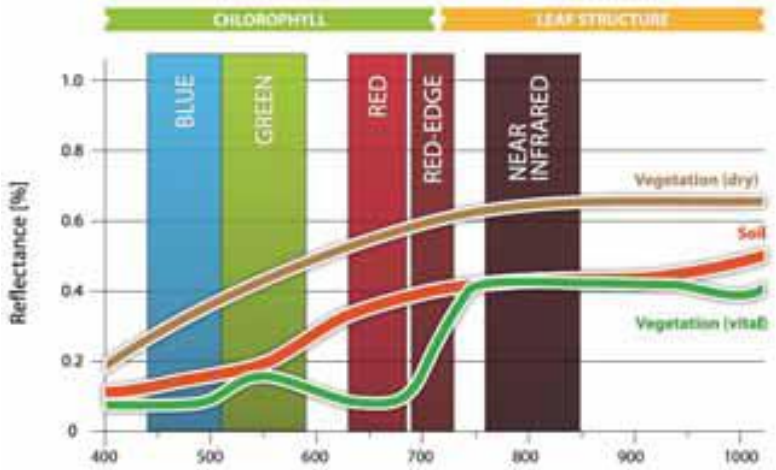

Figure 3.12: RapidEye Red Edge band.

To detect this flex are required very narrow spectral bands which could not be available in a simply multispectral analysis, where bands are too much large. With an hyperspectral analysis, where bands are much narrower, could be possible to detect precisely the flex. Once detected this flex, it's possible to combine the NDVI information with the Normalized Difference Red-Edge (NDRE) to obtain better LAI estimates. This allow to evaluate very well the chlorophyll concentration and the chlorophyll distribution by means of chlorophyll thematic maps and so the nitrogen content of plants. With a precise measurements of plants nitrogen content, is possible to establish a suitable application of fertilizer [42].

Short-Wave-Infrared (SWIR) channel *(from 1400 nm to 3000 nm)*

The Short-Wave-Infrared channel is very sensitive to moisture content of the soil, so it could be eventually exploited to measure and monitor this parameter as a complement to VIS and NIR observations [43].

Generally, observations in this portion of the electromagnetic spectrum requires low resolution levels (about 100 m) respect to those required in the other visible and infrared channels to provide the researched information [18], [30].

In last years the SWIR channel has assumed an higher degree of interest in relation to the possibility to perform a higher precision levels in the identification of vegetation type and so in the crop classification. It is mostly exploited by analysis which research optimum performance in terms of spectral resolution and which cover an extended portion of the electromagnetic spectrum respect to more common simply multispectral analysis, the hyperspectral analysis.

Finally, if coupled with NIR wavelengths, observations in the SWIR portion of the electromagnetic spectrum provide interesting benefits, including improved atmospheric transparency and materials identification. Materials like vegetation, are characterized by particular chemistries which cause specific reflectance and absorption features in the NIR and in the SWIR regions that allow their description from space [29].

Thermal-Infrared (TIR) channel *(from 3500 nm to 20 μm)*

This channel is mainly devoted to study the thermal state of land. Observations in this channel are essentially limited to produce

measurements of the temperature of the surfaces. Due to this, thermal IR observations find application mainly in the analysis of the heat stress of plants and into agricultural practices related to irrigation activities. Observations in this channel require a lower spatial resolution respect to other spectral domains; in particular, when looking for measures of the temperature of land, could be generally suitable also a coarse spatial resolution not better of about 100 - 500 m [31].

This channel could be also profitably exploited to detect wild fires, as in the case for example of the small instrument Compact InfraRed Camera (CIRC) mounted on the Advanced Land Observing Satellite-2 (Alos-2) and of the small instrument Hot Spot Recognition Sensor (HSRS) mounted on Bi-spectral InfraRed Detection (BIRD) [17], [18]. In the wild fire detection activity, parameters as fire fractional cover or fire temperature have to be measured with revisit time of at least 1 day [18].

3.9.2 Number of bands and bandwidth: multispectral and hyperspectral analysis

According to the required number of spectral bands, two types of spectral analysis have been considered appropriate for land and vegetation observation: the multispectral and the hyperspectral analysis.

Multispectral analysis is characterized by a reduced number of spectral bands, typically lower than 20. In a multispectral analysis the ratio between the value of the center wavelength of a selected band and the bandwidth of the band itself is of the order of 10. Hence, a multispectral analysis is performed by instruments that record electromagnetic reflected and/or emitted radiation over few broad bands. Multispectral observations are able to identify only the most important and evident land and vegetation spectral features, but are not able to deeply penetrate through the spectral response of studied targets. Hence, multispectral observations don't produce complete and very detailed reflectance curves of land and vegetation. Reflectance curves derived from multispectral instruments are obviously limited to a low number of discrete regions of the visible and infrared spectrum, so it is evident that this type of observations inevitably cause the loss of several information [3], [39].

Hyperspectral observations, differently, are characterized by an higher number of spectral bands and by the contiguous covering of the portions of interest of the electromagnetic spectrum, as shown by Figure 3.13:

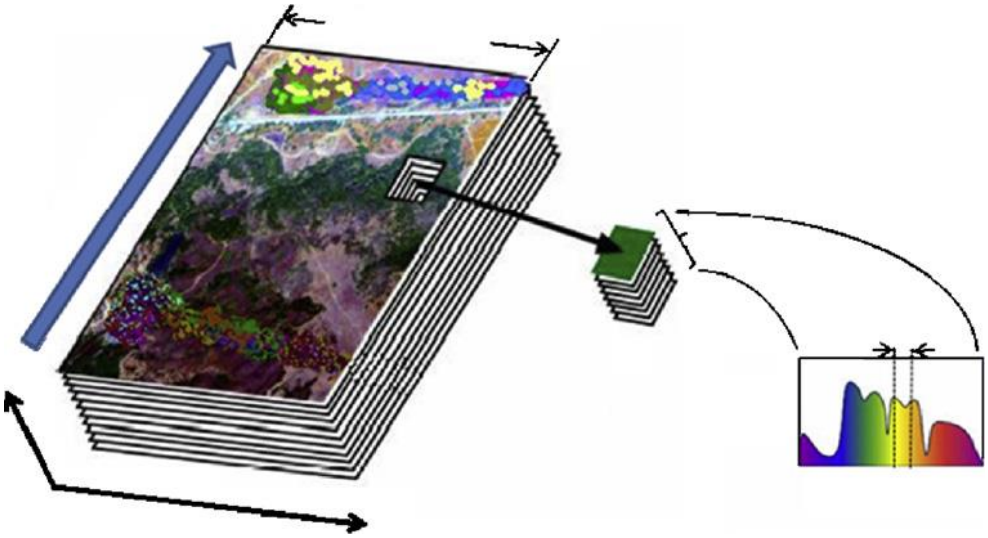

Figure 3.13: Hyperspectral imaging concept.

Typically, the bands present in hyperspectral observations go from several tens up to hundreds or even thousands very narrow bands. In an hyperspectral instrument the ratio between the value of the center wavelength of a certain band and the bandwidth of the band itself is of the order of 100. Hence, hyperspectral instruments bands are much narrower than in a multispectral analysis. The spectral bands division is represented in Figure 3.13 by the vertical dimension of the image reported.

Hyperspectral observations, especially in the last decade, cover also the SWIR wavelengths region [3], [39].

The selection of the number and of the type of desirable spectral bands is a determinant factor in the choice of the instrument and in the type of observations that the instrument will perform. Thanks to the capability of the sensor to discriminate and analyze the spectral response of a certain target, will be possible to obtain different types of products and to satisfy different requirements of farmers and all involved users [30].

For agricultural monitoring and management practices the minimum number of spectral bands generally required is 2, where the two essential channels to be recorded are the RED and the NIR channels, able to provide information about the NDVI [17].

These 2 channels could be integrated also by the GREEN and the BLUE channels, in order to offer the possibility to produce true color images. Anyway, they are of secondary importance in determining land and vegetation intrinsic properties respect to RED and near-infrared channels [17].

In conclusion, from a first analysis of typical requirements and of desired products, these 4 channels combined together allow a marginal capability of identification and discrimination of vegetation species and soil types, of description and quantification of the principal constituents of vegetation and of soil, a good monitoring of crops conditions, stress, pathologies and transformations. These abilities make the combined use of these four bands sufficient to guarantee the minimum spectral requirements for agricultural monitoring and management practices, from the crop acreage, to damage estimate, to verification of treatments success [17], [30].

Interesting information that could be profitably added to simple multispectral RGB and near-infrared observations are represented by acquisitions in the panchromatic channel. Coupling the 4 channels with the PAN channel, is possible to obtain images at a very high spatial resolution, guaranteed by the presence of the PAN channel, and at a sufficient spectral resolution, guaranteed by the presence of the multispectral channels [41].

In addition, to obtain a more detailed description of vegetation and land properties, for example to measure interesting biochemical and biophysical parameters, to describe and predict crop phenology cycle development and also to discriminate between different vegetation species that show very similar spectral responses, are generally necessary spectral performance more sophisticated, and so, an higher number of narrower spectral bands, like in the case of hyperspectral observations [39], [40].

Multispectral observation

Multispectral observations of land and vegetation refers to a concept and to a technology that has been well developed and consolidated during last years in the frame of optical remote sensing. From the preliminary analysis of the spectral requirements of agricultural users, this concept appears sufficient to satisfy the minimum spectral needs. A number of bands from 2 to 4 in the RED, GREEN, BLUE (RGB) and NIR channels guarantees to achieve a fair spectral analysis of the principal constituents of vegetation

and land: from multispectral observations the most relevant biochemical and biophysical parameters of crops are achievable. Therefore, multispectral observations, at a first analysis, seem able to guarantee a certain level of success in the application of satellite remote sensing to agricultural monitoring and management practices [30]. In addition, with a multispectral instrument could be possible to achieve those spatial resolution levels that are required to precisely analyze small units at the single farm local level in the frame of managed agriculture. These high spatial resolution levels are fundamental for purposes of precise management of targeted interventions; hence, a satellite system devoted to agriculture management practices has to guarantee the presence of an instruments that achieves these levels [30].

Anyway, respect to eventual analysis characterized by an higher number of spectral bands, like in the case of hyperspectral observations, multispectral images are able to perform only a coarse and superficial study of the spectral response of land and vegetation, and so they give only marginal information. This superficial study of spectral responses of vegetation and land causes the loss of many information which could be very important for several purposes. In particular, multispectral images provide limited performance in terms of: vegetation species discrimination and crop classification, crop health state accurate description and crop phenological development cycle monitoring. In multispectral observations bands have generally larger bandwidths respect to other types of spectrally improved images and this furthermore results in a reduced capability of deeply discerning spectral responses. Without a deep discern of spectral responses, it is very hard to accurately find those details which could reveal the little differences between different species that have similar but not identical spectral behaviors [39].

Hyperspectral observation

Hyperspectral observation is a more innovative concept of observation respect to the multispectral one.

A very high number of narrow bands, from several tens up to thousands, ensures the possibility to obtain spectral information very accurate and precise, that deeply describe the nature of the target.

Coupled with medium levels of spatial resolution, indicatively from 30 m to 100 m, hyperspectral images could improve very well the potential

performance in applications like vegetation species discrimination and crop classification. In this field, it could be also very important the recording of the SWIR region for the soil moisture content measurement.

In addition to an increased discrimination and classification capability, hyperspectral images could offer very accurate descriptions of crop health state, of crop stress (nitrogen, nutrients and mineral deficit), of crop damages (parasites and diseases). Not only, hyperspectral observations could be able to add some advantages also in the LAI and NPP estimation, in biomass quantification, in plants water content measurement and also in compiling suitable models for crop growth and yield. A very accurate capability of understanding crop biochemistry and biophysics is a vital feature for the actuation of preventive interventions. Thanks to this great potential support offered in the frame of prevention, hyperspectral instruments result very interesting candidates for a role in an optical remote sensing system devoted to agriculture and managed agriculture [40].

Unfortunately, hyperspectral images typically don't ensure those very high spatial resolution levels that are required to perform very accurate and targeted spatial interventions in particular and specific zones, especially for small field units and in particular if mounted on-board of small and very small satellites. Hence, they are not able to guarantee the complete satisfaction of all spatial requirements of users, especially in the frame of highly accurate and located management interventions. In this sense in fact, an hyperspectral instrument alone couldn't be sufficient to generate that source of very "ad-hoc" information that is required for very targeted applications, like for example precision agriculture [39].

Anyway, hyperspectral observations added to multispectral observations could offer many interesting complementary services useful to complete and to improve the capabilities offered by eventual multispectral instruments. For example, a systematic and repetitive hyperspectral observation of large sized lands could guarantee an optimum service of "early detection" of anomalies. This early detection capability could be the starting point on which targeted treatments are based: in fact, after an hypespectral preliminary identification of crop potential issues, more targeted and specific interventions devoted only to specific zones could be performed by coarser spectral resolution but very higher spatial resolution instruments.

This chain of systematic and logically distributed observations appears as an unique occasion to respond to the need of farmers in theme of prevention.

In conclusion, the presence of an hyperspectral instrument in an optical remote sensing system devoted to give aid and support to agricultural monitoring and management activities, could offer two kind of advantages respect to the use of a simple multispectral instrument alone. The first advantage is relative to the use of the hyperspectral instrument alone while the second one is relative to an hypothetical combination with an eventual multispectral instrument.

The first advantage consists in the capability of monitoring large land areas and, although with a spatial resolution not very high, to contemporarily discriminate very well the different species of vegetation present in the scene. In this sense, the use of an hyperspectral instrument offers a very reliable and accurate tool for the classification of croplands [40].

Differently, the second advantage is relative to the hyperspectral instrument capability in offering a potential service of early detection of anomalies. Thanks to this capability, a preliminary detection of anomalies or of bearing pathologies within a crop allows the system to drive another eventual instrument, characterized by an high spatial resolution, like multispectral instrument, in a specific zone or in a specific unit to perform further more accurate and spatially deep observation [30].

In conclusion, the combined multispectral and hyperspectral observation in successive moments, results very attractive both for prevention purposes, both for a very proper application and management of available resources, by means of targeted use of these resources where and when are necessary. In this way, agriculture costs and environmental impact result naturally and profitably reduced.

3.10 PRECISION AGRICULTURE

Precision agriculture *(or precision farming) is a system of production that promotes variable management practices within a field, according to site conditions* [44].

Precision agriculture is specifically devoted to study the dynamical variability within single units of small size, where targeted, specific and almost "chirurgical" interventions are required to increase agriculture profits by means of a proper use especially of chemical agents and water without exceeding environmental impact thresholds [45].

Precision agriculture is the agricultural practice which requires the most high performance possible, both in terms of temporal, spatial and spectral resolution. All these performance have to be improved respect to simple practices of agricultural monitoring, especially from the temporal and spatial resolutions point of view. Temporal performance (turn-around time and response time within 24 hours and an appropriate system revisit frequency) are of vital importance in precision agriculture. Activities related to precision agriculture are those that will drive the spatial resolution performance of the system, taking them to a level of values comprised between 2 and 5 m [22], [30].

This application requires all those capabilities that have to be ensured in the frame of general agricultural monitoring, like the individuation of crop and soil type, crop classification and crop acreage. Moreover, precision agriculture requires very precise information related to crop health, crop extension, crop growth dynamical processes, crop texture, nutrients state, NDVI and LAI at least weekly estimation, organic matter, biomass, chlorophyll and carotenoids quantification, potential production and crop stress. All these measurements allow to define very tailored and "in real-time" strategies of management, for example for the specific application of water for irrigation in zones with different moisture content or of fertilizer for fertilization in zones affected by different nitrogen content.

In relation to fertilizer, for example, by using very high resolution NDVI spatial distribution maps, it is possible to define strategies of variable-rate fertilizer application by differentiating the crop in specific zones identified by the NDVI thematic maps themselves. Thematic maps could then also be

used to verify the goodness of these interventions and their benefits. Hence, optical satellite remote sensing images are determinant for the creation of those "prescriptions" of fertilizer use which could allow farmers and all other users to prevent diseases and their destructive effects on crop. An example of NDVI variability study within small fields is provided by Figure 3.14, where the presence of red zones indicates low values of the NDVI.

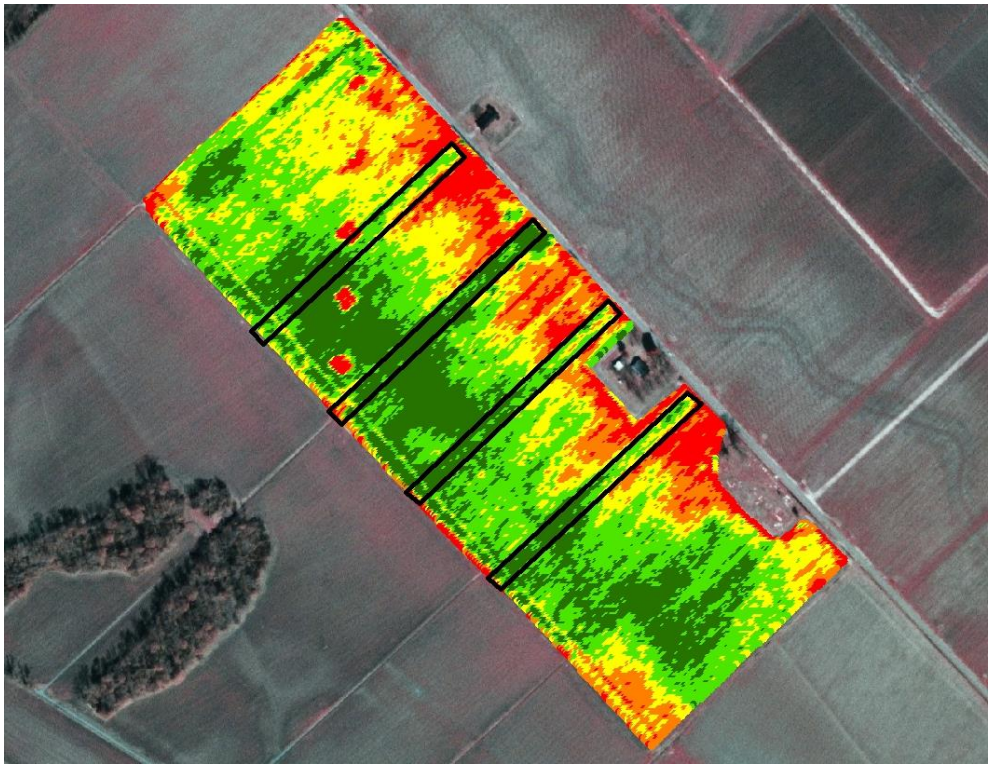

Figure 3.14: NDVI variability within adjacent small fields.

Hence, in precision agriculture, are very important both high accuracy and precision of measurement, in order to provide proper combinations of spatial and temporal descriptions, which are at the base of the term "Precision" and of the stringent timeliness that this application requires.

In precision agriculture is very important also the individuation of weeds and the consequent application of herbicides and also the application of pesticides and fungicides, which require a very precise identification of the specific zone of intervention. In this sense is fundamental to achieve a very high level of geo-location accuracy, typically within 1 pixel.

In precision agriculture is also required a good description of bare soils in order to plan a suitable definition of the so called management zone.

The accurate and specifically targeted use of these substances allows not also to reduce costs and increase the production, but also to reduce wastes and consequently to reduce the environmental impact of agricultural practices, which is one of the most important objectives of farmers and users.

Hence, it is evident how optical remote sensing images could be fundamental in supporting the process of decision making not also for agriculture in general but also at the single-small farm level, in the frame of crop management [15], [30], [37], [46], [47].

3.11 SUMMARY 3.2

User information requirements in the frame of agricultural monitoring an precision agriculture management practices (Table 3.2).

USER INFORMATION REQUIREMENTS	
Priority information	Application of: • fertilizer. • Herbicide. • Insecticide. • Irrigation.
Product delivery	< 24 hours.
Location accuracy	Within 1 resolution cell.
Measurement accuracy	70-75%
Revisit period	< 1 week.
Management unit	Up to 10-20 m.
Commercial product	Quantitative information.

Table 3.2: Chapter 3 Summary 2.

3.12 AN IMPROVED AND COMPLETE OPTICAL SYSTEM

The previous analysis of users requirements suggests to hypothesize a very interesting coupling of the capabilities of a multispectral instrument together with an hyperspectral instrument. This combination provides the design of an optical system characterized by different and selectable levels of spatial and spectral resolution performance. A system of this type would be able to generate many different kind of products and images, to respond at any possible different requests of users and at any different level in the scale of spatial and spectral performance.

A complete optical system covers any possible applications in the frame of land and vegetation observation. Multispectral and hyperspectral combined observations theoretically present only marginal deficiencies in the description of the vertical structure of vegetation and in the measurement of soil moisture content.

A system where multispectral and hyperspectral observations act both separately and both in couple ensures performance that could really improve the agricultural world, its sustainability and its development and find systematic application for commercial and national services.

Offering a system able to acquire images both at high spatial and spectral resolution provides the generation of a unique source of repetitive, systematic, reliable and accurate information. In fact, from one side, the achievement of very high spatial resolution levels (from 30 m to values lower than 5 m) is fundamental to study the variability within small management units; from the other side, the excellent spectral resolution level is instead fundamental for a good identification and quantification of materials in the scene, for a detailed analysis of the health state, for an accurate description of phenological cycles development and for a general understanding of functionality of land ecosystems at global level. Not only, thanks to the logic combinability of these images, this system is able to offer a very reliable service, where hyperspectral images are preliminary used for early detection of potentially dangerous anomalies and to direct multispectral instruments toward those zones which really need to be specifically treated with external agents.

Therefore, after a pure study of scientific requirements and of potential capabilities of multispectral and hyperspectral observation of land and

vegetation reflectance characteristics, it appears evident that a combined use of these two concepts could result very profitable.

Thanks to the possibility of producing identical recurring platforms and to equip them with different types of sensors, it is conceivable to design a system composed by multiple satellites which cover the whole field of optical observations in its all complexity thanks to the contemporary presence of multispectral and hyperspectral optical imager payloads.

The information and the indications derived from the study are clearly readable in a global perspective; the analysis performed is intended to understand all possible features involved in land and vegetation observation and in the exploitation of optical images to support and improve agricultural monitoring and management practices. Hence, it is possible to go from the general to the particular case and so to tailor the performance of the different optical instruments (and so, of the whole optical system of observation) to every specific needs.

The conclusion is that optical images could provide a very large variety of services and that could really improve agricultural monitoring and management practices.

Finally, to better and really understand the effective capabilities of the combined use of multispectral and hyperspectral observations together, and of optical land and vegetation observations in general, an accurate and complete analysis of the most relevant past, actual and planned Earth Observation missions will follow, with particular attention to those programs intended also to result in a support for agricultural monitoring and management practices.

3.13 SUMMARY 3.3

Optical remote sensing system specification for agricultural monitoring and precision agriculture management (Table 3.3).

USER INFORMATION REQUIREMENTS	
Spectral wavelengths	• Wide-band VIS/NIR. • Hyperspectral VIS/NIR/SWIR. • Thermal IR.
Spectral channels	• NIR: LAI, vegetation indices, crop vigor, soil and plant structure. • RED: LAI, vegetation indices, true color maps. • GREEN: NDVI-G, PRI, true color maps. • BLUE: aerosol corrections, true color maps. • XAN: PRI. • PAN: pan-sharpened multispectral images. Spatial resolution lower than 1 m. • SWIR: vegetation classification and soil moisture content. • TIR: land and vegetation thermal state.
Turnaround time	From 78 to 24 hours.
Image geolocation accuracy	Within 1 pixel.
Algorithm accuracy	70-75%
Nominal Repeat Cycle	From 3 days to 1 day.
Spatial resolution	• MS and HS products: 100-30 m, 30-10 m, < 5 m. • TIR products from 500 m to 100 m.
Product level	Surface reflectance and/or temperature.

Table 3.3: Chapter 3 Summary 3.

4 PAST, ACTUAL AND PLANNED EARTH OBSERVATION OPTICAL MISSIONS ANALYSIS

This chapter is intended to explore the wide world of past, actual and planned Earth Observation optical missions to validate indications found during scientific requirements analysis and to derive a preliminary idea about actual technology potentialities.

4.1 INTRODUCTION

Several specific characteristics and performance of actual and planned missions have been analyzed:

- orbital parameters.
- Revisit time capabilities.
- Geographical areas of coverage.
- Types and performance of the instruments carried on-board.
- Spectral bands covered.

Maintaining the reference application previously set, performance have been linked to those specific land and vegetation parameters measured by different missions to support agricultural practices. Examined missions have been divided in three large categories:

- multispectral missions.
- Hyperspectral missions.
- Thermal IR missions.

Within multispectral and hyperspectral categories, satellite missions have been divided in large and small satellites, in order to relate missions performance to platforms dimensions. This separation in terms of platform mass allows to obtain indications about the effective possibilities offered by satellites of reduced dimensions and to identify several interesting small instruments as potential payload candidates.

The analysis of spatial and spectral resolution levels found has made possible to relate actual services offered to the various results found during the analysis of scientific requirements. Only the characteristics of most representative missions have been reported, with a particular attention paid on these programs:

- the Landsat program, in the frame of multispectral large satellites [4].
- The RAPIDEYE constellation, in the frame of multispectral small satellite constellations [33].
- The PROBA (Project for On Board Autonomy) program, in the frame of hyperspectral small satellites [48].
- The DMC (Disaster Monitoring Constellation) satellites, due to the very interesting instrument carried on-board [2].

4.2 MULTISPECTRAL OPTICAL EARTH OBSERVATION MISSIONS

4.2.1 Large satellites multispectral missions

During large satellite multispectral Earth Observation mission analysis, many examples of programs devoted to produce optical images useful also for agricultural monitoring and management practices have been found.

Landsat program

The Landsat program is actually a series of six inactive and two operation satellites for high and medium resolution land and vegetation observation. It is an USA program developed in cooperation between the NASA (National Aeronautics and Space Administration) agency, responsible of the development of the space segment and of validation of its performance, and the USGS (United States Geological Survey) agency, responsible of mission requirements definition, development of the ground segment and full system operation. The result of this program is a long-term record of natural and human-induced changes on the global landscape. In fact, since 1972, Landsat satellites have continuously acquired space-based images of the Earth's land surface, coastal shallows, and coral reefs [4]. From an historical point of view, the first successfully launched satellite of the program was the Landsat-1, originally named ERTS (Earth Resources Technology Satellite). From that moment, all Landsat satellites have contributed to create a large archive of space remotely sensed data of land, archive that is a very reliable and systematic source of information for applications related to agriculture, geology, forestry, education, regional planning, mapping, and global change research. These information are used by government, commercial, industrial, civilian, military and educational communities throughout the United States and worldwide. Landsat program acquired data through the years allow for direct comparison of current specific site images with those taken months, years, or decades earlier. This comparison process can detect and study land-cover transformation that occur slowly and subtly, or quickly and devastatingly. Users could exploit time series of data over large areas to identify long-term trends and monitor the rates and the characteristics of land surface change. Landsat images are a fundamental resource for emergency response and disaster relief.

Actually, the last two satellites launched, the Landsat-7 and the Landsat-8, acquire each day hundreds of images of the Earth's surface all over the world to guarantee continuity of data creation to add to the Landsat general archive [4]. Landsat satellites generally acquire images while moving in a Sun-synchronus descending orbit (from north to south) over the sunlit side of the Earth. Landsat-1,2 and 3 were equipped with a multispectral medium-resolution instrument, the MSS (MultiSpectral Scanner). The MSS offered a spatial resolution of about 80 m in 4 spectral channels, a GREEN channel, a RED channel and two NIR channels. Landsat-4 and 5 were equipped with the MSS and with another multispectral medium resolution instrument, the TM (Thematic Mapper), which offered 7 multispectral bands at spatial resolution of about 30 m (and also a TIR channel at about 120 m) and a PAN channel at 15 m. Landsat-7 is equipped with a multispectral medium resolution optical instrument devoted to land and vegetation observation, the ETM+ (Enhanced Thematic Mapper Plus), direct result of the heritage of the entire Landsat program, especially from the point of view of the spectral bands. It acquires images in 6 multispectral bands at a spatial resolution of 30 m (and also a thermal IR channel at 120 m) and a panchromatic channel at 15 m, in order to have pan-sharpened multispectral images. An example is provided by Figure 4.1[4].

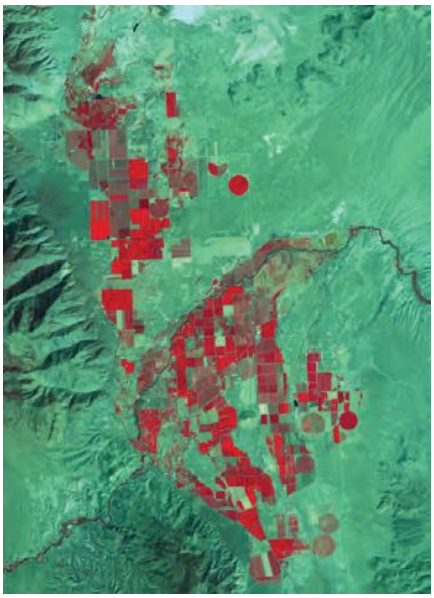

Figure 4.1: Agriculture in Nevada by Landsat-7.

Landsat-8

The Landsat-8 mission is an interesting still operational multispectral mission mainly devoted to optical land and vegetation observation. It is a 2623 kg satellite (Figure 4.2) launched in 2013. It is the first flight unit of the LDCM (Landsat Data Continuity Mission) program and so, the eighth flight unit of the Landsat program [2], [4], [18].

Figure 4.2: Landsat 8 satellite.

Orbital characteristics and derived temporal performance are the same of the Landsat-8 satellite [2], [18]:

- near-polar Sun-synchronus orbit at an altitude of about 700 km.
- Full-Earth-coverage cycle of about 16 days. Anyway, this satellite is offset to allow a 8-days repeat coverage of any Landsat scene area on the globe if necessary.

Landsat-8 is equipped with two multispectral medium resolution optical imagers devoted to land and vegetation observation. These instrument are called OLI (Operational Land Imager) and TIRS.

The OLI instrument offers also the possibility to acquire images in a panchromatic channel, in order to have pan-sharpened multispectral images [2], [4], [18]. Landsat-8 observations offer high quality and timely images in the visible and in the infrared domain. About 400 images are acquired each day.

An example is provided by Figure 4.3, where the progression of deforestation of Rondonia, Brazil, is shown [4].

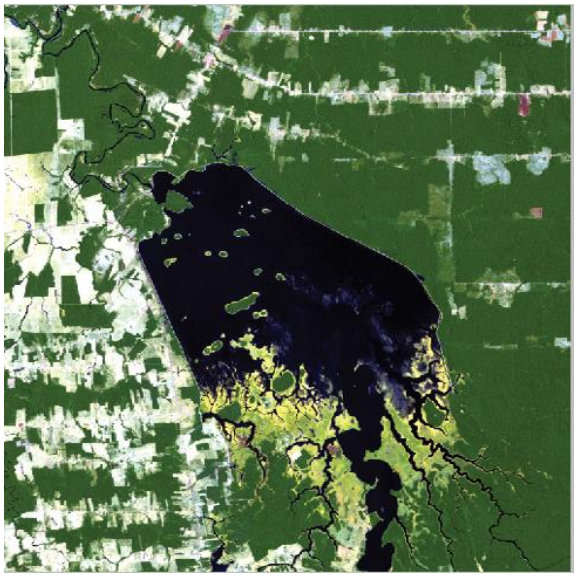

Figure 4.3: Deforestation in Rondonia, Brazil, by Landsat-8 (August 6, 2011).

OLI spatial resolution performance [4]:

- VNIR & SWIR GSD: 30 m.
- PAN GSD: 15 m.

OLI analyzed spectral channels [4]:

- COASTAL-AEROSOL: 430 – 450 nm. Used for coastal zones observations.
- BLUE-GREEN channel: 450 – 510 nm. Used for bathymetric mapping; to distinguish soil from vegetation; to distinguish deciduous from coniferous vegetation.
- GREEN channel: 530 – 590 nm. Used to emphasize peak vegetation, which is useful for assessing plant vigor.
- RED channel: 640 – 670 nm. Used to emphasize vegetation slopes.
- NIR channel: 850 – 880 nm. It is used to emphasize vegetation boundary between land and water, and landforms.
- SWIR channel I: 1570 – 1650 nm. Used to detect plant drought dress and to delineate burnt areas and fire-affected vegetation; it is also sensitive to the thermal radiation emitted by intense fires. It could be

used also to detect active fires, especially during nighttime when the background interference from SWIR in reflected sunlight is absent.

- SWIR channel II: 2110 – 2290 nm. Used to detect drought stress, burnt and fire-affected areas: it could be used also to detect active fires, especially at nighttime.
- CIRRUS channel: 1360 – 1380 nm. It is used to detect cirrus clouds.

Other large satellite relevant multispectral Earth observation missions

The principal characteristics of several other interesting multispectral actual and planned missions are presented in Table 4.1: Most representative large satellite multispectral missions principal characteristics. [2], [18], [29], [49], [50].

Mission	**Ikonos-2**	**GeoEye-1**	**Sentinel-2a&2b**	**SPOT-6&7**
S/c mass, [kg]	817	1955	1200	712
Launch	1999	2008	2015/2016	2012
Orbit, [km]	686, SSO	681, SSO	786, SSO	695, SSO
RT, [days]	3	4	10	3
Coverage	Global	Global	Global	Global
Instrument	*OSA*	*GIS*	*MSI*	*NAOMI*
Instrument mass, [kg]	171	452	275	18.5
GSD, [m]	VNIR: 3.3. PAN: 0.82	VNIR: 1.64. PAN: 0.41.	10-60 (depending on the band)	VNIR: 8. PAN: 2.
Spectral channels, [nm]	BLUE: 450–530. GREEN: 520-610. RED: 640 – 720. NIR: 760 – 860. PAN: 450 – 900.	BLUE: 450–520. GREEN: 520–600. RED: 625–695. NIR: 760–900. PAN: 450–900.	VNIR: 11 channels between 443 and 1375. SWIR: 2 channels between 1610 and 2190.	BLUE: 450–520. GREEN: 530–560. RED: 620–690. NIR: 760–890. PAN: 450–750.

Table 4.1: Most representative large satellite multispectral missions principal characteristics.

4.2.2 Small satellites multispectral missions

During small satellite multispectral Earth Observation mission analysis, many examples of programs devoted to produce optical images useful also for agricultural monitoring and management practices have been found. Between them, the RAPIDEYE and the Disaster Monitoring Constellation programs have been deeply analyzed in order to evaluate the state-of-art in the frame of small satellite constellations.

RapidEye

The RapidEye program consists in the RapidEye multispectral space mission specifically developed in the frame of agricultural market support and improvement. The RapidEye system is composed by 5 identical 150 kg satellites (Figure 4.4) equally spaced in a near-polar Sun-synchronus orbit, at an altitude of approximately 630 km, and launch at the end of 2008 [2], [18].

Figure 4.4: RapidEye satellites at SSTL prior to launch site shipment.

Within RapidEye services it is possible to find not only agricultural insurance, agricultural monitoring and mapping services, but also services

specifically devoted to precision agriculture, in particular to crop conditions and related management practices. RapidEye products provide international agencies and institutions with accurate and reliable predictions on future crop harvest; these predictions guarantee the needed timeliness of intervention to give subsidies and also emergency aids in case of disaster.

Finally, RapidEye images are also useful for cartography products, both in the commercial and also in the military market.

Thanks to the presence of 5 satellites in the same orbit, the RapidEye system guarantees a global daily revisit capability, which ensure to respond to specific request with a turn-around time lower than 24 hours. This capability is fundamental in the frame of the precision agriculture practices.

The RapidEye system gives particular attention to regions placed in Europe and in North America (Figure 4.5), which are completely covered by satellites images in a period lower than 6 days [2].

Figure 4.5: RapidEye image of Alaska, USA (September 11, 2012).

This ability ensures a frequent monitoring of croplands and so a frequent production of information, which is in line with the weekly planning

potentiality required by farmers. The RapidEye system is capable not only to optically image large regions, but also to analyze single small farm units. RapidEye images offer a very high level of quality for every product and application [33].

Although the mission objectives could be satisfied by just four satellites, there is a fifth satellite to introduce an external level of redundancy. All RapidEye satellites are based on a SSTL (Surrey Satellite Technology Ltd) platform and are equipped with an high-resolution optical imager mainly devoted to very-high-resolution land observation and disaster monitoring. [33] The instrument is a multispectral instrument called REIS (RapidEye Imaging System) and has a 43 kg mass. REIS spatial and spectral performance [2], [18]:

- VNIR GSD: 6.5 m.
- Spectral bands:
    - BLUE channel: 440 – 510 nm.
    - GREEN channel: 520 – 590 nm.
    - RED channel: 630 – 685 nm.
    - RED-EDGE channel: 690 – 730 nm.
    - NIR channel: 760 – 850 nm.

RapidEye system offers many products to precision agriculture applications; in particular, from RapidEye observation is possible to obtain [27]:

- True color maps, achievable with the combination of the RED, GREEN and BLUE bands.
- Soil brightness maps.
- Color coded maps, mostly intended to show the percentage of land covered by vegetation. It is useful to derive suitable data about crop yield and in particular for:
    - management zones individuation.
    - Variable planting rate.
    - Variable fertilizer application rate.
    - Yield estimation up to the field level.
- Chlorophyll maps; the knowledge of the chlorophyll content and distribution is used to:
    - identify specific areas with nutrients and nitrogen deficit.

- Identify specific areas affected by diseases or insects.
- Decision process support.

In conclusion, from the analysis of the RapidEye mission appears very evident the wide range of applications that optical remote sensing observations, while performed by a small satellites and over a limited number of spectral bands, could find not only in the frame of agricultural monitoring, but also for specific and targeted crop management, like precision agriculture.

The Disaster Monitoring Constellation (DMC)

The Disaster Monitoring Constellation is a DMC International mapping still operational mission composed by Algerian, Nigerian, Turkish, British and Chinese satellites built by SSTL, mainly devoted to land observation for disaster monitoring. These satellites are: AlSat-1, Beijing-1, Deimos-1 (Figure 4.6), NigeriaSat-1, NigeriaSat-X, UK-DMC-1 and UK-DMC-2 (Figure 4.6) [51]. They are 90-170 kg satellites all launched from 2002 to 2011. Orbital characteristics and derived temporal specifications [2], [18]:

- all satellites are placed in near-polar Sun-synchronus orbits at altitudes of about 700 km.
- Global coverage in 1 day thanks to the observations of all satellites.

Figure 4.6: UK-DMC-2 and Deimos-1 at the launch facility in Baikonur.

The DMC satellites AlSat-1, Beijing-1, NigeriSat-1 and UK-DMC-1 are equipped with an high-resolution optical imager devoted to high-resolution land observation and disaster monitoring, called SLIM-6 (Surrey Linear Imager Multispectral 6 channels – but 3 spectral bands). Similarly, Deimos-1, NigeriaSat-X and UK-DMC-2 are equipped with an improved-spatial resolution version of the SLIM-6, the SLIM-6-22. This instrument results interesting especially thanks to its performance and reduced mass (12 kg), appropriate for very small platforms. SLIM-6-22 spectral and spatial performance [51]:

- GSD:
    - multispectral GSD: 22 m.
- Spectral bands:
    - GREEN channel: 520 – 620 nm.
    - RED channel: 630 – 690 nm.
    - NIR channel: 760 – 900 nm.

Thanks to the observation in these bands, which are direct heritage of Landsat-7 bands 2, 3 and 4 and of SPOT HRV bands, the DMC produces many interesting data for agricultural monitoring and management (Figure 4.7) [2], [51], [52].

Figure 4.7: First image of NigeriSat-X, Auckland, New Zealand (August 21, 20119).

Other small satellite relevant multispectral Earth observation missions examples

The principal characteristics of other interesting multispectral actual and planned missions are presented in Table 4.2 [2], [18], [53], [54], [55], [56], [57].

Mission	**Hodoyoshi-4**	**PROBA-V**	**Sumbandilasat**	**VENµS**
Mass, [kg]	66	160	82	260
Launch	2014	2013	2009	2016
Orbit, [km]	630, SSO	820, SSO	500, SSO	720, SSO 400, SSO
Revisit Time, [day]	/	1-2	3-4	2
Coverage	/	Global	Global	Global
Instrument	HRMS	Végétation-P	MSI	VSSC
Instrument mass, [kg]	9	35	/	43.5
GSD, [m]	VNIR: 5	VNIR:	VNIR: 6.5	VNIR: 5.3

	(from 500 km).	300. SWIR: 600.		(from 720 km)
Spectral channels, [nm]	BLUE: 450–520. GREEN: 520–600. RED: 630–690. NIR: 760–900.	BLUE: 420–490. RED: 600–740. NIR: 740–930. SWIR: 1510–1780.	BLUE: 440–510. XAN: 520–540. GREEN: 520–590. RED: 630–690. RED-EDGE: 690–730. NIR: 845–890.	VNIR: 11 channels between 408 and 920.

Table 4.2: Most representative small satellite multispectral missions principal characteristics.

4.2.3 Multispectral optical Earth Observation missions analysis conclusions

The analysis of several past, actual and planned multispectral and multispectral optical Earth Observation missions devoted also to support agricultural practices has largely confirmed the indications found during the pure analysis of scientific requirements. The multispectral category offers a larger number of interesting examples and references, also in the frame of small satellite missions. It has been highlighted how a reduced number of spectral channels, at least 2 RED and NIR, with eventually also the GREEN and BLUE, if coupled with high spatial resolution performance satisfies a very wide range of scientific requirements. Thanks to these high spatial resolution levels and to a sufficiently deep content of spectral information, multispectral observations allow intense studies up to the single-farm level. From the temporal resolution point of view, analyzed missions shown a very wide range of frequencies (from 1 day to weeks), which are clearly influenced by the specific application and by the extension of the study. Multispectral missions examined have confirmed the expected capabilities in terms of measurement of significant parameters as:

- NDVI and LAI.
- Land cover.
- Soil type.
- Fraction of vegetated land.
- Vegetation type.
- Soil moisture at the surface.

Thanks to these measurements, multispectral observations are in synthesis able to provide (considering only agricultural practices):

- land-use identification and precise crop extension measurement.
- Fair discrimination of different crop and soil types.
- Accurate control of crops development.
- Reliable evaluation of treatments results and benefits.
- Reliable yielding estimates.
- Sufficient stress and pathologies mapping.
- Marginal description of crop phenology.
- Identification of zones with different contents of moisture.

From the orbital point of view, it has been noticed that:

- depending on instrument performance, a very wide range of altitudes could be exploited.
- All satellites analyzed are placed on Sun-synchronus orbits.

In conclusion, the actual state-of-art of multispectral observations guarantees the potential acquisition of a large amount of information suitable for several different government, commercial, industrial, military, civilian and educational agencies and communities involved in agricultural activities even with small instruments. A constellation of satellites devoted to land and vegetation multispectral optical observations hence seems to be an appropriate solution to provide timely, systematic and repetitive information about all types of cropland.

4.3 HYPERSPECTRAL OPTICAL EARTH OBSERVATION MISSIONS

Respect to multispectral missions, hyperspectral optical observations offer a reduced number of examples, due to the fact that this technology is relatively more innovative and of more recent definition and development respect to the multispectral one [39].

4.3.1 Large satellites hyperspectral missions

In the frame of large satellites hyperspectral mission, the EnMAP, the NMP-EO-1 and the PRISMA missions have been analyzed (Table 4.3) [2], [18], [58], [59].

Mission	**EnMAP**	**NMP-EO-1**	**PRISMA**
Mass, [kg]	871	588	550
Launch	2017	2000	2017
Orbit, [km]	643, SSO	690, SSO	614, SSO
RT, [day]	4	/	7
Coverage	Global	Global	Global
Instrument	HIS	Hyperion	HYC
Sensor mass, [kg]	/	49	90
GSD, [m]	VNIR/SWIR: 30.	VNIR/SWIR: 30.	VNIR/SWIR: 30. PAN: 5.
Spectral channels, [nm]	VNIR/SWIR: 240 channels between 420 and 2450.	VNIR/SWIR: 220 channels between 400 and 2500.	VNIR: 66 channels between 400 and 1010. SWIR: 171 channels between 920 and 2505. PAN: 400-700.
Spectral resolution, [nm]	VNIR: 5-10. SWIR: 10.	VNIR/SWIR: 10.	VNIR/SWIR: 10.

Table 4.3: Most representative large satellite hyperspectral missions principal characteristics.

4.3.2 Small satellites hyperspectral missions

In the set of studied hyperspectral missions, the most interesting small satellite mission found is the mission performed by the PROBA-1 satellite.

PROBA-1

The PROBA-1 (PRoject for On Board Autonomy-1) mission is an ESA still operational hyperspectral mission mainly devoted to vegetation and land observation. It is a 94 kg satellite launched in 2001. It is the first flight unit of the PROBA program, which consists in a series of mini-satellites technology demonstration missions. Orbital characteristics and derived temporal specifications [2], [18]:

- near-polar Sun-synchronus orbit at an altitude of about 600 km.
- nominal repeat cycle of about 1 week.

PROBA-1 is equipped with a very interesting low mass (14 kg) hyperspectral instrument. This instrument is called CHRIS (Compact High Resolution Imaging Spectrometer) and it is an medium-high resolution optical imager devoted to land observation for detailed analysis of vegetation produced by BNSC (British National Space Council). CHRIS spatial and spectral performance [2], [18]:

- GSD:
    - "reduced-spectral resolution observation mode" GSD: 18 m.
    - "Full-spectral resolution observation mode" GSD: 36 m.
- Spectral range: 400 – 1050 nm VNIR range.
    - "Reduced-spectral resolution mode": 18 spectral bands.
    - "Full-spectral resolution mode": 63 spectral bands.
- Spectral resolution:
    - "Reduced-spectral resolution mode": 5.6 nm.
    - "Full-spectral resolution mode": 32.9 nm.

PROBA-1 (Figure 4.8) images has found very interesting and effective applications in the frame of agricultural monitoring. In particular, PROBA-1 observations offer a good possibility to perform very detailed crop classification and also a very detailed and deep analysis of crop health conditions [48]. Hence, from the analysis of the PROBA-1 mission, appears evident the potential capabilities of application that optical remote sensing

observations, performed with an high number of spectral bands, could find especially in the frame of agricultural monitoring [2].

Figure 4.8: CHRIS image of Uluru, Australia (April, 2004).

Differently, from this mission appears harder to exploit hyperspectral data for very specific and targeted management practices, like precision agriculture, due to the not so much high spatial resolution level offered by this type of instrument.

4.3.3 Hyperspectral optical Earth Observation missions analysis conclusions

Hyperspectral missions analyzed have confirmed the expectations derived from the analysis of pure scientific requirements and also the effective advantages and improvements that the use of a very large number of narrow spectral bands in land and vegetation observation could ensures.

Hence, hyperspectral missions analysis in synthesis validates the expected capabilities of hyperspectral observation to:

- discriminate and quantify the matter within a scene.
- To deeply analyze chemical target characteristics.

- To describe accurately and reliably the phenological development and the physiological conditions of crops.
- To improve the classification performance offered by the multispectral observations.
- To very accurately detect plants stress (nitrogen, water and nutrients deficit).
- To deeply study foliar chemistry.
- To measure biomass, soil moisture and plants water content.

Therefore, from the parallel analysis of pure scientific requirements and of actual technological instruments capabilities, it has been confirmed that hyperspectral images offer an unique occasion to:

- understand how plants and soils react at changes on environmental conditions.
- Provide a fundamental tool to preliminary detect anomalies and potential pathologies, service determinant in the frame of crops damages prevention.

From the orbital point of view, it has been noticed that:

- depending on instrument performance, a very wide range of altitudes could be exploited.
- All satellites analyzed are placed on Sun-synchronus orbits.

In conclusion, the actual state-of-art of hyperspectral observations guarantees the potential acquisition of a large amount of information suitable for several different government, commercial, industrial, military, civilian and education agencies and communities involved in agricultural activities, even if there is a smaller amount of available examples respect to multispectral observations. A network of satellites devoted to land and vegetation hyperspectral optical observation hence seems to be an appropriate solution to provide timely, systematic and repetitive information about all types of cropland.

4.4 AN ATTRACTIVE OPPORTUNITY: THERMAL IR OBSERVATIONS

Information extracted from this channel are useful to monitor the thermal state of observed land, in particular the heat and hydric stress of surfaces and plants, and so result in a suitable complementary tool to properly manage water during irrigation practices.

Moreover, this portion of electromagnetic spectrum provides the ability of detecting and monitoring wild fires, skill that is not available with classical optical observations.

4.4.1 Thermal IR observation missions and instruments analysis

Two examples of optical imagers devoted to analyze the thermal IR radiation have been analyzed:

- The Alos-2 CIRC.
- The BIRD HSRS.

The Alos-2 CIRC instrument

The CIRC instrument is a low resolution optical imager which will be mounted on the JAXA land observation satellite Alos-2, planned to be placed on a Sun-synchronus orbit at an altitude of 640 km. CIRC will be devoted to detect wild fire with a global coverage cycle of 10 days. CIRC spectral and spatial performance [2], [18]:

- GSD:
    - thermal IR GSD: 200 m.
- Spectral range:
    - TIR channel: 8 – 12 μm.

In the frame of wild fire detection, the CIRC is able to measure [2], [18]:

- fire fractional cover, the fraction of a land area where fire is occurring.
- Fire temperature.
- Surface temperature [60].

The BIRD HSRS instrument

The HSRS instrument is a low resolution optical imager mounted on the land observation DLR BIRD inactive satellite, once placed on a Sun-synchronus orbit at an altitude of 572 km. HSRS has been devoted to land

observation and disaster monitoring. HSRS spectral and spatial performance [2], [18]:

- GSD:
  - thermal IR GSD: 372 m.
- Spectral range:
  - TIR channel I: 3.4 – 4.2 μm.
  - TIR channel II: 8.5 – 9.3 μm.

In the frame of land thermal state analysis and wild fire detection, the HSRS is able to measure [2], [18]:

- land surface temperature.
- Fire fractional cover.
- Fire temperature.
- Fire radiative power.

4.4.2 Thermal IR observation analysis conclusions

The brief analysis conducted on thermal IR observation instruments state-of-art confirms indications provided by users requirements analysis. In conclusion, parallel to multispectral and hyperspectral observations, it seems very interesting to add the potential contribution of a thermal IR optical imager, devoted only to:

- measure land surface temperature.
- Monitor hydric stress.
- Detect wild fire.

4.5 SUMMARY chapter 4

Combination of different instruments to build a complete optical system (Table 4.4).

COMPONENT	COMMERCIAL PRODUCT	POTENTIAL SERVICES
Multispectral Optical Imager	• Land and vegetation reflectance products at 10 – 30 m of GSD in RGB and NIR channels. • Land and vegetation reflectance products at 2 – 5 m of GSD in RGB and NIR channels.	• Land cover/use analysis. • Small fields fine spatial details analysis. • Precision agriculture.
Hyperspectral Optical Imager	• Land and vegetation reflectance products at 30 – 100 m of GSD in many narrow VIS, NIR and SWIR channels.	• Crop classification. • Vegetation processes analysis. • Crop early anomaly detection.
Thermal IR Optical Imager	• Land and vegetation temperature products at 100 – 500 m of GSD in a single TIR channel.	• Crop and soil thermal state monitoring. • Wild fire detection.

Table 4.4: Chapter 4 Summary.

5 SAR OBSERVATION

This chapter provides a general overview of the SAR concept, SAR potentialities and SAR application for land and vegetation observation. The purpose is to understand the real possibilities to equip a very small platform with a SAR and the improvements which could provide if coupled with optical sensors.

5.1 NON-OPTICAL OBSERVATIONS: MICROWAVES SPECTRAL DOMAIN AND SYNTHETIC APERTURE RADAR (SAR)

The SAR technology is an alternative way to perform remote sensing observations respect to passive sensors.

By means of the discussion about advantages and disadvantages, the analysis will try to find appropriate solutions to add a SAR instrument to the multispectral, hyperspectral and thermal IR expected to compose the observation system.

5.1.1 SAR technology concept and principle of functioning

The Synthetic Aperture Radar (SAR) concept is an evolution of remote sensing observations with imagining radar. With classical imaging radars, is very difficult to achieve very high spatial resolution levels. This is due to [70]:

- large antenna dimensions.
- Required power consumption.

The spatial resolution levels offered by imaging radar are generally very low also if these instruments are mounted on aircraft platform.

This limit is obviously more heavy in the case of very small spacecraft platforms, that have very reduced availability in terms of power and dimensions.

The SAR concept is the solution adopted in the frame of imaging radar to improve spatial resolution levels [70].

This method adopted consists in the synthesis of an apparently long antenna by making use of the forward linear motion of the space platform. The length of the synthetic aperture is defined by the time that a particular spot is irradiated by the radar.

The distance the SAR device travels over a target creates a large "synthetic" antenna aperture (the "size" of the antenna). As a rule of thumb one can assume that the larger the aperture is, the higher the image resolution becomes, regardless whether physical aperture or synthetic aperture: this allows SAR to create high resolution images with comparatively small physical antennas [70].

The concept of SAR is depicted by Figure 5.1:

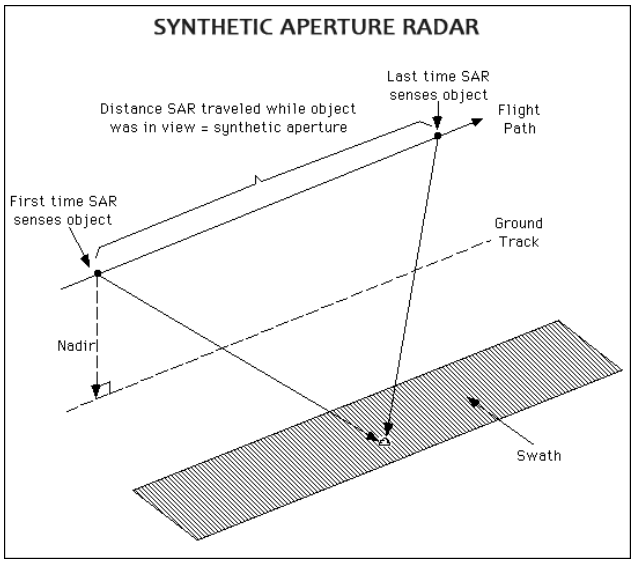

Figure 5.1: SAR concept representation.

To create a SAR image, successive pulses of radio waves are transmitted to "illuminate" a target scene, and the echo of each pulse is received and recorded. The pulses are transmitted and the echoes received using a single beam-forming antenna, with wavelengths used anywhere from a meter down to millimeters. As the SAR device onboard the aircraft or spacecraft moves, the antenna location relative to the target changes over time. Signal processing of the recorded radar echoes allows it then to combine the recordings from the multiple antenna locations – this forms the synthetic antenna aperture, and allows it to create finer resolution image than what would be possible with the given physical antenna aperture [71].

5.1.2 SAR signals target interaction mechanism

SAR observations are based on interaction between targets and emitted SAR signals.

This interaction involves the “backscattering mechanisms”. SAR are able to collect the signals “backscattered” from targets and to relate them to several properties of the scene. These backscattered signals depend on target surface scattering, on its volume scattering, and on these scatterings considered together.

The relative intensities of these different scatterings are influenced by surface roughness and from dielectric properties of the mean.

All these factors further depends on [70], [72]:

- SAR signal frequency.
- SAR signal polarization.
- SAR signal incidence angle.

Dominant scattering mechanisms involved in land and vegetation observation could be studied using [73]:

- the X-frequency band, which is sensitive to leaves scattering and which could offers the highest spatial resolution levels at fixed antenna dimensions.
- The L-frequency band, which is sensitive to ground scattering.
- The C-band frequency, which is sensitive both to leaves and ground scattering. This final ability makes it very largely used in the frame of some crop parameters monitoring.

SAR concept offers certain advantages respect to optical system that make it an interesting candidate to satisfy particular objectives [73]:

- ability to observe Earth in every meteorological conditions, fundamental for those regions of globe that are frequently affected by an intense cloud covering. This is very important to monitor particular phenological stages that occur during winter periods of the year, when clouds and fog largely limit the use of optical images. The knowledge of these phenological stages is very useful to study the vegetation development during the "late season". A reliable understanding of vegetation and crop potential development in this period of the year, allows users to have annual crop yielding "early seasons" predictions, available many months before the harvest time.
- Ability to observe in every kind of illumination conditions, especially during the night.
- SAR observations are not influenced by the presence of atmospheric constituents, like for example water vapor. This allows SAR signals to efficiently penetrate the atmospheric shield and so to reach targets without disturbances.

In the frame of land and vegetation observation, SAR images exhibit an high sensitivity to dielectric properties of the scene and to several soil characteristics [73]:

- the vegetation structure: dimensions, shape and orientation of leaves, stems and fruits.
- The plants water content.
- The soil surface roughness, moisture content and erosion.

Hence, SAR images offer a good occasion to study the physical morphology of land and vegetation, providing [74]:

- accurate crop identification and discrimination.
- Crop extension measurement.
- Improved management of hydric resources and so of irrigation practices.
- Quantification of biomass in the scene and description of the biomass regeneration process.

On the contrary, there exist some limits in SAR that make the practical application of this type of instrument very hard. SAR observation shows another limit linked to the difficulty in the visual interpretation which makes very hard also to relate SAR information to most relevant biophysical vegetation and soil parameters. These limits are mainly due to the complex interactions that occur between the target and the SAR signals [72]:

- radiometric and geometric signals distortions.
- SAR speckle effects.
- Topographical effects.

Anyway, even with these difficulties, add SAR observations to an optical system offers an interesting potential in the frame of [73]:

- vegetation species identification.
- Crop discrimination, surveillance and mapping.
- Verification of farmers declarations.
- Study of problematic regions affected by a frequent cloud covering, by a complex nature and by a reduced accessibility.

There exist three techniques that allow to improve the potentialities of SAR observations [20]:

- the multi-frequency SAR: the contemporary combination of different frequency bands.
- The SAR Polarimetry.
- The SAR Interferometry.

5.1.3 SAR Polarimetry (PolSAR)

Radar waves are characterized by a polarization. Different materials reflect radar waves with different intensities, but anisotropic materials such as vegetation often reflect different polarizations with different intensities. Some materials will also convert one polarization into another. By emitting a mixture of polarizations and using receiving antennas with a specific polarization, several images can be collected from the same series of pulses [71].

PolSAR is a variant of the pure SAR concept which could increase the capabilities of this technology, especially if combined with multi-frequency SAR. Multi-frequency PolSAR could offer good improvements in the phenology retrieval, in particular if the phenological development causes significant morphological transformations of plants. This high sensitivity results in an increased ability in the [25], [75]:

- crop classification, conditions analysis, yield predictions and clustering.
- Investigation of farming area specifications.

The use of PolSAR increases also the sensitivity of the observations to vegetation structure and to dielectric properties respect to the simple SAR. This increased sensitivity hence allows *a fortiori* a better discrimination between crop types (for example, the PolSAR is able to discriminate between different foils dimensions) and between vegetation and soil. Moreover, PolSAR improves [25], [75]:

- the soil moisture content estimate.
- The hydric content of plants measurement.
- The quantification of green biomass.

- Indisputable discrimination between winter and summer crops.

It is also possible, but the results are not so much accurate, to [25], [75]:

- preliminarily detect plant pathologies.
- map crop residues.
- Marginally estimate LAI.

5.1.4 Sar Polarimetry + SAR Interferometry (PolInSAR)

Rather than discarding the phase data, information can be extracted from it. If two observations of the same terrain from very similar positions are available, aperture synthesis can be performed to provide the resolution performance which would be given by a radar system with dimensions equal to the separation of the two measurements. This technique is called Interferometric SAR or InSAR. If the two samples are obtained simultaneously (perhaps by placing two antennas on the same aircraft or spacecraft, some distance apart), then any phase difference will contain information about the angle from which the radar echo returned. Combining this with the distance information, one can determine the position in three dimensions of the image pixel [71].

Actually, the use of the InSAR technology alone doesn't appear very suitable for agricultural applications, while on the contrary the combined use of PolSAR and InSAR, the "PolInSAR", seems interesting [20]. PolInSAR offers not only information about dielectric properties, shape and orientation of plants constituents, but especially about the vertical structure of plants. The accurate description of the vertical structure of vegetation guarantees interesting information about the vegetation height, an important biophysical vegetation parameter. The vegetation height, impossible to be analyzed with optical imagers, could be easily related to [20]:

- crop phenological stage:
- LAI measurements:
- crop biomass, thanks to the elimination of some disturbance factors that are inevitable with the use of the only PolSAR concept.
- Description of plants pathologies due to hydric stress and strictly related to plant water content.

5.2 PAST, ACTUAL AND PLANNED EARTH OBSERVATION SAR MISSIONS AND STUDIES ANALYSIS

An analysis of past, actual and planned SAR missions with extended application in the frame of agriculture has been conducted, although there exist a very limited number of examples, especially of very small satellites. In order to cover this gap, a research about studies of this type has been performed exploiting [2] and [18]. The lack of examples found within these database testifies that a profitable SAR applicability could result very hard to be confirmed and that an hypothetical use of this technology of observation could presents many more problems respect to optical technology.

5.2.1 Large satellite Earth Observation SAR missions analysis

The Sentinel-1 constellation characteristics have been reported because it has been considered the most appropriate and relevant mission within the Sentinel program and within all other large satellite examples found in the frame of SAR systems.

Also other large SAR satellite missions have been studied, like Alos-2, COSMO-SkyMed, RISAT-2, RadarSat-2, but for brevity their specifications haven't been reported [2], [18].

Sentinel-1

The Sentinel-1 mission is an ESA and EC SAR mission composed by two identical satellites, Sentinel-1a and Sentinel-1b, mainly devoted to all-weather ocean and land high-resolution multi-purpose observation. They are 2300 kg satellites: Sentinel-1a has been launched in 2014, while Sentinel-1b launch is planned for 2016. They are the first and the second flight unity of the Sentinel-1 program. Orbital characteristics and derived temporal performance [2], [18], [76]:

- near-polar Sun-synchronus orbit at an altitude of about 693 km.
- Global coverage from 5 days up to 3 months depending on the operation mode.

Sentinel-1a and Sentinel 1-b are equipped with an imaging radar SAR, an high-resolution all-weather multi-purpose imager for ocean, land and ice observation, called SAR-C (Sentinel-2).

A SAR-C image example is provided by Figure 5.2 [2]:

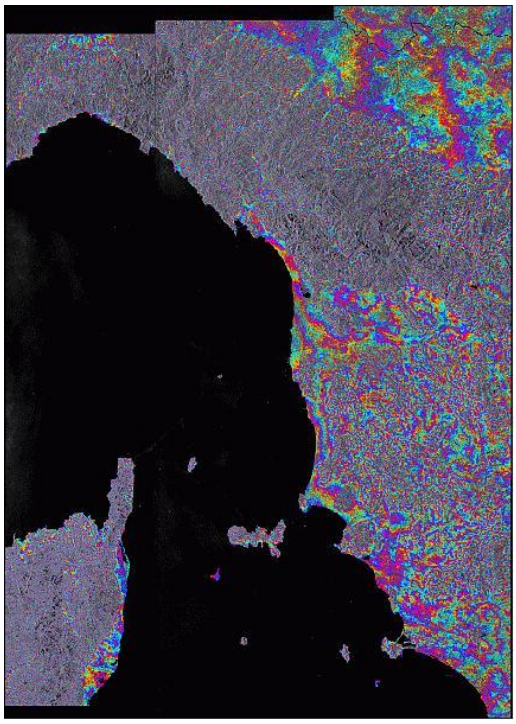

Figure 5.2: Sentinel-1a (IW) image of the Gulf of Genua, Italy (August, 2014).

The SAR-C (Sentinel-2) instrument is a C-band SAR [2], [18], [76]:

- Operation frequency: 5.405 GHz.
- Multipolarisation SAR.
- Variable swath/resolution in 4 different operation modes.
    - StripMap (SM) mode:
        - resolution: 4 x 5 m^2.
        - Swath: 80 km.
        - Polarisation: VV + VH or HH + HV.
    - ScanSar – Interferometric Wide-swath (IW):
        - resolution: 5 x 20 m^2.
        - Swath: 240 km.
        - Polarization: VV + VH or HH + HV.
    - ScanSar – Extra-wide swath (EW):
        - resolution: 25 x 80 m^2.
        - Swath: 400 km.
        - Polarization: VV + VH or HH + HV.

- WaVe (WV):
  - resolution: 20 x 5 m^2.
  - Swath: 20 x 20 km^2 every 100 km.
  - Polarization: VV or HH.

These large and interesting satellites produce some useful data for agricultural monitoring. Between these field, Sentinel-1a images (and, in the future, Sentinel-1b images) give some interesting measurements and parameters [2], [18], [76]:

- soil moisture at the surface.
- Fraction of vegetated land.
- Land cover.
- Soil type.
- Vegetation type.

5.2.2 Actual and planned studies about microsatellites SAR applications

Just few examples of very small satellite SAR studies have been found. The most interesting within them are those related to Coral [77], InSAR [78], [79], NovaSAR [80], PanelSAR mission [81], TECSAR [82] and WiSAR [83]. Studies analyzed noticed that SAR applications with very small satellite platforms are heavily limited, respect to optical sensors, by requirements in terms of dimensions and power levels. In particular:

- no microsatellites examples with mass lower than 120 kg have been found [79].
- No power levels consumption examples lower than 150 W have been found [79].

Therefore, the use of SAR with very small satellite platforms appears nowadays to be only at the level of an intricate challenge, by the fact that nothing has been found that could be used like consolidated heritage. In conclusion, the analysis conducted suggests that the actual state-of-art of SAR technology is not able to guarantee a reliable application in the field of very small satellites, in particular with mass lower than 100 kg. Although the power level required from SAR instruments could be almost reached by actual very small platforms, the SAR instruments range of mass found appears not suitable.

5.3 AGRICULTURE: OPTICAL IMAGES ARE SUFFICIENT

From the analysis of requirements, of potential improvements offered by SAR observations and of past, actual and planned SAR programs, it appears clear that SAR high spatial resolution images could provide interesting advantages if added to optical observations. SAR images are able to cover some intrinsic gaps of optical observations and contribute to create a very complete Earth Observation system. The high spatial resolution levels offered by SAR, combined to the possibility of different operation modes, results in an attractive occasion for very targeted agricultural management applications, such as precision agriculture. Actually, only constellations formed by large satellites, as in the case of Alos-2 and Alos-3, are effectively ready to be produced and it is impossible to find a consolidated and recurring application of SAR instruments on-board very small platforms [2], [18]. This lack of experience testifies that is not easy and convenient to design a mission based also on SAR instruments. The SAR potential improvements don't appear so intense to justify the level of complexity and uncertainty they introduce. Potential traps hidden by this technology are still excessively heavy if a low cost solution based on a small platforms is researched. Optical instruments are able to satisfy almost every kind of customers request, both in terms of large fields monitoring and also in terms of small unit management. Furthermore, the potentiality to design a constellation of satellites ensure to achieve very frequent revisit capabilities, and so to provide the possibility to acquire very frequently every target, largely reducing the relevance linked to the impossibility of optical systems to acquire images during the night or in case of adverse meteorological conditions. The conclusion is that it is more convenient to concentrate the attention only on optical instruments, profitable solution if something of reliable and simple has to be created with a low cost. Nevertheless, the analysis conducted on SAR technology is not completely useless: it is considered as a starting point for future improvements to an optical consolidated and operational system. When technology will be able to guarantee a reliable functioning of SAR instruments on-board very small satellite platforms, it would be possible to enrich optical observations with the eventual and successive launch of very small SAR satellites in orbit. This will allow to achieve a level of competitiveness and completeness which is unthinkable and unreachable nowadays [24].

5.4 SUMMARY Chapter 5

SAR observation characteristics: advantages and disadvantages (Table 5.1).

SAR OBSERVATIONS	
Advantages	***Disadvantages***
• Observations possible in every meteorological conditions. • Observations possible in every illumination conditions. • Very high spatial resolution levels achievable. • High sensitivity to vegetation structural attributes, mainly to vertical structure.	• Stringent limitations on mass (at least, 60 kg of payload) and power levels (at least, 150 W): apparently not suitable for micro-satellites applications. • Very limited heritage. • Hard visual interpretation of SAR data.

Table 5.1: Chapter 5 Summary 1.

SAR hypothetical contribution to an optical system devoted to provide information useful for agricultural monitoring and management practices (Table 5.2).

SAR POTENTIAL IMPROVEMENTS
• Continuous observation in every meteorological and illumination conditions. • Accurate description of vegetation structure, in particular vegetation vertical structure. • Accurate measurement of soil moisture. • Reliable “early season” predictions.

Table 5.2: Chapter 5 Summary 2.

6 PRELIMINARY MISSION ARCHITECTURE DESIGN

This chapter describes the analysis performed to identify the best mission architecture solutions to create a source of continuous, systematic, repetitive, accurate and complete land and vegetation observation system specifically devoted to be a support for the reference case of Tuscany agriculture. The analysis is based on general system technical specifications and on users scientific requirements. Through the discussion about possible orbital configurations and about state-of-art of different categories of small optical instruments, several interesting constellation architecture examples have been proposed.

6.1 CONSTELLATION DESIGN

The whole range of services at which all kind of users involved in agriculture could be potentially interested has been identified and a certain level of confidence with actual technology has been acquired. Optical observation resulted to be the best solution for a space observation system devoted to provide a source of continuous, systematic, repetitive, reliable, complete and accurate information to support in particular agricultural monitoring and management practices. A set of information provided by multispectral and hyperspectral images in the VIS, NIR, SWIR and TIR offers an attractive opportunity to achieve all spatial and spectral details related to land and vegetation. Before starting with an accurate sizing of the platform, a preliminary analysis to identify potential mission architectures is required.

This analysis is intended to select a range of possible orbital solutions which allow the platforms to match the capabilities and the objectives of all different types of instruments carried on-board. Initially, a reference mission devoted to produce data for hypothetical users involved in agricultural practices in a small region like the Tuscany is set as target of the analysis. The principal objectives of the mission analysis is to design:

- a low-cost mission, considering the satellite total mass and the total number of satellites as main cost drivers.
- A very performant mission, able to satisfy every kind of requirements in the frame of land and vegetation observation. The specific case of Tuscany will be used to derive general indications and relations that could be easily extended also to other different mission scenarios.

The mission analysis is based on three technical starting points:

- the maximum expected mass of the satellite: lower than 100 kg, in the frame of microsatellites [1].
- The presence of a micro-electric propulsion device on-board the microsatellite. In particular, the last version of the Alta SpA low power Hall thruster named HT100, the HT100D is expected to be carried on-board [6].
- The possibility to produce on large scale several microsatellites all based on a single standard platform.

These technical starting points presents several interesting advantages:

- firstly, microsatellites are characterized by a lower development and production cost respect to larger satellites.
- Finally, the HT100D ensures the unique and very innovative possibility to create a very performant and versatile observation system. Electric propulsion provides interesting potentialities in terms of atmospheric drag compensation for long periods even at very low altitude and with minimum propellant mass expense and further costs reduction by means of orbit differentiation after a single shared launch of all eventual microsatellites.

Such a system could be able to respond to many different and general tasks, and hence to perform a very large gamma of possible missions. The potential production of several microsatellites based on a single recurrent and versatile platform suggests to design a constellation of satellites able to:

- achieve very good temporal performance, better respect to larger satellites.
- Exploit all required observation payload types (multispectral, hyperspectral and thermal IR) together.

Considering the very small dimensions expected for the platform, the mission analysis is based on the assumption that just one observation payload could be carried on-board each satellite. Therefore, the mission analysis will be based on several steps:

- definition of most relevant technical requirements, system drivers and orbit parameters to design a suitable and appropriate Earth Observation constellation.
- The conceptual division of the complete constellation in "mini-constellations", each of one characterized by the presence of a specific payload and devoted to satisfy a particular portion of spatial and spectral requirements.
- Identification and analysis of several small existing instruments representative of each optical observation category.
- Separated design of each mini-constellation to find the best orbital solutions for each payload in terms of spatial and temporal resolutions.

6.1.1 A preliminary discrimination

When multiple satellites have to work together, depending on the characteristics of their configuration, they could compose a constellation, a formation or a swarm or cluster [61]:

***Constellation**: when several satellites flying in similar orbits without control of relative position, are organized in time and space to coordinate ground coverage. They are controlled separately from ground control stations [61].*

***Formation**: if multiple satellites with closed-loop control on-board provide a coordinated motion control on basis of relative positions to preserve the topology. It is the collective use of several spacecraft to perform the function of a single, large, virtual instrument [61].*

***Swarm or cluster**: if a distributed system of similar spacecraft is cooperating to achieve a joint goal without fixed absolute or relative positions. Each member determines and controls relative positions to the other satellites [61]*

6.1.2 Main technical requirements for an Earth Observation system

The main technical requirements for an Earth Observation system derive from the analysis of scientific requirements. In the particular case of land and vegetation observation the system performance which impact the orbit design process can be summarized in a limited number of peculiar figures of merit, such as [62]:

- Geographical coverage.
- Response time.
- Revisit time.
- On-ground resolution (spatial and spectral).
- Swath.

Linked to these fundamental requirements, there are a lot of other requirements that have to be provided contemporarily by the system, like for example [62]:

- image size and quality.

- Ground stations network available for launch, Early-Orbit-Phase and routine operations.
- Specific illuminations conditions, local time.
- Data availability and reliability.
- Volume of data produced by the payload.
- Data rate.
- Responsiveness, acquisition delay and latency.

6.1.3 System drivers

Strictly related to system technical requirements, there exist several technical parameters that drive the design of the system, like for example [62]:

- *mass and volume of the instrument and spacecraft*.
- *Budget constraints for manufacturing and operations during system lifetime*, which have to be carefully considered in order to design a low-cost mission together with the launch vehicle cost and availability.
- *System reliability and availability*, needed to ensure the possibility of every target acquisition by all interested users.
- *Timely continuity of data*.

6.1.4 Main parameters to define for an Earth Observation constellation design

The system drivers identify the main mission parameters influencing the achievement of the required performance vs. cost, risk and schedule for both space and ground segment. The mission parameters are mainly related to orbital characteristics that are selected to allow the highest level possible of system operation. In the frame of a constellation design, it is very important to specify [3]:

- the orbital shape.
- The orbital altitude.
- The orbital inclination.
- The number of orbital planes.
- The between-plane phasing.
- The number of satellites.
- The within-plane phasing.

6.2 ORBITAL CONSTRAINTS

To select several appropriate candidate mission architectures, many orbital solutions potentially suitable have to be studied. The objective is to produce a global description of every potential case to obtain a very wide gamma of suitable mission architectures. The identification of many different mission architectures will confirm:

- the versatility of the system.
- The ability to easily respond to many Earth Observation specific requirements.

Suitable ranges of most relevant orbital parameters and their appropriate combinations will be derived according to mission scientific requirements and to system specifications.

6.2.1 Orbital altitude range

The first step of orbital solutions analysis is to select a range of altitudes suitable to accommodate spacecraft platforms equipped with optical remote sensing instruments devoted to observe land and vegetation. The range of altitudes has to match the capabilities of all types of instruments expected in order to guarantee:

- the level of performance required to observations.
- Ideal operational conditions of the platform.

The upper limit of altitude range derives from the need to ensure appropriate system performance in terms of on-ground resolution. It is impossible for a small optical observation sensor to achieve high levels of spatial resolution from excessively high altitudes. This, linked to the statistical analysis of Earth Observation missions, suggests to set the upper limit at about 800 km. Considering a certain level of tolerance and the eventuality of a launch as secondary payload, the upper limit is initially set at about **1000 km**. This limit eliminates the possibility of Geo-synchronus orbits [63].

The lower limit of suitable altitude range results harder to be set. It is principally affected by the orbital decay related to atmospheric drag, which is the most important perturbation effect for low Earth orbits [3]. Atmospheric drag can be profitably balanced by means of electric propulsion; this makes possible to maintain very low altitudes with a limited

quantity of propellant on-board, unthinkable with other kind of propulsion. Further simulations will be performed to precisely quantify the effective possibilities of microsatellite platforms equipped with Alta SpA HT100D to maintain low altitudes for periods up to 5 years. Initially, according to statistical missions analysis, an appropriate lower limit seems to be 300 km [64]. Considering also a certain level of tolerance guaranteed, the lower limit is set at about **250 km** [63].

6.2.2 Orbital shape

The second step of orbital solutions analysis regards the discussion of advantages and disadvantages of two different elementary orbital geometries. The orbital geometries considered in this analysis regard:

- circular orbits (with $e = 0$).
- Elliptical orbits (with $0 < e < 1$).

Circular orbits

Circular orbits are the most frequently exploited type of orbits in the frame of Earth Observation satellites, as also clear from the mission analysis of Chapter 4. Circular orbits offer [3], [63]:

- an extended level of heritage.
- High reliability, fundamental to design an affordable and contemporarily low-cost Earth observation space mission.
- An attractive level of simplicity and stability.

In conclusion, circular orbits appear very interesting to accommodate spacecraft platforms equipped with optical observation instruments.

Elliptical orbits

Elliptical orbits are also an attractive orbit solution for Earth Observation purposes. Elliptical orbits offer an important advantage in terms of targeted coverage: they guarantee the possibility to observe a certain selected terrestrial hemisphere for a large period. Thanks to the particular geometry, when a satellite flies in an elliptical orbit, it stays for a longer period at the apogee crossing respect to other zones of the trajectory. This results in a prolonged coverage of a particular hemisphere respect to the other [63]. If only a specific geographical area has to be covered, this factor could result very interesting. The relevance of temporal observation prolongation

depends on the value of the eccentricity of the elliptical orbit [63]. The narrow range selected for orbit altitude, comprised between 250 and 1000 km, results in very low values of achievable eccentricities, with a maximum of 0.053. These small values of eccentricity result consequently in not significant advantages in terms of coverage of a specific hemisphere, hence the use of elliptical orbits is not very profitable. Moreover, elliptical orbits are typically characterized by a wide set of hard environmental perturbation conditions that makes these orbits very unattractive. Secondly, adequate performances of the observation sensors are not guaranteed because of the presence of variations of the altitude and of the velocity during the path. These variability doesn't allow optical instruments to maintain the necessary stability during the whole orbit [63]. As a consequence, elliptical orbits require very complex satellites to achieve a good level of operation and hence are not compatible with the objective of designing a very simple and low cost platform.

In conclusion, the use of elliptical orbits appears excessively unprofitable. The lack of examples found during the missions analysis is a further proof of the inadequacy of this type of orbits. Hence, the preliminary constellation design will be performed considering only the ideal case of **circular orbits**.

6.2.3 Orbital inclination

Equatorial orbits

Equatorial orbits are orbit with inclination angle equal to 0°. Orbits of this type aren't able to observe high or even mid-latitudes regions (like for example the Tuscany), and hence are immediately discarded [3].

Tropical or inclination orbits

Tropical or inclination orbits are characterized by inclination angles comprised between 0° and 90°. This type of orbit is very appropriate if a specific region or a specific latitude belt has to be observed. In a tropical or inclination orbit the inclination of the orbit itself is determined by the location of the region of interest [3]. There are not examples found during the missions analysis of tropical or inclination orbits, and it is mainly due to the fact that almost every missions analyzed is devoted to observe the entire

globe, purpose that is unachievable with a tropical inclination orbit. Added to this, two other great disadvantages derive from the use of tropical or inclination orbits:

- the impossibility to achieve conditions of Sun-synchronism, and hence the impossibility to observe the same place every time in the same illumination conditions. With tropical or inclination orbits the daily time of observation shifts every day of a certain quantity due to the combined action of Earth rotation and of J_2 effects [3].
- The need of a dedicated launch, due to the uncommon application of this orbital solution.

Polar and near-polar orbits

Polar orbiting satellites overfly higher latitudes even though the satellite does not pass directly over the poles. The altitude of polar orbiting satellites is normally lower than 2000 km hence they are suitable for the selected range of altitudes. Satellites placed in orbits with an inclination of 90° (polar) or slightly higher than 90° (near-polar) are able to observe almost all regions of the globe [3]. Polar and near-polar orbits are the most exploited by those missions devoted to cover the entire surface of the Earth, like for example the Landsat or the SPOT missions [Chap. 4]. So, polar and near-polar orbits result so very attractive for a launch as secondary payload. Moreover, near-polar orbits offer also the possibility to design Sun-synchronus orbits [3].

Inclination or near-polar orbits?

Both inclination and near-polar orbits offer some interesting advantages suitable to design a constellation of satellites for Earth Observation. Inclination orbits appear less adequate respect to near-polar orbits but, to maintain a very wide range of possibilities within which select the most appropriate orbital solutions to design the constellation, also inclination orbits will be considered in the frame of the identification of several suitable mission architectures.

6.3 SPECIALIZED ORBITS

6.3.1 Earthsynchronus Orbits: Repeating Ground Track Orbits (RGTO)

In order to compare the temporal evolution of observed scenes, the satellite should observe after a given period of time the same locations on the surface of Earth. It's possible to synchronize the motion of the satellite with the Earth rotation, in order to allow that after a predetermined period of time the satellite ground track repeats [3].

*The satellite **ground track** is the path of the sub-satellite point on the Earth's surface. The **sub-satellite point** is the point on the Earth's surface directly between the satellite and the center of Earth* [3].

*In a **Repeating Ground Track Orbit**, the spacecraft returns after one or more days to the same location with respect to the surface of the Earth such that the path of the spacecraft repeat itself. For this to occur, an integral number of orbit periods, j, must happens during an integral number of days, k* [3].

Due to the rotation of the orbit itself caused by the action of perturbations, the exact computation of the period of a RGT orbit results more complex than it appears. To have an harmonic rotation of the Earth respect to orbital plane, the rotation of the orbit due to oblateness of the Earth (in node, perigee and mean anomaly) has to be considered. This results in an iterative process of RGTO period calculation due to the fact that Earth oblateness effects depend on orbital altitude. [3] As first estimate of needed rotation period to have a RGTO, oblateness effects have not been initially taken into account. Without considering perturbation effects, a keplerian RGTO is described by the equation 5.1 [3]:

$$h_0 = \mu^{(1/3)} \times \left(\frac{2\pi j}{\tau_E \times k}\right)^{-(2/3)} - R_E \qquad (5.1)$$

where τ_E is the **sidereal rotation period of the Earth or sidereal day** (relative to the fixed stars): $\tau_E \cong 86164.10035$ s [3].

This type of orbit provides two great advantages [3]:

- the ground track and, therefore, the geometry relative to the surface of Earth, repeats. This in turn, means that the surface of the Earth from the can be seen from the same point of view on a recurring basis during all the mission and, therefore, one image or data set can be compared with another taken at a later time from the same orientation. This makes the interpretation of changes and variations far easier, fundamental to describe land and vegetation dynamical processes.
- In addition, the geometry of the satellite's path as seen by the ground station can be followed more easily since it evolves on a recurring basis.

These specialized orbits are very useful for Earth Observation purposes, especially for applications where temporal evolution analysis is required and the same location has to be acquired every short period of time [3]. In conclusion, a satellite motion synchronized with Earth Rotation motion appears a very attractive opportunity. RGT orbits have been very frequently exploited by past and actual missions [Chap. 4] and are at the base of many planned programs. Constellations like SPOT or RapidEye are based on RGTOs [65]. In order to guarantee the very frequent revisits of a certain place to provide continuous, systematic and repetitive optical observations of land and vegetation, to ensure almost daily turn-around and response times, RGTOs are an interesting opportunity. The identification of suitable mission architectures will proceed studying deeply the potential of these orbits, trying to find appropriate solutions which combine suitable altitudes and suitable repeat cycles. Therefore, every orbital solution will be based and this characteristic.

6.3.2 Sun-synchronus Orbits (SSO)

*A **Sun-synchronus orbit** is one in which the perturbation due to the Earth's oblateness causes the orbital plane to rotate in an inertial space at a rate equal to the average rate of the Earth's rotation about the Sun. Consequently, in a Sun-synchronus orbit, the position to the Sun relative to the orbit remains approximately constant* [3].

Sun-synchronus orbits find a large application thanks to the fact that they guarantee to maintain almost constant Sun angles, and this is very useful for optical Earth Observation purposes. Maintaining a constant Sun angle ensures the possibility to acquire a certain place every time in the same illumination conditions for all the mission, and this results determinant to improve and make easier the analysis of images [63]. In the following, Sun-synchronus orbits will considered potential candidates to accommodate the constellation. Parallel, also non-Sun-synchronus orbits, which on the contrary offer the possibility to observe a certain target in different illumination conditions over time, will be considered as potential candidates.

6.3.3 Sun-synchronus Repeating Ground Track Orbits (SSRGTO)

A **SSRGTO** is an orbit which provides contemporarily the capabilities of a repeating ground track orbit and also the capabilities of a Sun-synchronus orbit [65]. Chapter 4 shows that this solution is the most exploited by satellite land and vegetation observation optical systems. Due to this and to the combination of very interesting characteristics, SSRGT orbits are considered very appropriate. This orbital solution is well exploited for example by the Landsat, the SPOT and the RapidEye programs [65] and will be more deeply analyzed during this preliminary identification of suitable mission architectures.

6.4 SUMMARY 6.1

Optical Observation System drivers, technical requirements and orbital constraints (Table 6.1).

CONSTELLATION DESIGN	
System main driver	• Mass and volume of the instrument and spacecraft. • Budget constraints. • System reliability and availability. • Timely continuity of data.

Peculiar figures of merit	• Geographical coverage.
	• Response time.
	• Revisit time.
	• On-ground resolution.
	  o Spatial.
	  o Spectral.
	• Instrument swath width.

Orbital constraints and suitable ranges	• Orbital altitude.
	  o 250 – 1000 km.
	• Orbital shape.
	  o Circular orbits.
	• Orbital inclination.
	  o Tropical or inclination orbits.
	  o Polar or near-polar orbits.

Specialized orbits	• Geosynchronus orbits. • Repeating Ground Track orbits (RGTO). • Sun-Synshcronus orbits (SSO). • SSRGTO.

Table 6.1: Chapter 6 Summary 1.

6.5 GENERIC CONSTELLATION DESIGN

To identify several orbital solutions appropriate to sustain instruments capabilities and hence to satisfy the most important mission objectives, the constellation design initially starts analyzing the simplest case of multiple satellites with all main orbital parameters in common [3]:

- orbital shape.
- Altitude.
- Inclination.
- Satellites phase shift.

The study will proceed from the simplest case by changing separately or in combination one or more orbital parameter. The generic constellation orbital solutions analysis is conceptually equivalent for each mini-constellation which will form the complete constellation, and hence it will be considered indifferently applicable to all of them. Therefore, in the following paragraph, where only orbital parameters are studied independently from the specific type of optical instrument carried on-board and therefore analysis considerations are valid in a general sense, the generic term "constellation" could be referred to every hypothetical mini-constellation. At the end of the paragraph, the generic constellation will be conceptually divided in several mini-constellations according to different payload types needed. Finally, a specific mini-constellation design will be performed once identified several suitable instruments for all categories. The specific mini-constellations design will lead to quantitative mini-constellations examples, where will be proposed several optimum combinations between instruments performance and orbital parameters. These mini-constellations examples will be then combined together to compose complete constellation potential architectures, very appropriate for the specific case of the Tuscany region. The separated design of each mini-constellation will provide also users with the capability to select services offered by only one of them.

6.5.1 Repeat Cycle (RC) analysis to achieve the 1-day revisit time capability

First of all, it is necessary to design the constellation to have a nominal geometric RC suitable to repass very frequently over targets of interest. As

reference, the entire geographical area covered by the Tuscany region is set to be the specific target of interest. The analysis of scientific requirements noticed that optical images are required within time intervals such that farmers could be able to develop weekly plans for all agricultural practices. The Tuscany region is characterized by a small extension, about 22994 km^2 of area [66], and so, with just limited capabilities in terms of satellite pointing, a satellite directly passing over the Tuscany could be able to acquire every eventual target within the region. Therefore, constellation ground-track patterns will be tailored to pass as close as possible to the region. Satellites pointing capabilities would become fundamental if larger regions have to be observed, or if regions of interest are distributed all over the world. To achieve this, appropriate combinations between nominal RC and number of satellites have to be selected. Scientific requirements analysis set the system revisit time between 1 and 3 days. Considering a certain level of confidence, nominal RCs up to 5 days will be preliminary analyzed. The goal of this preliminary analysis is to achieve the ideal best revisit time of 1 day and to understand how this could be eventually extended to more relaxed temporal performance. From the relation of RGTOs expressed by equation 5.1, it is possible to derive the values of keplerian h_0 which gives the desired (j/k) ratios and hence the desired number of revolutions per day needed to achieve RCs from 1 to 5 days.

RC computation

Actually, the proposed computation of altitudes to achieve required nominal geometric RCs doesn't take into account, besides the Earth's oblateness, the value of orbit inclination. This allows to identify indicative values of altitude from which derive a global understanding of constellation pattern trends in function of different combinations of RCs and number of satellites. Without paying particular attention on inclination it is possible to maintain available both inclination orbits and both near-polar orbits. These altitudes will be used to execute simulations useful to derive general trends of long-term atmospheric decay in function of different values of satellites total mass and to identify preliminary mini-constellation quantitative examples. To calculate altitudes correspondent to desired nominal RCs, the relation expressed by equation 5.2 has to be satisfied [62], [63]:

$$\frac{j}{k} = \left\{ \sum_{I\,=\,13{,}16} I + \left[\sum_{\substack{t\,=\,2{,}5 \\ z\,=\,1{,}(t-1)}} \frac{b}{t} \right] \right\} \tag{5.2}$$

The following nominal altitudes are derived and shown in Table 6.2.

j/k	**h_0, [km]**	**RC, [days]**
16	262	1
15	554	1
14	880	1
15.5	404	2
14.5	713	2
13.5	1059	2
15.66	358	3
15.33	454	3
14.66	661	3
14.33	769	3
13.66	1000	3
15.75	332	4
15.25	478	4
14.75	632	4
14.25	795	4
13.75	968	4
15.8	318	5
15.6	375	5
15.4	433	5
15.2	493	5
14.8	617	5
14.6	680	5
14.4	746	5
14.2	812	5
13.8	951	5
13.6	1022	5

Table 6.2: Values of altitude to achieve a nominal (RC) from 1 to 5 days.

Number of satellites

A ground-track graphical analysis has been performed using the AGI Systems Tool Kit (STK). 1- and 2-days RC schemes will be presented to derive universal analytical relations theoretically applicable to every case.

1-day RC scheme

Starting Time

Initially, the satellite (SC, in blue) is perfectly placed over the region of interest (Figure 6.1).

Figure 6.1: The satellite SC is directly placed over Tuscany at the starting time.

1st day

Perfectly after 1 sidereal day, the satellite is placed again directly over the region of interest (Figure 6.2)**.**

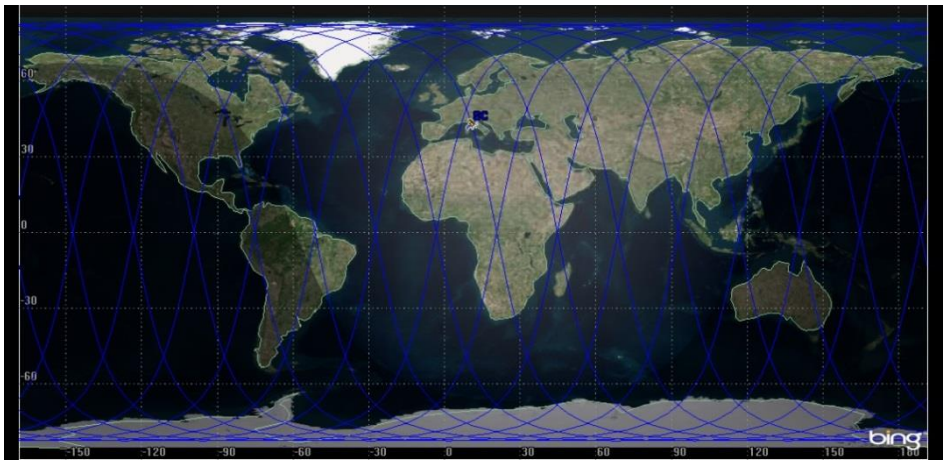

Figure 6.2: The satellite SC is again directly placed over Tuscany after 1 sidereal day.

2-days RC scheme with 1 satellite

Starting Time

Initially, the satellite (SC, in blue) is perfectly placed over the region of interest (Figure 6.3).

Figure 6.3: The satellite SC is directly placed over Tuscany at the starting time.

1^{st} day

Perfectly after 1 sidereal day, the satellite ground track is shifted respect to the starting time and the satellite doesn't repass directly over the region of interest (Figure 6.4).

The satellite ground track is shifted respect to the starting time of a quantity which is function of the (j/k) ratio and of the latitude of the region of interest:

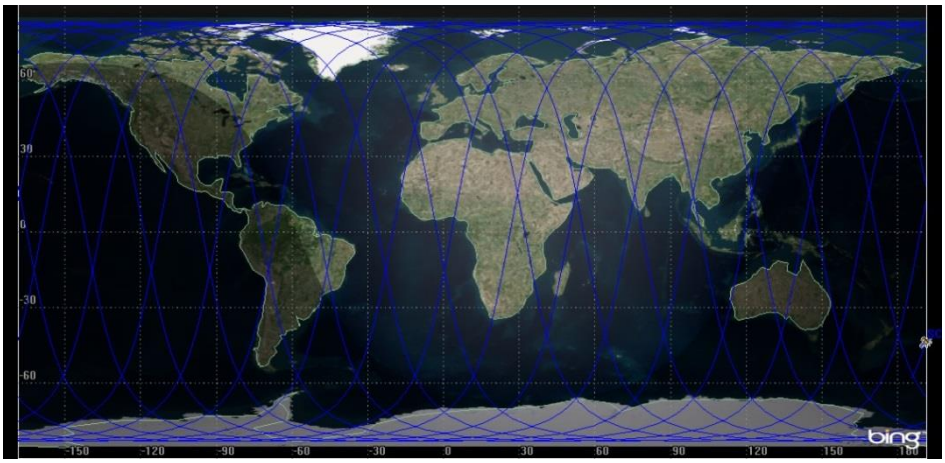

Figure 6.4: The ground-track is shifted after 1 sidereal day and the satellite SC doesn't repass over the Tuscany.

2nd day

After 2 sidereal days, the satellite is placed again perfectly and directly over the region of interest (Figure 6.5) like in the starting time, as expected. Its ground tracks are more densely distributed all over the entire world respect to the 1-day RC case previously visualized.

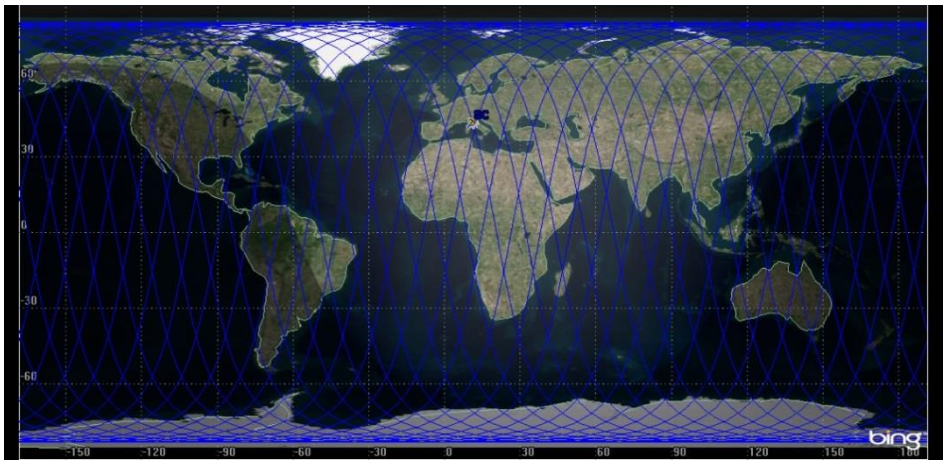

Figure 6.5: Satellite is again directly placed over Tuscany after 2 sidereal days.

2-days RC scheme with 2 satellites

Starting Time

The spacecraft 1 (SC1, in blue) is placed directly over the region of interest and the spacecraft 2 (SC2, in red) is properly phased respect to it: therefore, it is shifted of about 180° within the same identical orbit respect to SC1 (figure 5.6).

Figure 6.6: The satellite SC1 is directly placed over the region of interest at the starting time.

1st day

After 1 sidereal day, the SC2 occupies the position previously occupied by SC2 and it is placed directly over the region of interest (Figure 6.7).

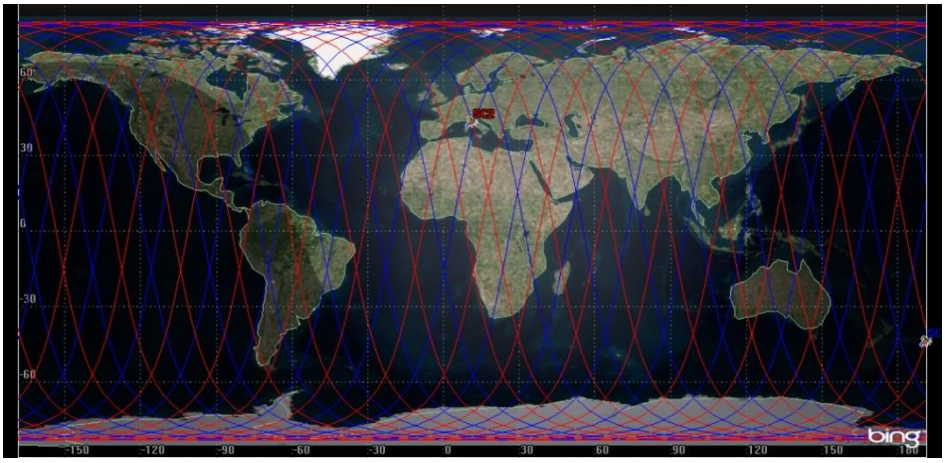

Figure 6.7: After 1 sidereal day, the satellite SC2 is directly placed over the Tuscany.

2nd day

After 2 sidereal days, the positions of satellites become again as at the starting time, with the satellite SC1 placed directly over the Tuscany. In conclusion, during the second day, SC1 has described the ground track described by SC2 during the previous day and *vice versa* (Figure 6.8). Hence, during the 2-days RC, all satellites passed directly over the region of interest once and every day the region of interest has been in view at least from one satellite.

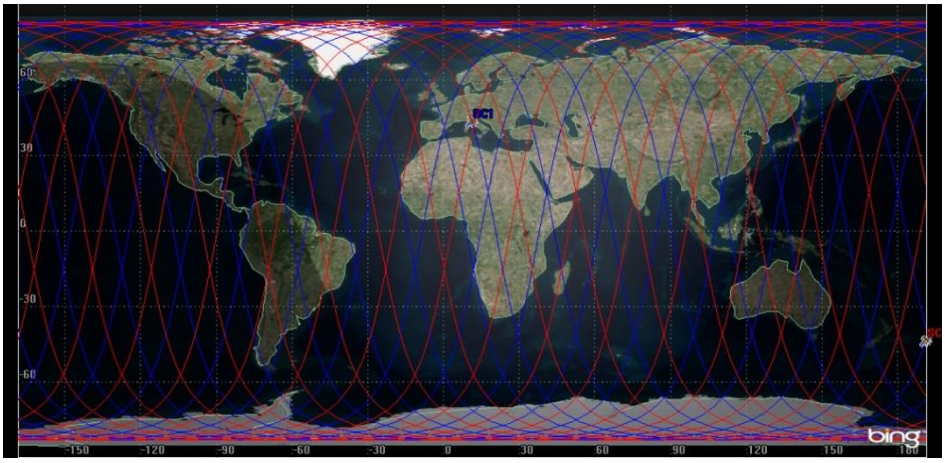

Figure 6.8: After 2 sidereal days, the satellite SC1 is again placed directly over the Tuscany.

RC analysis conclusions

The schemes shown by images can be easily extended to all RC cases. As expected, a generalized relation could be computed to quantify the daily ground-track shift D_{Shift} relative to every nominal RC case in function of (j/k) and latitude. The generalized formula is shown by equation 5.3:

$$D_{Shift} = \frac{2\pi R_E}{(\frac{j}{k})} \times \frac{1}{RC} \times \cos\lambda \tag{5.3}$$

where λ is the latitude of the region of interest. According to equation 5.3 and considering results reported by figures relative to the 2-days RC, to repass every day directly over the region of interest is needed a number of satellites at least equal to the value of the nominal RC. The analysis shows also that high values of nominal RC are in favour of a denser coverage of the globe but are not in favour of a limited number of satellites for the same revisit time performance. Therefore, to design a low-cost mission with a low number of satellites, the choice of values of RC not higher than 5 days has been confirmed in this sense very appropriate. Moreover, altitudes identified in the RC computation cover homogeneously the whole range of altitude selected. In conclusion, the analysis appears complete and coherent. To design a very capable system, the target performance of 1 day revisit time frequency has been selected as starting point. Lower performance could be easily achieved by adequately tailoring analytical relation reported by previous equations. In conclusion, all the altitude solutions found are suitable to achieve the 1-day revisit time frequency potentially required by agricultural applications with a limited number of satellites and hence will be used as starting points to derive appropriate constellation and mini-constellation architectures.

6.5.2 Repeat coverage analysis to observe the whole Tuscany every day

The analysis proceeds trying to find suitable solutions to cover every day the whole extension of the region of interest. There exist a slight difference between:

- *revisit time of every eventual target within the entire region.*
- *Repeat coverage of every target within the entire region*.

In the first case, if a satellite passes directly over the region of interest every day, it can *"potentially"* acquire every target by means of appropriate pointing, but not *"all"* target during one pass. This is different from the situation in which every target *"is"* effectively acquired every day. In the coverage of the entire region, are determinant the extension of the Tuscany and the swath width of instruments carried on-board. Supposing to divide the Tuscany in *"strips"*, each of them geometrically characterized by an horizontal dimension W_{Strip} equal to the generic instrument swath width S_W, there is a number of strips N_{Strip} (equation 5.4):

$$N_{Strip} \cong \frac{D_{Tuscany}}{W_{Strip}} \tag{5.4}$$

where $D_{Tuscany}$ is assumed to be the maximum longitudinal dimension of Tuscany. If each of these strips is specifically allocated to a single satellite of the constellation, this means that this satellite is devoted to observe *"only"* that strip and to acquire only that specific portion. So, the number of satellites N^* needed to cover the entire region, at a first analysis, becomes (equation 5.5):

$$N^* = \frac{D_{Tuscany}}{W_{Strip}} = \frac{D_{Tuscany}}{S_w} = N_{Strips} \tag{5.5}$$

To allow each satellite to acquire exactly a specific strip with the highest image quality possible (quasi-nadir mode), satellites relative positions within the orbit plane have to be properly phased. This results in a constellation where satellites aren't equally spaced within the orbit plane. Relative angular positions $\Delta\varphi_{relative}$ can be calculated according to equation 5.6:

$$\Delta\varphi_{relative} = \left[\left(\frac{\tau_E \times S_w}{2\pi R_e \cos\lambda}\right) \times \frac{360}{\tau}\right] \tag{5.6}$$

where τ is the keplerian orbit period. Examples are provided by following figures, where 3 satellites, able to provide a swath width of about 60 km

from an altitude of 554 km, are needed to cover the entire Tuscany region. Figure 6.9 shows the passage of the first satellite (Strip1, in red), devoted to acquire the most easterly strip. The swath width edges of the first satellite are indicated by the red lines.

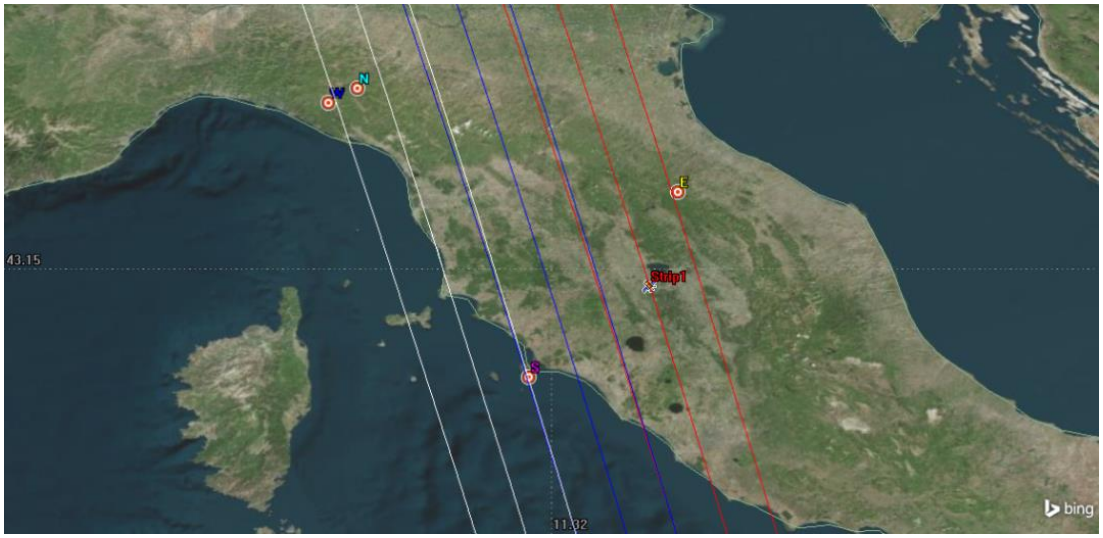

Figure 6.9: The Strip1 satellite images the most easterly Tuscany side during one pass.

Figure 6.10 and Figure 6.11 show the successive passages of the second satellite (Strip2, in blue) and of the third satellite (Strip3, in white), devoted to acquire the central and the most westerly strip, respectively. The swath width edges of satellites are indicated by the blue and the white lines.

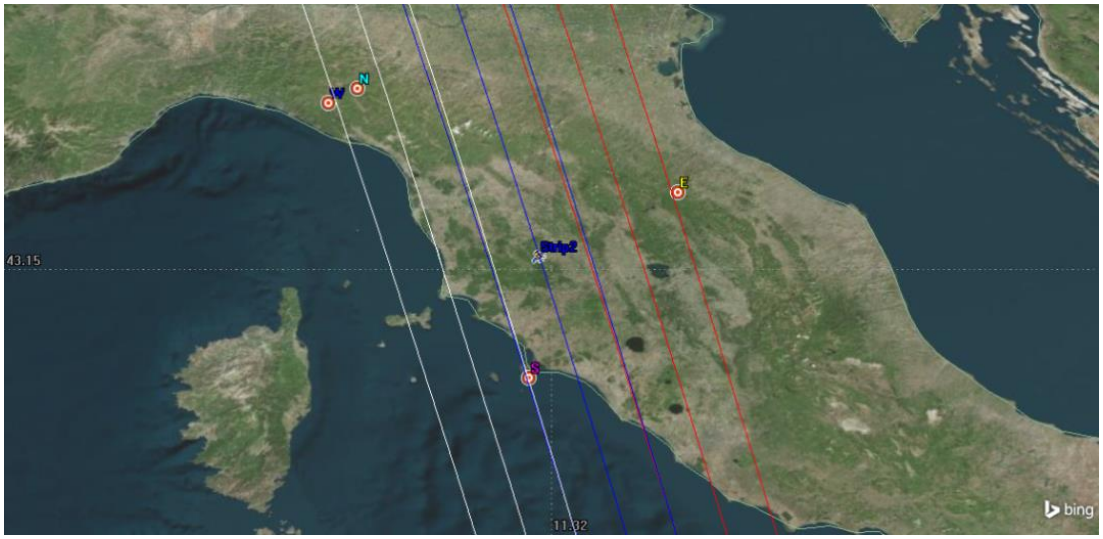

Figure 6.10: The Strip2 satellite images the central portion of Tuscany during one pass.

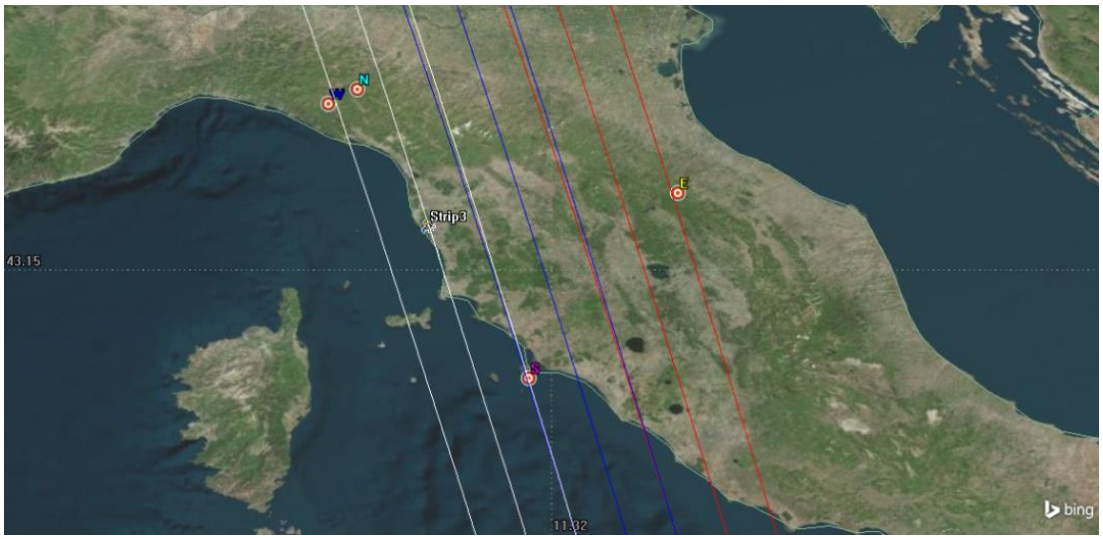

Figure 6.11: The Strip3 satellite images the most westerly Tuscany side during one pass.

Figures show that Tuscany could not easily be geometrically approximated and also that orbit inclination is important to identify the real number of strips. Satellites in the example are placed on a near-polar orbit. As a reference, in the figures are reported 4 relevant points [66]:

- N, the most northerly Tuscany point.
- S, the most southerly Tuscany point.
- W, the most westerly Tuscany point.
- E, the most easterly Tuscany point:

The distance between points E and O is the longest distance within the entire region, about 210 km. Therefore, $D_{Tuscany}$ can be initially taken equal to 210 km at this first step of computation, when many different altitudes and instrument swath width capabilities have to be considered. In future computation steps, when the number of possibilities will be reduced, more precise graphical analysis will be conducted with AGI STK (Systemas Tool Kit) to really quantify N_{Strip}. This approximation allows to perform an easier initial estimate of number of strips without initially considering inclination. If, the eventual selected instrument is characterized by a swath width such that (equation 5.7):

$$S_w \geq D_{Tuscany} \tag{5.7}$$

hence, it would be possible to divide the whole region in a single hypothetical strip and to acquire it with just one satellite. This concept is shown by the Figure 6.12 (where an inclination of 55° has been selected).

Figure 6.12: Acquisition of the entire Tuscany during a single pass from an inclination orbit.

An example of land division in strips is provided by RapidEye observation of the Germany (Figure 6.13). In this case, the repeat coverage of the entire country is performed every 5 days with 5 satellites. The less frequent repeat coverage is due to the larger dimensions of Germany respect to Tuscany and to the fact that the RapidEye constellation has to observe lands all over the world [27].

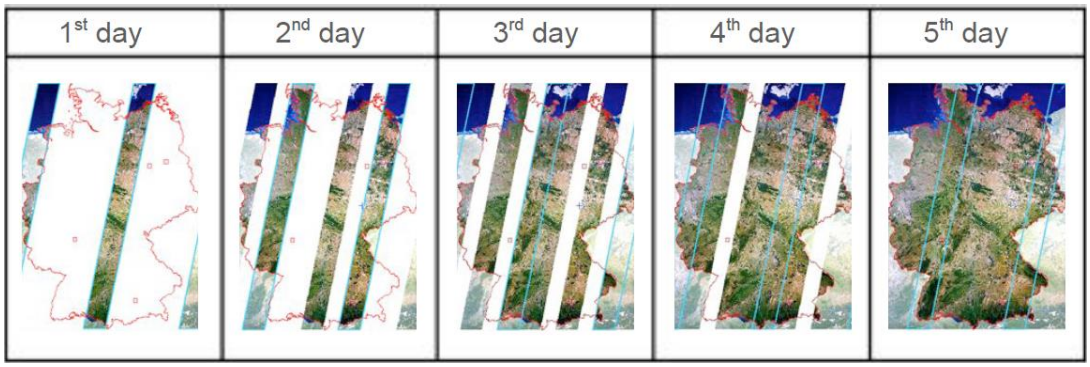

Figure 6.13: 5-days acquisition of the Germany by RapidEye constellation.

Number of satellites for a daily repeat coverage of the whole Tuscany calculation

To cover the entire region in quasi-nadir mode, the constellation needs a number of satellites at least equal to the number of strips. If satellites are equipped with an instrument characterized by a swath width such that the Tuscany could be divided into n strips, hence the constellation needs at least n identical satellites adequately phased. If satellites are placed at an altitude such that the orbit nominal RC is higher than 1 day, n satellites aren't sufficient to observe the whole region every day. To have a daily full coverage of the whole region with an orbit nominal RC higher than 1 day, is required a number of satellites equal to the number of strips over the region during every day of the nominal cycle. The total number of satellite N_S therefore becomes (equation 5.8):

$$N_S = RC \times N_{Strips} \tag{5.8}$$

These results are valid in a first approximation for each altitude identified in the 1 to 5-days nominal RC range and generally for every value of RC, even if more accurate graphical analysis are needed to verify them. This highlights the need to select multispectral and hyperspectral instruments characterized by a proper combination of:

- spatial resolution performance.
- Swath width capabilities.

This combination would have to provide the required level of performance with a limited number of satellites. Equivalently to the daily revisit time number of satellites computation, this analysis is devoted to identify the best possible solutions to *cover the entire region of interest every day*. Depending on different users that could be involved, the coverage frequency could be relaxed from the 1-day performance to more extended temporal performance and targets of interest, if heterogeneously distributed within the region, could be properly selected . In this particular case, the total number of satellites could be easily determined by proportionally tailoring previous relations to the specific request.

6.6 SUMMARY 6.2

Generic constellation characteristics identification (Table 6.3).

CONSTELLATION DESIGN	
Single set of satellites with all orbital parameters in common	• Orbital shape. • Altitude. • Inclination. • Satellites phase shift.
Repeat cycle RC computation	• From 1 day to 5-days nominal repeat cycle (RC).

Revisit frequency of every eventual target within the region capability	• $\boldsymbol{N_S} < RC$.
	  ○ If the revisit is not required every day.
	• $\boldsymbol{N_S = RC}$.
	  ○ If a daily revisit is required.

Tuscany division in strips and repeat coverage of the entire region capability	• $\boldsymbol{N_S} < RC \times \boldsymbol{N_{Strips}}$.
	  ○ If the repeat coverage is not required every day.
	• $\boldsymbol{N_S = RC \times N_{Strips}}$.
	  ○ If a daily revisit is required.

Table 6.3: Chapter 6 Summary 2.

6.7 SPECIFIC-OPTICAL TASK MINI-CONSTELLATIONS

In this paragraph the nature of each mini-constellation which will compose the complete constellation will be specified. The division in mini-constellations is based on the different nature of optical instruments needed to satisfy all spatial and spectral requirements.

6.7.1 Specific-optical observation task mini-constellations

Due to the reduced dimensions of the expected platform and therefore to the reduced volume and mass available for the single payload, will be selected optical instruments able to satisfy only one specific characteristic required to the entire system. In fact, the study performed in Chapter 4 noticed that sensors which offer a compromise between a good spatial resolution and a moderately high number (more than 10) of spectral bands, are characterized by excessively heavy mass, not suitable for microsatellite applications. This is for example the case of the VENμS VSCC (43.5 kg). Therefore, three different types of optical instruments have been considered suitable to provide useful information in the frame of agricultural monitoring and management practices, both separately and both in cooperation:

- a ***multispectral*** instrument with very good spatial resolution performance (< 30 m), combined with good swath width capabilities and characterized at least by the 2 fundamental spectral channels (RED and NIR) and eventually also with the BLUE and the GREEN channels.
- An ***hyperspectral*** instrument with medium spatial resolution performance (30 - 100 m) characterized by many very narrow spectral bands covering the VIS, the NIR and the SWIR.
- A single ***thermal IR*** channel instrument.

The previously analysis on the orbital design of a generic constellation could be extended to each type of specific-optical task mini-constellations:

- a ***base specific-multispectral optical observation*** mini-constellation devoted to cover every day the whole extension of the Tuscany, providing images with a spatial resolution at least lower than 30 m. This mini-constellation is intended to produce information useful to satisfy a very large part of scientific requirements, especially from

the point of view of land and agricultural monitoring, mapping, acreage and management. This mini-constellation has to be the *"core"* of the mission and all other mini-constellations are principally intended to complete and sustain it.

- a ***base specific-hyperspectral optical observation*** mini-constellation devoted to cover every day the whole Tuscany with a spatial resolution at least lower than 100 m. It is intended to acquire very fine spectral details needed to improve the multispectral vegetation species discrimination and crop classification, to describe very accurately crop health conditions and phenology cycle, and to measure the soil moisture content. It is also expected to provide a service of early anomalies detection, fundamental to identify specific problematic zones where accurately direct the attention of the more spatially refined multispectral mini-constellation.
- a ***base specific-thermal IR optical observation*** mini-constellation formed by satellites equipped with a single (or double) channel TIR instrument devoted to perform additionally large-scale thermal measurements of land and soil, to identify specific zones where intensive and targeted irrigation practices are needed. Finally, thermal IR mini-constellation has to be able also to provide a service of wild fire detection and monitoring. It is the mini-constellation which has to provide the lowest spatial resolution performance, from 100 to 500 m.

From the orbital point of view, for each mini-constellation the best solution appears to be the simplest configuration: all satellites adequately phased within a single orbit plane and all at the same altitude. Several constellation architecture examples will be proposed in the following after a quantitative analysis of instrument specifications, mass and performance. These examples will be indicative and only a part of the wide range of possible architectures, as a confirm of the high versatility of the mission under study.

6.8 ACTUAL AND PLANNED SMALL MULTISPECTRAL, HYPERSPECTRAL AND THERMAL IR LAND AND VEGETATION OBSERVATION INSTRUMENTS

The identification of suitable mission architectures needs more detailed information about instruments specifications:

- levels of spatial resolution and swath width.
- Number, type and width of spectral channels recorded.
- Mass.

Several suitable instruments have been yet described in the Chapter 4 in relation to their respective missions and satellites. In this section a bigger attention will be paid only on significantly small instruments, in order to identify general technological trends compatible with microsatellite platforms. Only instruments with a mass lower than 20 kg have been considered.

6.8.1 Multispectral optical Earth Observation sensors

During small multispectral optical Earth Observation instruments analysis, many examples of sensors devoted to produce optical images useful also for agricultural monitoring and management practices have been found. Between them, the Hodoyoshi-4 HRMS, the SPOT-6 & 7 NAOMI and the DMC SLIM-6-22 have been already mentioned in Chapter 4. In this paragraph, also the characteristics of the X-Sat IRIS, the IMS-1 Mx-T [18], [2], the Rising-2 HPT [67], and the Hodoyoshi-1 OC [53], [54], will be shown. Multispectral instruments satellite, operation altitude and mass are shown in Table 6.4:

Instrument	Satellite	Altitude, [h]	Mass, [kg]
HPT	Rising-2	700	< 10
HRMS	Hodoyoshi-4	630	9
IRIS	X-Sat	820	12
Mx-T	IMS-1	632	5.8
NAOMI	SPOT 6-7	695	18.5
OC	Hodoyoshi-1	500	15
SLIM-6-22	DMC	686	12

Table 6.4: Multispectral analyzed instruments and their satellite, altitude and mass.

Multispectral instruments spatial and spectral performance are shown in Table 6.5:

Instrument	GSD, [m]	Swath, [km]	Spectral bands
HPT	5	3	RGB & NIR
HRMS	5 (from 500 km)	20	RGB & NIR
IRIS	12	50	RG & NIR
Mx-T	36	150	RGB & NIR
NAOMI	8, MS; 2, PAN	25	RGB, NIR & PAN
OC	6.7	27.8	RGB & NIR
SLIM-6-22	22	600	RG & NIR

Table 6.5: Multispectral analyzed instruments and their spatial and spectral performance.

Multispectral observations: the advantage of using different instruments

An interesting solution suggested by the small multispectral instruments analysis could be to select a combination of two types of multispectral instruments:

- one characterized by a fair spatial resolution (in the 10 - 30 m range) combined with a very good swath width to satisfy the full daily coverage of the entire region with a limited number of satellites.
- An additional sensor characterized by a very good spatial resolution (smaller than 5 m).

With such different multispectral instruments, the multispectral mini-constellation could result divided into *two* multispectral mini-constellations:

- a *base multispectral mini-constellation*, devoted to observe the whole region every day and to offer a continuous land monitoring service, especially on large scale.
- an *add-value multispectral mini-constellation*, able to satisfy every additional specific request of very high spatial resolution acquisition every day without daily covering the whole region (and hence, designed to have only the 1-day revisit time capability). The add-value mini-constellation could be for example designed to operate at a lower altitude respect to the base mini-constellation to further improve spatial resolution.

The mini-constellations combination will provide:

- even with a low number of satellites, continuous and systematic observations suitable for many agricultural monitoring purposes.
- Very high spatial resolution performance, sufficient to satisfy precision agriculture requests.

For the *base multispectral* mini-constellation, the SLIM-6-22 could be seriously considered a potential candidate to represent the technological specifications and performance required. SLIM-6-22 is particularly favorable thanks to its reduced mass, to its fair spatial resolution performance and especially to its very large swath width. Despite some unattractive characteristics, for the *base multispectral* mini-constellation other two instruments could be considered potential candidate to marginally represent the technological specifications and performance required:

- The Hodoyoshi-1 OC.
- The Indian Mini-Satellite-1 (IMS-1) Mx-T.

For the *add-value multispectral* mini-constellation, the Hodoyoshi-4 HRMS (Figure 6.14) and the Rising-2 HPT could be seriously considered potential candidates to represent the technological specifications and performance required, especially thanks to their low mass and to their very good spatial resolution performance.

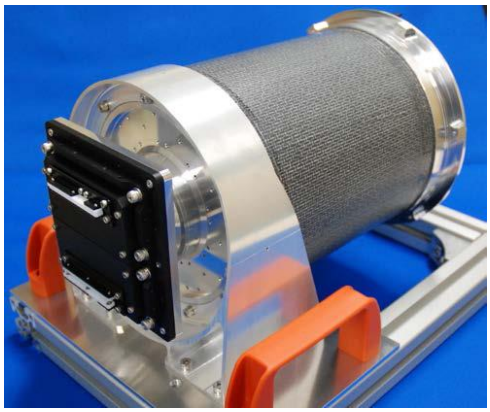

Figure 6.14: Hodoyoshi-4 HRMS.

Moreover, thanks to the RGB channels presence and therefore to the possibility of creating true color maps, they could cover the lack in this

sense of the SLIM-6-22, which hasn't the BLUE channel. These instruments are very similar but show two differences:

- the HRMS swath width is larger respect to HPT. The selection of one of them depends on the size of targets to be acquired.
- The observations in the NIR channel. The HRMS has a single NIR channel, while HPT is equipped with particular filters, the Liquid Crystal Tunable Filters (LCTF). The LCTF can electrically change the central wavelength in the unit of 1 nm. This means that LCTF has 400 potential spectral bands in the NIR region. This makes HPT multispectral observations in the NIR region equivalent to hyperspectral observations [67].

Despite some unattractive characteristics, for the *add-value multispectral* mini-constellation also the X-Sat IRIS could be considered a potential candidate to marginally represent the technological specifications and performance required. On the contrary, the SPOT 6-7 NAOMI doesn't offer very interesting advantages in terms of spatial resolution or swath width capabilities respect to others. Therefore, this instrument won't be used to derive multispectral mini-constellations architecture examples.

6.8.2 Hyperspectral optical Earth Observation sensors

During small hyperspectral optical Earth Observation instruments analysis, many examples of sensors devoted to produce optical images useful also for agricultural monitoring and management practices have been found. Between them, the CHRIS and the COMIS instruments have been already analyzed in Chapter 4. Another interesting instrument under development, the compact hyperspectral imager breadboard Phytomapper [68], [69], will be shown to identify general performance technological trends and to verify effective compatibility with the *base hyperspectral* mini-constellations purposes. Hyperspectral instruments satellite, operation altitude and mass are shown in Table 6.6:

Instrument	Satellite	Altitude, [h]	Mass, [kg]
CHRIS	PROBA-1	600	14
COMIS	StSat-3	700	4.3
PHYTOM.	/	600	5

Table 6.6: Hyperspectral analyzed instruments and their satellite, altitude and mass.

Hyperspectral instruments spatial and spectral performance are shown in Table 6.7:

Instrument	GSD, [m]	Swath, [km]	Spectral bands
CHRIS	18-36	14	VNIR: 18-63
COMIS	30-60	15-30	VNIR: 64
PHYTOM.	100	360	VNIR & SWIR: up to 2400

Table 6.7: Hyperspectral analyzed instruments and their spatial and spectral performance.

For the *base hyperspectral* mini-constellation, the Phytomapper could be seriously considered a potential candidate to represent the technological specifications and performance required, especially thanks to its very low mass, to its very large swath width and to the high number of spectral channels recorded over a large portion of the electromagnetic spectrum. The Phytomapper, principally thanks to its large swath width, is expected also to provide an optimum service of early anomalies detection [68]. Multispectral instruments, depending on specific user and hence on spatial resolution level required, will be directed to better analyze the zone interested by the anomaly. Despite some unattractive characteristics, for the *base hyperspectral* mini-constellation also the COMIS could be considered a potential candidate to marginally represent the technological specifications and performance required. On the contrary, the CHRIS, which is characterized by very similar performance respect to the COMIS but it has an higher mass, won't be used to derive base hyperspectral mini-constellation architecture examples.

6.8.3 Single Thermal IR channel optical Earth Observation sensors

During scientific requirements and small thermal optical Earth Observation instruments analysis, two very interesting examples of sensors devoted to produce optical images useful also for agricultural monitoring and management practices have been found, the CIRC and the HSRS instruments, already mentioned in Chapter 4 [18]. TIR instruments satellite, operation altitude and mass are shown in Table 6.8:

Instrument	Satellite	Altitude, [h]	Mass, [kg]
CIRC	Alos-2	640	2.6
HSRS	BIRD	572	13.9

Table 6.8: TIR analyzed instruments and their satellite, altitude and mass.

TIR instruments spatial and spectral performance are shown in Table 6.9:

Instrument	GSD, [m]	Swath, [km]	Spectral bands
CIRC	200	128	Single TIR
HSRS	392	190	Double TIR

Table 6.9: TIR analyzed instruments and their spatial and spectral performance.

For the *base thermal IR* mini-constellation, both instruments could be considered potential candidate to represent the technological specifications and performance required.

6.8.4 Specific mini-constellations satellites number analysis

According to equation 5.8, each analyzed instrument has been used to derive preliminary indications about the number of satellites required to satisfy each mini-constellation temporal requirement for the specific case of the Tuscany. The analysis depends on operation altitude and nominal RC.

Base multispectral mini-constellation number of satellites analysis results and conclusions

As expected:

- the lowest satellites number could be obtained exploiting a very large swath instrument like the SLIM-6-22.
- Values of nominal RC higher than 1 or 2 days are very unfavorable and unjustified if are used instruments characterized by a narrow swath width.

Therefore, the SLIM-6-22 results to be the best solution to represent performance required to the potential instrument for the base multispectral mini-constellation.

Add-value multispectral mini-constellation number of satellites analysis conclusions

As expected, the satellites number results are equivalent for all three instruments in relation to reduced Tuscany extension. Instruments swath width capabilities don’t affect the number of satellites analysis, only altitudes and the respective nominal RC. Considering that the Hodoyoshi-4 has an higher swath width respect to Rising-2 HPT and a spatial resolution

and a mass almost identical, it results to be the best solution to represent performance required by potential instrument for the add-value multispectral mini-constellation. Anyway, both the HPT and also the X-Sat IRIS represent valid alternative to the HRMS, even if the IRIS appears less appropriate respect to other two instruments.

Base hyperspectral mini-constellation number of satellites analysis conclusions

As expected:

- the lowest satellites number could be obtained exploiting a very large swath instrument like the Phytomapper.
- Values of nominal RC higher than 1 or 2 days are very unfavorable and unjustified with instruments characterized by a narrow swath width.

Therefore, the Phytomapper results to be the best solution to represent performance required to the potential instrument for the base hyperspectral mini-constellation.

Base thermal IR mini-constellation number of satellites analysis conclusions

As expected:

- satellites number results are better for the instrument with the largest swath, the BIRD HSRS.
- Values of nominal RC higher than 1 or 2 days are very unfavorable and unjustified with instruments characterized by a narrow swath width.

Anyway, considering that the Alos-2 CIRC has a much lower mass respect to BIRD HSRS and a much better spatial resolution, it results to be the best solution to represent performance required to the instrument for the base thermal IR mini-constellation.

6.9 COMPLETE OPTICAL CONSTELLATION PRELIMINARY ARCHITECTURE EXAMPLES

Previous results provide general indications about the best solution for daily acquisition by each specific mini-constellation in terms of:

- instrument type.
- Operation altitude.
- Satellites number.
- Achievable spatial resolution levels.

Several potential combinations of mini-constellations could generate mission architecture examples which ensure to respond to every kind of requests coming from government, commercial, industrial, civilian and educational users. An hypothetical complete optical system composed by proposed mini-constellations should provide the same level of spatial and spectral performance ensured by a large single satellite equipped with multiple different instruments but with very better temporal performance and with a very reduced cost. Previously mini-constellations, if appropriately combined, can generate images useful in many fields, not only focused on agriculture.

6.9.1 Proposed complete constellation architecture examples

Following complete constellation architecture examples derive from the combination of all mini-constellations for the specific case of the Tuscany region and only the most interesting of them will be shown in this frame. Architecture examples, shown from following figures, have been created and classified according to the:

- research of the lowest possible number of satellites.
- Achievement of all required performance.
- Research, where possible, of the best compromise in terms of minimum satellites number and best performance.

The classification is based on 4 levels of suitability:

- **FAIR.**
- **GOOD.**
- **VERY GOOD.**
- **OPTIMUM.**

Optical Task	Instrument	h, [km]	GSD, [m]	N_S
Base MS	SLIM-6-22	404	14	2
Add-Value MS	HRMS	404	4	2
Base HS	PHYTOM.	404	67	2
Base TIR	CIRC	554	173	2
Total N_S = 8				

Table 6.10: Architecture example n°1.

Optical Task	Instrument	h, [km]	GSD, [m]	N_S
Base MS	SLIM-6-22	554	18	1
Add-Value MS	HRMS	404	4	2
Base HS	PHYTOM.	404	67	2
Base TIR	CIRC	554	173	2
Total N_S = 7				

Table 6.11: Architecture example n°2.

Optical Task	Instrument	h, [km]	GSD, [m]	N_S
Base MS	SLIM-6-22	554	18	1
Add-Value MS	HPT	554	4	1
Base HS	PHYTOM.	404	67	2
Base TIR	CIRC	554	173	2
Total N_S = 6				

Table 6.12: Architecture example n°3.

Optical Task	Instrument	h, [km]	GSD, [m]	N_S
Base MS	SLIM-6-22	554	18	1
Add-Value MS	HPT	554	4	1
Base HS	PHYTOM.	554	92	1
Base TIR	CIRC	554	173	2
Total N_S = 5				

Table 6.13: Architecture example n°4.

Optical Task	Instrument	h, [km]	GSD, [m]	N_S
Base MS	SLIM-6-22	554	18	1
Add-Value MS	HPT	554	4	1
Base HS	PHYTOM.	554	92	1
Base TIR	CIRC	880	275	1
Total N_S = 4				

Table 6.14: Architecture example n°5.

Optical Task	Instrument	h, [km]	GSD, [m]	N_S
Base MS	SLIM-6-22	554	18	1
Add-Value MS	HPT	554	4	1
Base HS	PHYTOM.	554	92	1
Base TIR	HSRS	554	380	1
Total N_S = 4				

Table 6.15: Architecture example n°6.

Optical Task	Instrument	h, [km]	GSD, [m]	N_S
Base MS	SLIM-6-22	554	18	1
Add-Value MS	HRMS or HPT	358	< 3	1
Base HS	PHYTOM.	404	67	1
Base TIR	CIRC	404	126	2
Total N_S = 5				

Table 6.16: Architecture example n°7, relaxed temporal performance coming from the combination of previous examples and using a further lower altitude.

Optical Task	Instrument	h, [km]	GSD, [m]	N_S
Base MS	SLIM-6-22	554	18	1
Add-Value MS	HPT	554	4	1
Base HS	COMIS	880	75	5
Base TIR	CIRC	554	173	2
Total N_S = 9				

Table 6.17: Architecture example n°8.

Optical Task	Instrument	h, [km]	GSD, [m]	N_S
Base MS	OC	880	12	4
Add-Value MS	HPT	554	4	1
Base HS	PHYTOM.	554	92	1
Base TIR	CIRC	554	173	2
Total N_S = 8				

Table 6.18: Architecture example n°9.

Optical Task	Instrument	h, [km]	GSD, [m]	N_S
Base MS	Mx-T	404	23	1
Add-Value MS	IRIS	404	6	1
Base HS	PHYTOM.	404	67	1
Base TIR	CIRC	554	173	2
Total N_S = 5				

Table 6.19: Architecture example n°10.

6.9.2 Proposed complete constellation architecture examples discussion and selection of the most interesting examples

Examples proposed show that:

- all temporal, spatial and spectral resolution requirements for Tuscany agriculture could be satisfied with a very limited number of small satellites, from a minimum of 4 to a maximum of 9.
- Not very low altitudes (generally higher than 400 km) could be profitably exploited to satisfy on-ground resolution requirements.
- Satellites could work well at close orbital altitudes: hence propellant expense for maneuvers after launch could be maintained low.
- Further simulations are needed to understand the real total mass needed to carry on-board proposed instruments and to maintain selected altitudes.
- The mission design by means of the division in mini-constellations allows an eventual customer to select within a very wide range of possibilities, going from the complete optical constellation services to the services offered by a single mini-constellation.
- As expected, such very frequent and complete acquisitions could provide benefits not only in the frame of agriculture, but also in many other fields, like natural resources management and disaster

monitoring, strictly linked to agriculture. This is testified by the presence of instruments like the SLIM-6-22, in particular able to detect and control fires and floods, very important in the case of Tuscany, and also like the Phytomapper. The role of the thermal IR mini-constellation in the wild fire detection further evidences this conclusion. This last consideration confirms how the previous analysis could be extended to a large part of Earth Observation purposes, especially in the case of land and vegetation management.

Moreover, examples 7 and 10 show a complete optical constellation where acquisition frequencies are relaxed from the 1 day temporal performance, and confirm:

- the large versatility of the mission design.
- The possibility to simply scale the 1-day repass frequency to every other tailored frequency for all mini-constellation.

6.9.3 Description of most interesting selected architectures

In conclusion, 3 examples are considered very suitable and appropriate for Tuscany observation: examples number 2, 6 and 7, shown again in Table 6.20, Table 6.21 and Table 6.22. The proposed mission architecture I (Table 6.20) derives from the example 2. It represents the best compromise in terms of performance and satellites number. The entire range of spatial and spectral resolution levels required by users is covered. Every day, all instruments are able to repass directly over Tuscany to generate products useful for all applications and for all kind of user.

Optical Task	Instrument	h, [km]	GSD, [m]	N_S
Base MS	SLIM-6-22	554	18	1
Add-Value MS	HRMS	404	4	2
Base HS	PHYTOM.	404	67	2
Base TIR	CIRC	554	173	2
Total N_S = 7				

Table 6.20: Proposed mission architecture I.

The proposed mission architecture II (Table 6.21) derives from the example 6. It represents the best way to achieve daily frequencies and sufficient performance with a minimum number of satellites. In this sense,

the HPT and the HSRS replace the HRMS and the CIRC. Architecture I has the further advantage that all satellites are placed at the same altitude. The entire range of spatial and spectral resolution levels required by users is covered. Every day, all instruments are able to repass directly over Tuscany to generate products useful for all applications and for all kind of user.

Optical Task	Instrument	h, [km]	GSD, [m]	N_S
Base MS	SLIM-6-22	554	18	1
Add-Value MS	HPT	554	4	1
Base HS	PHYTOM.	554	92	1
Base TIR	HSRS	554	380	1
Total N_S = 4				

Table 6.21: Proposed mission architecture II.

The proposed mission architecture III (Table 6.22) derives from the example 7. The add-value MS and the base HS mini-constellations are in this case characterized by relaxed temporal performance respect to other mission architectures (3 days) but provide very improved spatial resolution levels thanks to the very low altitudes assigned. The entire range of spatial and spectral resolution levels required by users is covered. The contemporary presence of the HRMS and of the HPT evidences the large versatility of the mission design and the possibility to select one of them depending on the spatial resolution level required and especially on the swath width capabilities expected from the add-value MS mini-constellation. Two satellites could be assigned to the base TIR mini-constellation to maintain a daily dual source of wild fire monitoring and detection in combination with the base MS mini-constellation.

Optical Task	Instrument	h, [km]	GSD, [m]	N_S
Base MS	SLIM-6-22	554	18	1
Add-Value MS	HRMS or HPT	358	< 3	1
Base HS	PHYTOM.	358	60	1
Base TIR	CIRC	404	126	1 – 2
Total N_S = 4 – 5				

Table 6.22: Proposed mission architecture III.

These 3 examples:

- cover the whole range of temporal, spatial and spectral requirements.

- A very large gamma of instrument mass, from the 2.6 kg of the CIRC to the 13.9 of the HSRS.
- Reach the interesting low altitude of about 358 km.

Therefore, considering the very high performance achievable, the very large number of services potentially offered in many fields and the very low number of satellites expected, they will further analyzed to identify the total mass required to perform the mission architecture they propose.

6.10 SUMMARY 6.3

Mini-constellation definition, instruments analysis and complete optical constellation architectures identification (Table 6.23).

SPECIFIC MINI-CONSTELLATIONS AND COMPLETE CONSTELLATION DESIGN	
Constellation conceptual division in specific-optical task mini-constellation	Mini-constellation concept: • Identical platform. • Identical instruments within each mini-constellation. • Different instruments from a mini-constellation to another.

Specific-optical task mini-constellations	According to scientific requirements:
	• Base MS mini-constellation.
	  ○ GSD lower than 30 m.
	  ○ RED and NIR bands.
	• Add-Value MS mini-constellation.
	  ○ GSD lower than 5 m.
	  ○ RGB and NIR bands.
	• Base HS mini-constellation.
	  ○ GSD lower than 100 m.
	  ○ VIS, NIR and SWIR bands.
	• Base TIR mini-constellation.
	  ○ TIR channel.

Separated design of each mini-constellation	Singular achievement with the minimum number of satellites of required performance in terms of: • Temporal resolution. • Spatial resolution.

Several optical instruments analysis	• Mass ranging from 2 to 18.5 kg.
	• Different levels available in terms of:
	  ○ Spatial resolution.
	  ○ Spectral resolution.
	  ○ Achievable swath width.

Several mini-constellation architecture examples	Mini-constellation specific examples: • Performance. • Number of satellites.
Several complete constellation architecture examples	Starting from separate mini-constellation design and examples, several architectures of the complete constellation have been identified and classified in terms of: • Performance. • Total number of satellites. • Suitability with an eventual secondary-payload launch.
Very interesting complete constellation examples	3 very interesting examples of complete constellation architectures have been identified.

Table 6.23: Chapter 6 Summary 3.

7 SATELLITE PRELIMINARY MASS BUDGET

This chapter describes the process followed to preliminary evaluate the mass of different microsatellite platform subsystems, in order to estimate the available mass to carry on-board an optical payload and the propellant required to compensate atmospheric drag at several altitudes.

7.1 SATELLITE PRELIMINARY MASS BUDGET

With the aim to preliminary size satellite subsystems, several fundamental steps have been followed:

- satellite conceptual division to identify main parts.
- Subsystems indicative mass quantification.
- Derivation of approximated available mass for payload and propellant in function of altitude and satellite total mass.

7.1.1 Satellite conceptual subdivision

The satellite could be conceptually divided in three principal parts [3]:

- The satellite platform, which comprises all main subsystems:
    - the *Electric Propulsion* subsystem, and in particular the Alta SpA HT100D [6].
    - The *Telemetry, Tracking and Command* subsystem.
    - The *Primary Structure*.
    - The *Thermal Control* subsystem.
    - The *On-Board Computer* subsystem.
    - The *Attitude Determination and Control* subsystem.
    - The P*ower Generation* subsystem.
- The payload.
- The propellant needed to maintain the designed orbit and to perform eventual maneuvers.

The satellite platform preliminary mass is derived in relation to a satellite total mass ranging from 40 to 80 kg, compatible with the definition of microsatellite (10 – 100 kg) [1].

Several mass budget examples have been used to identify general indications about the different subsystems mass. Exploited microsatellite mass budget examples refer to:

- NEMO-HD, an University of Toronto under development microsatellite [84].
- Leonidas, an University of Hawaii under development microsatellite, used in particular in relation to the TT&C system [85].
- Three different preliminary studies conducted by:
    - the Amirkabir University of Technology (AUT) [86].
    - The Carleton University [87].

  - The University of Madrid [88].
- The large analysis on LEO satellites with propulsion shown by [3].

7.1.2 Electric Propulsion subsystem: the Alta SpA HT100D

The first subsystem considered is the thrusting module, which in this case represents the most important component of the platform. Thrust on-board would be provided by the last version of the Alta SpA low power Hall thruster named HT100, the HT100D (Figure 7.1).

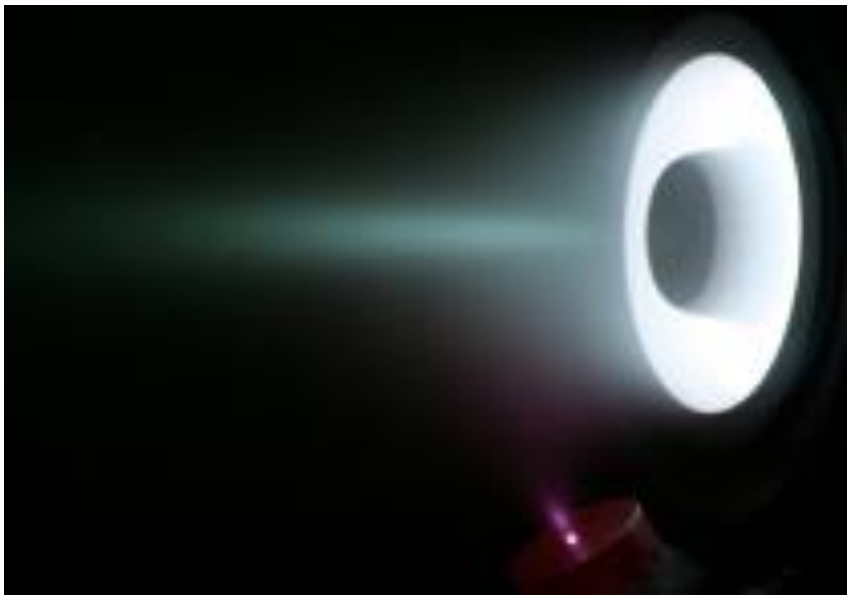

Figure 7.1: Alta SpA HT100D in operation.

The Alta SpA HT100D is designed to guarantee the performance shown in Table 7.1 [6]:

Performance	Value
Thrust, [mN]	6 – 18
Power, [W]	120 – 400
Specific Impulse, [s]	1000 – 1600
Thrust Efficiency	Up to 0.4
Lifetime, [h]	~ 2000
Mass, [kg]	0.4

Table 7.1: HT100D performance range.

In the frame of preliminary mass budget derivation, considering the respective mass of HT100D, of cathode and of the expected mass for the

Power Processing Unit (PPU), the mass of the entire Electric Propulsion subsystem is expected to be of about 7.7 kg (Table 7.2) [6].

Element	HT100D	Cathode	PPU
Mass, [kg]	0.436	0.200	0.700
Total dry mass = 7.700 kg			

Table 7.2: Electric Propulsion subsystem components mass.

HT100D stable operation points are shown in Figure 7.2and Figure 7.3[6]:

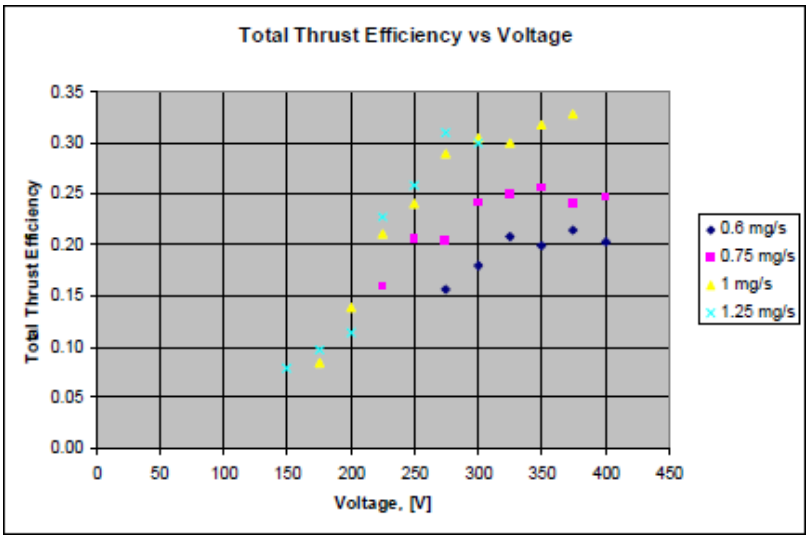

Figure 7.2: Experimental HT100D total thrust efficiency.

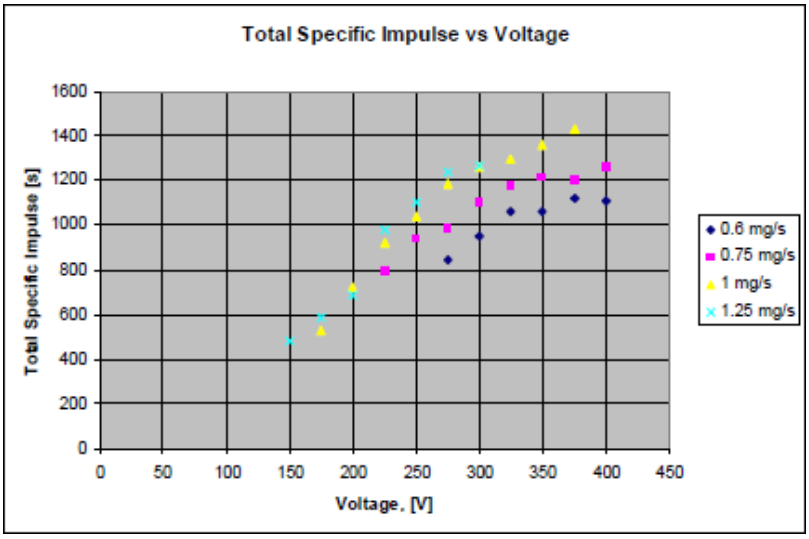

Figure 7.3: Experimental HT100D Total Specific Impulse.

As a reference, an anodic specific impulse of 1200 s has been adopted in correspondence of 3 different cases of thrust levels. Each thrust level is characterized also by a specific power level and an AMFR and is sufficient to counteract the atmospheric drag for altitudes down to 250 km [3]. These quantities will be used in the Power Generation subsystem mass budget derivation, in particular for secondary batteries sizing. Thrust levels are summarized in Table 7.3, where power consumption considers also a factor of 0.88 to take in to account the efficiency of the electronic transmission [6]:

Case #	Thrust, [mN]	Power, [W]	AMFR, [mg/s]
1	9	200	0.75
2	12	250	1.0
3	15	340	1.25

Table 7.3: Thrust levels adopted to describe the HT100D operation with a nominal Total Specific Impulse of about 1200 s.

7.1.3 Telemetry, Tracking and Command subsystem (TT&C)

To provide preliminary indications about realistic mass of the TT&C subsystem, a statistical analysis about existing components is required. The mass of the complete TT&C subsystem reported by cases analyzed in this frame are shown in Table 7.4 [84], [85], [86], [88]:

Example	NEMO-HD	LEONIDAS	AUT	Madrid Un.
Mass, [kg]	1.308	1.341	2.750	2.500

Table 7.4: TT&C subsystem mass for different cases.

Considering the very low mass expected by NEMO-HD and by Leonidas, and a margin of confidence, the satellite preliminary mass budget will consider a maximum mass for the TT&C subsystem of about 2.75 kg.

7.1.4 Primary structure

Percentage values of primary structure mass respect to satellite total mass shown by different microsatellites examples have been considered. The percentage mass of the primary structure subsystem respect to satellite total mass reported by cases analyzed in this frame are reported in Table 7.5 [3], [84], [87]:

Example	NEMO HD	AEGIS	SMAD
Mass, [%]	< 14	27	20

Table 7.5: Primary structure percentage mass of satellite total mass for different cases (data derived by [3] are referred to the satellite dry mass).

Once derived a statistical idea about realistic percentage values of the primary structure mass respect to the satellite total mass, further and more precise indications have been derived using [88]. This study is specifically devoted to create a model of a simple prismatic and aluminum structure for a microsatellite. The satellite under study is expected to be potentially launched as a secondary payload and its total mass covers the 20 – 70 kg range. Hence, this study appears fairly suitable to be applied to a general case of microsatellite within the 40-80 kg mass range, as in this preliminary step of analysis. Percentage values of the satellite total mass for the primary structure reported by [88] have been used to derive an approximated model, described by equation 6.1:

$$m_{st} = -1.25 \times 10^{-3} \times m_{tot}^2 + 0.27 \times m_{tot} \quad (6.1)$$

The equation gives the variation of indicative primary structure mass in function of satellite total mass:

- from a minimum of about 9 kg , at the 40 kg total mass case, in correspondence of a lateral dimension of 0.4 m,
- to a maximum of about 14 kg, at the 80 kg total masse case, in correspondence of a lateral dimension of 0.5 m

The model reported is clearly approximated and very simplistic, but it has been considered sufficiently conservative in this preliminary step of mass budget derivation.

7.1.5 Thermal Control (TC), On-Board Computer (OBC) and Attitude & Determination Control (ADC) subsystems

In these cases, the statistical analysis refers only to percentage values of TC, OBC and ADC mass respect to the satellite total mass. The percentage mass of the complete TC, OBC and ADC subsystems respect to satellite total mass reported by cases analyzed in this frame are shown in Table 7.6, Table 7.7 and Table 7.8 [3], [84], [87], [88]:

Example	**NEMO HD**	**AEGIS**	**SMAD**	**Madrid Un.**
Mass, [%]	1	3.7	2	2

Table 7.6: TC subsystem percentage mass of satellite total mass for different cases (data derived by [3] are referred to the satellite dry mass).

Example	NEMO HD	SMAD	Madrid Un.
Mass, [%]	3	5	5

Table 7.7: OBC subsystem percentage mass of satellite total mass for different cases (data derived by [3] are referred to the satellite dry mass).

Example	NEMO HD	AEGIS	SMAD	Madrid Un.
Mass, [%]	< 5	13.6	6	10

Table 7.8: ADC subsystem percentage mass of satellite total mass for different cases (data derived by [3] are referred to the satellite dry mass).

Considering a certain margin of confidence, the satellite preliminary mass budget will consider the percentage mass for these subsystems shown in Table 7.9:

Subsystem	TC	OBC	ADC
Mass, [%]	2	4	10

Table 7.9: Percentage mass of the satellite total mass assigned to TC, OBC and ADC subsystems.

7.1.6 Power Generation and Storage Subsystem

The Power Generation subsystem needs a particular and more detailed discussion due to the large expense of electric power required by the HT100D.

The Power Generation and Storage subsystem is formed by two main elements:

- the solar array subsystem.
- The secondary batteries subsystem, fundamental if solar panels are not able to provide the whole amount of electric power during different operations.

Solar array subsystem

The solar array subsystem is expected to be formed by cells mounted on five identical surfaces, coincident with the microsatellite cross-section, which is expected to vary with the total mass from a minimum of 0.16 m^2 (for 40 kg total mass), to a maximum of 0.25 m^2 (for 80 kg total mass). The idea is to equip the microsatellite with at least a single set of body-mounted solar cells coupled with four additional deployable panels. Deployable panels could be stacked one up each other on a single microsatellite face at the moment of the launch and then deployed in orbit.

Expected solar panel technology refers to the triple junction GaInP/GaAs/Ge 3G30C Azur Space Cells, described by Table 7.10 [89]:

Performance	3G30C Azur Space Cells
Efficiency	30%
Dimensions, [m^2]	0.04 x 0.08
Generated Power per cell, [W]	1
Specific Power, [W/kg]	97

Table 7.10: Triple junction GaInP/GaAs/Ge 3G30C Azur Space Cells characteristics.

The mass of the entire solar array subsystem therefore approximately ranges from 2.5 kg to 3 kg, considering a certain margin of confidence.

Secondary batteries subsystem

Assuming to separate the thruster operation from images acquisition or data transmission, HT100D ignitions represent the largest requests in terms of power. Initially, also about 10 W of power have been considered to take into account a generic base consumption of the platform [84]. Therefore, solar arrays have to generate a power such that (equation 6.2):

$$P_{s/a} \geq P_{Thruster} + P_{Platform} \tag{6.2}$$

If the relation described by the equation 6.2 is verified, secondary batteries are sized only to provide power during eclipse periods. According to [3], secondary batteries mass in this case is described by equation 6.3:

$$m_{batt} = \frac{\left(\frac{P_{Batt.} \times \Delta t_{Ecl.}}{DOD \times 0.9}\right)}{ED} \tag{6.3}$$

where:

- $P_{Batt.} = 10\ W$, is the standard platform consumption during eclipse.
- $\Delta t_{Ecl.}$, is the duration of the eclipse.
- DOD, is the battery depth of discharge.
- ED, is the battery energy density.

Eclipse duration have been precisely quantified using the System Tool Kit (STK) simulator only for those altitudes identified in Chapter 6 and initially only under keplerian assumptions. If the relation described by the equation 6.2 is not verified, hence secondary batteries have to be sized also to provide power to sustain thruster operation. Secondary batteries mass in this case is described by equation 6.4:

$$m_{batt} = \frac{\left(\frac{P_{Batt.Th.} \times \Delta t_{Th.}}{DOD \times 0.9}\right)}{ED} \tag{6.4}$$

where:

- $P_{Batt.Th.} = P_{Th.} + 10\ W - P_{s/a}$, is the power to be added to solar array subsystem generation to sustain the thruster operation.
- $\Delta t_{Th.}$, is the duration of the thrusting.

To have a reliable sizing of the secondary batteries, several suitable simulations have been performed. General Mission Analysis Tool (GMAT) simulations have been used to estimate the short-period semi-major axis decay in the hypothesis of maximum solar activity. Know the semi-major axis decay, the Δv needed to compensate drag during a single thrusting cycle has been quantified. The number of maximum thrusting cycles is set to be 3500 for the whole mission. Considering a maximum duration for the mission of about 5 years, it is hence possible to compensate drag theoretically every 12.5 hours. By the fact that the thrusting time duration depends on the thrust level, batteries mass and capacity will vary in function of selected thrust level. According to an analysis about actually available secondary batteries products, ABSL 18650 HC Li-Ion [90] has been initially chosen to compute the secondary batteries capacity and mass (Table 7.11) [91], [92]:

Performance	**ABSL 18650 HC Li-Ion cells**
Depth of Discharge	10% (80000 cycles, to be exploited for eclipse) 30% (10000 cycles, to be exploited for HT100D ignitions)
Energy Density, [Whr/kg]	130

Table 7.11: ABSL 18650 HC Li-Ion cell characteristics.

7.2 PRELIMINARY MASS BUDGET RESULTS

7.2.1 Mass budget results

Mass budget results derived according to described process are illustrated from Figure 7.4 to Figure 7.8 for the three thrust nominal cases.

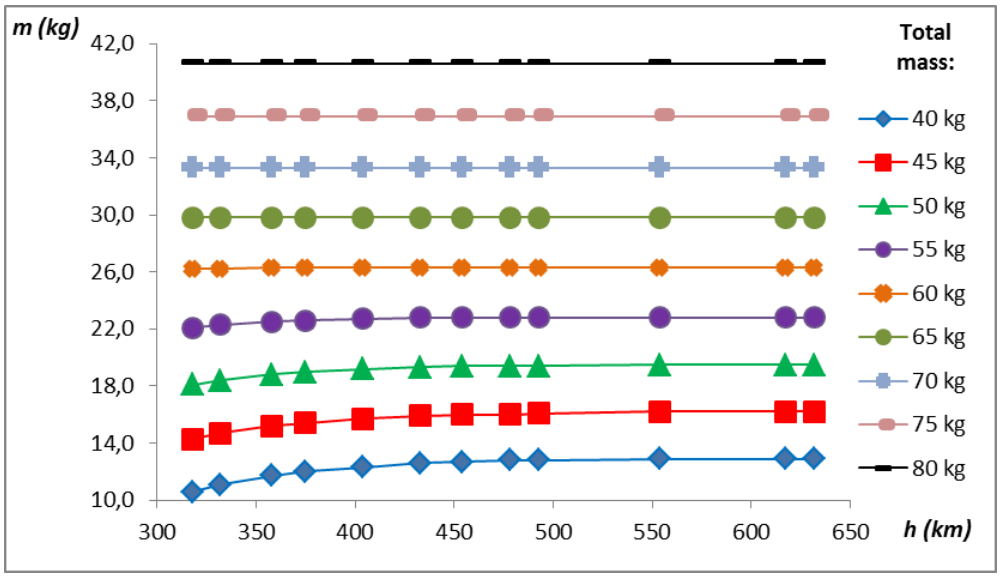

Figure 7.4: GMAT available mass to carry on-board a payload and propellant in the case of a thrust of 9 mN for altitudes comprised between 318 and 632 km.

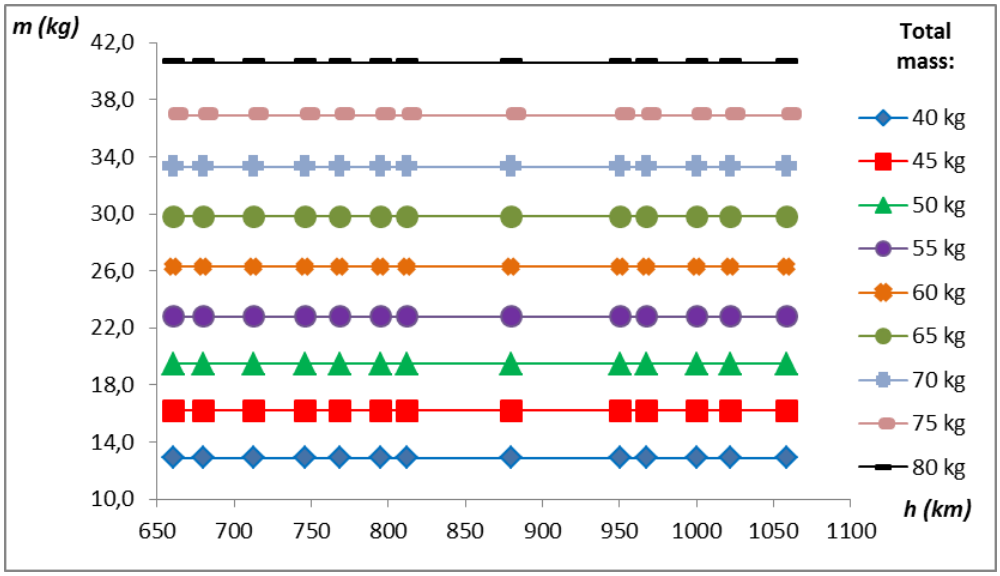

Figure 7.5: GMAT available mass to carry on-board a payload and propellant in the case of a thrust of 9 mN for altitudes comprised between 661 and 1059 km.

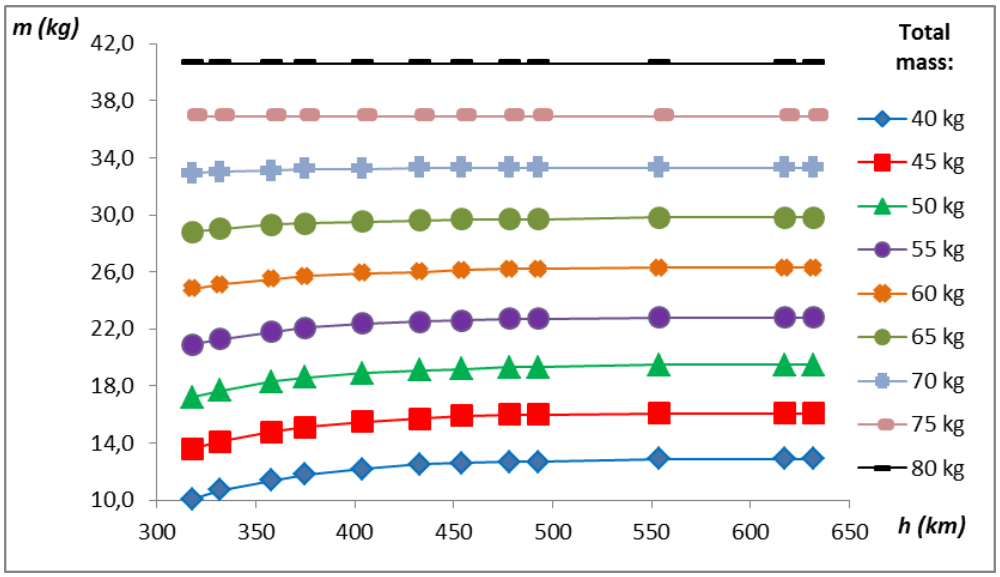

Figure 7.6: GMAT available mass to carry on-board a payload and propellant in the case of a thrust of 12 mN for altitudes comprised between 318 and 632 km.

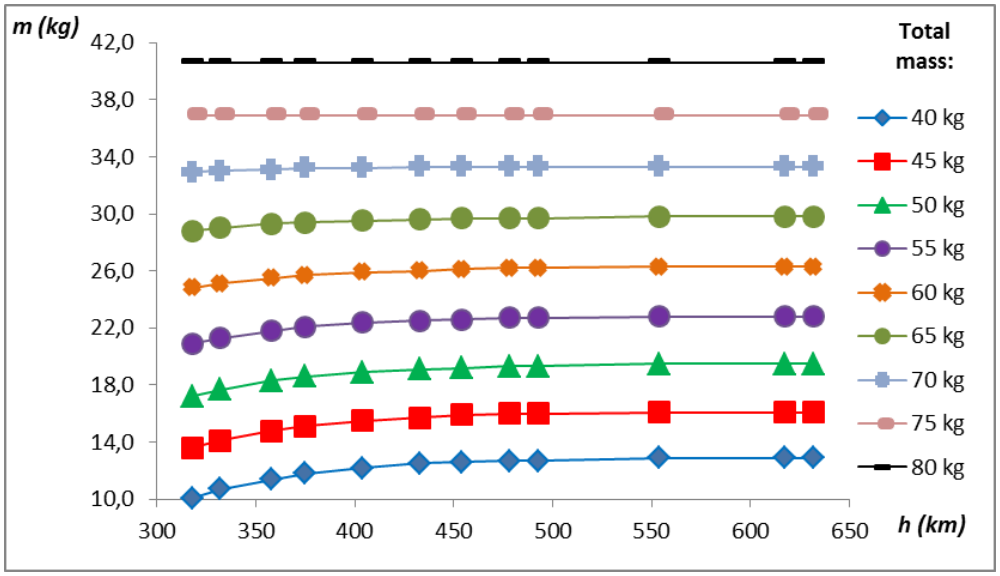

Figure 7.7: GMAT available mass to carry on-board a payload and propellant in the case of a thrust of 12 mN for altitudes comprised between 661 and 1059 km.

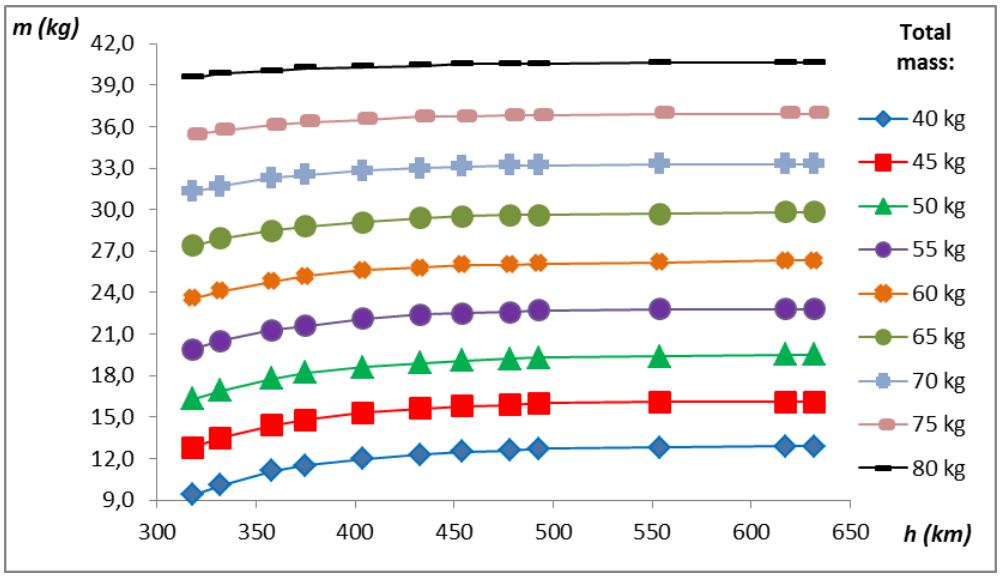

Figure 7.8: GMAT available mass to carry on-board a payload and propellant in the case of a thrust of 15 mN for altitudes comprised between 318 and 632 km.

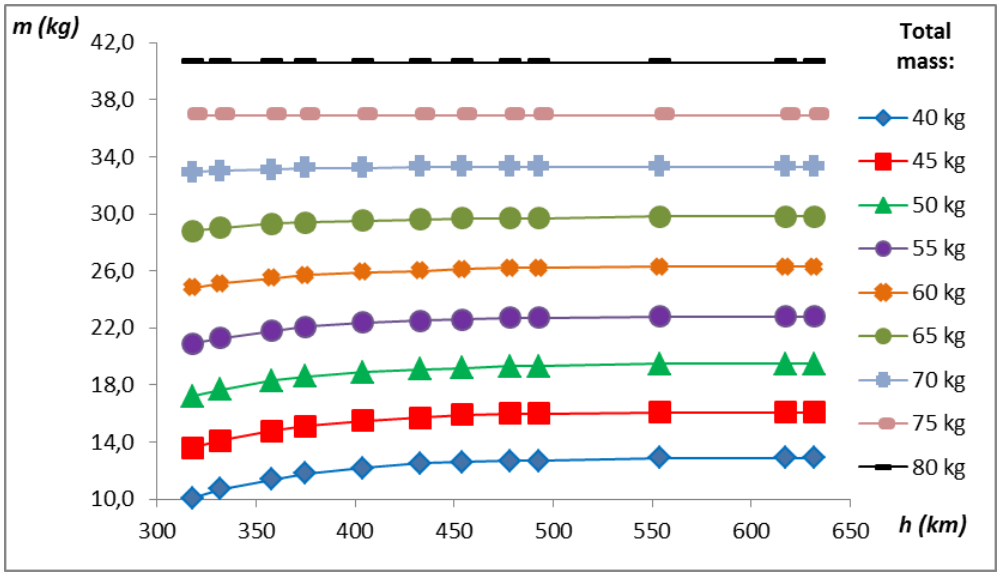

Figure 7.9: GMAT available mass to carry on-board a payload and propellant in the case of a thrust of 15 mN for altitudes comprised between 661 and 1059 km.

7.2.2 GMAT simulations and preliminary mass budget results discussion and conclusions

Previous preliminary mass budget results show that:

- there exist interesting possibilities to carry an optical payload and a good amount of propellant (up to 42 kg) also at low altitudes even with very low satellite total mass.
- Altitude influence is weak and affects only secondary batteries.
- Highest total mass values have a panel assembly surface sufficient to sustain lower thrust levels of HT100D operation also without the support of secondary batteries.

Preliminary mass budget results conclusions are that:

- seems possible to provide a sufficient mass availability to perform missions with expected small instruments (up to 12-15 kg) also if upper limit of satellite total mass is reduced to 60 kg.
- Further simulations are needed to precisely quantify the propellant needed to maintain altitude for a 5 years mission.
- A more precise second step of subsystems sizing is required, together with a definitive indication about satellite total mass, external layout and dimensions, and with the selection of state-of-art components able to guarantee a suitable operation of the platform in the whole selected altitude range.

7.3 SUMMARY Chapter 7

Quantification of available mass for an optical payload and for propellant in function of altitude and of satellite total mass (Table 7.12).

Subsystem	Mass, [kg]	% of total mass
Electric Propulsion	7.7	/
TT&C	2.75	/
TC	/	2
OBC	/	4-5
ADC	/	10
Primary Structure	9 – 14	/
Solar Array	2.5 – 3	/
Secondary Batteries	Up to 2.4 kg	/
Total mass range = 40 – 80 kg		
Nominal thrust levels = 9, 12, 15 mN		

Table 7.12: Chapter 7 Summary.

8 FIVE YEARS DRAG COMPENSATION AND ORBITAL TRANSFER SIMULATIONS

This chapter reports results obtained with the GMAT and Alta SpA SATSLab simulators relative to long-period altitude maintenance and orbital maneuvers. Simulations provided a preliminary quantification of propellant needed to perform the mission in many different conditions, and therefore a general description of the Alta SpA HT100D behavior.

8.1 DRAG COMPENSATION GMAT SIMULATIONS

According to preliminary mass budget results of Chapter 7, semi-major axis decay has been simulated only for a satellite total mass ranging from 40 to 60 kg (and therefore a drag surface between 0.8 and 1.0125 m^2). The atmospheric model exploited by GMAT losses significance if periods longer than 1 year are simulated. Therefore, GMAT 1-year results are used only initially to derive indicative orders of magnitude of propellant expense for a 5-years missions. For GMAT simulations, the following input parameters have been selected:

- mean atmospheric solar density, computed with a value of the F10.7 flux of 150. The value is selected according to [3].
- A typical value for the drag coefficient of about 2.2 [3].
- A thrust of 9 mN, sufficient to counteract the atmospheric drag in the selected altitude range.
- A maximum of 3500 thruster ignitions to compensate drag.
- A reflection coefficient of 2 for the Solar Radiation Pressure [3].

8.1.1 Five-years propellant expense GMAT simulations results

GMAT simulations results are shown by Figure 8.1 and Figure 8.2 only for altitudes up to 554 km (higher altitude considered in proposed architectures), where atmospheric decay is still a significant effect:

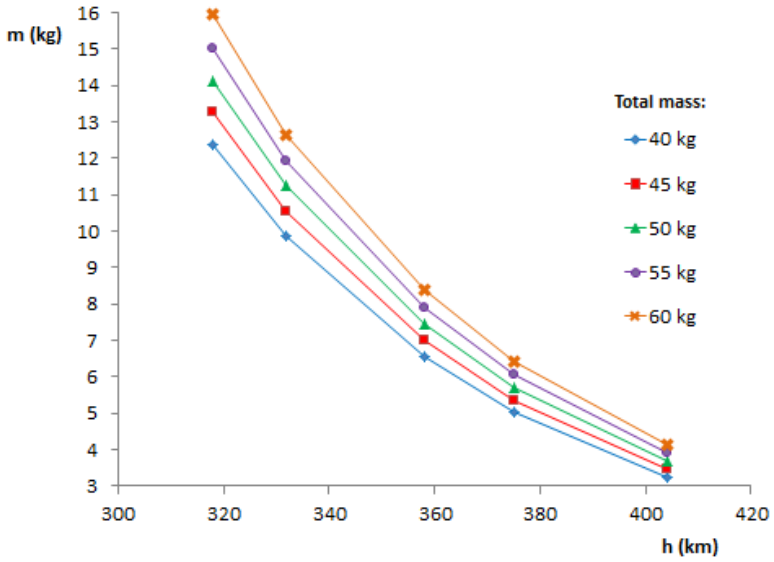

Figure 8.1: Propellant expense to maintain altitude for 5 years up to about 404 km.

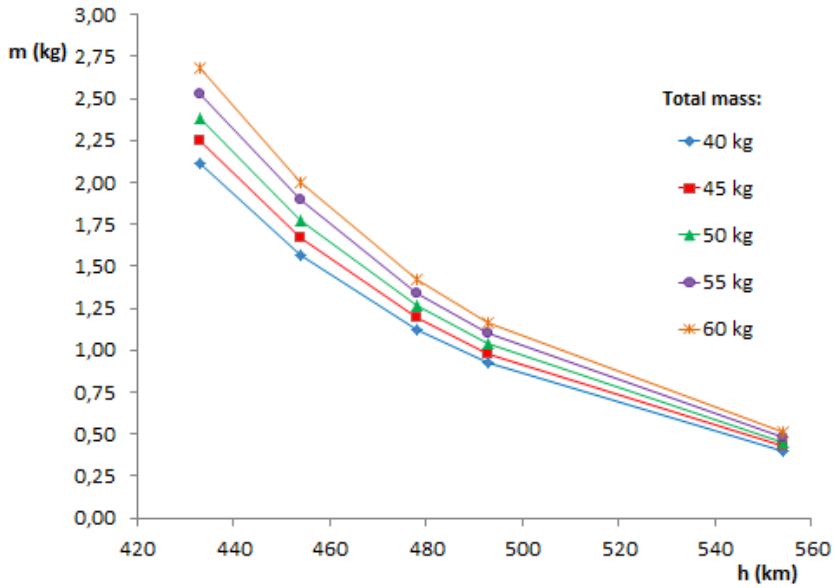

Figure 8.2: Propellant expense to maintain altitude for 5 years up to about 554 km.

Results relative to altitudes higher than 554 km are not shown because the propellant expense is very low, very near to zero.

8.1.2 Available mass for an optical sensor derivation

Previous GMAT simulations results have been used to quantify the mass available on-board the satellite to carry an optical payload. Results derived according also to preliminary mass budget are shown by Figure 8.3 and Figure 8.4.

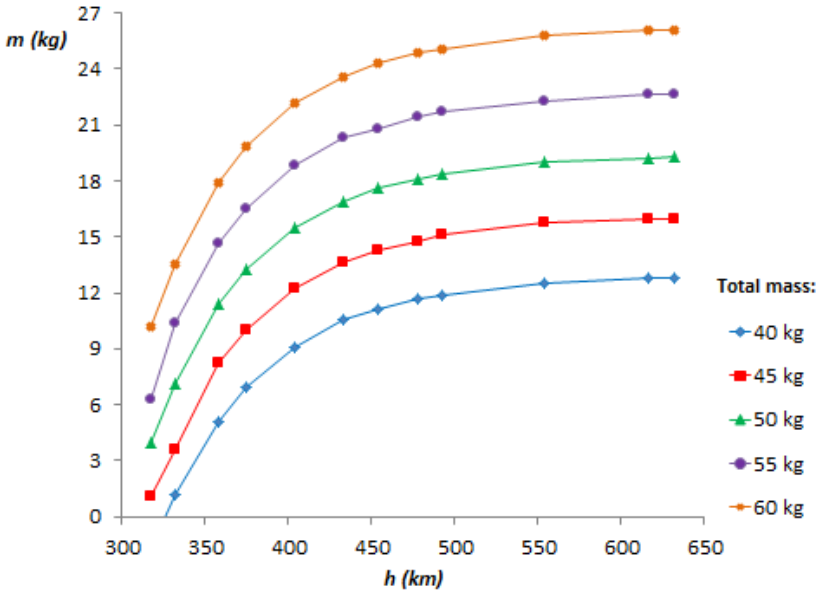

Figure 8.3: Available mass to carry on- board an optical payload.

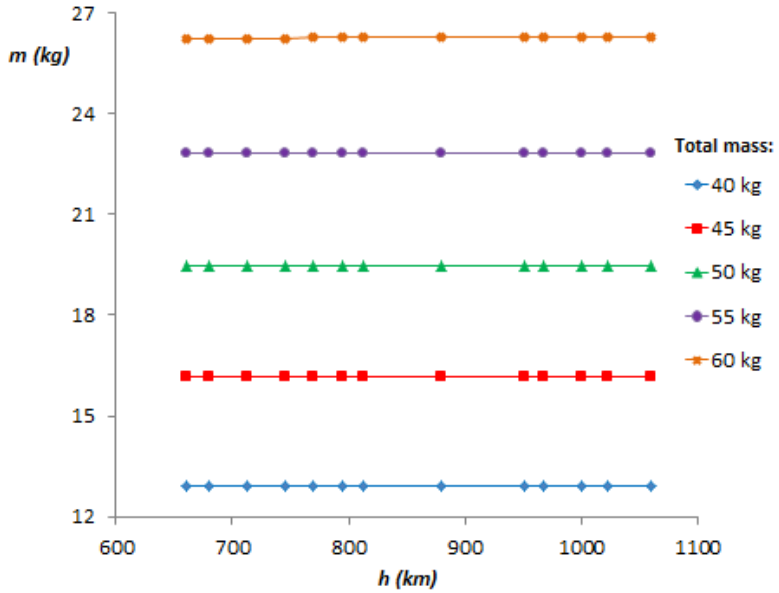

Figure 8.4: Available mass to carry on- board an optical payload.

Figure 8.4 confirms that the impact of the propellant needed to maintain the orbit at altitudes higher than 600 km on the available mass for the payload is almost unappreciable.

8.1.3 Total mass selection for complete constellation architectures

Previous combined preliminary mass budget and GMAT results have been used to identify values of satellite total mass suitable to perform appropriate simulations of constellation architectures proposed in Chapter 6 using the Alta SpA SATSLab simulator.

A maximum total mass of 50 kg and the correspondent drag cross-section of about 0.9 m^2 (derived according to Chapter 7 results and to the hypothesis of solar panels completely deployed) have been considered appropriate for each architecture, in relation to altitudes and instruments mass expected, and have been set as input parameters to initially approach SATSLab simulations.

8.2 Alta SpA SATSLab SIMULATIONS

8.2.1 FIVE YEARS CONSTELLATION ARCHITECTURES Alta SpA SATSLAB SIMULATIONS

Alta SpA SATSLab simulator has been used to derive precise quantifications of propellant expense to maintain a 50-kg microsatellites at those altitudes expected by proposed mission architectures.

To perform SATSLab simulations, the following input parameters have been selected:

- The NRLMSISE-00 atmospheric density model. In relation to the model adopted, the indicative date of launch is set to be in October 2023, in correspondence of a period of maximum solar activity.
- A typical value for the drag coefficient of about 2.2 [3].
- A drag surface of about 0.9 m^2.
- A thrust of 9 mN, sufficient to counteract the atmospheric drag in the selected altitude range.
- A control on the semi-major axis (SMA) suitable box. Box amplitude is a function of altitude and has been iteratively tailored for each case to achieve indicative values of HT100D ignitions to compensate drag lower than 3500.
- A reflection coefficient of 2 for the Solar Radiation Pressure [3].

SATSLab simulations specific orbital input parameters and derived results are shown by Table 8.1:

Altitude, [km]	358	404	554
Inclination, [°]	96.9	97.0	97.6
Eccentricity	0	0	0
RAAN, [°]	0	0	0
Argument of perigee, [°]	0	0	0
SMA box, [m]	1000	500	100
Propellant, [kg]	5.850	2.510	0.270

Table 8.1: Mass of propellant needed to maintain 5 years a 50-kg microsatellite at three different altitudes.

Propellant mass consumption during the first six months of operation have been plotted for each altitude case and are reported by Figure 8.5, Figure 8.6 and Figure 8.7.

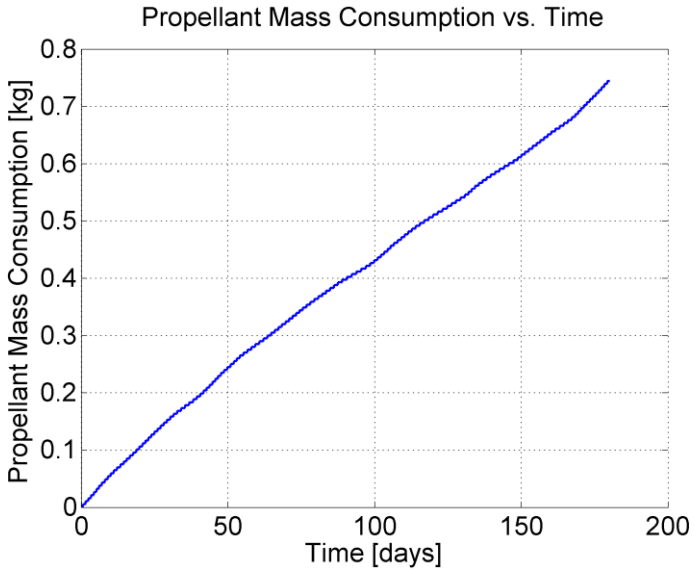

Figure 8.5: Propellant mass consumption during the first 6 months of life at 358 km.

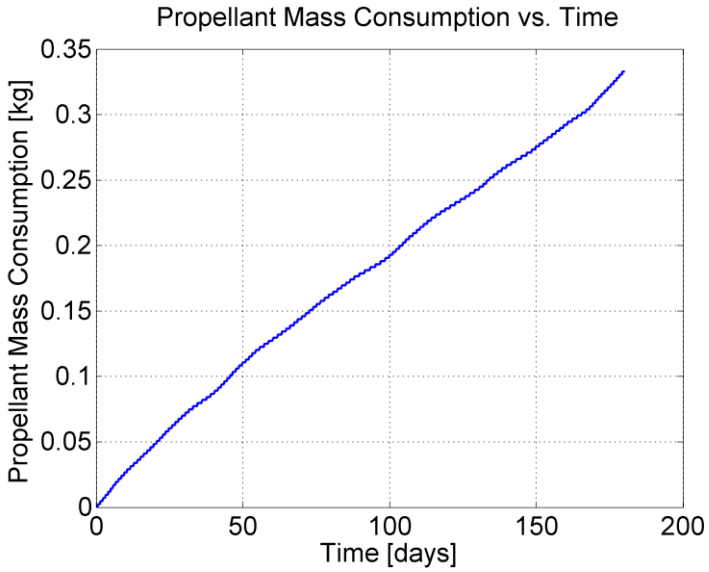

Figure 8.6: Propellant mass consumption during the first 6 months of life at 404 km.

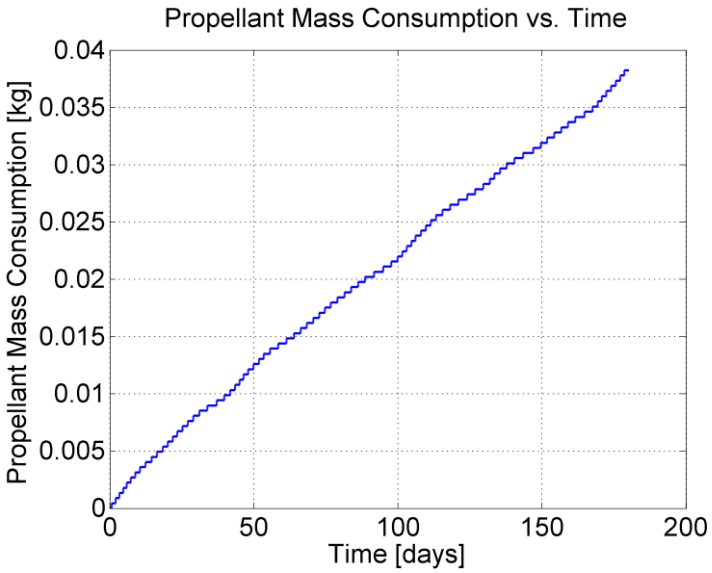

Figure 8.7: Propellant mass consumption during the first 6 months of life at 554 km.

Previous plots show that the consumption of propellant needed to compensate drag is not a perfectly linear function of time and that could significantly vary if short periods have to be studied. To complete the analysis, also propellant mass consumption relative to last 6 months of microsatellites operation has been plotted and is reported by Figure 8.8, Figure 8.9 and Figure 8.10 for all different altitudes.

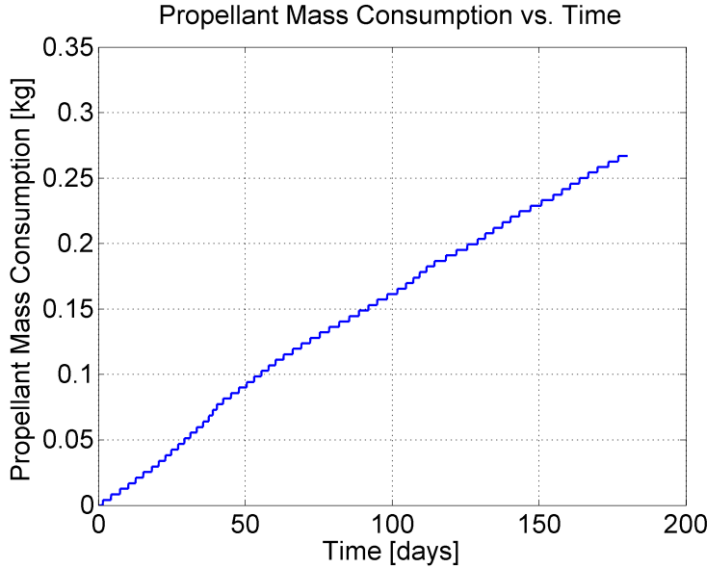

Figure 8.8: Propellant mass consumption during the last 6 months of life at 358 km.

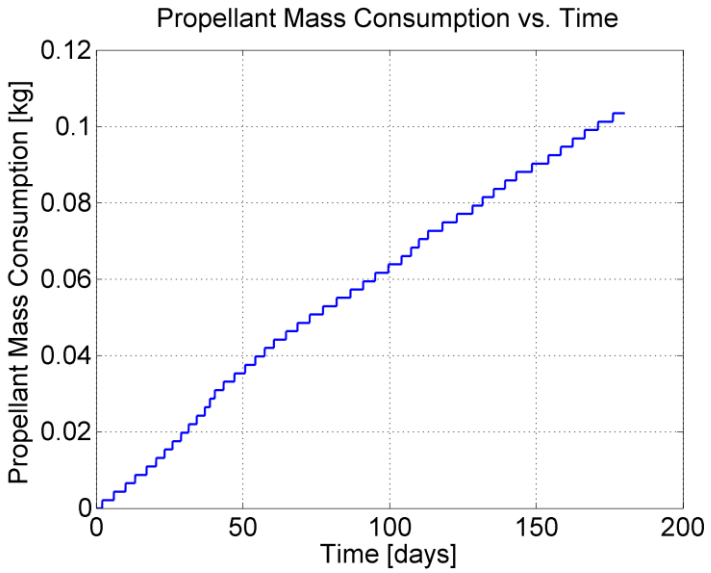

Figure 8.9: Propellant mass consumption during the last 6 months of life at 404 km.

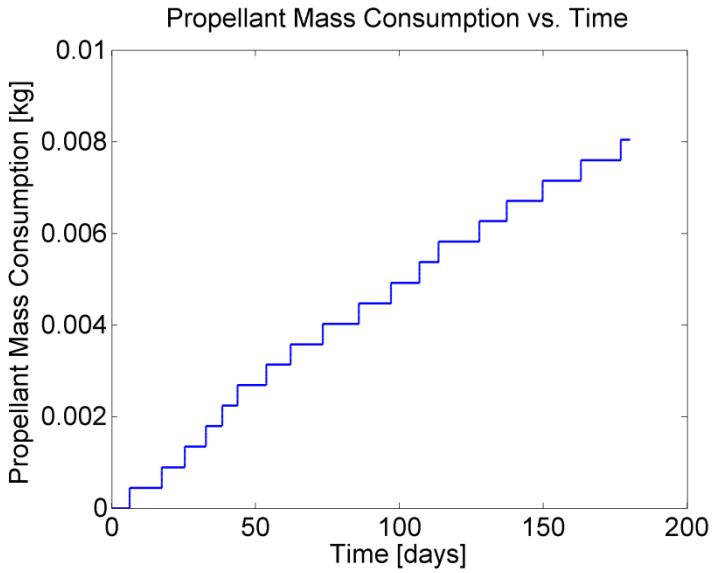

Figure 8.10: Propellant mass consumption during the last 6 months of life at 554 km.

Plots relative to last 6 months of operation of an hypothetical 5-years mission confirm the different intensity of atmospheric drag experienced by the 50-kg microsatellite in a period of minimum solar activity respect to a period of maximum solar activity.

The reduced number of ignitions shown by figures 7.9, 7.10 and 7.11 testifies that the value of the semi-major axis box control has been

appropriately selected and that the expected quantity of thruster ignitions needed during the entire mission to compensate drag is lower than the supposed limit value of 3500.

8.2.2 Alta SpA SATSLab simulations to model hypothetical orbital transfers

Alta SpA SATSLab simulator offers also the possibility to model orbital transfers using the COE (Classical Orbital Elements) change function. This tool has been exploited to indicatively quantify the mass of propellant needed to move a 50-kg microsatellite within a large range of Sun-synchronus orbits, from the lowest orbit expected by proposed architectures (358 km) to about 820 km, altitude reached by the VEGA launcher in the case of multi-payload launch configuration with the adapter VESPA in occasion of the PROBA-V launch [93].

Results of several of these simulations are shown by Table 8.2 for transfers where the SMA is increased (and therefore, the atmospheric drag has to be counteracted) and by Table 8.3 for transfers where the SMA is decreased (and therefore, the atmospheric drag makes the transfer easier):

Initial h, [km]	**Final h, [km]**	**Initial i, [°]**	**Final i, [°]**	**Propellant mass, [kg]**
358	404	96.9	97.0	0.260
358	554	96.9	97.6	0.920
404	554	97.0	97.6	0.760

Table 8.2: Transfers between Sun-synchronus orbits (with SMA increase) propellant mass expense results.

Initial h, [km]	**Final h, [km]**	**Initial i, [°]**	**Final i, [°]**	**Propellant mass, [kg]**
404	358	97.0	96.9	0.220
554	358	97.6	96.9	0.880
554	404	97.6	97.0	0.700
820	358	98.7	96.9	2.454
820	404	98.7	97.0	1.950
820	554	98.7	97.6	1.300

Table 8.3: Transfers between Sun-synchronus orbits (with SMA decrease) propellant mass expense results.

Transfers simulations results show that the transfer between the same two Sun-synchronus orbits is more convenient in the case of decrease of the SMA thanks to the action of the atmospheric drag. Clearly, if a very low altitude has to be maintained, as in the case of 358 km, the amount of propellant needed to compensate drag could be very large and a too much expensive transfer couldn't be allowed.

8.2.3 Alta SpA SATSLab simulations results discussion

SATSLab simulations, both in terms of 5-years continuous drag compensation and of orbital transfers, demonstrated that:

- all proposed architectures could be conservatively performed by a 50-kg microsatellite: therefore, 50 kg appears to be an appropriate solution for the successive and more refined steps of platform sizing.
- A wide range of transfers between Sun-synchronus orbits with limited expense of propellant could be performed, resulting in a very high degree of flexibility for the possible mission scenarios.
- Propellant tank will be sized to maintain for 5 years the lowest simulated altitude (358 km) and considering in addition also the quantity of propellant needed to perform the largest simulated transfer from 820 km to 358 km.
- Mission refinements are needed to even more precisely quantify the definitive value of propellant needed to compensate drag once the effective satellite drag-cross section will be defined.

8.3 SUMMARY Chapter 8

Microsatellite expected total mass to perform architecture examples according to GMAT simulations (Table 8.4).

GMAT Simulations			
Architecture	I	II	III
Total mass, [kg]	≤ 50	≤ 50	≤ 50

Table 8.4: Chapter 8 Summary 1.

Propellant mass needed to maintain for 5 years low and very low Sun-synchronus altitudes according to SATSLab simulations (Table 8.5).

Altitude, [km]	358	404	554
Propellant, [kg]	5.850	2.510	0.270
SMA box, [m]	1000	500	100

Table 8.5: Chapter 8 Summary 2.

Propellant mass needed to perform orbital transfers within a very wide range of Sun-synchronus altitudes according to SATSLab simulations (Table 8.6).

Initial h, [km]	**Final h, [km]**	**Initial i, [°]**	**Final i, [°]**	**Propellant mass, [kg]**
358	404	96.9	97.0	0.260
358	554	96.9	97.6	0.920
404	358	97.0	96.9	0.220
404	554	97.0	97.6	0.760
554	358	97.6	96.9	0.880
554	404	97.6	97.0	0.700
820	358	98.7	96.9	2.454
820	404	98.7	97.0	1.950
820	554	98.7	97.6	1.300

Table 8.6: Chapter 8 Summary 3.

Microsatellite total mass expected to be used for platform sizing and design according to SATSLab simulations (Table 8.7).

Total Mass, [kg]	50

Table 8.7: Chapter 8 Summary 4.

9 PLATFORM SIZING AND DESIGN

This chapter describes the process adopted to design a microsatellite platform able to perform 5-years Earth Observation missions in the selected altitude range. General mission scenario and platform logic architecture are provided, together with a conceptual division of platform operation modes. Exploitable mass, volume and power for a candidate payload are finally computed, in combination with a quantification of the maximum propellant capability.

9.1 SATELLITE SUBSYSTEMS SIZING AND COMPONENT SELECTION

With the aim to size satellite subsystems, several fundamental steps have been followed:

- Computation of subsystems requirements computation in the entire expected altitude range.
- Selection of suitable components off-the-shelf.

9.1.1 Platform dimensions

Initially, the satellite is supposed to be a cube with a side of 0.5 m and with a total mass up to 50 kg, according to the preliminary mass budget analysis [Chap. 7] and to SATSLab simulations [Chap.8].

9.1.2 Power Generation subsystem and platform bus

According to preliminary mass budget hypothesis about the presence of 4 deployable solar panels in addition to a set of body-mounted solar array [Chap. 7], the total area available for solar cells is 1.25 m^2. This results in a maximum power generation of 250 W BOL and of about 224 W EOL, according to [89].

The bus platform is supposed to be unregulated with a voltage of 28 V, according to [3].

9.1.3 Primary Structure

Two different solutions have been considered for primary structure materials:

- an all metallic solution, in particular Al 6061, as proposed by [3].
- A composite aluminum solution, as exploited by PROBA-V [2], and SATEX-1 [94].

According to [2] and [94], the material selected for the composite skin is the Al 2024 while for the honeycomb is proposed the Al 3003, exploited by SATEX-1 [94].

For the honeycomb, it appears interesting also the Al 5056, which has better mechanical properties respect to Al 3003 [97]. Both selected composite materials could be an appropriate base to easily satisfy stiffness requirements.

Table 9.1 summarizes principal characteristics of previous materials [97]:

Material	Al 6061	Al 2024	Al 3003	Al 5056
Density, [kg/m^3]	2700	2780	54	54
Modulus of elasticity, [GPa]	70	70	0.540	0.620
Average Strength, [Mpa]	240	270	2.5	2.6

Table 9.1: Principal characteristics of proposed materials.

The primary structure has to satisfy frequency requirements imposed by the launch vehicle. VEGA and DNEPR are initially assumed as possible candidates. Requirements traduce in a minimum value of the moment of inertia calculated at the launch vehicle interface (Table 9.2) [3], [95], [96]:

Launch vehicle	VEGA	DNEPR
Longitudinal f, [Hz]	$20 \div 45$ or > 60	≥ 20
Lateral f, [Hz]	≥ 15	≥ 10
I, [kgm^2]	$\geq 2.18 \times 10^{-6}$	

Table 9.2: VEGA and DNEPR frequency requirements.

The value of the minimum moment of inertia has been calculated using a cantilever beam assumption and considering:

- 50 kg of microsatellite total mass.
- 0.5 m of microsatellite length as a beam.
- 70 GPa for the aluminum modulus of elasticity.

All selected materials allow to easily satisfy moment of inertia requirements.

Initially, the honeycomb solution has been considered more appropriate, besides its typical advantages (very low weight, high stiffness and durability and cost savings), also to reduce the needs in terms of secondary structures. Composite allows to easily attach components directly to structural panels, and this is ideal to reach an high degree of flexibility in the management of internal envelops and therefore to have a primary structure the simplest and the most light possible [3]. The primary structure mass will be only indicatively quantified according to SATEX-1 experience, using a thickness of 5 mm for the honeycomb and of 0.8 mm for the skins [94]. A more precise layout of the structure will be provided in paragraph 8.3, when different subsystems components dimensions will be known.

9.1.4 Thrusting Module

The Thrusting Module is composed by [6]:

- Two HT100D (for cold redundancy).
- Power Processing Unit (PPU).
- Propellant tank and propellant.
- Fluidics.

To refine mission requirements, a second step of SATSLab simulations have been performed to quantify the mass propellant required to maintain the altitude of 358 km and to perform the largest transfer hypothesized in Chapter 8, from 820 km to 358 km. Mission refinement simulations input parameters are shown in Table 9.3:

Input parameter	Value
Exposed cross-section, [m^2]	0.25
Ballistic mass, [kg]	50
Drag coefficient	2.2
Period of operation	2023 (maximum solar activity)

Table 9.3: Simulations input parameters.

Propellant mass consumption needed to compensate drag results to be about 0.18 kg. Projecting this value in the hypothesis of a 5-years mission, the resulting value of total propellant needed to compensate atmospheric drag is set to be 1.8 kg (conservative assumption).

Minimum tank propellant capability has been calculated considering contributions reported by Table 9.4.

The contribution of additional maneuvers like small inclination changes to maintain the condition of Sun-synchronism or initial orbit phasing, has been computed as equivalent to a 10% of the total propellant mass expense for the drag compensation.

Contribution	Value
Drag compensation, [kg]	1.8 (at 358 km)
Additional maneuvers, [kg]	0.2
Transfers	Up to 2.2
Required capability ≥ 4.5 kg	

Table 9.4: Minimum tank capability computation.

The propellant to be exploited for the HT100D operation is the gas xenon (Table 9.5) [6]:

Storage pressure, [MPa]	15
Storage temperature, [K]	293
Density, [kg/m^3]	1700 – 1800
Molecular weight, [g/mol]	131

Table 9.5: Physical properties of xenon.

An interesting spherical titanium pressurant tank is produced by the ATK company. Tank characteristics are summarized by Table 9.6 [98]:

Internal diameter, [mm]	194.5
Minimum wall, [mm]	2.337
Volume, [l]	3.851
Operating pressure, [MPa]	24.82
Max design weight, [kg]	1.533

Table 9.6: ATK spherical titanium pressurant tank specifications.

The selected tank is perfectly able to satisfy gas xenon storage requirements.

The maximum mass of propellant storable in the tank is about 6.5 kg.

In conclusion, the characteristics of the elements of the thrusting module are summarized by Table 9.7 [6], [98]:

Element	HT100D	PPU	Tank
Mass, [kg]	0.436	< 7.000	1.533
Power, [W]	200	-	-
Volume, [mm^3]	60x60x100	150x120x115	199x199x199
Quantity	2	1	1
Total dry mass = 9.805 kg			

Table 9.7: Summary of Thrusting Module elements characteristics.

Finally, also the possibility to isolate the thrusting module respect to the rest of the platform using a conical plume shield has been considered and studied [99].

Details of the plume shield size, shape, collocation and specific functions will be reported in Paragraph 8.4.

9.1.5 Telemetry, Tracking and Command subsystem (TT&C)

According to indications provided by [3] and to some examples reported in [2], an X-band system has been selected to ensure an high-rate payload data and telemetry downlink. In particular, two suitable and reliable components have been identified to compose the X-band transmission subsystem:

- The Syrlinks EWC28 X-band transmitter (Figure 9.1) [100].
- The RUAG X-band helix antenna (Figure 9.2) [101].

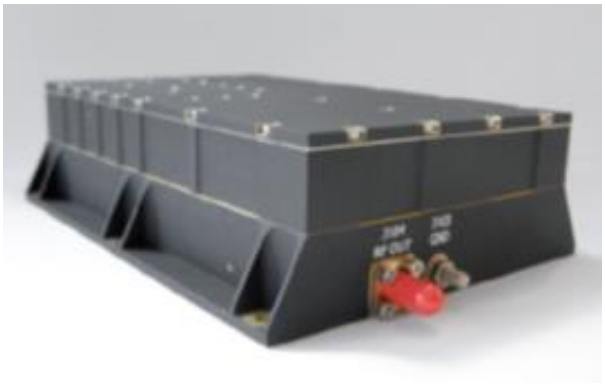

Figure 9.1: EWC28 Syrlinks X-band transmitter and S-band receiver.

Figure 9.2: RUAG X-band helix antenna.

Alta SpA SATSLab has been used to completely simulate a downlink activity with a dedicated ground station supposed to be placed in Florence, Tuscany, Italy. The simulator allows to study and quantify the duration of the contact with the ground-station and also the achievable channel capability at two extremes of the selected altitude range of proposed mission architectures (358 km and 554 km). Simulations input parameters, according

to [3], [8] and to components performance, are reported by Table 9.8, while Table 9.9 report results.

Altitude, [km]	358	554
Min elevation angle, [°]	5	5
Frequency, [GHz]	8	8
RF output power, [W]	8	8
Tx antenna gain, [dBi]	5	5
Rx antenna gain, [dBi]	58 (10-m dish)	58 (10-m dish)
System noise T, [W]	250	250
Bandwidth, [MHz]	400	400
Conditions	Dry	Dry

Table 9.8: Simulations input parameters.

Altitude, [km]	358	554
Max T in view per pass, [min]	7.56	9
Channel capacity, [Mbit/s]	Up to 58	Up to 25

Table 9.9: Simulations results.

From Figure 9.3 to Figure 9.6 ground station visibility (only during sunlight passes) and channel capacity for both altitudes are shown.

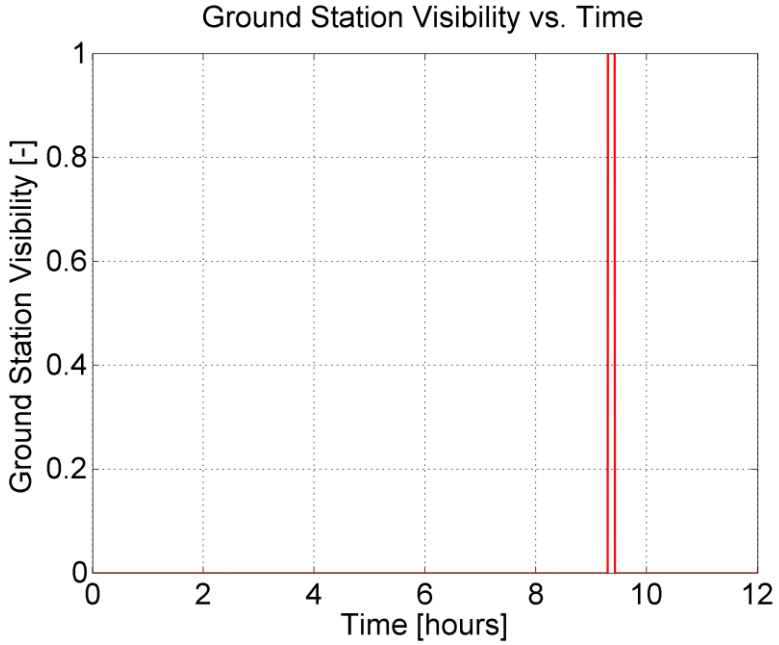

Figure 9.3: Ground station visibility from an altitude of 358 km.

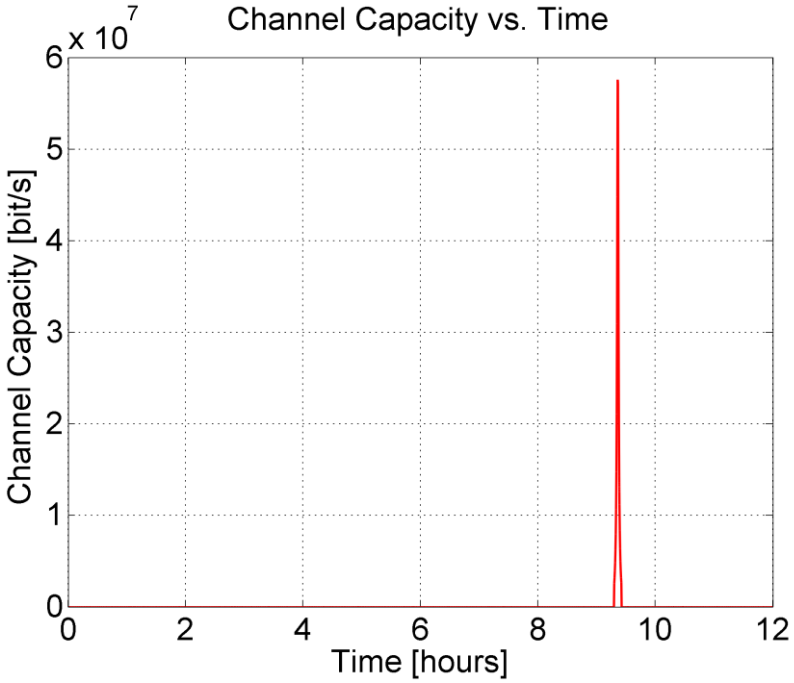

Figure 9.4: Available channel capacity from an altitude of 358 km.

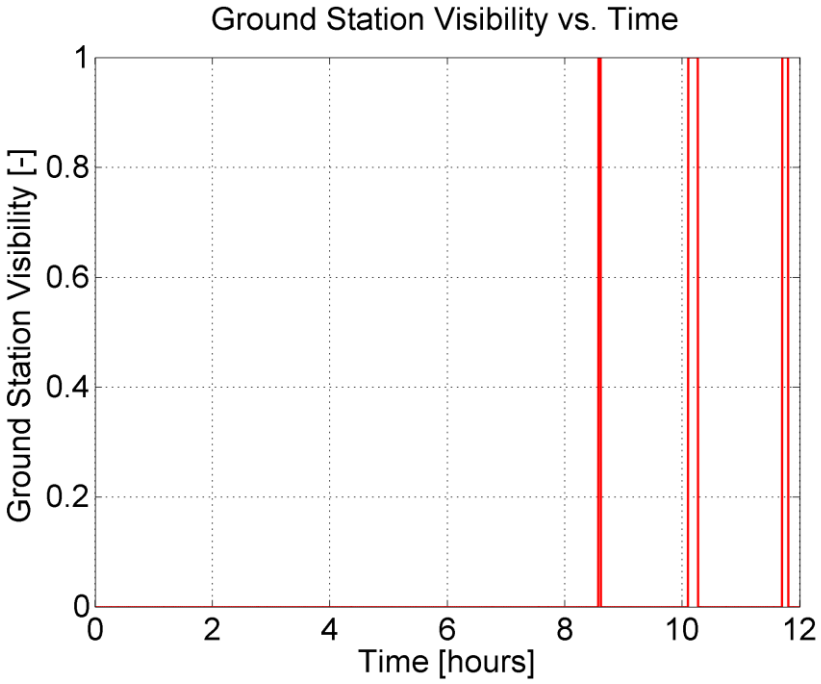

Figure 9.5: Ground station visibility from an altitude of 554 km.

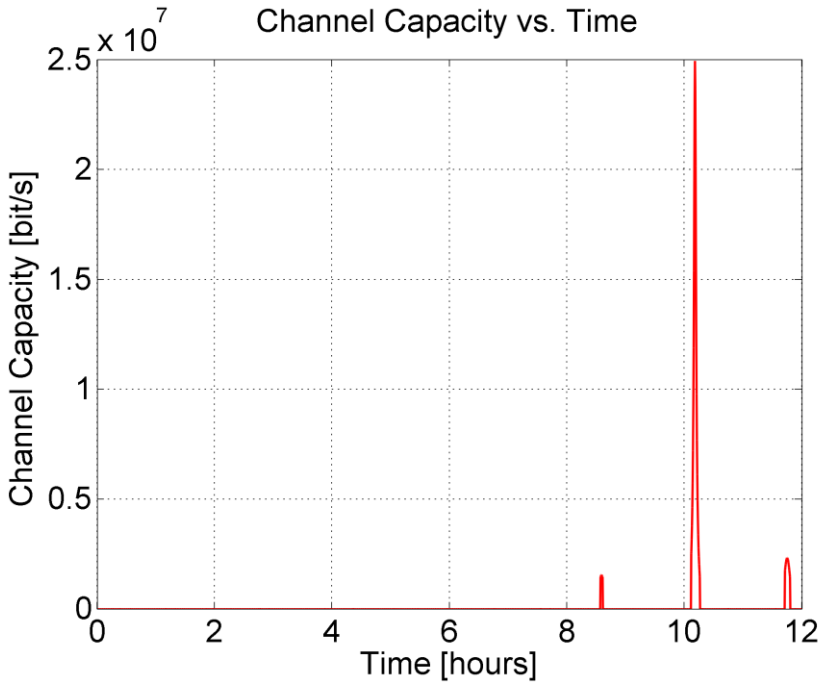

Figure 9.6: Available channel capacity from an altitude of 554 km.

Results shown by plots confirm that the downlink chain hypothesized for the satellite is sufficient to meet requirements imposed by the SLIM-6-22, which is the instrument characterized by the highest data rate between sensors analyzed in Chapter 6. In particular, it operates with a downlink rate up to 8 Mbit/s [2].

To achieve a very high-date rate capability, the TT&C subsystem will be composed by two couples of EWC28 transmitter and helix antenna. According to [100], it possible to achieve a total maximum data rate of 200 Mbit/s (100 Mbit/s per each antenna).

Moreover, according to [100], EWC28 is also perfectly able to receive telecommand uplink in the S-band. Therefore , EWC28 are expected to be used also for the uplink.

They will be combined with two S-band patch antennas, like for example those produced by ISIS, appropriately placed in two opposite directions to provide omni-directional coverage [102].

Telecommand reception is supposed to be operational in every moment of the mission.

In conclusion, the characteristics of the elements of the TT&C subsystem are summarized by Table 9.10 [100], [101], [102]:

Component	**EWC28**	**X-Antenna**	**S-Antenna**
Quantity	2	2	2
Unit mass, [kg]	1.000	0.400	< 0.080
Rx Power, [W]	1.6	-	-
Tx Power, [W]	3.5 – 35	-	-
Vol., [mm^3]	160x115x46	90x90x240	50x50x3.2
Company	SYRLINKS	RUAG	ISIS
Total mass < 3.000 kg			

Table 9.10: Characteristics of TT&C subsystem components.

9.1.6 Attitude Determination and Control subsystem (ADC)

The ADC subsystem has been sized according to process described by [3] while the available components are selected according to indications provided by [1]. According to [103], [53], [67] and to many examples found in [2], the pointing accuracy required by optical Earth Observation is typically lower than 0.1°.

As testified by [3], this means that a very fine attitude control mode is required for Earth Observation, in order to allow also instruments with the narrowest field of view to acquire very accurate optical images, fundamental for example for precision agriculture purposes [2]. Therefore, satellite is supposed to be Earth-oriented and 3-axis stabilized [3], [8]. This configuration allows to observe the Earth and contemporarily direct the HT100D axis along the velocity direction. To perform a 3-axis stabilization with an accuracy lower than 0.1°, star trackers and reaction wheels are required [3]. The same fine attitude control mode is supposed to be used also during thruster operation. To desaturate reaction wheels, magnetic torquers are required. Moreover, if combined with coarse Sun sensors, they allow the spacecraft to be able to operate also in a coarser attitude control mode, for example during acquisition phases, eclipses or in safety mode [3]. This solution, is adopted from many Earth Observation satellites [2]. The ADC finally has to be completed by a magnetometer, a 3-axis MEMS gyroscope and also a GPS for orbit determination [3]. According to [3], the first step of ADC actuators sizing is the quantification of worst cases of external disturbance torques. Disturbance torques have been analytically

computed using input parameters shown by Table 9.11, selected thanks to [3], [8], [53]:

Disturbance torque	**Solar Radiation Pressure**	
Altitude, [km]	358	554
Reflectivity coefficient	1	1
Solar constant, [W/m^2]	1366	1366
Exposed area	1.25	1.25
rc_s, [m]	0.1	0.1
Torque amplitude, [Nm]	1.14×10^{-6}	1.14×10^{-6}
Disturbance torque	**Atmospheric Drag**	
Altitude, [km]	358	554
Density, [kg/m^3]	1.923×10^{-11}	1.420×10^{-13}
Drag surface, [m^2]	0.25	0.25
Drag coefficient	2.2	2.2
cp_a, [m]	0.050	0.050
Torque amplitude, [Nm]	1.565×10^{-5}	1.125×10^{-7}
Disturbance torque	**Magnetic Field**	
Altitude, [km]	358	554
B, [T]	5.1×10^{-5}	4.7×10^{-5}
s/c dipole, [Am^2]	0.5	0.5
Λ	2	2
Torque amplitude, [Nm]	2.55×10^{-5}	2.35×10^{-5}
Disturbance torque	**Gravity Gradient**	
Altitude, [km]	358	554
θ, [°]	1	1
I, [kgm^2]	3.015	3.015
I_y, [kgm^2]	2.881	2.881
Torque amplitude, [Nm]	9.15×10^{-9}	8.39×10^{-9}

Table 9.11: External torque acting on the satellite in the expected altitude range.

Table 9.11 highlights that the worst disturbance case are the external torques imposed by the magnetic field and the atmospheric drag at 358 km of altitude.

Considering a safety margin of 2, as suggested by [3], this results in a minimum disturbance rejection capability required to reaction wheels of about 8.46×10^{-5} Nm to counteract the sum of all torques.

The momentum storage requirement is dominated by the atmospheric drag torque, which acts constantly for the entire orbital period for an Earth-pointing satellites, [103] while other torques are cyclic, and accumulate in a quarter of the orbit [3], [103].

Therefore, momentum capability required to reaction wheels is shown in Table 9.12 [3], [103]:

Altitude, [km]	358	554
Momentum storage, [mNms]	112	31

Table 9.12: Momentum storage required to RWs in the expected altitude range.

The large difference between momentum storage requirement at considered altitudes is due to the significant difference in the atmospheric drag intensity.

To maintain a certain margin, fundamental considering the very fast maneuvers that could be imposed by Earth Observation purposes, for example for site-to-site observations, reaction wheels of Astround Feinwerktechnik Adlershof GmbH with a momentum storage capability of 340 mNms have been selected (Figure 9.7) [104].

Figure 9.7: RW 90 of Astround Feinwerktechnik Adlershof GmbH reaction wheel.

Finally, magnetic torquers able to counteract the worst case of external disturbance torque and sufficient to guarantee a certain margin, fundamental for fast momentum dumping purposes, have been selected.

Considering the method suggested by [3] and the conservative case of minimum magnetic field available for actuators, the minimum dipole capability required to magnetic torquers is of about 3.32 Am^2.

To maintain a certain margin, the ZARM MT5-2 magnetic torquers, with a capability up to 5 Am^2, have been selected (Figure 9.8) [105]. If necessary, also ZARM MT6-2 and MT10-2-H, with higher dipole capabilities, could be used.

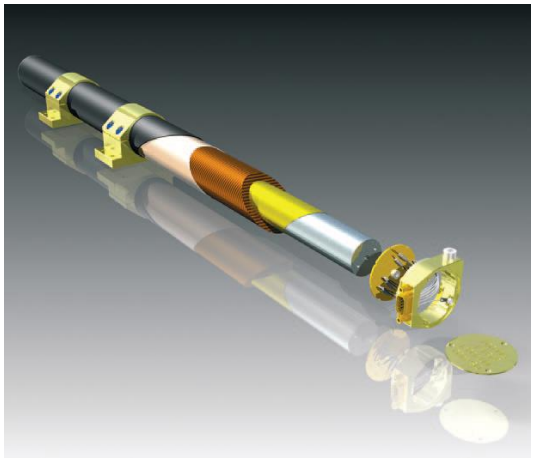

Figure 9.8: ZARM MT5-2 magnetic torquer.

ZARM magnetic torquers could be integrated by the use of a ZARM AMR digital magnetometer. This device is able to work up to an absolute value of the magnetic field of 240 μT, perfectly in line with expected magnetic field intensity (Figure 9.9) [106].

Figure 9.9: AMR ZARM digital magnetometer.

To select a suitable tracker, many examples found in [2] and also the specific case of [53] and [67] have been followed. The ST-16 Star Tracker

produced by Sinclair, with a pointing determination accuracy lower than 7 arc-sec, has been considered very appropriate (Figure 9.10) [107].

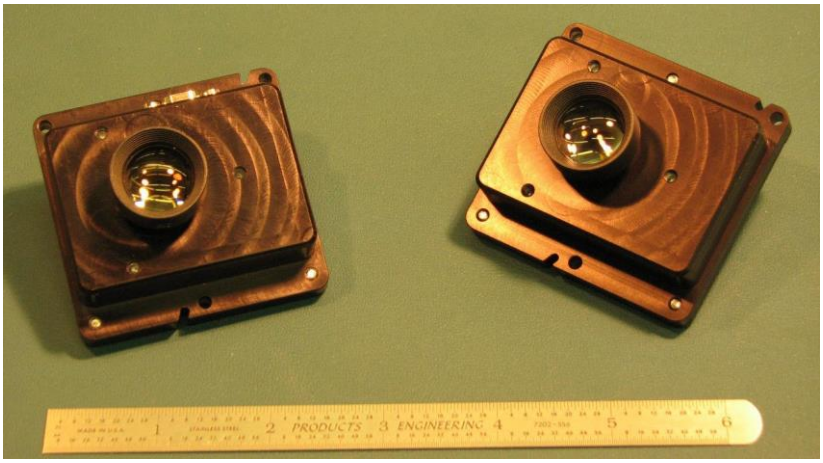

Figure 9.10: ST-16 Sinclair star trackers.

The set of sensors is completed by Space Micro CSS-01,02 coarse Sun sensors [108] (Figure 9.11), which offer a very large field of view (up to 120°) and a good accuracy (5°), and by a small 3-axis MEMS gyro produced by Sensonor, the STIM300 (Figure 9.12) [1], [109].

The bias instability offered by the STIM300, of about 0.5 deg/hour, is in line with indications provided by [110] in terms of line of sight stability requirement of 5 μrad/s for rotational measurements accuracy (in presence of a PAN channel, which requires the most stringent value).

Figure 9.11: CSS-01,02 Space Micro coarse Sun sensor.

Figure 9.12: STIM300 Sensonor 3-axis MEMS gyroscope.

The characteristics of the ADC subsystem actuators are summarized by Table 9.13:

Component	**RW 90**	**MT5-2**
Quantity	4	3
Unit mass, [kg]	0.900	0.900
Unit power, [W]	1.8 – 15	2.310
Unit vol., [mm^3]	103x101x80	18x18x240
Company	Astround Feinwerktechnik Adlershof GmbH	ZARM

Table 9.13: characteristics of ADC actuators components.

The characteristics of the ADC subsystem actuators are summarized by Table 9.14:

Component	**ST-16**	**CSS-01,02**	**STIM300**	**AMR**
Quantity	2	6	1	1
Unit m., [kg]	0.130	0.010	0.055	0.055
Unit p., [W]	1.5	/	/	0.6
Unit v., [mm^3]	59x56x66.5	23x23x9	39x45x21	56x36x17
Company	Sinclair Interplanetary	Space Micro	Sensonor	ZARM

Table 9.14: Characteristics of the ADC subsystem sensors.

The Attitude Determination & Control subsystem is finally completed by a device for the Spacecraft Trajectory Navigation and Control Systems [3],

in particular for autonomous navigation, the Phoenix Spaceborne GPS receiver (and related antenna) [111].

9.1.7 On-Board Computer (OBC) and data storage subsystems

In this second step of platform sizing, OBC has been studied in terms of of on-board storage capabilities.

According to preliminary mass budget [Chap.7], a mass of about 2.5 kg has been selected for the complete OBC subsystem while, a power consumption of about 5 W is set to be taken into account [84]. In the frame of the platform design, a small volume will be defined to host an on-board computer.

On-board storage capability has been sized according to SLIM-6-22 largest image dimension [112]:

- 600 x 700 km.
- 3.5 GBytes.

To provide such data storage capability, it appears interesting to exploit a light SSDR (Solid State Data Recorder) as proposed by [1].

9.1.8 Thermal Control subsystem (TC)

The thermal control subsystem has not been deepen for this preliminary sizing analysis.

According to preliminary mass budget of Chapter 7, a 2% of the satellite total mass has been taken into account for the entire Thermal Control subsystem.

9.2 PLATFORM LOGIC DESIGN AND FUNCTIONS INDIVIDUATION

9.2.1 Mission scenario

The proposed mission scenario is schematically composed by following phases after the launch (Table 9.15):

Phase	Attitude control mode	Function
Acquisition	Coarse	Solar panels deployment.
Transfer	Fine	Achievement of final orbit.
Operation	Fine & coarse	Housekeeping, Earth Observation, payload data transmission, orbit control.

Table 9.15: General mission scenario after the launch.

As shown by table 8.15, once achieved the nominal operational orbit, the mission is divided in 4 sub-phases. Principal functions and related attitude control mode of each sub-phase are shown by Table 9.16:

Phase	Attitude control mode	Function
Housekeeping	Coarse	Power savings, telecommand reception
Earth Observation	Fine	Target acquisition
Payload data transmission	Fine	Telemetry and images transmission
Orbit control	Fine	Altitude and inclination maintaining

Table 9.16: Principal functions of nominal operational orbit sub-phases.

The housekeeping phase is supposed to be operative for the entire fraction of the orbit during which no observations or transmissions are performed (e.g. during the eclipse). It is thought especially to save power and therefore to minimize the capacity required to secondary batteries.

The Earth Observation and payload data transmission phases are supposed to be potentially operative contemporarily for the most extended possible fraction of the sunlight period of the orbit. This means that the

platform could be able to image a region and at the same time transmit to a dedicated ground station placed there.

Finally, the orbit control mode is supposed to be operative both in sunlight and in eclipse, in order to perform drag compensation maneuvers in correspondence of orbit nodes, and therefore to maintain a value of the eccentricity close to zero.

9.2.2 Platform logic architecture

Figure 9.13 summarizes the platform logic architecture, linking different operation modes and phases to involved components.

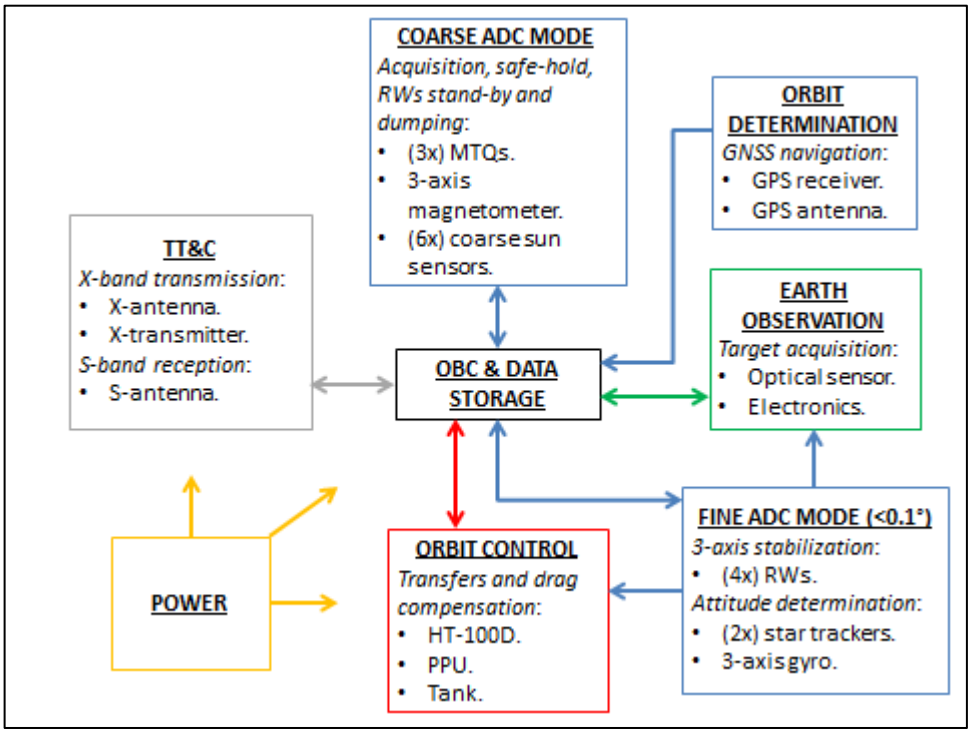

Figure 9.13: Platform logic architecture.

9.2.3 Platform begin of life (BOL) power budget and power storage subsystem sizing

Power budget is computed in relation to a 10:30 am-10:30 pm (or *viceversa*) orbit, which is considered more appropriate for optical Earth Observation respect for example to a *noon-midnight* orbit or a *twilight* orbit [3]. This type of orbit is suggested by many examples found in [2]. The available power during an year in a Sun-synchronus and Earth-oriented orbit

depends on the value of the Sun angle. The concept is shown by Figure 9.14, where a *noon-midnight* orbit (β = 0°), a *twilight* orbit (β = 90°) and a general orbit (0° < β < 90°) are shown. The *twilight* orbit is more convenient from the point of view of secondary batteries (absence of eclipse) but optical observations would result in too much long shadows, and therefore they aren't appropriate [3]. In a 10:30 am-10:30 pm orbit (β = 22.5°), the configuration is very similar to the *noon-midnight* orbit. Therefore, with the instrument optical axis oriented toward nadir, the best configuration for the solar panels is with the normal aligned along the zenith.

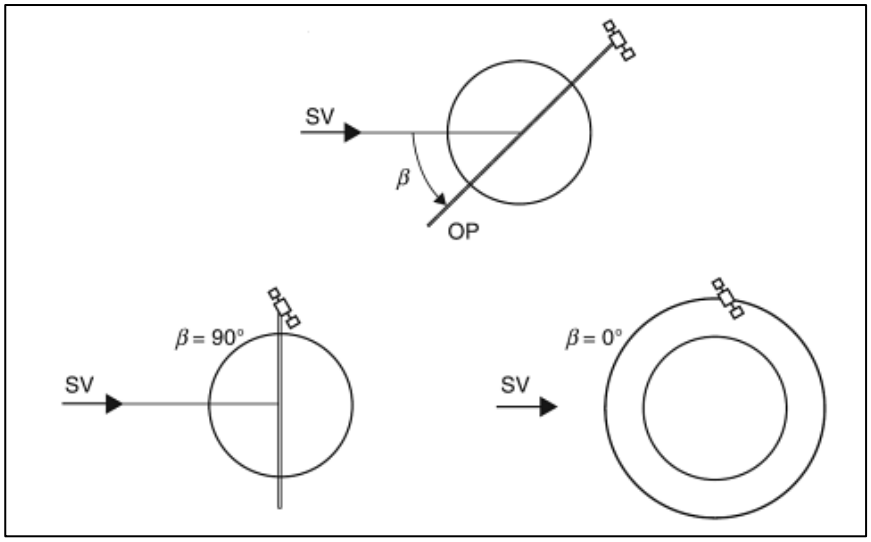

Figure 9.14: Different Sun-synchronus orbit configuration with respect the Sun vector.

SATSLab has been exploited to simulate the variation of power generation during the year and to confirm if the proposed solar panels configuration is effectively suitable. Simulations results are shown by Figure 9.15 (first half of the year, from April to October) and Figure 9.16 (second half of the year).

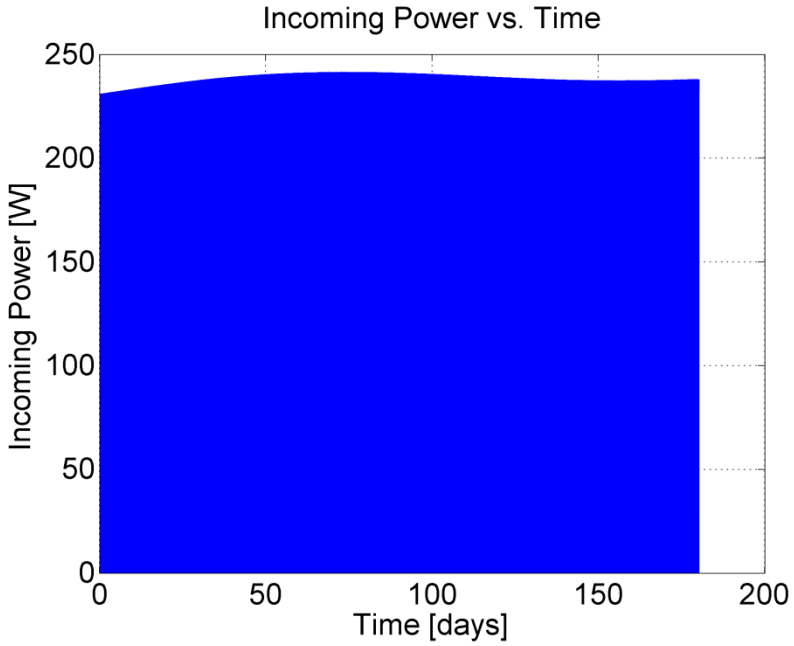

Figure 9.15: Power Generation variation in relation to Sun-angle (first half of the year).

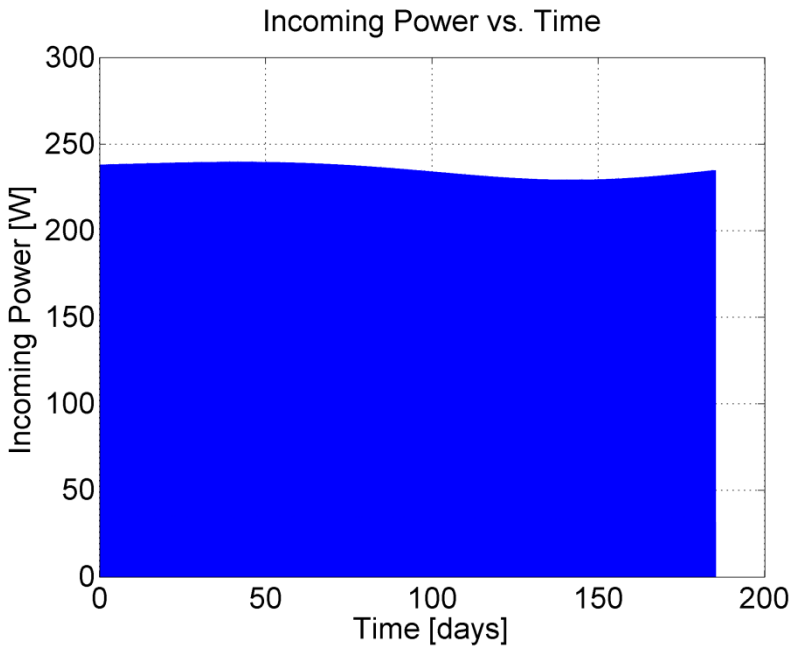

Figure 9.16: Power Generation variation in relation to Sun-angle (second half of the year).

Previous simulations highlighted a minimum power generation during the year of about 220 W (conservative value). This value has been used to conservatively compute the BOL power budget.

In Table 9.17, it is shown the BOL power budget for all supposed operational mission phases.

Subsystem	HK, [W]	Thrusting, [W]	Pl&Tx, [W]
HT100D	-	200	-
Payload	-	-	30 – 111
TT&C	3.2	3.2	75.2
ADC	12	28.8	28.8
OBC	5	5	5
Platform total	20.2	237	109
Total	20.2	237	$\leq$ 220

Table 9.17: BOL platform Power Budget for each mission nominal phase.

The power assigned to payload is derived considering the possibility to observe and contemporarily be able to transmit (at maximum RF output power) at all latitudes comprised between +60° and – 60° (and therefore the Tuscany is comprised).

The minimum value of 30 W guaranteed is perfectly in line with the power expense required by the SLIM-6-22, which has the largest consumption between studied instruments. Other latitudes, if required, could be eventually observed but a specific analysis of the particular case is needed.

In relation to power needed for the housekeeping phase (which covers at least an half of each orbit), and to results derived in Chapter 7 during the preliminary Power Storage subsystem sizing, secondary batteries have been initially selected to provide a minimum capacity of 220 Wh (DOD of 10% for ABSL 18650 HC Li-Ion cells long-life cycles) [92].

A conservative capacity of about 65% of the initial one at the end of a 5 years mission (about 30000 cycles) is estimated. Therefore, two existing 8 by 3 arrangements of ABSL 18650 HC Li-Ion cells (126 Wh) would be connected in parallel to achieve a good compromise between a fair capacity (252 Wh) and limited mass (3 kg) [92].

Figure 9.17 shows the batteries BOL DOD trend during each revolution within 24 hours of operation in the hypothesis that both observation and

transmission are performed contemporarily and continuously in the proposed latitude range (HT100D ignitions are not considered).

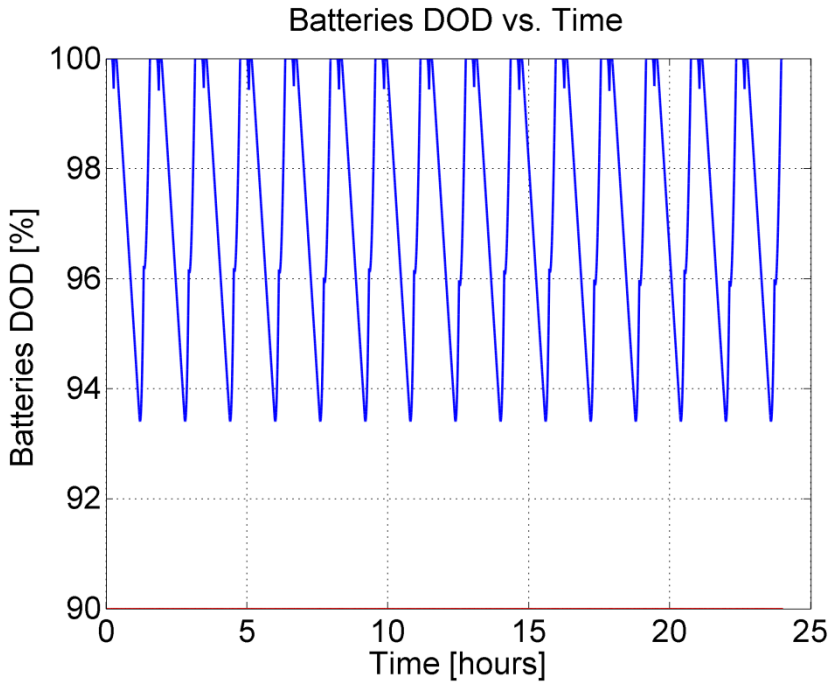

Figure 9.17: Batteries DOD BOL vs time if observation and transmission are performed every orbit between +60° and -60° of latitude.

Finally, in the hypothesis of a maximum of 3500 HT100D ignitions useful to compensate drag (Chap. 7 and Chap. 8) the HT100D is supposed to be in operation for a maximum of 2 times per day.

At the beginning of the mission (supposing maximum solar activity), SATSLab simulations at the lowest expected altitude of 358 km shown that the orbit could be maintained with two daily ignitions of about 16.2 minutes.

Such short durations allow to better manage the thruster from the point of view of thermal control, in particular at the interface with the platform. Thruster operating temperature with a power consumption of 175 are shown by Figure 9.18.

In particular, the green curve T2 INTERF refers to this interesting interface temperature, and confirms that it could be maintained very close to the good temperature of about 50°C if ignition durations are lower than 30 minutes.

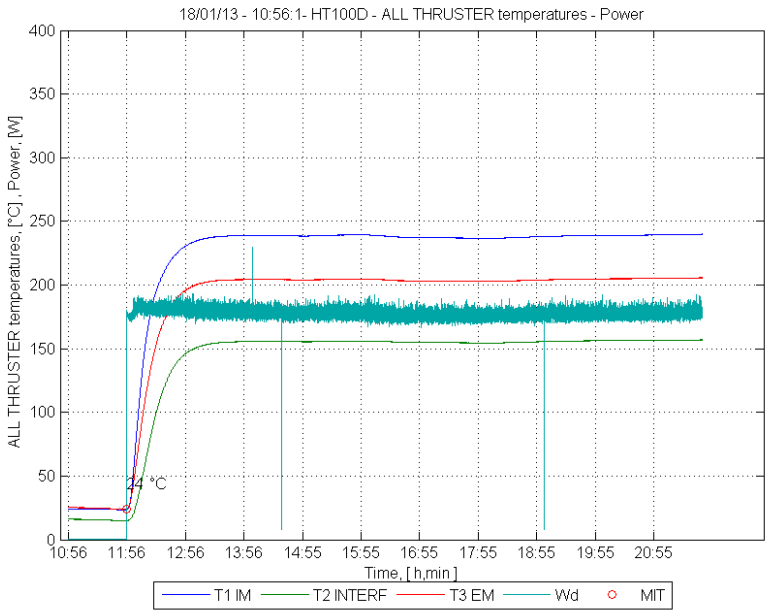

Figure 9.18: HT100D operation temperature.

The SMA daily maintenance at the beginning of the mission is shown by Figure 9.19 (SMA box of about 0.3 km):

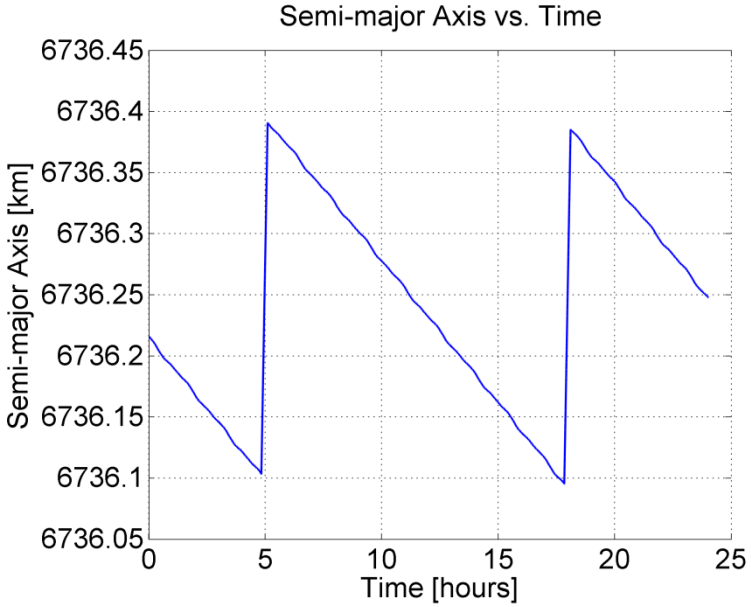

Figure 9.19: Daily SMA BOL maintaining at 358 km of altitude.

9.2.4 Platform end of life (EOL) power budget and power storage subsystem sizing

In Table 9.18, it is shown the EOL power budget for all supposed mission phases. A conservative maximum available power of 200 W is considered.

Subsystem	HK, [W]	Thrusting, [W]	Pl&Tx, [W]
HT100D	-	200	-
Payload	-	-	From 30 to 91
TT&C	3.2	3.2	75.2
ADC	12	28.8	28.8
OBC	5	5	5
Platform total	20.2	237	109
Total	20.2	237	$\leq$ 200

Table 9.18: EOL platform Power Budget for each mission nominal phase.

The unique difference respect to BOL power budget regards the maximum power generation during the observation and transmission phase. Figure 9.20 shows the batteries DOD EOL trend in the hypothesis of observation and transmission performed contemporarily and continuously during each revolution in the proposed latitude range.

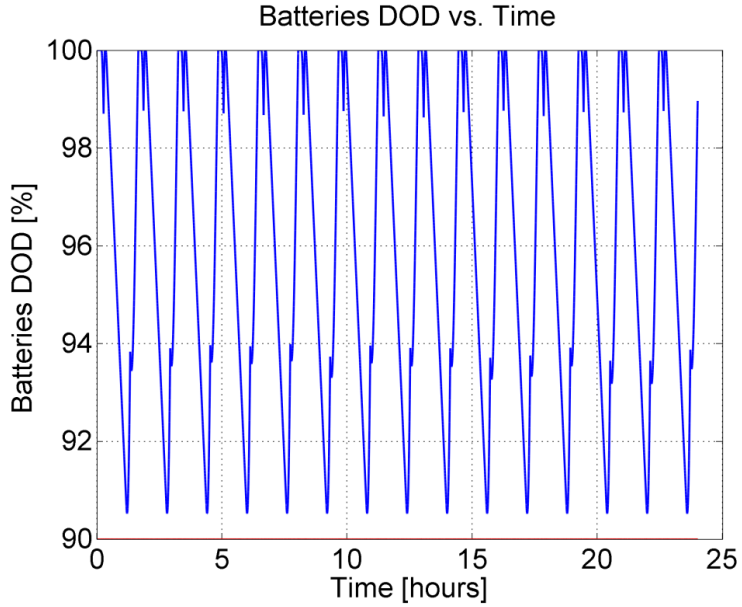

Figure 9.20: Batteries DOD EOL vs time.

Supposing to reach the EOL of the mission in a period of very low solar activity, the daily thrusting phase could be composed by a maximum of 2 ignitions of about 4.15 minutes each one. The SMA daily maintenance at the end of the mission is shown by Figure 9.21:

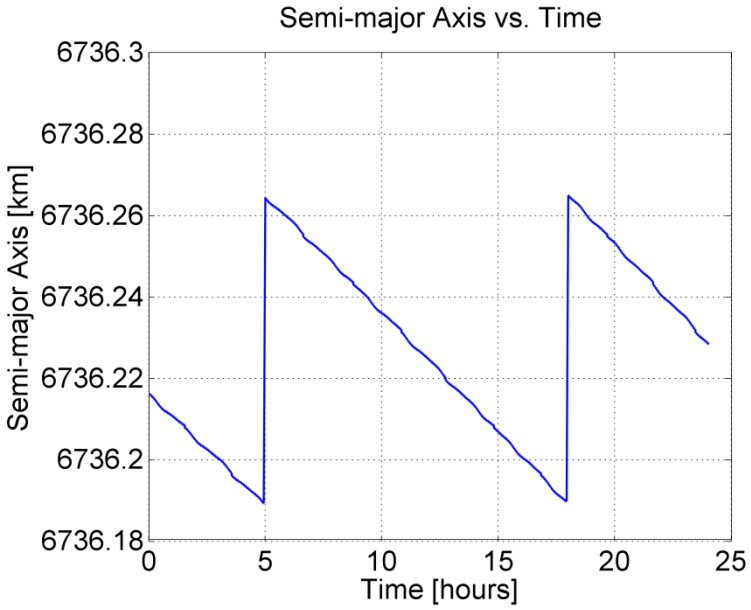

Figure 9.21: Daily SMA maintaining EOL at 358 km of altitude.

The very low duration of HT100D thrusting during period of low solar activity, allows to think also to a strategy of longer but less frequent ignitions, in order to maintain ignitions total number well below the accepted threshold.

9.2.5 Alta SpA SATSLab simulations of complete mission BOL

From Figure 9.22 to Figure 9.25 is represented the energetic state at the beginning of the life (with the minimum expected power generation of to 220 W) for one single day during which all mission phases are performed. The simulated altitude is 358 km.

Simulations performed consider data transmission only to a dedicated ground station centered in Tuscany.

The payload is supposed to operate contemporarily to data transmission and to consume 30 W.

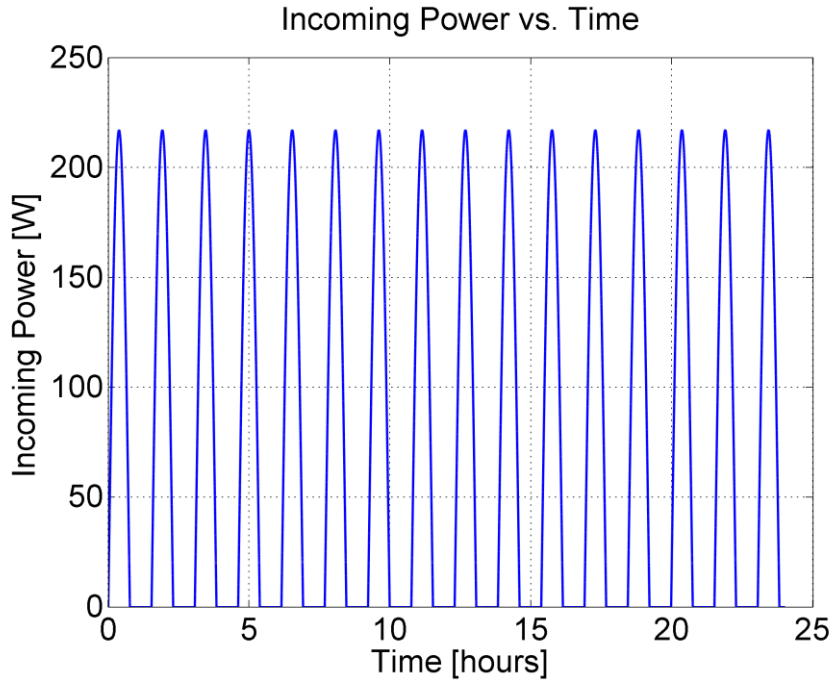

Figure 9.22: Power generation BOL during one completely operational day.

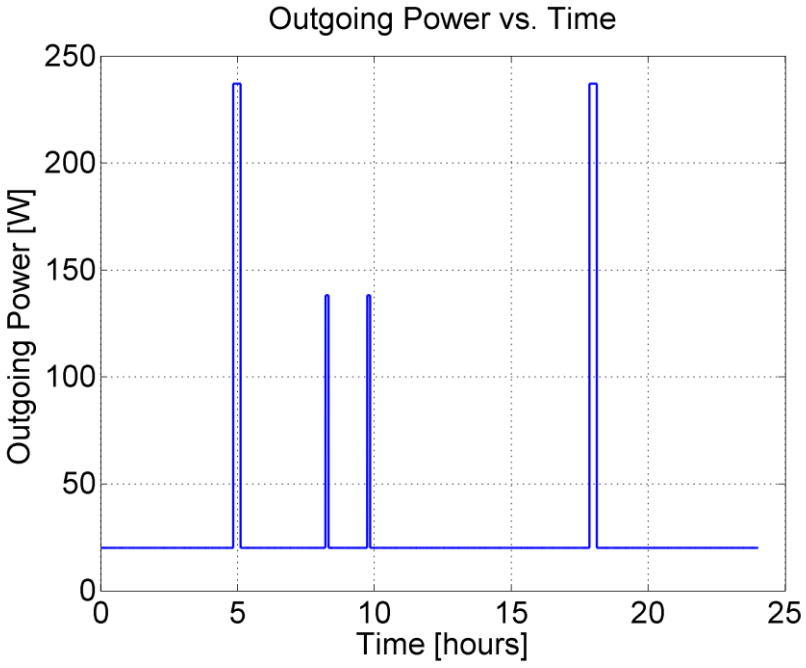

Figure 9.23: Power Consumption BOL during one operational day. HT100D ignitions are represented by the first and the last step.

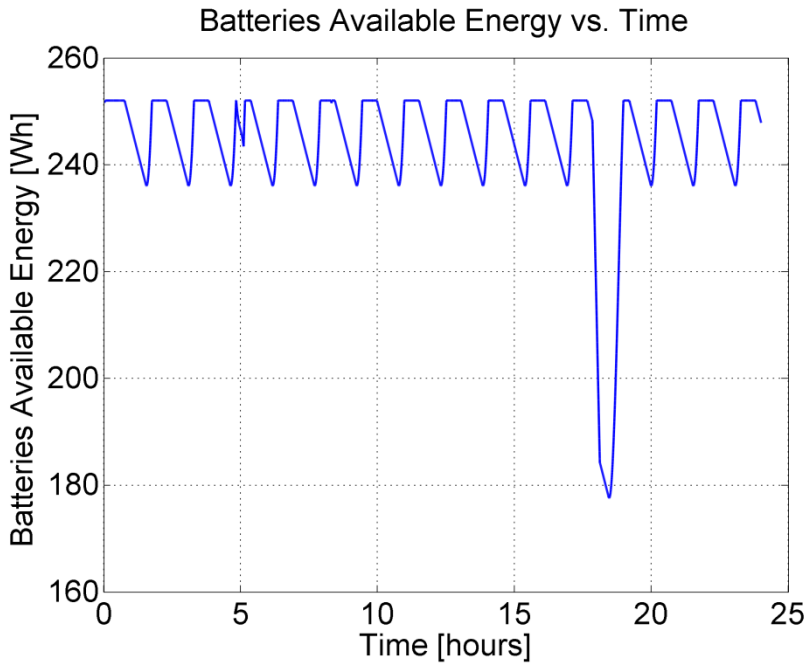

Figure 9.24: Batteries Available Energy BOL during one completely operational day.

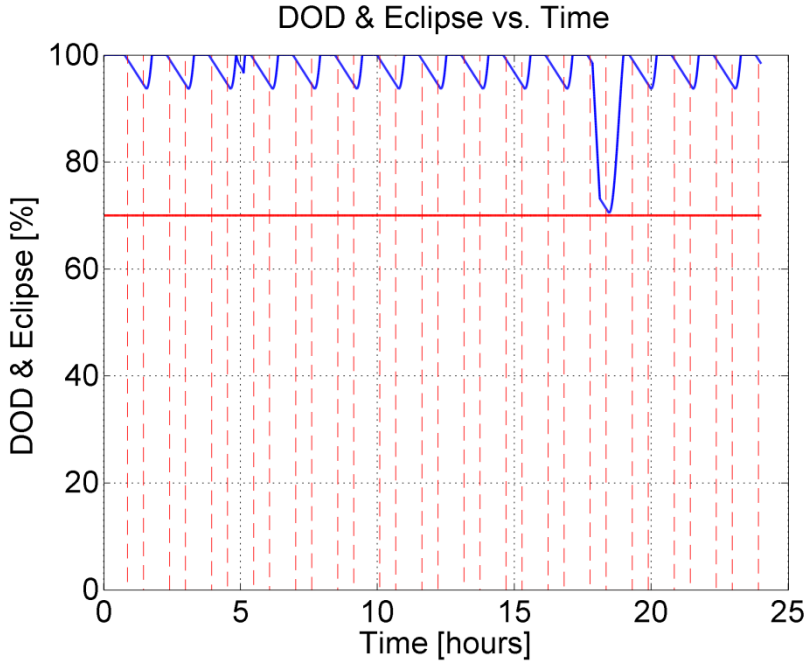

Figure 9.25: Batteries DOD and eclipse BOL during one completely operational day. Eclipse- thrusting is represented by the largest DOD decrease.

Therefore, figures show that the spacecraft is perfectly able to operate from the energetic point of view. Figure 9.23 distinguishes power expense for HT100D thrusting phases (highest steps) from power expense for transmission and observation (smallest central steps). Figure 9.25 highlights that HT100D operation is perfectly possible also during eclipse, with a batteries DOD lower than 30%. Considering that HT100D eclipse-ignitions are well below a number of 2000, 30% is conservatively in line with batteries performance shown by [92], which shown that it is possible to reach a 70% of DOD if cycles number is very limited.

9.2.6 Alta SpA SATSLab simulations of complete mission EOL

From Figure 9.26 to Figure 9.29 is represented the daily energetic state of the spacecraft but at the end of the life.

Simulations consider a very conservative decrease of battery capacity down to 65% [92], a maximum power generation of 200 W and 2 HT100D ignitions of 4.15 minutes.

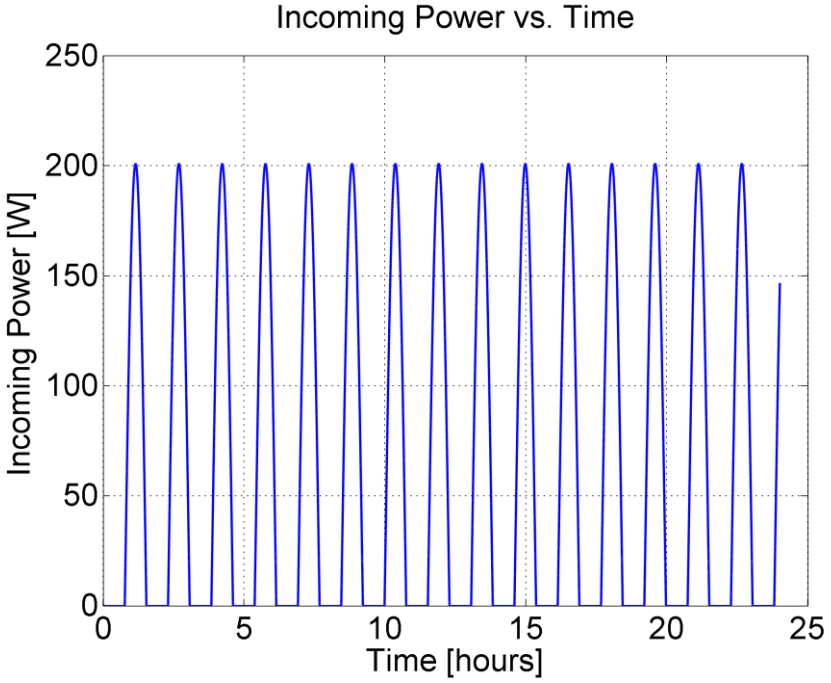

Figure 9.26: Power generation EOL during one completely operational day.

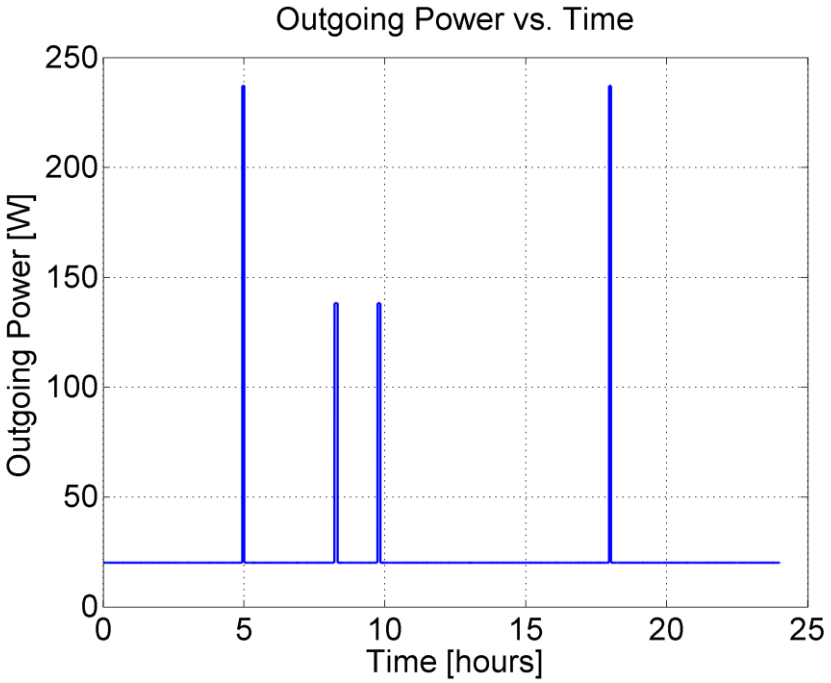

Figure 9.27: Power Consumption EOL during one completely operational day. HT100D ignitions are represented by the first and the last step.

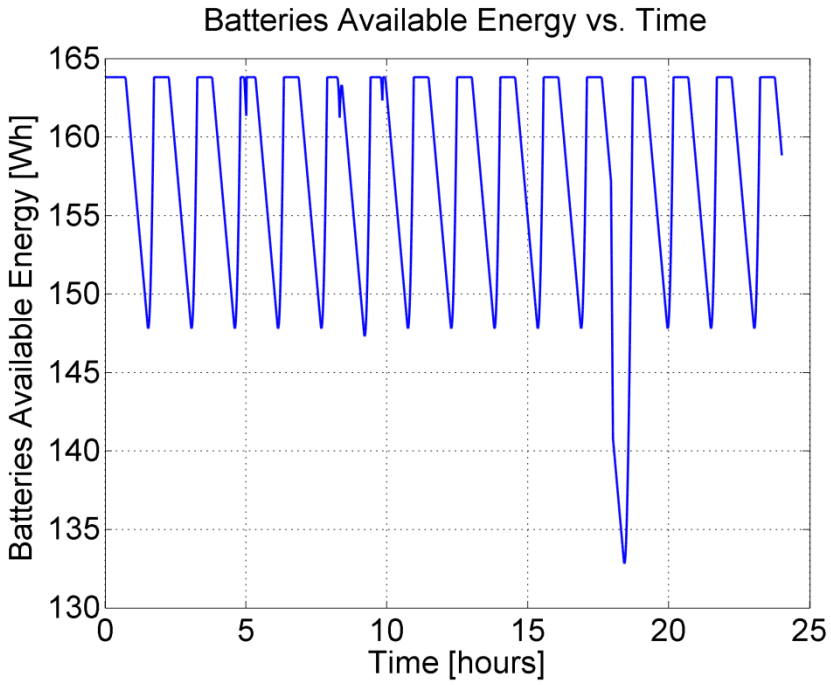

Figure 9.28: Batteries Available Energy EOL during one completely operational day.

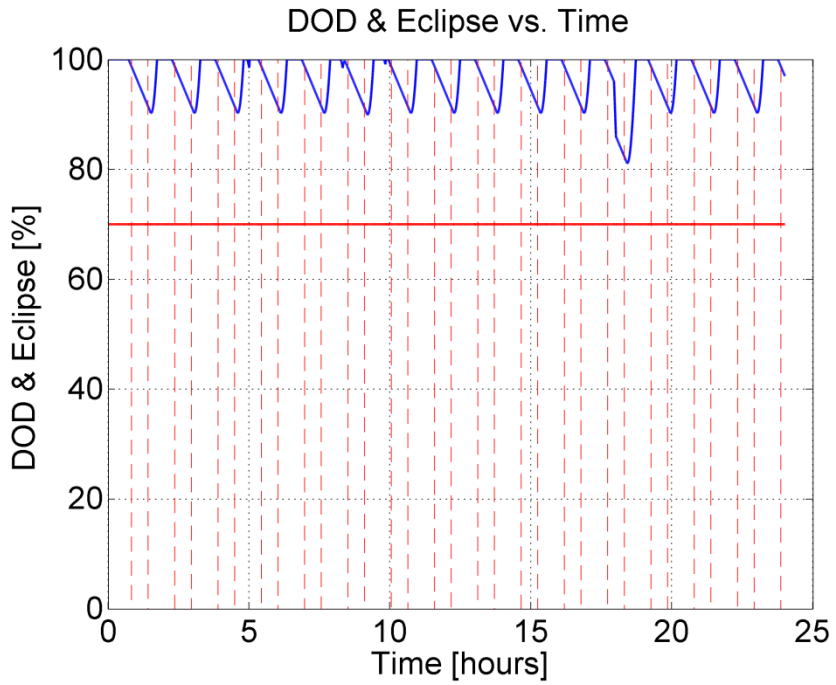

Figure 9.29: Batteries DOD and eclipse EOL during one completely operational day. Eclipse- thrusting is represented by the largest DOD decrease.

Figures confirmed the spacecraft capability to reliably sustain its operation from the energetic point of view also at the EOL, with batteries DOD lower than 10%.

Figure 9.29 evidences that from the battery point of view it is possible to perform also longer ignitions respect to simulated 4.15 minutes.

9.3 PLATFORM DESIGN

This paragraph describes the general guidelines followed to design the platform and shows detailed representation of internal and external layouts.

The final design is devoted to demonstrate the achievement of the primary objective of the thesis: design a platform for Earth Observation with very small envelops at the launch and equipped with electric propulsion.

9.3.1 Platform conceptual definition

Several guidelines have been followed to define the physical architecture and the conceptual organization of the platform:

- creation of a primary structure as simple as possible, in order to have only the surfaces strictly needed to attach components and to satisfy launch requirements.
- Definition of a free volume exploitable as *payload vane*, to host the instrument and the associated electronics. The vane needs anchorages to stably mount the payload and will be sized according to dimensions of studied instruments [2].
- Balance of internal mass to enable the platform to host a payload up to at least 12 kg (SLIM-6-22 mass) [2].
- Individuation of a reliable collocation for the *thrusting module*, with particular attention to isolate it from the rest of the platform and to place the tank center of mass perfectly coincident with the spacecraft center of mass.
- Placement of the 3 principal reaction wheels perfectly aligned with spacecraft principal axis to maintain as simple as possible the attitude control system.
- Definition of an internal volume to place a small computer.
- Placement of external components like star trackers, coarse Sun sensors and antennas in their correct orientation.
- Maintenance of a certain margin for additional envelops due to cables and to eventual secondary structures.

9.3.2 Platform external layout

The platform design has been performed with the Dassault Systems software CATIA V5. The external envelope of the platform could be schematized as a prism with dimensions of about 0.5x0.4x0.5 m^3 without

appendices. This results in a surface exposed to drag of about 0.2 m^2, perfectly in line with the one used for previous mission refinement simulations. From Figure 9.30 to Figure 9.38 are shown several views and details of the external layout of the satellite.

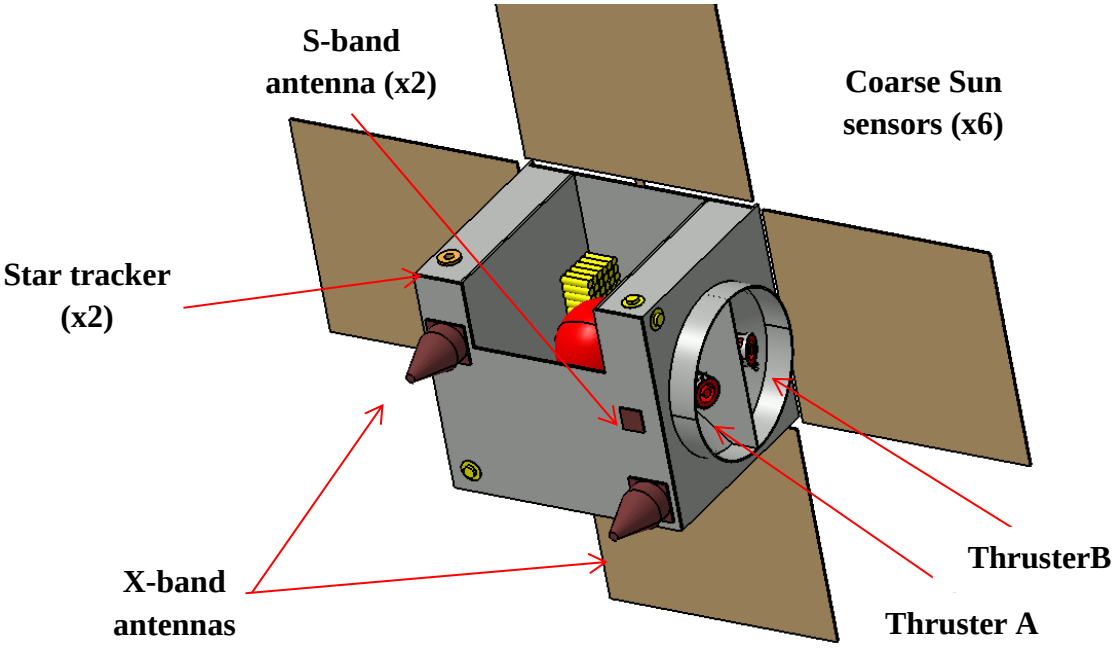

Figure 9.30: Isometric external view of the deployed platform.

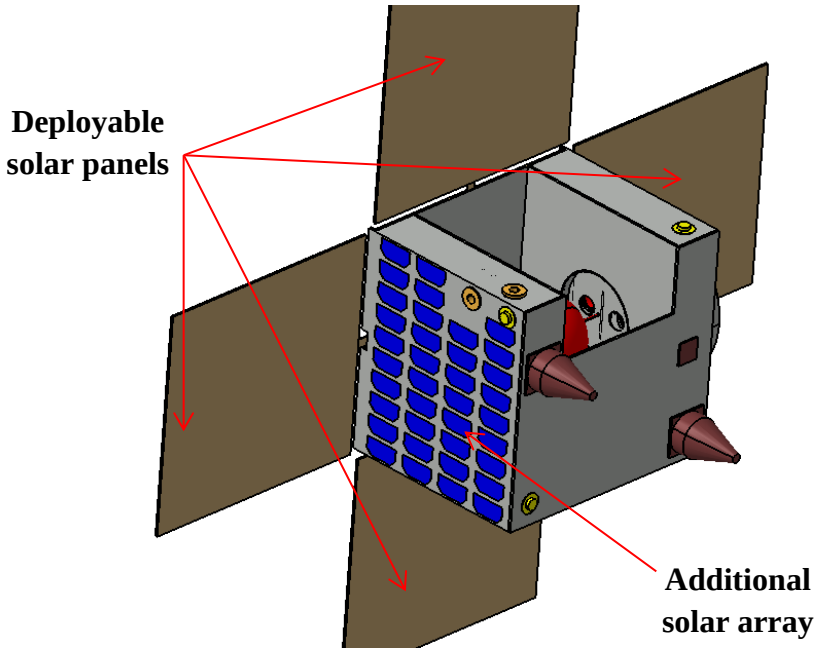

Figure 9.31: Isometric external view of the deployed platform.

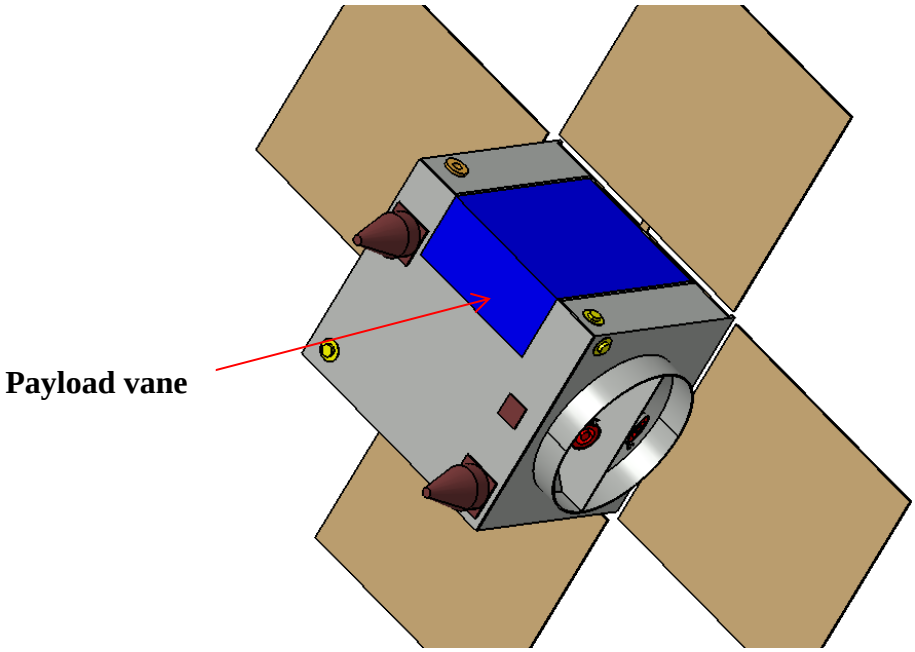

Figure 9.32: Isometric view of the deployed platform with in evidence the available volume of the *payload vane* (in blue).

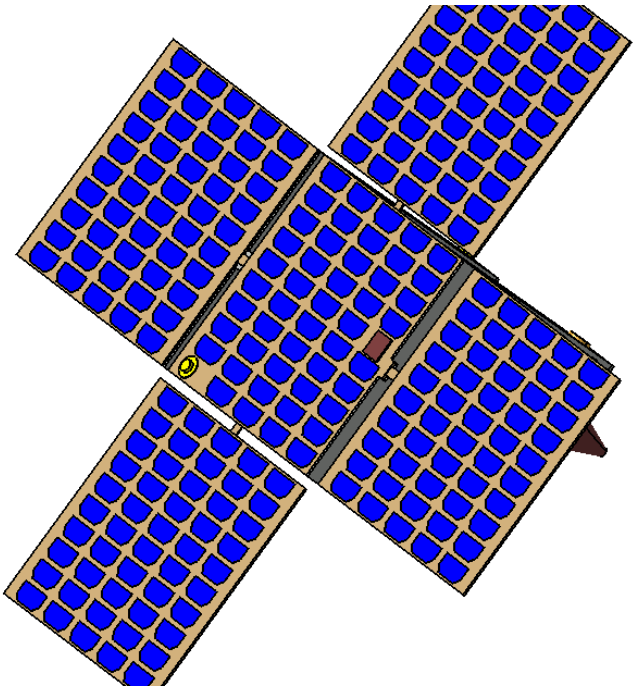

Figure 9.33: Isometric external view of the deployed platform, solar panels side.

Previous figures show several isometric views of the platform in the deployed configuration.

Payload vane dimensions allow to mount a payload with a volume internal to the platform of 0.315x0.420x0150 m^3.

Thrusters (in red, named respectively “Thruster A” and “Thruster B”) are mounted almost completely internally to the platform, with a resultant external protrusion of about 30 mm.

Solar panels (in brown) are placed in a configuration perfectly suitable for a 10:30 am-10:30 pm orbit in terms of power generation, as shown by previous SATSLab simulations.

Figure 9.31 introduces the additional body-mounted solar cells (in blue) devoted to supply power at the exit of eclipses. Also the two star trackers (in orange) are shown.

In particular it is interesting to note the collocation of S-band patch antennas on two opposite surfaces.

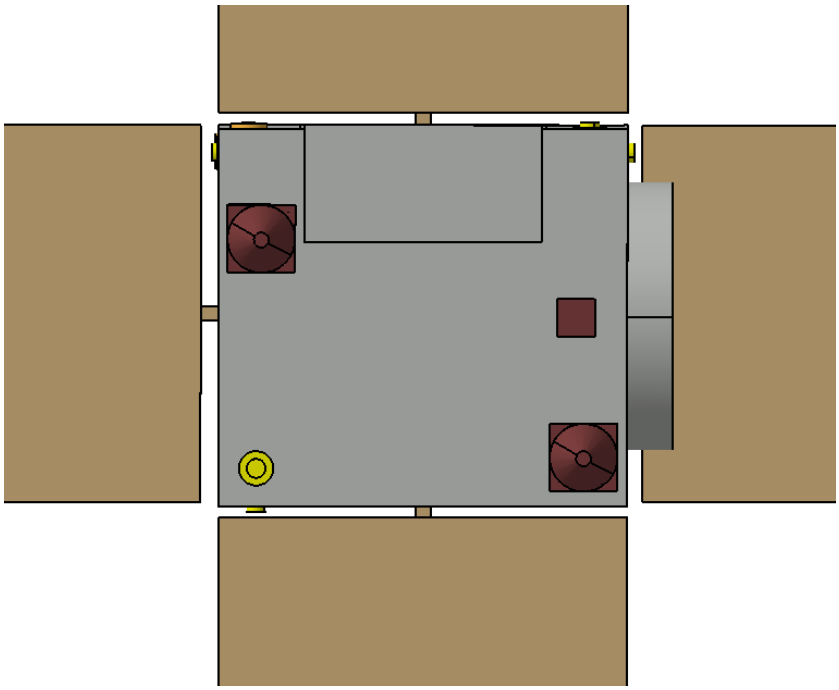

Figure 9.34: External view of the deployed platform, front of the *payload vane*.

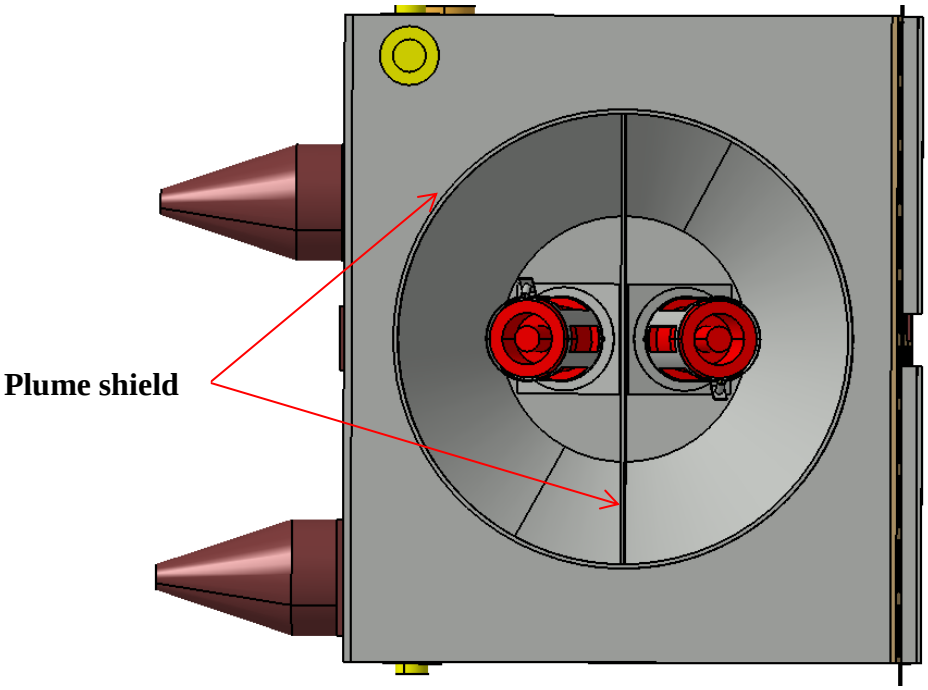

Figure 9.35: External view of the deployed platform, in front of the *thrusting module*.

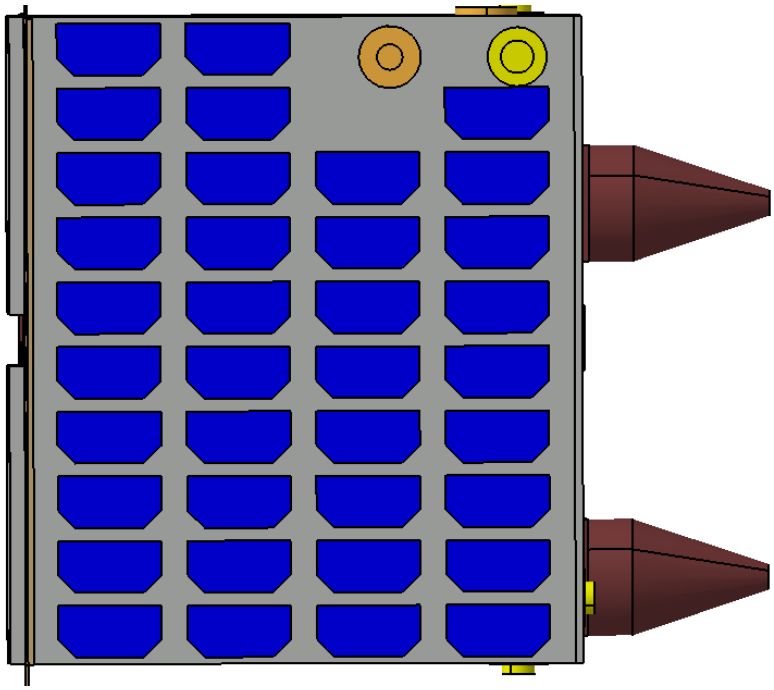

Figure 9.36: External view of the deployed platform, in front of the *thrusting module*.

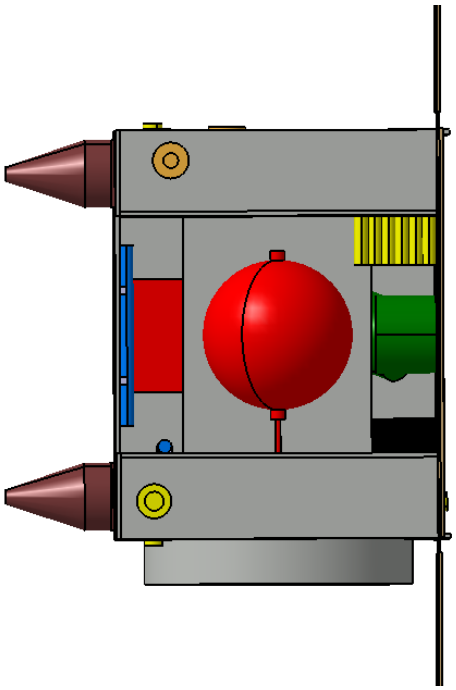

Figure 9.37: External view of the deployed platform, from the top of the *payload vane*.

Figure 9.34, Figure 9.35, Figure 9.36 and Figure 9.37 show four normal views, respectively in front of the *payload vane*, of the *thrusting* module, of the 37 additional body mounted solar cells and finally from the top of the platform.

In particular, Figure 9.34 and Figure 9.35 show the shape and the dimensions of the plume shields used to isolate thrusters from the rest of the platform (cylindrical shield) and also to protect the redundant thruster from the operative one (wake-region shield) [99]. The cylindrical shield external length is set to be about 50 mm while the diameter is of about 360 mm: this allows to provide a reliable and extended coverage to the entire platform without affecting the HT100D principal plume [99]. Other details of the design of the *thrusting module*, like the internal supporting and isolating structure, thrusters separation distance and wake-region shield will be provided in sub-paragraph 8.3.3.

Figures provide also an idea about the additional envelope imposed by helix antennas (characterized by an external length of about 140-150 mm, depending on the configuration).

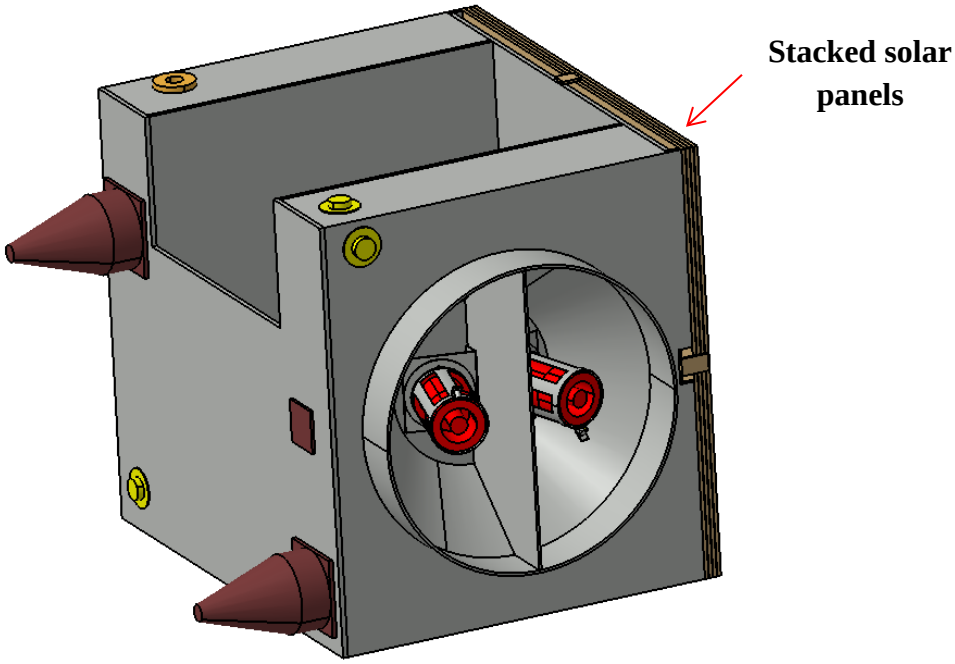

Figure 9.38: External view of the platform in the hypothetical launch configuration.

Finally, Figure 9.38 gives a schematic representation of the platform configuration at the moment of the launch, with deployable solar panels stacked on a single surface.

9.3.3 Platform internal layout

From are shown several views of the internal layout of the platform. These figures show the management of components collocation and the relative fulfillment of envelope requirements, the simplicity and compactness of the primary structure (grey), the very isolated configuration designed for the *thrusting module*, the appropriate collocation of the central tank (red), of reaction wheels (green) and of magnetic torquers (blue).

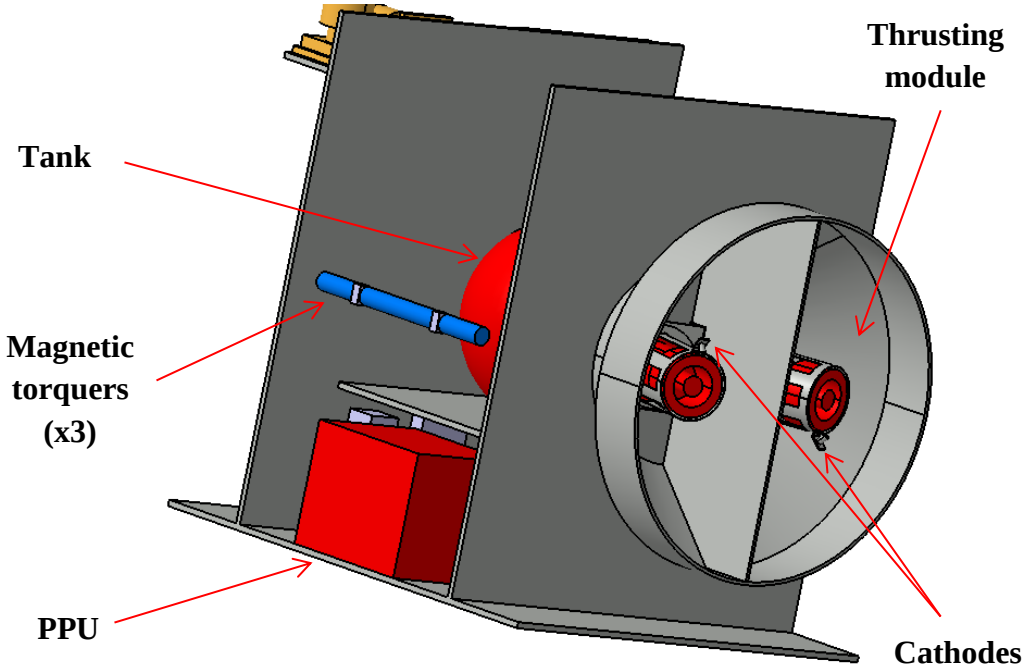

Figure 9.39: Isometric internal view of the platform.

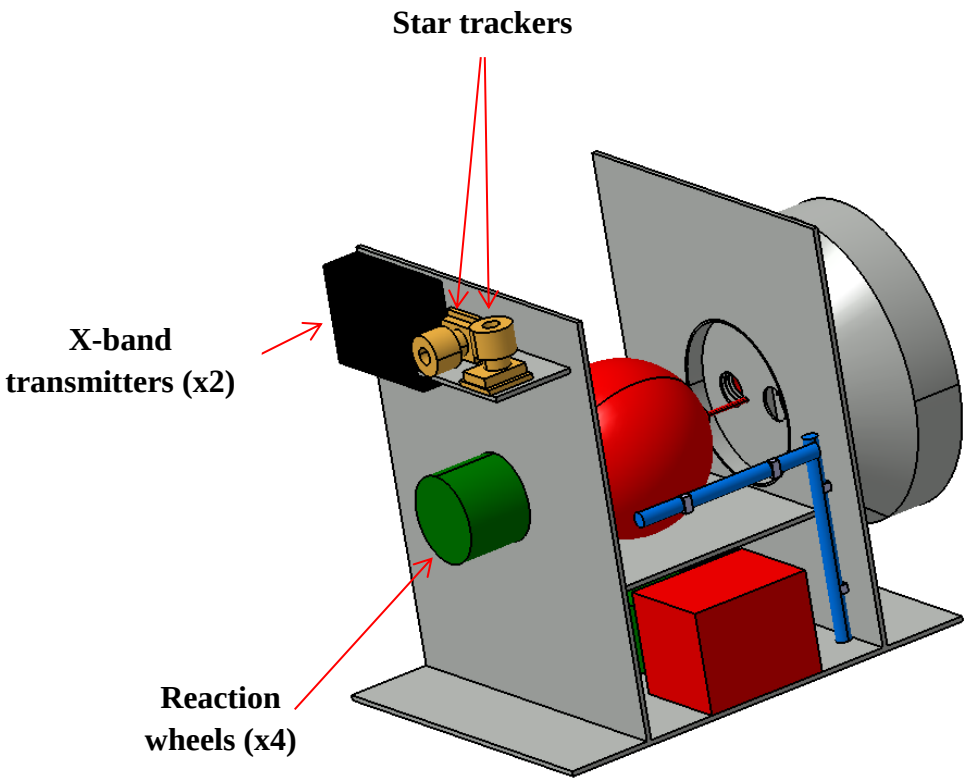

Figure 9.40: Isometric internal view of the platform.

Figure 9.39 and Figure 9.40 provide detailed isometric views of the internal layout of the platform. In particular, show that thrusters are arranged with a misalignment respect to the velocity vector of about 15.189°, resulting in a useful thrust of 8.69 mN, perfectly able to counteract the atmospheric drag, as demonstrated by further SATSLab simulations, used to quantify again the mass of propellant needed to compensate drag. The derived value is almost identical respect to the 1.8 kg previously estimated. Figure 9.39 shows the presence of one cathode per each thruster and the shape of the wake-region plume shields which divide separate thrusters. It is important to underline that CEX ions effects aren't considered potentially critical for the platform in terms of view of contamination, degradation or spacecraft charging. Therefore, shields (potentially built with the same materials of the structure or with stainless steel) are used mostly to mitigate these effects [99], [113], [114].

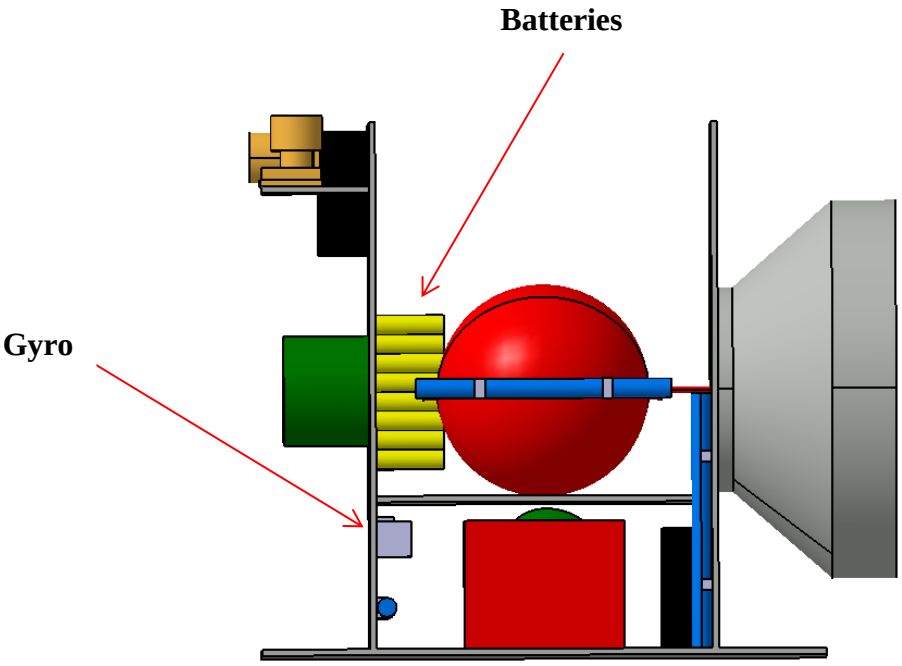

Figure 9.41: Internal view of the platform, front.

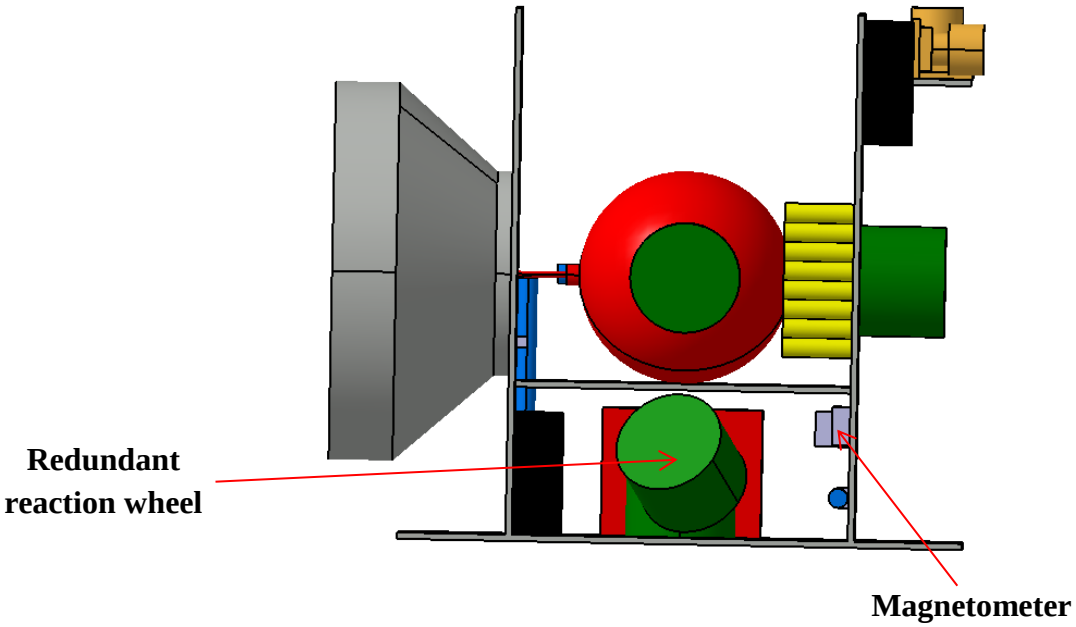

Figure 9.42: Internal view of the platform, back.

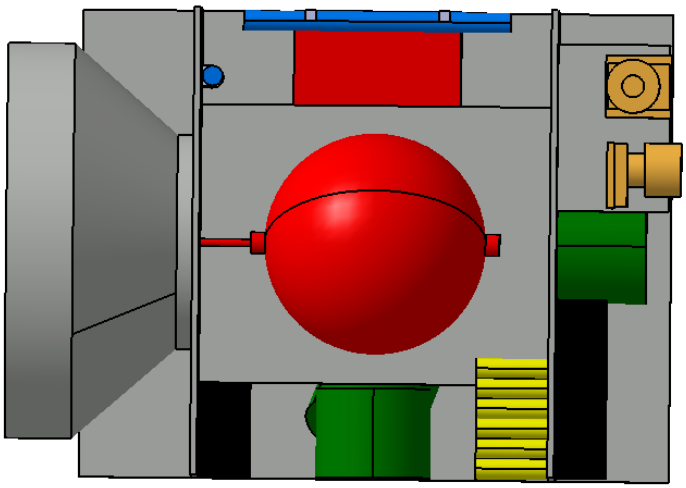

Figure 9.43: Internal view of the platform, top.

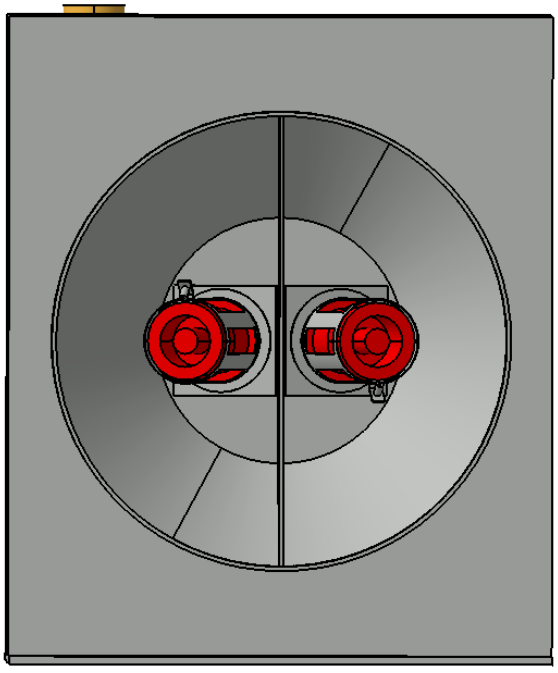

Figure 9.44: Internal view of the platform, in front of the *thrusting module*.

Figure 9.41, Figure 9.42, Figure 9.43 and Figure 9.44 provide a complete overview of the internal components arrangement.

In conclusion, they underline:

- the presence of a very simple structure.
- the appropriate disposal of internal masses, which allow to maintain the platform center of mass very near to the geometric center of mass, considering also the presence of a payload up to 12 kg. Vertical arms of the primary structure will be used as anchorages for the payload.
- The conical shape of the internal supporting structure of the *thrusting module*, which allow to sustain thrusters and to thermally isolate them from the internal of the platform. The shape is selected according to the historical example provided by SMART-1 [113]. Moreover, it allows to save mass and overall internal envelope respect for example to a cylindrical structure.
- The proposed presence of individual back plate radiators for each HT100D to further reduce the temperature at the interface with the spacecraft. The back plate radiators could eventually receive heat collected at the back of the thrusters thanks to appropriate heat guides [115]. Anyway, a more detailed analysis of the thermal exchange between the thruster and the interface is required.
- The coincidence of tank center of mass with the spacecraft center of mass.
- The alignment of reaction wheels with spacecraft principal axis and the presence of a redundant reaction wheel correctly placed on the trisectrix of spacecraft principal axis.
- The correct placing of magnetic torquers parallel to spacecraft principal axis. The possibility to mount an additional magnetic torquer for redundancy is considered.
- The definition of a free volume for the OBC, on the opposite side respect to the *thrusting module*.
- The presence of a margin for additional envelopes.

9.3.4 Platform mass budget

Table 9.19 shows the definitive platform mass budget. The 10% of margin takes into account the additional mass for plume shields, for the launch vehicle interface ring, for cables and for eventual secondary structures. Solar panels substrate is supposed to be a conventional Al /CFRP (Carbon Fiber Reinforced Plastic) sandwich, as suggested by PROBA platforms [2], [116]. Also a kapton foil of 1 mm of thickness is considered to be used for solar panels [89].

Subsystem	Estimated mass, [kg]
Structure	7.000
Solar cells and panels	5.000
Batteries	3.000
HT100D & PPU	8.272
Propellant tank	1.533
TT&C	2.960
ADC	4.825
OBC	2.500
ADC	1.000
Dry platform w/o payload (10% margin)	< 40
Propellant	Up to 6.5
Payload	Up to 12
Total	< 60 kg

Table 9.19: Platform mass budget.

9.4 ALTERNATIVE PLATFORM DESIGN

One interesting issue individuated with previous platform design is related to the potentially dangerous effects of the interactions between the deployable solar panel placed in the proximity of the *thrusting module*, and the principal plume of the thruster B, as depicted by Figure 9.45[6]:

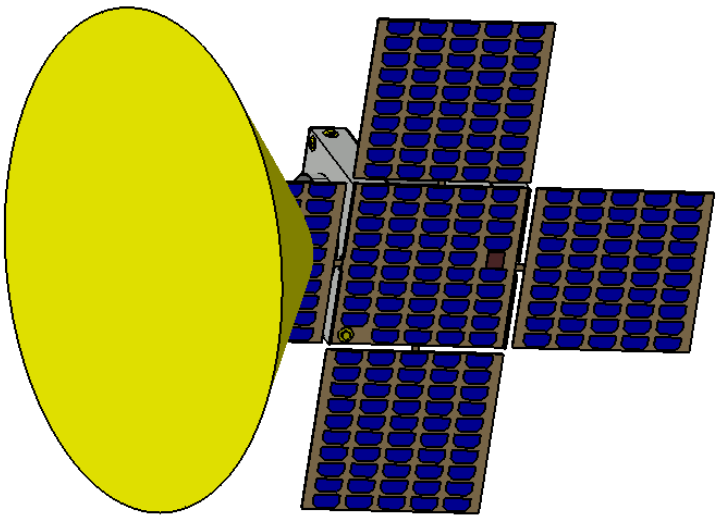

Figure 9.45: Interaction between the plume and the solar panel.

On the contrary, interactions impact due to the other thruster A is very limited and almost inexistent. This means that the thruster A is more appropriate to be considered the principal one, while the thruster B as redundant. To compensate drag, the principal HT100D is expected to operate for a total period lower than 600 hours (value derived thanks to appropriate SATSLab simulations), which is well below the 2000 hours of maximum operative life expected [6]. Considering the very low cost of the platform and the possibility to produce it on large scale, it appears admissible to accept the eventual negative effects related to the use of the redundant thruster. These negative effects don't regard the solar cells degradation (almost unappreciable), but for example the eventual contamination for example of the optics coming from solar panels eroded

materials backsputtering. Following paragraph shows an alternative configuration intended to eliminate this problem.

9.4.1 Alternative configuration

To completely eliminate the problem, one solution defined and proposed in alternative to the previous one (still considered the "principal one") for successive steps of study and development of the platform regards the use of only 3 deployable solar panels, as shown by Figure 9.46:

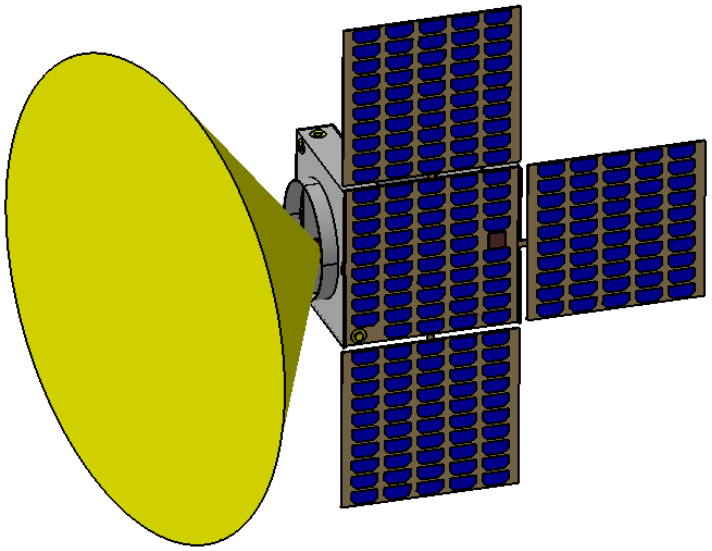

Figure 9.46: Platform external layout with only 3 deployable solar panels.

Therefore, it is more interesting to study this configuration from the point of view of the available power, which is reduced from a maximum of 248 W EOL to 198 W BOL. In relation to previous considerations about the orbit, the minimum available power generation decreases from 220 W BOL to about 175 W BOL, which results in 157 W EOL [89]. With this power generation it is needed a further study of the energetic state to understand if it is possible to maintain the same performance of previous configuration. SATSLab simulations show that it is impossible to reproduce the same performance of the principal configuration with this reduced power generation. Therefore, for example, one solution could be to increase secondary batteries capacity, like the one guaranteed by the use of an 8 by 8

ABSL 18650 HC Li-Ion cells arrangement (336 Wh) [92]. This selection results in an increase of batteries mass of 0.500 kg. With these assumptions, the BOL power budget becomes (Table 9.20):

Subsystem	HK, [W]	Thrusting, [W]	Pl&Tx, [W]
HT100D	-	200	-
Payload	-	-	30 – 66
TT&C	3.2	3.2	75.2
ADC	12	28.8	28.8
OBC	5	5	5
Platform total	20.2	237	109
Total	20.2	237	≤ 175

Table 9.20: BOL platform Power Budget for each mission nominal phase.

BOL power budget illustrated by table 8.21 is almost equal to the BOL power budget of the principal configuration, with the minimum of 30 W ensured to the payload between +60° and -60° of latitude and in the hypothesis of a potentially contemporary transmission. The concept is demonstrated by Figure 9.47, where the BOL batteries DOD of an hypothetical operational day during which observation and transmission are performed contemporarily in the entire proposed latitude range is shown.

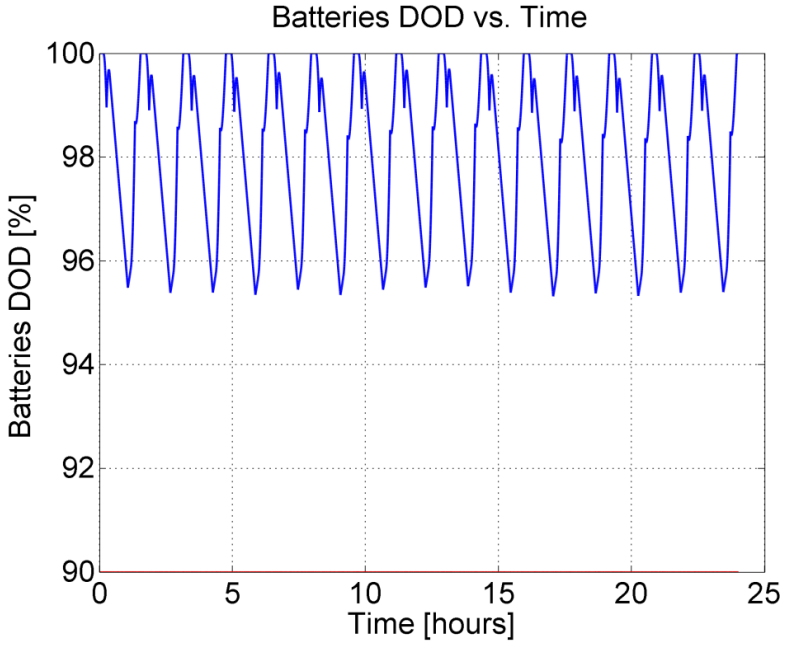

Figure 9.47: Batteries DOD BOL vs time.

From Figure 9.48 to Figure 9.51 is shown the daily energetic state BOL.

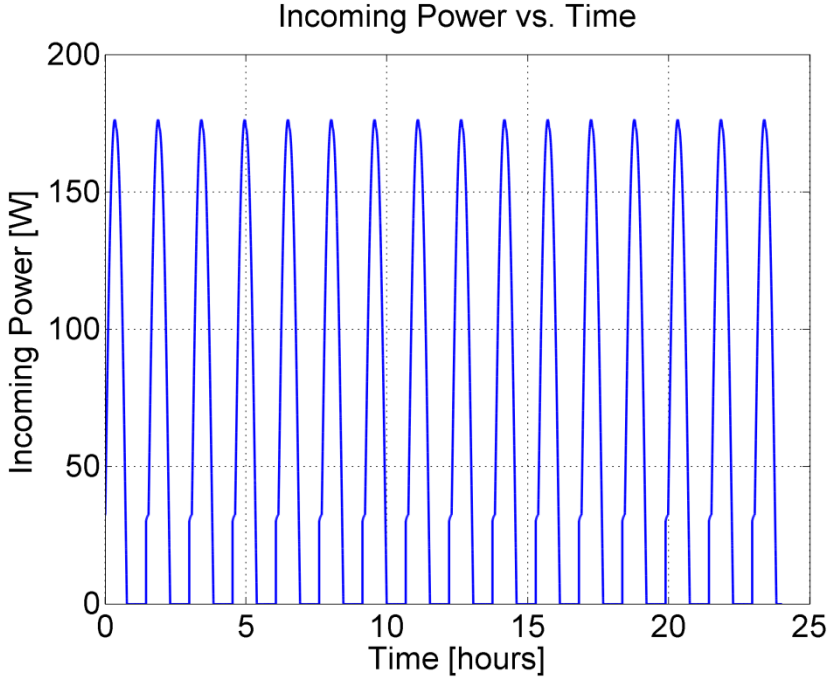

Figure 9.48: Power generation BOL during one completely operational day.

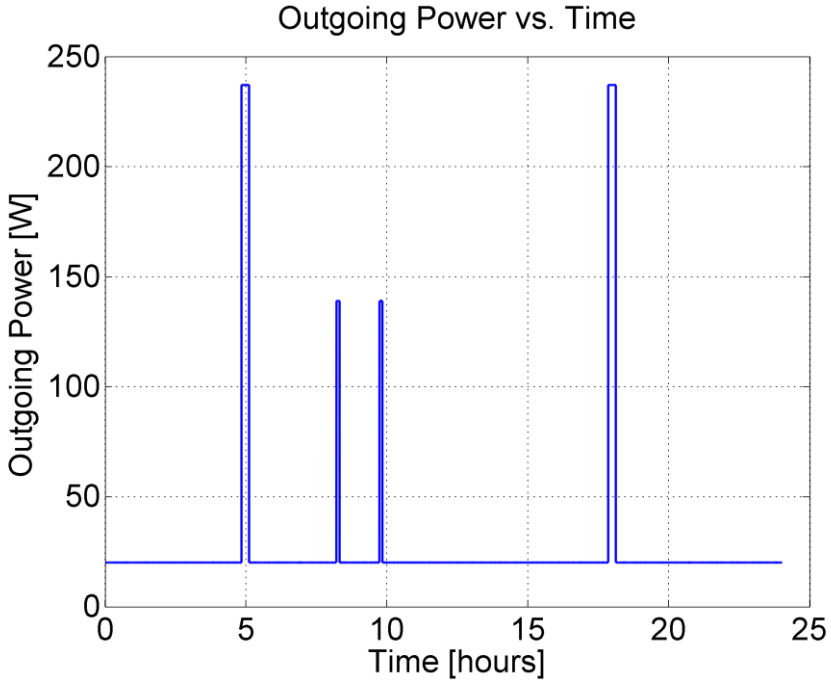

Figure 9.49: Power Consumption BOL during one completely operational day.

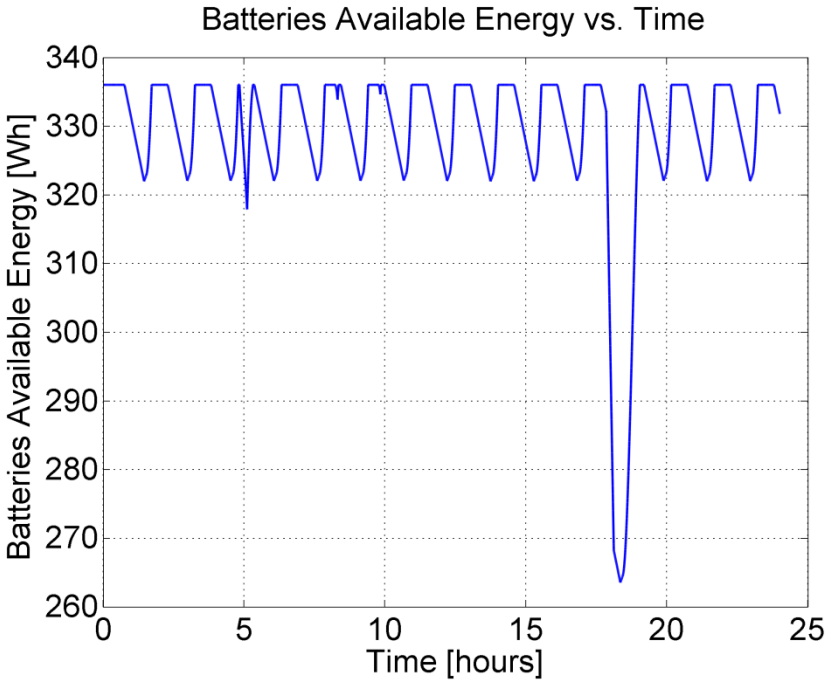

Figure 9.50: Batteries Available Energy BOL during one completely operational day.

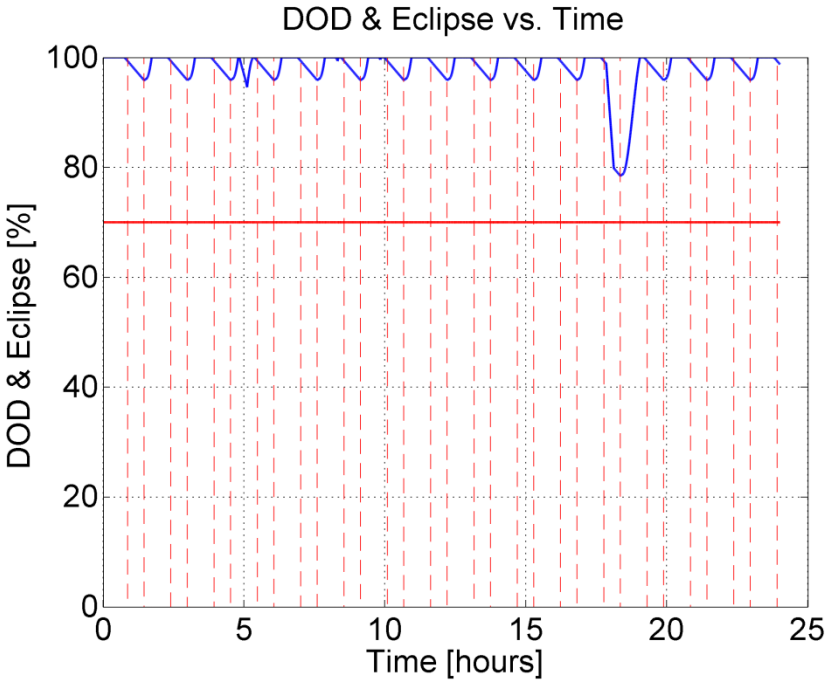

Figure 9.51: Batteries DOD and eclipse BOL during one completely operational day. Eclipse- thrusting is represented by the largest DOD decrease.

Similarly, the EOL power budget becomes (Table 9.21):

Subsystem	HK, [W]	Thrusting, [W]	Pl&Tx, [W]
HT100D	-	200	-
Payload	-	-	From 30 to 48
TT&C	3.2	3.2	75.2
ADC	12	28.8	28.8
OBC	5	5	5
Platform total	20.2	237	109
Total	20.2	237	$\leq$ 157

Table 9.21: EOL platform Power Budget for each mission nominal phase in the alternative configuration.

Again, the EOL power budget of the new configuration is almost the same of the EOL power budget in the principal configuration.

The concept is confirmed by Figure 9.52, where the EOL batteries DOD of an hypothetical operational day during which observation and transmission are performed contemporarily in the entire proposed latitude range is shown:

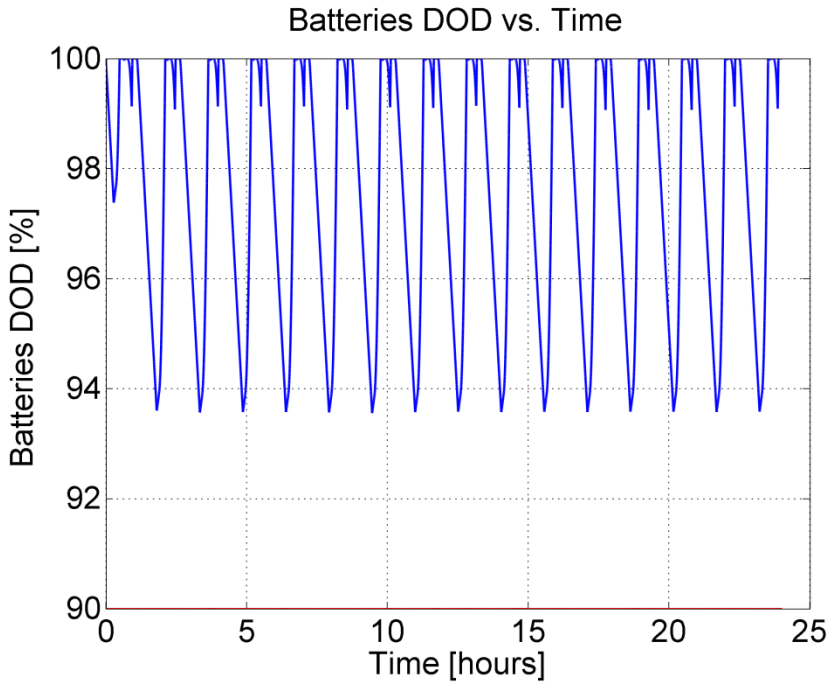

Figure 9.52: Batteries DOD BOL vs time.

From Figure 9.53 to Figure 9.56 is shown the daily energetic state EOL in the alternative configuration:

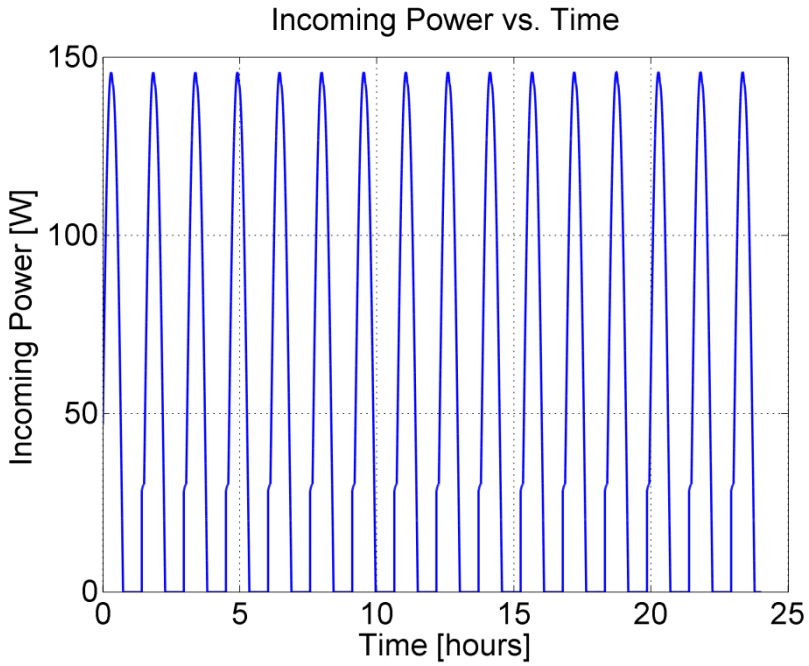

Figure 9.53: Power generation EOL during one completely operational day.

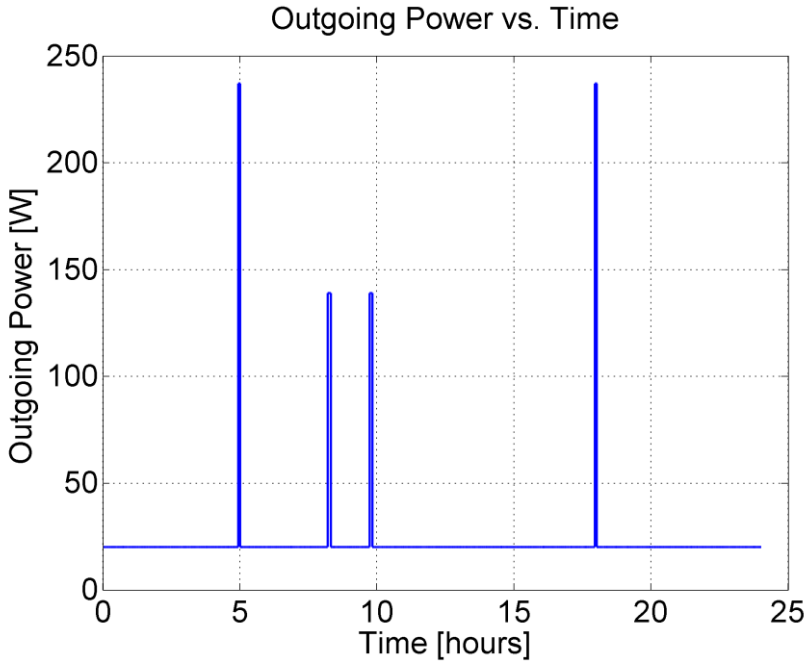

Figure 9.54: Power Consumption EOL during one completely operational day.

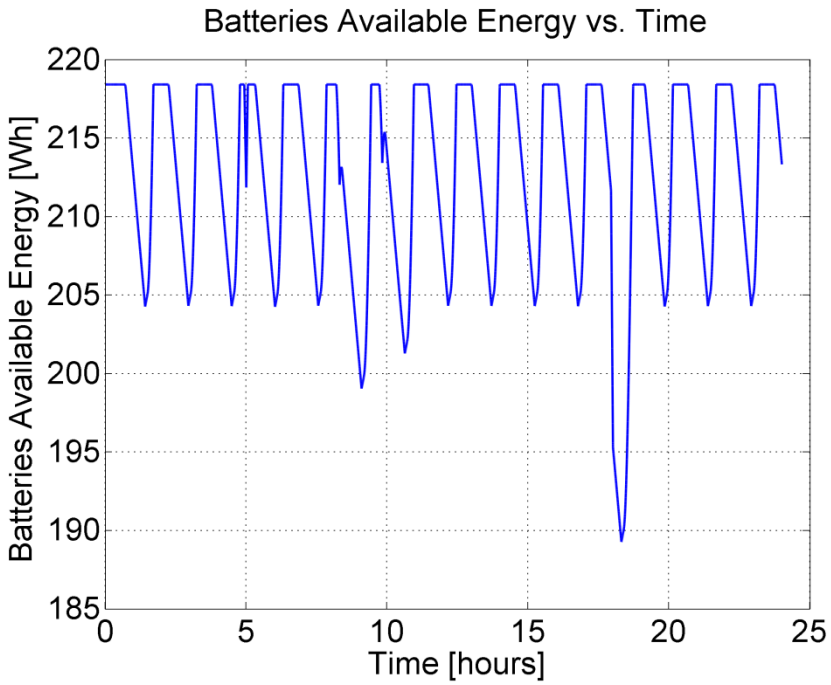

Figure 9.55: Batteries Available Energy BOL during one completely operational day.

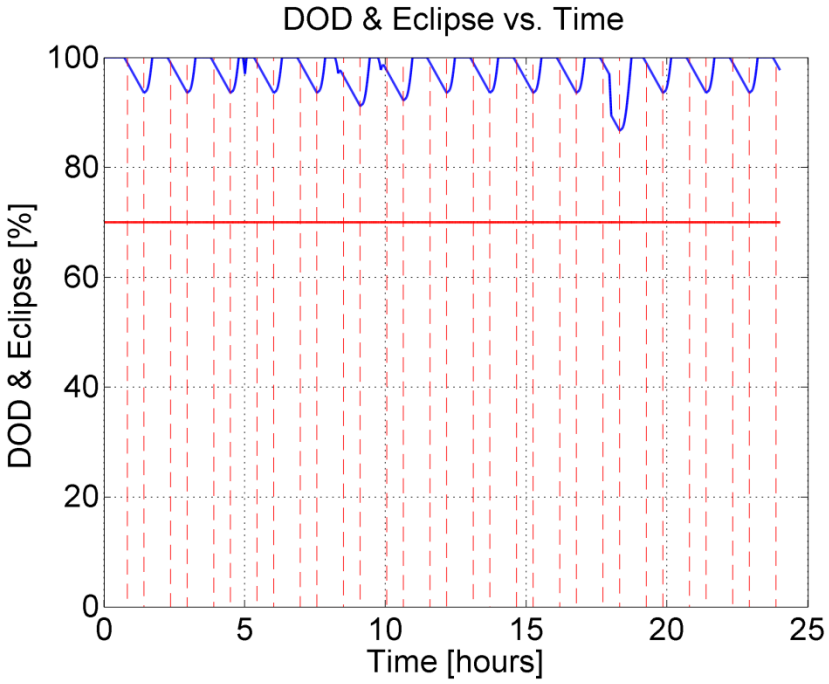

Figure 9.56: Batteries DOD and eclipse BOL during one completely operational day. Eclipse- thrusting is represented by the largest DOD decrease.

Finally, table 8.23 shows the alternative configuration mass budget:

Subsystem	Estimated mass, [kg]
Structure	7.000
Solar cells and panels	4.000
Batteries	3.500
HT100D & PPU	8.272
Propellant tank	1.533
TT&C	2.960
ADC	4.825
OBC	2.500
ADC	1.000
Dry platform w/o payload (10% margin)	< 40
Propellant	Up to 6.5
Payload	Up to 12
Total	< 60 kg

Table 9.22: Platform mass budget.

In conclusion, respect to the first one, this alternative configuration ensures more reliability in terms of the eliminations of interactions between the redundant HT100D ant the solar panel.

Further studies are needed to understand if principal plume interactions are effectively dangerous to justify the increase of battery capacity (fundamental to maintain the same performance but harder to be fully recharged) and the loss of the symmetry imposed by the lack of the solar panel.

Finally, it has to be taken into account also that all these considerations have to be related to specific users' objectives and that the needs in terms of payload operation and data transmission will be clearer only when one definitive observation plane will be established.

9.5 PLATFORM SIZING AND DESIGN CONCLUSIONS

- It is possible to design the platform selecting components within a large variety of available off-the-shelf occasions, ensuring also a minimum of 30 W for the payload power consumption
- SATSLab simulations of the specific case of the Tuscany highlighted the full operational daily capability of the platform in every mission phase. Anyway, a more detailed observation and transmission plane is required to understand the effective need in terms of daily operations.
- SATSLab simulations show that drag compensation could be energetically sustained also during the eclipse, allowing to define a very suitable thrusting strategy and to appropriately manage the number of HT100D ignitions and their duration. Moreover, it is possible to isolate the *thrusting module* from the rest of the platform by means of appropriate structures and shields.
- Several difficulties have been found from the point of view of interactions between the solar panel next to the *thrusting module*: an alternative configuration with only 3 deployable panels have been studied, demonstrating the existence of a simple solution able to maintain the same performance of the principal configuration. This alternative configuration requires more detailed studies to understand the effective dynamical impact of an asymmetrical solar array layout.
- Further studies are needed from the point of view of the primary structure dynamical behavior, of the on-board computer, of the thermal control, on effective impact of CEX ions contamination and of eroded solar panel materials backsputtering and therefore the real need to study more in detail issues linked to the alternative configuration.

9.6 SUMMARY Chapter 9

Summary of principal platform characteristics and available performance in both configurations (Table 9.23).

Configuration	Principal	Alternative
Cube external envelope, [m^3]	0.53x0.42x0.50	0.53x0.42x0.50
Dry platform mass w/o payload (10% margin), [kg]	< 40	< 40
Power generation BOL, [W]	248	198
Base consumption, [W]	20.2	20.2
Battery capacity, [Wh]	252	336
Fine pointing accuracy, [°]	< 0.1	< 0.1
Payload available mass, [kg]	Up to 12	Up to 12
Payload available volume, [m^3]	0.315x0.42x0.15	0.315x0.42x0.15
Payload available power, [W]	30 – 91	30 – 48
Propellant available mass, [kg]	Up to 6.5	Up to 6.5
Drag cross-section, [m^2]	0.21	0.21
Maximum SMA box control, [km]	0.15	0.15
Maximum thrust duration, [min]	16.2	16.2
Available data rate, [Mbit/s]	Up to 200	Up to 200

Table 9.23: Chapter 9 Summary.

10 CONCLUSIONS

This thesis was aimed at the study of a constellation of microsatellites with electric propulsion for Earth Observation and at the preliminary design of a simple, standard and low-cost platform while maintaining high performance.

The study conducted to understand the effective potentialities of a systematic and frequent application of optical images to support land and vegetation-related human activities, like agricultural monitoring and management practices in the region of Tuscany, and recent technological advances (high efficiency solar cells development, operational reliability of electric thrusters achievement, off-the-shelf components availability), demonstrated the feasibility of such a low-cost and high performance constellation.

The mission analysis resulted in the identification of a wide gamma of interesting mission scenarios with the aim of ensuring an easy access to space-data at a large number of different users and communities (institutional, commercial, industrial, military and educational).

Mission scenarios are based on the contemporary and cooperative presence of a number of optical sensors (multispectral, hyperspectral, thermal infrared) on-board the same recurring platform bus and placed at different Sun-Synchronus Repeating Ground Track orbits, designed *ad-hoc*.

All mission architectures identified rely on a number of satellites small enough to guarantee that the entire constellation could be launched exploiting a single launch vehicle, if necessary.

The mission analysis has been followed and completed by the design of a small (60 kg class spacecraft) and compact (external envelope fitting in a cube of 0.5 m of side) platform bus.

The platform guarantees significant performance in terms of power generation (up to 250 W), available payload power (30 W at least) and mass (up to 12 kg), data transfer speed (up to 200 Mbit/s), pointing accuracy (down to 0.025 deg), and, thanks to the 6.5 kg of Xe propellant capability, also altitude maintenance (down to 350 km) and large orbital transfers.

Alta SpA SATSLab simulator allowed to realistically simulate proposed mission scenarios, paying particular attention on the use of electric propulsion for long-periods drag compensation (up to 5 years) and on the behavior of platform power and energy sources (e.g. batteries discharge during electric thruster eclipse operation). Simulations were therefore aimed to testify the high performance ensured by the Alta SpA low power Hall thruster named HT100 and by different subsystems (payload, data transmission, attitude determination and control).

The overall design and simulations process was aimed at the achievement of an easy compatibility with an extended range of existing small optical instruments and of a reliable capability to conveniently operate down to very low altitudes.

These performance are the most significant results obtained in the frame of this thesis, especially if related to the interesting improvements in terms of optical observation completeness and instruments on-ground resolution levels achievable.

To conclude, the achievement of all objectives initially imposed has been confirmed: versatile constellations of microsatellites equipped with electric propulsion, able to realize many different low-cost missions while ensuring better performance (revisit frequency, ground coverage, mission lifetime, operational flexibility) respect to larger satellites or other platforms based on classical chemical propulsion, have been designed.

As a future development of the work, the study demonstrated also interesting possibilities to enlarge the area of interest to many other applications. Therefore, not only agriculture or disaster monitoring, but also climatology (atmospheric, terrestrial and oceanic domains) or hydrology, could be for example conveniently considered, with the aim to respond to a wider range of users distributed all over the world.

Further analysis and studies are required to improve the structural design (dynamical behavior description) and to better analyze effects linked to the use of the electric propulsion, in particular its thermal coupling with the rest of the platform, or other secondary effects, like CEX ions contamination, or solar panel and redundant HT100D plume interactions.

BIBLIOGRAPHY

[1] Mission Design Division Staff, *Small Spacecraft Technology State of the Art*, Ames Research Center, Moffett Field, California, NASA/TP-2014-216648, 2014
[2] https://directory.eoportal.org/web/eoportal/home, 2014
[3] J.R. Wertz, D.F. Everett and J.J Puschell, Microcosm Press, *Space Mission Engineering: The New SMAD*, Space Technology Library, 2011
[4] U.S. Department of the Interior, U. S. Geological Survey, USGS science for a changing world, *Landsat – A Global Land Imagining Mission*, Fact Sheet 2012-3072, 2013
[5] Gottfried Konecny, *SMALL SATELLITES – A TOOL FOR EARTH OBSERVATION?*, University of Hannover, Germany
[6] Ducci C., Oslyak S., Dignani D.. Albertoni R., Andrenucci M., *HT100D performance evaluation and endurance test results*, 33rd International Electric Propulsion Conference, The George Washington University – Washington, D.C. – USA, October 6 – 10, 2013
[7] Canada Centre for Remote Sensing, *A Canada Centre for Remote Sensing Tutorial: Fundamentals of Remote Sensing*, Canada Natural Resources
http://www.nrcan.gc.ca/earth-sciences/geomatics/satellite-imagery-air photos/satellite-imagery-products/educational-resources/9309, 2014
[8] S. Marcuccio, *Satellite Instrumentation Lectures*, University of Pisa, 2011
[9] J. D. Foley and A. Van Dam, Addison-Wesley, *Fundamentals of Interactive Computer Graphics*, 1982
[10] NZ Aerial Mapping Ltd, *Frequently Asked Questions: What is Ground Sample Distance?*,
http://nzam.com/, 2014
[11] Global Strategy IMPROVING AG-STATISTICS, Global Strategy Research Plan, *Developing more efficient and accurate methods for using remote sensing*, Review of the literature, June, 30th, 2013

[12] R. Vintila, C. Lazar, V. Poenaru, C. Radnea and P. Voicu, *A first reference spatial remote sensing and agronomic knowledge base for precision agriculture and related applications*, Stiinta Solului – Soil Science XLVI (1), 2012
[13] P. Timon McPhearson and Osman C. Wallace, *Remote Sensing Applications to Biodiversity Conservation*, Synthesis Document, 2007
[14] P. J. Pinter, Jr., J. L. Hatfield and J. S. Schepers, E. M. Barnes, M. S. Moran, C. S.T. Daughtry and D. R. Upchurch, *Remote Sensing for Crop Management*, © American Society for Photogrammetry and Remote Sensing, Photogrammetric Engineering & Remote Sensing, Vol. 69, No. 69, pp. 646-664, June, 2003
[15] David J. Mulla, *Twenty five years of remote sensing in precision agriculture: Key advances and remaining knowledge gaps*, Dept. Soil, Water and Climate, University of Minnesota, USA, SciVerse ScienceDirect, BIOSYSTEMS ENGINEERING II4 pp. 358-371, 2103
[16] E. Maliet and V. Poinsignon, *A Superspectral microsatellite system for GMES land cover applications*, Acta Astronautica 59 pp. 107-112, 2006
[17] Shunlin Liang, Xiaowen Li and Jindi Wang, *Advanced Remote Sensing*, Elsevier Inc., April, 2012
[18] Observing Systems Capability Analysis and Review Tool, http://www.wmo-sat.info/oscar/, 2014
[19] D. Haboudane et al., *Estimation of leaf area index using ground spectral measurements over agriculture crops: prediction capability assessment of optical indices*, University of Boul., Chicoutimi, Quebec, Canada
[20] J. M. Lopez-Sanchez and J.D. Ballester-Berman, *Potentials of polarimetric SAR interferometry for agriculture monitoring*, RADIO SCIENCE, VOL. 44, 2009
[21] R. D. Jackson and Alfredo R. Huete, *Interpreting vegetation indices*, Elsevier Science Publishers B. V., Amsterdam, Preventive Veterinary Medicine, 11 pp. 185-200, 1991
[22] E. Raymond Jr et al., *A visible band index for remote sensing leaf chlorophyll content at the canopy scale*, International Journal of Applied Earth Observation and Geoinformation 21 pp. 103-112, 2013
[23] Bradley D. Johnson, *Stranger Creek Watershed and Landcover Analysis*, ES 775 Advanced Image Processing, 2011

http://academic.emporia.edu/aberjame/student/johnson4/strangercreek.html, 2014
[24] Remote Sensing Exploitation Division ESRIN, *Agricultural monitoring*, ESA Publications Division, BR-128/II
[25] Juan M. Lopez-Sanchez et al., *Agriculture: Phenology Retrieval*, 2nd Advanced Course on Radar Polarimetry
[26] Shibendou Shankar Ray, *Remote Sensing Applications: Indian Experience*, Department of Agriculture & Cooperation, New Delhi, India
[27] Dr. Georg Losel/RapidEye AG, *Earth Observation Solutions from RapidEye for agricultural needs*, Wageningen, October 6th, 2009
[28] T. A. Doerge, *Management Zone Concepts*, Site-Specific Management Guidilines, SSMG-2, Potash & Phosphate Institute (PPI)
[29] Kumar Navulur, Fabio Pacifici, and Bill Baugh, *Trends in Optical Commercial Remote Sensing Industry*, IEEE GEOSCIENCE AND REMOTE SENSING MAGAZINE, December, 2013
[30] M. Susan Moran, *New imaging sensor technologies suitable for agricultural management*, Aspects of Applied biology 60, 2000
[31] Henry R. Hertzfeld and Ray A. Williamson, *The Social and Economic Impact of Earth Observing Satellites*, National Research Council, Committee on Earth Science and Applications from Space, *Earth Science and Applications from Space: National Imperatives for the Next Decade and Beyond*, Washington DC: National Academy Press, 2007
[32] Elisabetta Peccol, *Nuovi dati da satellite ad alta risoluzione per l'analisi del territorio rurale*, University of Udine, GENIO RURALE N.11, 2008
[33] Dr. George Tyc et al., *RapidEye – An Earth Observation Smallsat Constellation for Daily Agricultural Monitoring*, SSC03-VIII-06, 17th AIAA/USU Conference on Small Satellites, 2003
[34] F. Baumann et al. *TUBIN – A Nanosatellite Mission with Infrared Imager Payload*, S14-5, The 4S Symposium, 2012
[35] R. Vintila et al., *Definition of the required satellite revisit frequency to fulfill farmer information needs – Use of GNSS in precision agriculture*, ADAM Project: Assimilation of spatial Data by AgroModeling
[36] Prof. Graciela Metternicht, *Use of remote sensing and GNSS in precision agriculture*, UN-Zambia-ESA Regional Workshop on the Applications of GNSS in Sub-Saharan Africa, June, 2006

[37] U. Shapira et al., *Field spectroscopy for weed detection in wheat and chickpea fields*, International Journal of Remote Sensing, Vol. 34, No. 17 pp. 6094-6108, 2013
[38] M. Ferreiro-Arman, J.-P. da Costa, S. Homayouni and J. Martìn-Herrero, *Hyperspectral Image Analysis for Precision Viticulture*, 2009
[39] M. Guelman, F. Ortenberg, *Small satellite's role in future hyperspectral Earth Observation missions*, Acta Astronautica 64, 2009
[40] P. S. Thenkaball, R. B. Smith, and E. De Pauw, *Evaluation of Narrowband and Broadband Vegetation Indices for Determining Optimal Hyperspectral Waveband for Agricultural Crop Characterization*, *Remote Sensing for Crop Management*, © American Society for Photogrammetry and Remote Sensing, Photogrammetric Engineering & Remote Sensing, Vol. 68, No. 6, pp. 607-621, June, 2002
[41] A. Schoonwinkel et al., *Integrated Hyperspectral, Multispectral and Video Imager for Microsatellites*, SSC05-I-6, 19th AIAA/USU Conference on Small Satellites, 2005
[42] F. Campo and V. de Luca, *RapidEye e la banda Red Edge per la creazione di mappe di Clorofilla*, GEOmedia, No. 4, 2012
[43] J. Rogan and D. Chen, *Remote Sensing Technology for mapping and monitoring land-cover and land-use change*, Progress in Planning 61 pp. 301-325, 2004
[44] S. K. Seelan et al., *Remote sensing applications for precision agriculture: A learning community approach*, Remote Sensing of Environment 88 pp. 157-169, 2003
[45] G. W. Morgenthaler, N. Khatib and B. Kim, *Incorporating A Constrained Optimization Algorithm Into Remote Sensing/Precision Agriculture Methodology*, Acta Astronautica 53 pp. 429-437, 2003
[46] S. L. Liaghat and S. K. Balasundram, *A Review: the role of remote sensing in precision agriculture*, American Journal of Agricultural and Biological Sciences 5 (1) pp. 50-55, ISSN 1557-4989, © 2010 Science Publications, 2010
[47] Dr. J. F. Paris, *Precision Remote Sensing and Image Processing for Precision Agriculture (PA)*, Colorado State University, Fort Collins, CO, 2005
[48] B. Hoersch and F. Teston, P*ROBA-1 10 YEARS IN ORBIT*, ESA, 4S Conference, 2012

[49] M. Rao et al., *Resourcesat-1: A global multi-observation mission for resources monitoring*, Acta Astronautica 57 pp. 534–539, 2005
[50] François Spoto, Philippe Martimort, Omar Sy and Paolo Laberinti, Sentinel-2 Project team, ESA/ESTEC, *Sentinel-2 Optical High Resolution Mission for GMES Operational services*, Sentinel-2 Preparatory Symposium, Frascati (Rome) Italy, 23-27 April, 2012
[51] http://www.satpalda.com/product/dmc/, 2014
[52] www.deimos-imaging.com, 2014
[53] S. Nakasuka, *Environment Monitoring of Fukushima and Chernobyl Areas using a Constellation of Micro Observation satellites and ALOS-2*, Japan-Ukraine Cooperation Technical Demonstration Program for Supporting Aftermath Response to Accidents at Nuclear Power Stations, University of Tokio, 2013
[54] S. Nakasuka, *Current Status and Future Vision of Hodoyoshi Microsatellites – Systems for Quick and Affordable Space Utilizations*, University of Tokio
[55] Stefano Santandrea, ESA- Proba-V System Engineer, *Proba-V Mission*, IAA Symposium, Berlin, 2011
[56] S. Mostert et al., *Sumbandilasat – An operational technology demonstrator*, Acta Astronautica 63 pp. 1273-1282, 2008
[57] J. Herscovitz and A. Karnieli, *VENμS Program: Broad and New Horizons for Super-Spectral Imaging and Electric Propulsion Missions for a Small Satellite*, SSC08-III-1, 22nd Annual AIAA/USU Conference on Small Satellites, 2008
[58] T. Stuffler et al., *The EnMAP hyperspectral imager – An advanced optical payload for future applications in Earth observation programmes*, Acta Astronautica 61 pp.115-120, 2007
[59] M. Folkman, J. Pearlman, L. Liao, and P. Jerecke, *EO-1/Hyperion hyperspectral imager design, development, characterization, and calibration*, 2000
[60] CEOS EO HANDBOOK – INSTRUMENT SUMMARY, 2014
[61] Prof. Dr. K. Schilling, *MISSION ANALYSIS FOR LOW-EARTH OBSERVATION MISSIONS WITH SPACECRAFT FORMATIONS*, RTO EN-SCI-209, University of Wurzburg
[62] A. Ciccolella – ESA, *MISSION ANALYIS ASPECTS FOR EARTH OBSERVATION MISSIONS*, Summer School Alpbach, 2010

[63] P. Spera, A. Gallon, *Constellation Orbit Design Criteria for a Dual Use EO System*, RTO SET Symposium on "Space-Based Observation Technology, Island of Samos, Greece, 16-18 October 2000
[64] H. Atir, *Microsatellites at Very Low Altitude*, SSC06-II-3,20th Annual AIAA/USU Conference on Small Satellites, 2006
[65] P. Muri, J. McNair, J. Anton, A. Gordon-Ross, K. Cason, N. Fitz-Coy, *Topology Design and Performance Analysis for Networked Earth Observing Small Satellites*
[66] Statistiche demografiche ISTAT, 2010
http://demo.istat.it (Accessed 2014)
[67] Toshinori Kuwahara et al., *Constellation of Earth Observation Micro Satellites with Multi-spectral High-resolution Telescopes*, SSC13-IV-7, 27th Annual AIAA/USU Conference on Small Satellites, 2013
[68] L. Maresi et al., *Compact Hyperspectrals*, SSC11-I-4, 25th Annual AIAA USU Conference on Small Satellites, 2011
[69] L. Maresi et al., *Compact Hyperspectral Imager Breadboard*, 8th IAA Symposium on Small Satellites for Earth Observation, April 04-08, Berlin, 2011
[70] J. A. Richards, *Remote Sensing with Imaging Radar*, Signals and Communication technology, Springer, 2009
[71] L. J. Cutrona, Radar Handbook: Synthetic Aperture Radar, Chapter 23, McGraw Hill, 1970
[72] T. Le Toan, *Use of SAR data for Agriculture Applications*, ESA, DRAGON 2, Advanced Training Course in Land Remote Sensing, Lecture D4L2, Wuhan University, 13 – 18 October, 2008
[73] J. Shang, H. McNairn, C. Champagne and X. Jiao, *Application of Multi-Frequency Synthetic Aperture Radar (SAR) in Crop Classification*, Research Branch, Agriculture and Agri-Food Canada, Canada, Advances in Geoscience and Remote Sensing, 2009
[74] J. M. Lopez-Sanchez, *Agriculture Monitoring Using Time Series of Satellite Polarimetric Images*, Edinburgh Earth Observatory, University of Edinburgh, 2010
[75] H. Inahata and H. Koyama, *Evolution of SAR satellite for Agricultural Applications*, APRSAF-18, Mitsubishi Electric Corporation, 2011

[76] A. Regan, P. Silvestrini, D. Fernandez, N. Leveque, S. Eves, *Sentinel-Convoy: Synergetic Observations with Satellites Flying in Formation with European Operational Missions*, The 4S Symposium, 2012
[77] S. W. Schenk, R. Burt, *Coral: A High Performance Design Expanding CubeSat Mission Output*, SSC10-III-4, 24th Annual AIAA/USU Conference on Small satellites, 2010
[78] E. H. Peterson, R. E. Zee, *InSAR Microsatellite Constellations Enabled by Formation Flying and Onboard Processing Capabilities*, SSC11-IX-1, 25th Annual AIAA/USU Conference on Small satellites, 2011
[79] E. H. Peterson, R. E. Zee, *Possible Orbit Scenarios for an InSAR Formation Flying Microsatellite Mission*,
[80] P. Davies et al., *Nova-SAR – Bringing Radar Capability to the Disaster Monitoring Constellation*, The 4S Symposium, 2012
[81] P. van Duijn, M. Pastena, *PanelSAR: a smallsat radar instrument*, SSC13-I-5, 27th Annual AIAA/USU Conference on Small satellites, 2013
[82] N. Ahmed, C. Underwood, *An Extended Chirp Mode Pulsed SAR Concept for Low-Cost Micro-Satellite SAR*, IAA-B9-1301, 9th IAA Symposium on Small Satellites for Earth Observation, Berlin, 2013
[83] P. A. Fox et al., *WiSAR^{TM}: A New Solution for High-Performance, Smallsat-Based Synthetic Aperture Radar Missions*, SSC08-VI-1, 22nd Annual AIAA/USU Conference on Small satellites, 2013
[84] F.M. Pranajaya et al., *NEMO-HD: HIGH RESOLUTION MICROSATELLITE FOR EARTH MONITORING AND OBSERVATION*, SSC12-I-4, 26th AIAA/USU Conference on Small Satellites, 2010
[85] Dennis D. Dugay, *TELECOMMUNICATIONS SUBSYSTEM FOR THE LEONIDAS MICROSATELLITE*, University of Hawaii at Manoa Honolulu
[86] H. Bonyan, *System engineering approach toward the problem of required level of in-orbit autonomous-operation of a LEO microsatellite mission*, Amirkabir University of Technology (AUT)
[87] Carleton University Spacrecraft Design Project 2003, *Executive Report: AEGIS Microsatellite System*, Carleton University, March, 2003
[88]Ali Ravanbakhsh and Sebastian Franchini, *Rapid Sizing Tool for a Low Cost University Microsatellite Structure Subsystem*, University of Madrid, 2011

[89] S. Gregucci, *Pannelli fotovoltaici a basso costo per piccolo satelliti: progettazione, sviluppo e qualifica per applicazione su UniSat5*, University of Pisa, 2011-2012
[90] K. Schrantz, C. Pearson, N. Russel, *Experiences From the Early Evolution of the Lithium-ion Space Battery Sector*, ABSL SPACE PRODUCTS, 2008
[91] Michelle A. Manzo et al., *NASA Aerospace Fligth Battery Program, Generic Safety, Handling and Qualification Guidelines for Lithium-Ion (Li Ion) Batteries, Availability of Source Materials for Lithium-Ion (Li-Ion)Batteries, Maintaining Technical Communications Related to Aerospace Batteries (NASA Aerospace Battery Workshop)*, NASA/TM-2010-216727/Volume II, NESC-RP-08-75, 2010
[92] Tami Max, *ABSL's COTS Li-Ion Cell Suite Development 2007 NASA Battery Workshop*, ABSL Space Products, 2007
[93] EADS CASA Espacio, *VESPA VEGA Secondary Payloads Adapter*, VV02, ASTRIUM CASA ESPACIO, 2013
[94] R. Peralta et al., *STRUCTURAL DESIGN, DEVELOPMENT AND TESTING OF A SMALL EXPERIMENTAL SATELLITE: SATEX-1*
[95] *Vega User's Manual*, Issue 4 Revision 0, April 2014
[96] *DNEPR User's Guide*, Issue 2, November 2001
[97] HEXCEL COMPOSITES, *HexWebTM HONEYCOMB SANDWICH DESIGN TECHNOLOGY*, Publication No. AGU 075b, 2000
[98] ATK Part Number 80326-1 Data Sheet, 2014
[99] J. Lee et al., *Simulation of the Spacecraft Electric Propulsion Interaction on DubaiSat-2 using SPIS*, 32nd International Electric Propulsion Conference, Wiesbaden, Germany, September 11 – 15,2011
[100] Syrlinks X-Band Transmitter EWC28 Data Sheet, 2014
[101] RUAG Space X-band Helix Antenna Data Sheet, 2014
[102]http://www.cubesatshop.com/index.php?page=shop.product_details&flypage=flypage.tpl&product_id=85&category_id=6&option=com_virtuemart&Itemid=70&vmcchk=1&Itemid=70 (Accessed 2014)
[103] POLITECNICO DI MILANO, *ADCS (ATTITUDE DETERMINATION AND CONTROL SUBSYSTEM)*, Sistemi Spaziali – Anno Accademico 2009-2010

[104] Astround Feinwerktechnik Adlershof GmbH, Space Technology AOCS-Components, *Reaction Wheel RW 90 for Small and Micro satellites*, RW 90 Data sheet
[105] ZARM Technik AG, *Intelligent Solutions to reduce Space Mission Costs, Magnetic Torquers for Spacecraft Attitude Control*, MT5-2 Data sheet
[106] ZARM Technik AG, *Small Devices – Great Benefit, Magnetometers for S/C Attitude Determination*, AMR Digital Data sheet
[107] Sinclair Interplanetary, ST-16 Star Tracker Data sheet, 2014
[108] CSS-01,02 Space Micro Coarse Sen Sensors Data sheet, 2014
[109] Sensonor ButterflyGyroTM STIM300 Inertia Measurement Unit Data sheet, July 2014
[110] M. Aguirre, J-L Bézy, *ESA Activities Related to High Resolution Imaging from GEO*, European Space Agency, High resolution GEO user consultation at ESRIN 14 and 15, April 2010
[111] Phoenix Spaceborne GPS Receiver Data Sheet, Issue 1.1, January 2007
[112] Surrey Satellite Technology Ltd., *Wide Swath DMC Multi-Spectral Imager*, 2014
[113] D. Estublier, G. Saccoccia and J. G. del Amo, *Electric Propulsion on SMART-1*, A Technology Milestone, ESA Technical & Quality
[114] James Szabo et al., *Iodine Propellant Space Propulsion*, 33rd International Electric Propulsion Conference, The George Washington University – Washington, D.C. – USA, October 6 – 10, 2013
[115] J. Kurzyna and D. Danilko, *IPPLM Hall Effect Thrusters – design guidilines and preliminary tests*, 33nd International Electric Propulsion Conference, Wiesbaden, Germany, September 11 – 15, 2011
[116] Ruelle V et al., *Low Concentration Solar Array Experimento on-board PROBA-2*